

**MOLECULAR ALTERATIONS IN PATIENTS WITH
BENIGN THYROID GOITRE AND PAPILLARY THYROID
CANCER: GENOMIC AND PROTEOMIC
INVESTIGATIONS**

MARDIATY IRYANI BINTI ABDULLAH

**FACULTY OF MEDICINE
UNIVERSITY OF MALAYA
KUALA LUMPUR**

2018

**MOLECULAR ALTERATIONS IN PATIENTS WITH
BENIGN THYROID GOITRE AND PAPILLARY
THYROID CANCER: GENOMIC AND PROTEOMIC
INVESTIGATIONS**

MARDIATY IRYANI BINTI ABDULLAH

**THESIS SUBMITTED IN FULFILMENT OF THE
REQUIREMENTS FOR THE DEGREE OF DOCTOR OF
PHILOSOPHY**

**FACULTY OF MEDICINE
UNIVERSITY OF MALAYA
KUALA LUMPUR**

2018

UNIVERSITY OF MALAYA
ORIGINAL LITERARY WORK DECLARATION

Name of Candidate: **Mardiaty Iryani Binti Abdullah**

Matric No: **MHA 110036**

Name of Degree: **Doctor of Philosophy**

Title of Project Paper/Research Report/Dissertation/Thesis (“this Work”):

**MOLECULAR ALTERATIONS IN PATIENTS WITH BENIGN THYROID
GOITRE AND PAPILLARY THYROID CANCER: GENOMIC
AND PROTEOMIC INVESTIGATIONS**

Field of Study: **Molecular Medicine**

I do solemnly and sincerely declare that:

- (1) I am the sole author/writer of this Work;
- (2) This Work is original;
- (3) Any use of any work in which copyright exists was done by way of fair dealing and for permitted purposes and any excerpt or extract from, or reference to or reproduction of any copyright work has been disclosed expressly and sufficiently and the title of the Work and its authorship have been acknowledged in this Work;
- (4) I do not have any actual knowledge nor do I ought reasonably to know that the making of this work constitutes an infringement of any copyright work;
- (5) I hereby assign all and every rights in the copyright to this Work to the University of Malaya (“UM”), who henceforth shall be owner of the copyright in this Work and that any reproduction or use in any form or by any means whatsoever is prohibited without the written consent of UM having been first had and obtained;
- (6) I am fully aware that if in the course of making this Work I have infringed any copyright whether intentionally or otherwise, I may be subject to legal action or any other action as may be determined by UM.

Candidate’s Signature

Date:

Subscribed and solemnly declared before,

Witness’s Signature

Date:

Name:

Designation:

ABSTRACT

MOLECULAR ALTERATIONS IN PATIENTS WITH BENIGN THYROID GOITRE AND PAPILLARY THYROID CANCER: GENOMIC AND PROTEOMIC INVESTIGATIONS

Benign thyroid tumours account for most nodular thyroid diseases. However, determination of whether a thyroid nodule is benign or malignant is a clinical dilemma. Hence, molecular diagnosis may contribute to an improved assessment of thyroid nodules for the distinction of benign and malignant tumours. In the present study, molecular alterations in patients with benign thyroid goitre (BTG) and papillary thyroid cancer (PTC) were profiled using genomic and proteomic approaches. In the genomics study, nucleotide alterations in thyroid tissues were screened using whole-exome sequencing (WES) in patients with BTG (n = 4) and PTC (n = 5). WES led to the discovery of 340 variants in 36 thyroid neoplasm-related genes. Filtering of variants against public databases revealed 23 novel nucleotide alterations, including 12 in the intronic regions, 6 non-synonymous and 4 synonymous changes, and 1 frame-shift deletion. *In silico* functional analyses indicated that the following novel mutations; c.5908T>C and c.4604A>G of *TG*, c.1082G>T of *TPO*, c.353G>A of *TRH*, and c.262A>C of *RASSF1* affected normal activity of the encoded proteins. Further transcript investigation of thyroid tissue of a PTC patient with a frame-shift deletion, termed c.19-50_53CTGdel, verified for the presence of a novel LGALS3-IFI27 chimeric mRNA. Molecular analysis using multiple OMIC techniques was followed up on one of the patients who had concurrent benign and malignant thyroid tissues. WES of her PTC tissue identified c.1799T>A and c.353G>A mutations in the *BRAF* and *TRH* genes, respectively. However, only the *TRH* c.353G>A mutation was detected when PCR direct sequencing was performed on the benign cyst of the patient. Both the malignant and benign tissues had high *BRAF* expression with decrease or loss of expression of multiple iodide

metabolism genes. Analyses by 2-dimensional electrophoresis and Ingenuity Pathway analysis indicated “reactive oxygen species insult”, “tissue injury/inflammation”, “cell proliferation” and “apoptosis and necrosis inhibitions” in the benign cyst. Both the tissues demonstrated different expression patterns of activated signal transducer and activator of transcription 3 (pY-STAT3) in western blot experiments, with the benign tissue expressing a novel putative 28 kDa STAT3 isoform, termed STAT3 ϵ . In the subsequent proteomics study, a gel-based approach was performed to analyse the expression of proteins in tissue and serum samples of PTC patients without (PTCa; n = 8) and with a history of BTG (PTCb; n = 6), relative to patients with BTG (n = 20). While higher levels of alpha-1 antitrypsin (A1AT) and heat shock 70 kDa protein were associated with PTCa, lower levels of A1AT, protein disulfide isomerase, and ubiquitin-conjugating enzyme E2N seemed apparent in PTCb. In case of the serum proteins, higher abundances of A1AT and alpha 1-beta glycoprotein were detected in PTCa, while PTCb was associated with enhanced apolipoprotein A4 and alpha 2-HS glycoprotein (AHSG). The different altered expression of tissue and serum A1AT as well as serum AHSG between PTCa and PTCb patients were validated by ELISA. The distinctive altered abundances of the tissue and serum proteins form preliminary indications that PTCa and PTCb may be two distinct cancers of the thyroid that are etiologically and mechanistically different.

Keywords: papillary thyroid cancer, benign thyroid goitre, whole exome sequencing, tissue proteomics, serum proteomics

ABSTRAK

Tumor tiroid benigna merangkumi sebahagian besar penyakit tiroid nodular. Walau bagaimanapun, penentuan samaada nodul tiroid adalah benigna atau kanser merupakan suatu dilema klinikal. Oleh itu, diagnosis molekul dijangka dapat menyumbang kepada penambahbaikan penilaian nodul tiroid dalam membezakan tumor benigna dan kanser. Dalam kajian ini, perubahan molekuler di kalangan pesakit goiter tiroid benigna (BTG) dan kanser tiroid papilari (PTC) telah diprofilkan melalui pendekatan genomik dan proteomik. Dalam kajian genomik, perubahan nukleotid dalam tisu tiroid telah disaring menggunakan penjujukan keseluruhan ekson (WES) pada pesakit BTG (n = 4) dan PTC (n = 5). WES telah membawa kepada penemuan 340 variasi dari 36 gene berkaitan tiroid neoplasma. Penyaringan varian menggunakan pangkalan-pangkalan data awam telah mendedahkan 23 perubahan nukleotid novel, termasuk 12 yang terletak di kawasan intronik, 6 perubahan bukan sinonim dan 4 perubahan sinonim, dan 1 delesi anjakan rangka. Analisis *in silico* menunjukkan bahawa mutasi novel yang berikut; c.5908T>C dan c.4604A>G di *TG*, c.1082G>T di *TPO*, c.353G>A di *TRH*, dan c.262A>C di *RASSF1* menjejaskan aktiviti normal protein-protein yang dikodkan. Kajian transkrip yang selanjutnya pada tisu tiroid seorang pesakit PTC dengan mutasi delesi anjakan rangka, diistilahkan sebagai c.19-50_53CTGdel, telah mengesahkan kehadiran novel LGALS3-IFI27 mRNA kimerik. Analisis molekul menggunakan pelbagai teknik OMIK telah dijalankan pada salah seorang pesakit yang memiliki tisu tiroid benigna dan malignan secara serentak. WES dari tisu PTC pesakit wanita tersebut telah mengenalpasti mutasi c.1799T>A dan c.353G>A di gen *BRAF* dan *TRH*, masing-masing. Walau bagaimanapun, hanya mutasi *TRH* c.353G>A ditemui apabila PCR penjujukan langsung dijalankan ke atas sista benigna pesakit tersebut. Kedua-dua tisu kanser and benigna mempunyai ekspresi *BRAF* yang tinggi dengan penurunan atau kehilangan ekspresi pelbagai gen berkaitan metabolisme iodida. Analisis menggunakan elektroforesis dwi-

dimensti dan *Ingenuity Pathway analisis* menunjukkan "kerusakan akibat daripada spesies oksigen reaktif" dan "kecederaan tisu/keradangan", "proliferasi sel", dan "perencatan apoptosis dan nekrosis" dalam sista benigna. Dalam analisis Western blot, kedua-dua tisu tersebut menunjukkan corak ekspresi yang berbeza bagi transduser isyarat dan pengaktif transkripsi 3 yang diaktifkan (pY-STAT3), dengan tisu benigna mengekspresikan isoform 28 kDa STAT3 putatif novel, dipanggil STAT3 ϵ . Dalam kajian proteomik yang selanjutnya, pendekatan berasaskan gel telah dilakukan untuk menganalisis ekspresi protein dalam tisu dan serum dari sampel pesakit PTC tanpa (PTCa; n = 8) dan dengan latar belakang BTG (PTCb; n = 6), berbanding dengan pesakit BTG (n = 20). Sementara aras yang lebih tinggi alfa-1 antitripsin (A1AT) dan protein haba kejut 70 kDa dikaitkan dengan PTCa, aras yang lebih rendah A1AT, protein disulfida isomerase, dan enzim konjugasi-ubikuitin E2N adalah ketara dalam PTCb. Dalam kes protein serum, kelimpahan yang tinggi A1AT dan alfa 1-beta glikoprotein telah dikesan dalam PTCa, manakala PTCb dikaitkan dengan peningkatan apolipoprotein A4 dan alfa 2-HS glikoprotein (AHSG). Perbezaan pengekspresan untuk tisu dan serum A1AT serta serum AHSG di antara pesakit PTCa dan PTCb juga telah disahkan oleh ELISA. Perubahan kelimpahan protein tisu dan serum yang tersendiri menjadi petunjuk awal bahawa berkemungkinan PTCa dan PTCb merupakan dua jenis kanser tiroid yang berbeza secara etiologi dan mekanikal.

Kata kunci: kanser tiroid papilari, goiter tiroid benigna, penjujukan keseluruhan ekson, proteomic tisu, proteomik serum

ACKNOWLEDGEMENTS

First of all, I praise Allah, the Almighty, merciful and passionate, for providing me this opportunity and granting me the capability to proceed successfully.

I am indebted to all of generous individuals for their efforts, encouragement and kindness. I acknowledge with gratitude the assistance received from Prof. Dr. Onn B. Haji Hashim, A/P Dr. Sarni Bt. Mat Junit and A/P Dr. Ng Khoon Leong, my supervisors for their continuous support in the research project and for their interest and comments throughout the project. The motivation, patience as well as persistent effort of them have been invaluable, for which I extremely grateful.

I would like to thank the Ministry of Higher Education (MOHE) and International Islamic University Malaysia (IIUM) for giving me the opportunity and scholarship for my PhD candidature.

I would also like to express my special appreciation to the entire member of staff at the Department of Molecular Medicine and Medical Biotechnology Laboratory, Faculty of Medicine, University Malaya for the considerable help. I am sincerely grateful to Alfred and Jamie for their guidance, advice and help rendered to me.

To my colleagues, Firasysafra, Lee Cheng Siang, Lim Chor Yin, Maryam Khalilzadeh, Mohd Aizat, Nazirah, Nur Hikmah, Siti Nur Fatimah, Thanewary, and Wan Izlina, you really deserve a warm appreciation from me. Allow me to say 'thank you' for your kind heartedness that made the atmosphere in the workplace more joyful and for the meaningful guidance and support. I am so glad to be with and working with you guys.

I thank all the participants of this research and endocrine surgery team for their effort and time, I humbly acknowledge their contribution.

Above all, this thesis would not have been possible without the valuable courage given by my parents, Tuan Haji Abdullah B. Haji Hashim and Puan Hajah Zainab Bt. Haji Yusuf. I want to say 'thank you' for your continuous prayers, unconditional love and supports, faith on me and being my pillar of strength. I owe everything to them and am extremely grateful.

To my husband, Amir Fatihi who remains willing to engage with the struggle. I am truly thankful. Alfateh Ihraz, 'my little angle', I consider myself very lucky for having you in my life. I wish to thank my siblings, who have brought great joy to my life.

Finally, and by no means least, I also dedicate my thesis to all those who formally and informally gave me benefit of their interest, knowledge, views and experiences.

Mardiaty Iryani Bt. Abdullah, 2017

TABLE OF CONTENTS

Abstract	iii
Abstrak	v
Acknowledgements	vii
Table of Contents	viii
List of Figures	xii
List of Tables	xiv
List of Symbols and Abbreviations	xvi
CHAPTER 1: INTRODUCTION	1
CHAPTER 2: LITERATURE REVIEW	6
2.1 The Thyroid Gland	6
2.1.1 Embryology and anatomy	6
2.1.2 Physiology of thyroid hormones	8
2.2 Thyroid Neoplasms.....	10
2.2.1 Benign thyroid tumours.....	12
2.2.2 Malignant thyroid tumours.....	13
2.3 Papillary Thyroid Cancer.....	14
2.3.1 Aetiology of PTC	14
2.3.2 Diagnosis of PTC	15
2.3.3 Prognosis and treatment of PTC.....	16
2.3.4 Genetic alterations in PTC	17
2.3.4.1 <i>BRAF</i> oncogene and PTC.....	17
2.3.4.2 <i>RET/PTC</i> chromosomal rearrangements	18
2.3.4.3 <i>RAS</i> oncogenes and PTC	21

2.3.5	Biomarkers for PTC	22
2.3.5.1	Genome-based biomarkers	23
2.3.5.2	Proteome-based biomarkers	24
2.3.5.3	MicroRNA biomarkers	27
2.4	Malignancy among Nodular Goitre	27
2.4.1	Incidence of PTC malignancy in nodular goitre.....	31
2.4.2	Risk predictors of PTC malignancy in nodular goitre.....	32
CHAPTER 3: MATERIALS AND METHODS		33
3.1	Materials	33
3.1.1	Chemicals	33
3.1.2	Commercial kits and assays.....	35
3.1.3	Serological reagents	36
3.1.4	DNA ladder	37
3.1.5	Primers.....	37
3.2	Methods	38
3.2.1	Subjects of study	38
3.2.2	Medical history of patients	38
3.2.3	Sample preparation.....	43
3.2.3.1	Human tissue samples.....	43
3.2.3.2	Human serum samples.....	43
3.2.4	Genomics analysis	43
3.2.4.1	Tissue lysate preparation	43
3.2.4.2	Isolation of DNA	44
3.2.4.3	Total cellular RNA (tcRNA) extraction	44
3.2.4.4	Determination of yield and quality of genomic DNA and tcRNA	45

3.2.4.5	Whole-exome sequencing.....	45
3.2.4.6	Thyroid neoplasm-related genes screening	47
3.2.4.7	Characterisation of nucleotide alterations in thyroid neoplasm-related genes	50
3.2.4.8	mRNA transcript analysis.....	51
3.2.4.9	Expression analysis of <i>BRAF</i> , <i>NIS</i> , <i>TG</i> , <i>TPO</i> , and <i>TSHR</i> genes ..	56
3.2.5	Proteomic analysis.....	58
3.2.5.1	Extraction of protein from human tissue and serum samples.....	58
3.2.5.2	2-DE.....	58
3.2.5.3	Silver staining of 2-DE gels.....	60
3.2.5.4	Analysis of 2-DE gels.....	61
3.2.5.5	In-gel tryptic digestion.....	61
3.2.5.6	Q-TOF LC/MS	62
3.2.5.7	Database search	62
3.2.5.8	Functional analysis using Ingenuity Pathway Analysis software	63
3.2.5.9	Western blot.....	63
3.2.5.10	Enzyme-linked immunosorbent assay	64
3.2.5.11	Statistical analysis.....	64
CHAPTER 4: RESULTS.....		66
4.1	Genomic Studies.....	66
4.1.1	Further analyses of the nucleotide variants in thyroid neoplasm-related genes in patients with PTC and BTG	68
4.1.2	Genetic susceptibility of <i>RET</i> , <i>TG</i> , <i>TPO</i> and <i>TSHR</i> genes polymorphisms on PTC and BTG.....	78
4.1.3	Characterisation of novel variants in the individual index patients	83

4.1.3.1	<i>In silico</i> analysis of the novel non-synonymous variants in the <i>LGALS3</i> , <i>RASSF1</i> , <i>TG</i> , <i>TPO</i> , and <i>TRH</i> genes	88
4.1.3.2	The effect of the novel mutations in the <i>BRAF</i> , <i>LGALS3</i> , <i>PAX8</i> , <i>PIK3CA</i> , <i>RET</i> , <i>SLC26A4</i> , <i>TG</i> , <i>TPO</i> , and <i>TSHR</i> genes on intronic splicing.....	92
4.1.4	Further evaluation on a novel c.353G>A (p.Arg118Gln) mutation in PCP9	101
4.2	Proteomic Studies	104
4.2.1	Protein profiles of concurrent benign thyroid cyst and malignant tissues of a patient with PTC	105
4.2.1.1	2-DE tissue profiles	105
4.2.1.2	Pathway interactions and biological process analysis	107
4.2.1.3	Quantitative western blot analysis of STAT3 phosphorylation.	114
4.2.2	Proteomic analyses of patients with BTG, PTCa, and PTCb	120
4.2.2.1	2-DE tissue profiles	120
4.2.2.2	2-DE serum profiles.....	122
4.2.2.3	Analysis of tissue and serum proteins expression by ELISA	126
CHAPTER 5: DISCUSSION		130
CHAPTER 6: CONCLUSION.....		154
REFERENCES.....		156
LIST OF PUBLICATIONS.....		189
APPENDIX		193

LIST OF FIGURES

Figure 2.1: The thyroid gland.....	7
Figure 2.2: Schematic presentation of thyroid hormone synthesis in the follicular cell..	9
Figure 4.1: Single nucleotide variants (SNVs) detected in 34 out of 36 thyroid neoplasm-related genes in patients with A) PTC and B) BTG.	69
Figure 4.2: Number of insertion deletion (InDel) variants against 36 thyroid neoplasm-related genes in patients with A) PTC and B) BTG.	71
Figure 4.3: A summary of A) the number of SNVs and InDels in the 34 out of 36 thyroid neoplasm-related genes and B) patterns of SNVs and InDels in patients with PTC and BTG.....	73
Figure 4.4: A summary of A) number of nucleotide alterations in the 12 thyroid neoplasm-related genes and B) distinct profiles of nucleotide alterations in patients with PTC and BTG.....	76
Figure 4.5: A Venn diagram to illustrate nucleotide variants that were detected in patients with PTC and BTG.	77
Figure 4.6: Genetic algorithm analysis of a novel variant c.158C>A (p.Ala53Asp) of <i>LGALS3</i> gene in a patient with PTC (PCP7).	89
Figure 4.7: Genetic algorithm analysis of a novel variant c.262A>C (p.Thr88Pro) of <i>RASSF1</i> gene in a patient with BTG (BGP4).....	90
Figure 4.8: Genetic algorithm analysis of a novel variant c.5908T>C (p.Phe1970Leu) of <i>TG</i> gene in a patient with BTG (BGP4).....	91
Figure 4.9: Genetic algorithm analysis of a novel variant c.4604A>G (p.Asp1535Gly) of <i>TG</i> gene in a patient with PTC (PCP8).....	93
Figure 4.10: Genetic algorithm analysis of a novel variant c.1082G>T (p.Arg361Leu) of <i>TPO</i> gene in patients with PTC (PCP3) and those with BTG (BGP23).	94
Figure 4.11: Algorithm analysis of a novel variant c.353G>A (p.Arg118Gln) of <i>TRH</i> gene in a patient with PTC (PCP9).	95
Figure 4.12: Transcript analysis of the <i>LGALS3</i> gene in a patient with PTC, PCP5, with a novel c.19-50_53CTGdel.	100
Figure 4.13: DNA sequencing electropherograms showing the A) c.353G>A (p.Arg118Gln) mutation in exon 3 of the <i>TRH</i> gene and B) wild type allele.	102

Figure 4.14: Real time PCR analysis.	103
Figure 4.15: Representative 2-DE maps of benign thyroid cyst and PTC tissue.....	106
Figure 4.16: IPA graphical representation of the molecular relationships in A) “cancer, endocrine system disorders, organismal injury, and abnormalities” network and B) “amino acid metabolism, small molecule biochemistry, nuclei acid metabolism” network in benign cyst vs PTC tissues.....	111
Figure 4.17: Western blot and Image-J densitometric analyses.....	119
Figure 4.18: Representative 2-DE tissue protein profiles of BTG, PTCa, and PTCb patients.	121
Figure 4.19: Percentage volume contribution of 2-DE tissue proteins that were differentially expressed in patients with BTG, PTCa, and PTCb.	124
Figure 4.20: 2-DE analyses of serum proteins derived from BTG, PTCa, and PTCb patients.	125
Figure 4.21: Average percentage of volumes that were differentially expressed between BTG, PTCa, and PTCb patients.	128
Figure 4.22: ELISA analyses of tissue (panels A and B) and serum (panels C and D) proteins in BTG, PTCa, and PTCb patients.	129
Figure 5.1: RNA processing events that generate IFI27-LGALS3 chimeric mRNA of PCP5.....	137
Figure 5.2: Proposed transitional changes in A) benign thyroid cyst and B) PTC tissue in a single patient, PCP9.	147

LIST OF TABLES

Table 2.1: Physiological effects of thyroid hormones	11
Table 2.2: Characteristic features of PTC with specific genetic alterations.	19
Table 2.3: Gene expression profile in patients with PTC.	25
Table 2.4: Potential biomarkers for PTC from various sample using proteomic techniques.....	28
Table 3.1: Demographic and clinical profiles of subjects.....	39
Table 3.2: Phred quality scores	47
Table 3.3: List of genes associated with thyroid diseases.....	48
Table 3.4: Nucleotide sequence of PCR primers for mRNA transcript analysis.....	52
Table 3.5: Sequences of the primers used for quantitative real-time PCR analysis	57
Table 4.1: Type of nucleotide variants identified in the index patients.....	67
Table 4.2: Frequencies of selected SNVs genotypes and alleles in patients with PTC and BTG.....	79
Table 4.3: Summary of detected nucleotide variants of the candidate genes in patients with PTC and BTG.	84
Table 4.4: The effect of the novel mutations in the <i>BRAF</i> , <i>LGALS3</i> , <i>PAX8</i> , <i>PIK3CA</i> , <i>RET</i> , <i>SLC26A4</i> , <i>TG</i> , <i>TPO</i> , and <i>TSHR</i> genes on intronic splicing.....	96
Table 4.5: List of proteins with differential abundance identified by Q-TOF LC/MS	108
Table 4.6: Upstream regulators predicted to be regulated in different tissues using IPA software.....	115
Table 4.7: Prediction of disease or function annotation in different tissues using IPA software.....	117
Table 4.8: Involvement of the seven identified proteins in the free radical scavenging activity.....	118
Table 4.9: Identification of spots from 2-DE tissue proteins profiles using Q-TOF LC/MS.....	123

Table 4.10: List of serum proteins with differential abundance identified by Q-TOF LC/MS..... 127

University of Malaya

LIST OF SYMBOLS AND ABBREVIATIONS

2-DE	: Two-dimensional electrophoresis
A ₂₃₀	: Absorbance at 230 nm
A ₂₆₀	: Absorbance at 260 nm
A ₂₈₀	: Absorbance at 280 nm
A1AT	: Alpha-1 antitrypsin
A1B	: Alpha 1-beta glycoprotein
ACTG1	: Actin gamma 1
ADCY10	: Adenylate cyclase 10
ADORA1	: Adenosine A1 receptor
AHR	: Aryl hydrocarbon receptor
AHSG	: Alpha 2-HS glycoprotein
ALDH4	: Aldehyde dehydrogenase 4
ALDH5A1	: Aldehyde dehydrogenase 5 family member A1
ALDHA1	: Aldehyde dehydrogenase isoform 1A1
ANG1	: Angiopoietin 1
ANKRD37	: Ankyrin repeat domain 37
ANXA1	: Annexin A1
ANXA3	: Annexin A3
APEH	: Acylaminoacyl-peptide hydrolase
APOA4	: Apolipoprotein A4
APOC1	: Apolipoprotein C1
APOC3	: Apolipoprotein C3
ATG101	: Autophagy-related protein 101
ATP5B	: ATP synthase subunit beta, mitochondrial

ATP5H	: ATP synthase D chain, mitochondrial
BAX	: BCL2 associated X, apoptosis regulator
bp	: base pair
BCA	: Bicinchoninic acid
BCCIP	: BRCA2 and CDKN1A interacting protein
BCL2	: Apoptosis regulator
BGLAP	: Bone gamma-carboxyglutamic acid-containing protein
BMP2	: Bone morphogenetic protein 2
BMP5	: Bone morphogenetic protein 5
BRAF	: V-raf murine sarcoma viral oncogene homolog b
BTG	: Benign thyroid goitre
CA4	: Carbonic anhydrase 4
CALCA	: Calcitonin-related polypeptide alpha
CCDC6	: Coiled-coil domain containing 6
CCND1	: Cyclin D1
CD3	: Cluster of differentiation E
CDH1	: Cadherin 1
CDH3	: Cadherin 3
CDH16	: Cadherin 16
CDKN1A	: Cyclin-dependent kinase inhibitor 1A
cDNA	: Complementary DNA
CHAPS	: 3-[(3-cholamidopropyl)dimethylammonio]-1-propanesulfonate
CHI3L1	: Chitinase 3 like 1
CI	: 95% confidence intervals
CITED1	: Cbp/P300-interacting transactivator 1

CNKS2	: Connector enhancer of kinase suppressor of ras 2
CNN3	: Calponin 3
COMP	: Cartilage oligomeric matrix protein
CRABP1	: Cellular retinoic acid binding protein 1
CST6	: Cysteine proteinase inhibitor
CTNNB1	: Catenin Beta 1
CTSB	: Cathepsin B
CTXN1	: Cortixin 1
CYR61	: Cysteine rich angiogenic inducer 61
dbSNP	: Single Nucleotide Polymorphism database
DDA1	: DET1 and DDB1 associated 1
DEHAL1	: Iodotyrosine deiodinase
DIO1	: Deiodinase, iodothyronine type I
DIO2	: Deiodinase, iodothyronine type II
DIT	: Diodotyrosine
DLG3	: Disks large homolog 3
DMWD	: Dystrophia myotonica WD repeat-containing protein
DNA	: Deoxyribonucleic acid
DPP4	: Dipeptidyl peptidase 4
DTT	: Dithiothreitol
DTX4	: Deltex E3 ubiquitin ligase 4
DUOXs	: Dual oxidases
DUSP1	: Dual specificity protein phosphatase 1
DUSP6	: Dual specificity protein phosphatase 6
EGF	: Epidermal growth factor
ELISA	: Enzyme-linked immunosorbent assay

EMG1	: Ribosomal RNA small subunit methyltransferase NEP1
EMID1	: Emilin and multimerin domain-containing protein
EPS8	: Epidermal growth factor receptor pathway substrate 8
ERK1/2	: Extracellular signal-regulated kinase 1 and 2
FAM21A/FAM21C	: Family with sequence similarity 21, member A/C
FCGBP	: Fc fragment of IgG binding protein
FGB	: Fibrinogen beta chain
FGF	: Fibroblast growth factor
FGFR2	: Fibroblast growth factor receptor 2
FGG	: Fibrinogen gamma chain
FN1	: Fibronectin 1
FNAC	: Fine needle aspiration cytology
FOSB	: FBJ murine osteosarcoma viral oncogene homolog B
FOXA2	: Forkhead box A2
ft4	: free thyroxine
GADD153	: DNA damage inducible transcript 3
GALE	: UDP-galactose-4-epimerase
GAL3	: Galectin 3
GAPDH	: Glyceraldehyde-3-phosphate dehydrogenase
GBAS	: Glioblastoma amplified sequence
GLDC	: Glycine decarboxylase
GNAS	: Guanine nucleotide-binding protein
GNB1	: G protein subunit beta 1
GNB2	: G protein subunit beta 2
GPC1	: Glypican 1
GPR51	: G-protein coupled receptor 51

H ₂ O ₂	: Hydrogen peroxide
HBA1	: Hemoglobin subunit alpha 1
HDL	: High density lipoprotein
HGD	: Homogentisate 1,2-dioxygenase
HGFR	: Hepatocyte growth factor receptor
HIBADH	: 3-hydroxyisobutyrate dehydrogenase
HIF1	: Hypoxia-inducible factor-1
HLA-B	: Major histocompatibility complex, class I, B
HLA-DBP1	: Major histocompatibility complex, class II, DP beta 1
HMGA2	: High mobility group AT-hook 2
HP	: Haptoglobin
HPLC	: High-performance liquid chromatography
HPN	: Hepsin
HRAS	: Harvey rat sarcoma viral oncogene homolog
HSP70	: Heat shock 70 kDa
HW	: Hardy-Weinberg
I ⁻	: Iodide
ICAM1	: Intercellular adhesion molecule 1
ID1	: Inhibitor of DNA binding 1
ID3	: Inhibitor of DNA binding 3
InDel	: Insertions and deletion
IEF	: Isoelectric focusing
IGF1	: Insulin like growth factor 1
IGFBP5	: Insulin like growth factor binding protein 5
IHC	: Immunohistochemistry
IL1	: Interleukin 1

IL6	: Interleukin 6
IPA	: Ingenuity pathway analysis
IPG	: Immobilised pH gradient
IST1	: Increased sodium tolerance 1 homolog
ITPR1	: Inositol 1, 4, 5-trisphosphate receptor type 1
iTRAQ	: Isobaric tag for relative and absolute quantitation
KCNJ2	: Potassium voltage-gated channel subfamily J member 2
kDa	: Kilo dalton
KIF11	: Kinesin family member 11
KISS1R	: KISS1 receptor
KLK7	: Kallikrein related peptidase 7
KRAS	: Kirsten rat sarcoma viral oncogene homolog
KRT10	: Keratin 10
KRT19/CK19	: Keratin 19
LAMB3	: Laminin, beta 3
LC	: Liquid chromatography
LDBH	: Lactate dehydrogenase B
LGALS1	: Lectin, galactoside-binding, soluble, 1
LGALS3	: Lectin, galactoside-binding, soluble, 3
LGALS3BP	: Lectin, galactoside-binding, soluble, 3 binding protein
LGALS8	: Lectin, galactoside binding soluble 8
Lh	: Luteinising hormone
LIFR	: Leukemia inhibitory factor receptor alpha
LM-PCR	: Ligation-mediated polymerase chain reaction
LRP4	: LDL receptor related protein 4
LRRC47	: Leucine rich repeat containing 47

LYVE1	: Lymphatic vessel endothelial hyaluronan receptor 1
M	: Molar
MAFB	: MAF BZIP transcription factor B
Map	: Mitogen-activated protein
MAPK	: Mitogen-activated protein kinase
MCM3	: Minichromosome maintenance complex component 3
MET	: MET proto-oncogene, receptor tyrosine kinase
MEN1	: Multiple endocrine neoplasia type 1
miRNA	: Micro ribonucleic acid
MIT	: Monoiodotyrosine
MKP	: Kinase phosphatase 1
MKP2	: MAP kinase phosphatase 2
MLEC	: Malectin
MMP11	: Matrix metalloproteinase 11
mRNA	: Messenger ribonucleic acid
MRPL20	: Mitochondrial ribosomal protein L20
MS	: Mass spectrometry
MS/MS	: Tandem mass spectrometry
MYC	: V-myc avian myelocytomatosis viral oncogene homolog
MYO5A	: Myosin VA
NCOA4	: Nuclear receptor coactivator 4
NDUFS1	: NADH ubiquinone oxidoreductase core subunit S1
NF- κ B	: Nuclear factor-kappa B
NGEF	: Neuronal guanine nucleotide exchange factor
NGS	: Next-generation sequencing
NIS	: Sodium/iodide symporter

NKX2-1	:	NK2 homeobox 1
NMU	:	Neuromedin U
NPNT	:	Nephronectin
NRAS	:	Neuroblastoma ras viral (v-ras) oncogene homolog
NRCAM	:	Neuronal cell adhesion molecule
NRP2	:	Neuropilin 2
OTOS	:	Otospiralin
P	:	Probability
P38 MAPK	:	P38 mitogen-activated protein kinase 14
PAX8	:	Paired box 8
PDGFA	:	Platelet derived growth factor subunit A
PDI	:	Protein disulfide isomerase
PHB	:	Prohibitin
pI	:	Isoelectric points
PIK3CA	:	Phosphatidylinositol-4,5-biphosphate 3-kinase, catalytic subunit alpha
PKC	:	Protein kinase C
PKD1	:	Polycystin 1
PLAB	:	Placental bone morphogenetic protein
PPARG	:	Peroxisome proliferator-activated receptor gamma
ppm	:	parts per million
PPP2R1B	:	Protein phosphatase 2 regulatory subunit A, beta
PPP6R3	:	Protein phosphatase 6 regulatory subunit 3
PRDX	:	Peroxiredoxin
PROS1	:	Protein S alpha
PSD3	:	Pleckstrin and sec7 domain containing 3

PSMC2	: Proteasome 26S subunit, ATPase 2
PTC	: Papillary thyroid cancer
PPARA	: Peroxisome proliferator-activated receptor alpha
PTEN	: Phosphatase and tensin homolog
PTH	: Parathyroid hormone
qRT-PCR	: Quantitative real time-polymerase chain reaction
Q-TOF	: Quadrupole time-of-flight
RASSF1	: RAS accociation domain-containing protein
RASSF1A	: RAS association domain family member 1
RB1	: RB transcriptional corepressor 1
RET	: Ret proto-oncogene
RNH1	: Ribonuclease/angiogenin inhibitor 1
rpm	: revolutions per minute
RPP14	: Ribonuclease P/MRP subunit P14
RT-PCR	: Reverse transcription-polymerase chain reaction
RUNX1	: Runt-related transcription factor 1
RXRG	: Retinoid X receptor
S100A6	: S100 calcium binding protein A6
S100A13	: S100 calcium binding protein A13
SAGE	: Serial analysis of gene expression
SCEL	: Sciellin
SDC4	: Syndecan 4
SDS	: Sodium dodecyl sulphate
SDS-PAGE	: Sodium dodecyl sulphate-polyacrylamide gel electrophoresis
SELDI-TOF	: Surface enhanced laser desorption ionisation time of flight
SELENBP1	: Selenium binding protein 1

SEM	: Standard error of mean
SERPINA1	: Serpin peptidase inhibitor 1
SERPINA7	: Serpin peptidase inhibitor 7
SH3BP1	: SH3 domain binding protein 1
SHC	: Src homology 2 domain containing transforming
SLC4A4	: Solute carrier family 4 member 4
SLC5A5	: Solute carrier family 5 member 5
SLC26A4	: Pendrin
SLC34A2	: Solute carrier family 34 member 2
SNV	: Single nucleotide variation
SOX4	: SRY-box 4
STAT3	: Signal transducers and activators of transcription 3
SWATH	: Sequential window acquisition of all theoretical spectra
SYND4	: Syndecan 4
SYTL5	: Synaptotagmin like 5
T3	: Triiodothyronine
T4	: Thyroxine
TACSTD2	: Tumour-associated calcium signal transducer 2
TBG	: Thyroxine-binding globulin
TBP	: Tata-box binding protein
tcRNA	: total cellular RNA
TEMED	: N,N,N',N'-tetramethylethylenediamine
TFCP2L1	: Transcription factor CP2 like 1
TFF3	: Trefoil factor 3
TG	: Thyroglobulin
TIMP1	: Timp metalloproteinase inhibitor 1

TIMP3	: Timp metallopeptidase inhibitor 3
TM7SF4	: Transmembrane 7 superfamily member 4
TMSB4X	: Thymosin beta 4
TMSB10	: Thymosin beta 10
TNIP2	: TNFAIP3 interacting protein 2
TSSC3	: Tumour-suppressing subchromosomal transferable fragment candidate gene 3 protein
TTR	: Transthyretin
TNF- α	: Tumour necrosis factor-alpha
TP53	: Tumour protein 53
TPO	: Thyroid peroxidase
TRH	: Thyrotropin releasing hormone
TSH	: Thyroid stimulating hormone
TSHR	: Thyroid stimulating hormone receptor
TWF2	: Twinfilin actin binding protein 2
UBA5	: Ubiquitin like modifier activating enzyme 5
UBC	: Ubiquitin C
UBE2N	: Ubiquitin conjugating enzyme E2N
UBE2Q2	: Ubiquitin conjugating enzyme E2 Q2
UMMC	: University of Malaya Medical Centre
USP46	: Ubiquitin specific peptidase 46
VEGFB	: Vascular endothelial growth factor B
YKL40	: Chitinase 3 like 1
WES	: Whole-exome sequencing

Abbreviations for standard units of measurement such as length, volume, mass, temperature and concentration were omitted from the list.

LIST OF APPENDICES

- APPENDIX A : Medical Ethics Committee Approval Letter
- APPENDIX B : The distribution of per-base sequencing depth and cumulative depth distribution in target regions in target regions for A) PCP3 B) PCP5 C) PCP7 D) PCP8 and E) PCP9 patients.
- APPENDIX C : The distribution of per-base sequencing depth and cumulative depth distribution in target regions in target regions for A) BGP4 B) BGP8 C) BGP20 D) BGP23 patients.
- APPENDIX D : Summary of metrics of whole-exome sequencing (WES) in patients with papillary thyroid cancer (PTC)
- APPENDIX E : Summary of metrics of whole-exome sequencing (WES) in patients with benign thyroid goitre (BTG)
- APPENDIX F : Summary of detected nucleotide variants in exonic region of the candidate genes in PCP3
- APPENDIX G : Summary of detected nucleotide variants in intronic region of the candidate genes in PCP3
- APPENDIX H : Summary of detected nucleotide variants in exonic region of the candidate genes in PCP5
- APPENDIX I : Summary of detected nucleotide variants in intronic region of the candidate genes in PCP5
- APPENDIX J : Summary of detected nucleotide variants in exonic region of the candidate genes in PCP7
- APPENDIX K : Summary of detected nucleotide variants in intronic region of the candidate genes in PCP7
- APPENDIX L : Summary of detected nucleotide variants in exonic region of the candidate genes in PCP8
- APPENDIX M : Summary of detected nucleotide variants in intronic region of the candidate genes in PCP8
- APPENDIX N : Summary of detected nucleotide variants in exonic region of the candidate genes in PCP9
- APPENDIX O : Summary of detected nucleotide variants in intronic region of the candidate genes in PCP9
- APPENDIX P : Summary of detected nucleotide variants in exonic region of the candidate genes in BGP4
- APPENDIX Q : Summary of detected nucleotide variants in intronic region of the candidate genes in BGP4
- APPENDIX R : Summary of detected nucleotide variants in exonic region of the candidate genes in BGP8

- APPENDIX S : Summary of detected nucleotide variants in intronic region of the candidate genes in BGP8
- APPENDIX T : Summary of detected nucleotide variants in exonic region of the candidate genes in BGP20
- APPENDIX U : Summary of detected nucleotide variants in intronic region of the candidate genes in BGP20
- APPENDIX V : Summary of detected nucleotide variants in exonic region of the candidate genes in BGP23
- APPENDIX W : Summary of detected nucleotide variants in intronic region of the candidate genes in BGP23

University of Malaya

CHAPTER 1: INTRODUCTION

Papillary thyroid cancer (PTC) is one of the few cancers whose incidence is on the rise (Enewold et al., 2009; Raposo et al., 2017). It is a follicular cell-derived cancer and accounts for 80% of all thyroid malignancies (Dralle et al., 2015). Most patients with PTC are considered to be of low risk (Garas et al., 2013), with 99% survival at 20 years after surgery (Kakudo et al., 2004; Shaha, Shah, & Loree, 1997). Status of malignancy of the patients can be confirmed or nullified by a fine needle aspiration cytology (FNAC). However, approximately 10-20% of the FNAC cytopathologic diagnosis results are inconclusive (Chow, Gharib, Goellner, & van Heerden, 2001), which leads to unnecessary thyroidectomy in some of the patients (Akgül, Ocak, Göçmen, Koc, & Tez, 2010). FNAC has low predictive value on malignancy in patients with benign lesions due to the presence of multiple nodules (Luo, McManus, Chen, & Sippel, 2012). Ultrasound features, such as hypoechoic appearance, microcalcifications, irregular borders, and increased vascularity, are increasingly used to help distinguish malignancy in PTC patients with benign thyroid goitre (BTG) (Kim et al., 2008).

The emerging OMICS technologies, including genomics, epigenomics, proteomics, cytomics, metabolomics, interactomics, and bioinformatics, are being increasingly used for cancer research (Cho, 2010). There is an extreme interest in applying OMICS signatures to foster an understanding of tumour development and progression, as well as develop new cancer biomarkers for diagnosis and early detection (Mordente, Meucci, Martorana, & Silvestrini, 2015). In addition, the OMICS research has so far discovered hundreds of potential molecular players in PTC-tumorigenesis (Krause, Jessnitzer, & Fuhrer, 2009). It is also capable in distinguishing benign from malignant thyroid nodules (Finley, Arora, Zhu, Gallagher, & Fahey, 2004) and explaining the molecular events that are deregulated during tumorigenesis (Vucic et al., 2012).

In genomics, next-generation sequencing (NGS), also known as massive parallel sequencing, refers to a number of technologies capable of performing high-throughput DNA sequencing. The technology aims to simultaneously sequence multiple different short captured DNA fragments or amplicons, termed reads. The sequences of these reads are then mapped to a reference genome sequence, i.e., human genome build37 (hg19). This is followed by multistep filtering that narrows down the identified possible causing variants, against public databases such as 1000 Genome Project¹², dbSNP, and HapMap (www.hapmap.org) (Gilissen, Hoischen, Brunner, & Veltman, 2011; Shendure & Ji, 2008). Recently, an application of the NGS technology, known specifically as whole-exome sequencing (WES), has become the most widely used targeted sequencing method in cancer research (Lennon, Adalsteinsson, & Gabriel, 2016). WES targets all exons encoding proteins and non-protein coding RNAs including intronic boundary regions, which represents about 1% of the genome. It is now considered by many to be the preferred method than the genome sequencing. It is typically cheaper, quicker, and gives greater coverage of reads. This method also produces less data simplifying bioinformatics analysis and minimising the discovery of variants of uncertain significance. The application of WES technology to cancer genomics has dramatically increased the efficiency of mutation discovery. WES was first published in 2011 as having successfully identified genes associated with gastric cancer (Wang et al., 2011) and pheochromocytoma (Comino-Mendez et al., 2011).

Cancer is a complex disease caused by genetic mutations (germline or somatic) or environmental factors that drives a normal cell to a malignant phenotype (Parsa, 2012). The cells undergo metabolic and behavioural changes, leading them to proliferate in an excessive and untimely way. Low level genomic instability, resulted from genetic alterations, is a key feature of PTC (Finn et al., 2007; Ward et al., 2007). It is a major driving force for tumourigenesis that lead to an activation of thyrocyte signalling

pathways. Numerous molecular alterations have been documented in PTC for more than 20 years. Earlier studies have reported the alterations of genes, such as *BRAF*, *PAX8*, *PIK3CA*, *RAS*, *TG*, *TP53*, and *TPO* involved in thyroid neoplasm (Citterio et al., 2013; Eberhardt, Grebe, McIver, & Reddi, 2010; Garcia-Rostan et al., 2005; Howell, Hodak, & Yip, 2013; Ris-Stalpers & Bikker, 2010; F. Wang et al., 2014; Qing Zhang, Liu, Guan, Chen, & Zhu, 2016). In addition, different genetic alterations involving the axis RET-RAS-BRAF of the mitogen-activated protein kinase (MAPK) signalling pathway have been described as causal somatic changes in PTC (Landa & Robledo, 2011). Recently, the search for other genetic variants predisposing to the thyroid neoplasm have been made (Nagy & Ringel, 2015). In the present study, a similar attempt to identify nucleotide alterations in BTG patients as well as those with PTC, but using the state-of-art technique, WES, was made.

Proteomics is defined as a large-scale characterisation of the entire protein complement of the genome in complex biological samples (Chandramouli & Qian, 2009). In general, proteomics-based strategy can be used for: (1) proteome profiling, (2) comparative analysis of protein expression, (3) the localisation and identification of posttranslational protein modifications, and (4) the study of protein-protein interactions. In recent years, proteomic studies of cancer have generated many notable findings and led to the discovery of potential biomarkers (Honda et al., 2013; Sallam, 2015; Wulfschlegel, Paweletz, Steeg, Petricoin, & Liotta, 2003). One of the most frequently used laboratory techniques in proteomics is two-dimensional electrophoresis (2-DE) and mass spectrometry. The approach can be used in combination with more traditional techniques, including western blotting and affinity column chromatography. The strength of 2-DE lies in its capacity to fractionate and visualize thousands of proteins simultaneously in a single gel as well as its ability to differentiate truncated fragments from native proteins.

Over the years, many cases of PTC associated with BTG have been reported (Bombil, Bentley, Kruger, & Luvhengo, 2014; Gandolfi et al., 2004; Hanumanthappa et al., 2012; Htwe, 2012; Pang & Chen, 2007; Rahman et al., 2015; Ullah, Hafeez, Ahmad, Muahammad, & Gandapur, 2014). However, the molecular mechanisms underlying tumorigenesis of a long-standing thyroid nodule remains unclear. The relationship between gene expressions measured at mRNA level and proteins are complex. There are several reports emphasising the disparity between mRNA transcript and protein expression levels (Greenbaum, Colangelo, Williams, & Gerstein, 2003; Koussounadis, Langdon, Um, Harrison, & Smith, 2015; Varambally et al., 2005). Makki et al. (2013) has demonstrated the serum levels of ANG1, CK19, TIMP1, YKL40, and GAL3 were not significantly different between patients with benign thyroid tumour and those with PTC, although their corresponding genes in the PTC tissues have been consistently shown to be up-regulated (Baris et al., 2005; Jarzab et al., 2005). Hence, genomic analysis alone is unable to provide adequate information on the underlying tumourigenic mechanisms in PTC. With this in mind, a holistic OMICS strategies may hold promise for a better understanding of the molecular events at the gene and protein levels that underlie the development and progression of PTC. Thus, the present study was performed via multiple OMICs techniques, including WES, PCR-direct sequencing, gel-based 2-DE, which were then followed by Ingenuity Pathway analysis and western blotting.

A significant number of proteomic analyses of tissue and/or blood samples from patients with BTG and those with PTC have been previously reported (Dinets et al., 2015; Giusti et al., 2008; Moretz et al., 2008; Sofiadis et al., 2012; Srisomsap et al., 2002). Among the proteomic signatures of PTC that were previously identified include CTSB, ATP5H, PHB, LGALS1, S100A6, PRDX, and HSP70 (Brown et al., 2006; Srisomsap et al., 2002; Torres-Cabala et al., 2006). However, to date, comparative studies of the expression of proteins in the tissue and serum samples of PTC patients with and without

benign background have not been performed. This is important as the two types of PTC maybe totally unrelated, both etiologically as well as mechanistically. With this in mind, a study was also undertaken to analyse the expression of proteins in tissue and serum samples of PTC patients with and without a background of thyroid nodules relative to those with BTG via 2-DE.

Objectives of the study

The present study was performed:

1. to screen for nucleotide alterations in thyroid tissues using WES in patients with BTG and those with PTC,
2. to further characterise the novel nucleotide alterations in patients with BTG and PTC,
3. to elucidate and hypothesise molecular mechanisms underlying tumourigenesis of a long-standing thyroid nodule in a patient with concurrent BTG and PTC by performing proteomic analyses of her thyroid tissues and,
4. to analyse for differences in tissue and serum protein abundances in 2-DE profiles generated by silver staining using Image Master 2D platinum software between PTC patients with and without benign background and those with BTG.

CHAPTER 2: LITERATURE REVIEW

2.1 The Thyroid Gland

The thyroid gland was named after the shape of the thyroid cartilage which looks like a shield (Greek: thyreos = shield) (Stathatos, 2016) (Figure 2.1). The gland is situated low down in front of the neck. An adult thyroid gland generally weighs about 25 g but can increase considerably in size and weight due to pathological conditions.

2.1.1 Embryology and anatomy

Thyroid is the first glandular tissue to develop in the embryo (Blankenship, Chin, & Terris, 2005; Park & Chatterjee, 2005). The gland begins to form in the third gestational week from a median endoderm by merger of the fourth pouch of the primordial pharynx with the tongue base median line (Bursuk, 2012). As the tongue grows, the embryonic thyroid gland descends in the neck and passes ventrally to the developing laryngeal cartilages and hyoid bone (Khatawkar & Awati, 2015a). The hollowed thyroid primordium soon becomes solid and divides into right and left lobes, connected by the isthmus of the thyroid gland. By the 7th gestational week, the thyroid assumes its definitive shape and reaches its final site in the neck (Moore & Persaud, 2003).

The thyroid gland consists of two lobes, with the right lobe being normally larger than the left lobe (Khatawkar & Awati, 2015a). The two thyroid lobes are connected by the isthmus, which ties them anteriorly at the 2nd and 3rd tracheal rings. The thyroid gland is capsulated with an envelope of pretracheal fascia, which is thickened posteriorly and attached to the upper tracheal rings and cricoid cartilage (Sharma, Milas, Weber, & Carlson, 2010). The gland is rich with blood supplied from the superior and inferior thyroid arteries (Singh, 2014).

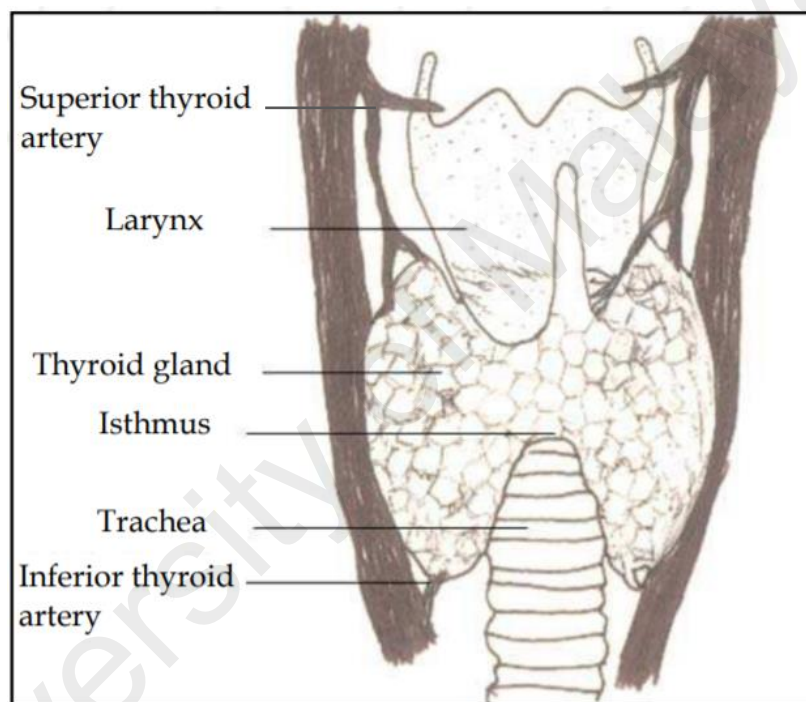


Figure 2.1: The thyroid gland (source from Bursuk, 2012)

2.1.2 Physiology of thyroid hormones

The thyroid gland, one of the largest endocrine organs in the human body, is important in regulating systemic metabolism through thyroid hormones (Bursuk, 2012). The gland consists of two distinct hormone-producing cell types, i.e., the follicular and C cells. Follicular cells comprise most of the epithelium and are dedicated to the production of thyroid hormones and for iodine uptake, while C cells are scattered parafollicular cells that are responsible for the synthesis of the calcium-regulating hormone, calcitonin.

Triiodothyronine (T3) and thyroxine (T4) are the two major thyroid hormones secreted by the follicular cells, with T3 being more active (Khatawkar & Awati, 2015a). The hormones are secreted directly into the blood stream or stored in the colloid as part of thyroglobulin (TG) until needed. Of the circulating thyroid hormones, 80% is bound to thyroxine-binding globulin, 10% to albumin and 10% to prealbumin (Seeböck, Haybaeck, & Tsybrovskyy, 2017). Biosynthesis and secretion of the thyroid hormones occur in several steps in the thyroid gland (Figure 2.2). Iodide (I^-) is initially transported from the blood stream into the thyroid cells by the sodium/iodide symporter (NIS) in the basolateral membrane and further transported into the follicular lumen by pendrin. In presence of hydrogen peroxide (H_2O_2) produced by dual oxidases (DUOXs), the tyrosine residues within TG are iodinated by the enzyme thyroid peroxidase (TPO) at the apical surface of thyrocytes forming monoiodotyrosine (MIT) and diiodotyrosine (DIT). Further coupling of DIT with MIT and DIT on TG, which is also catalysed by TPO, forms T3 and T4, respectively. When thyroid hormone is required, TG is internalised by pinocytosis and hydrolysed in the lysosome. This then leads to the release of T3 and T4 into the blood stream, as well as MIT and DIT which can be reutilised for further coupling reactions. T3 is also synthesised in the peripheral tissues by deiodination of T4.

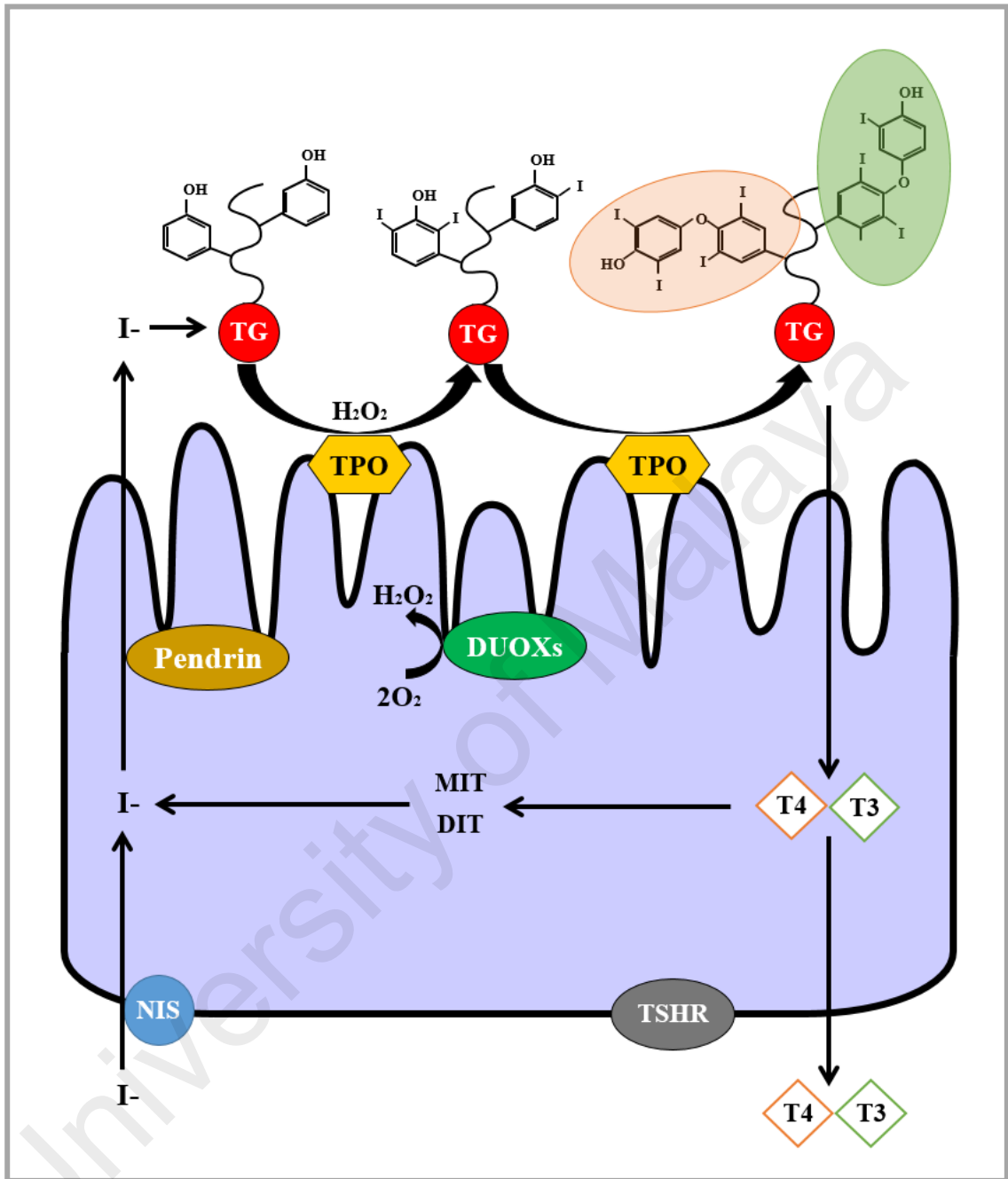


Figure 2.2: Schematic presentation of thyroid hormone synthesis in the follicular cell

[Abbreviation: DIT, Diodotyrosine; DUOXs, Dual oxidases; I, Iodine; H₂O₂, Hydrogen peroxide; O₂; Oxygen; MIT, Monoiodotyrosine; NIS, Sodium/iodide symporter; T₃, Triiodothyronine; T₄, Thyroxine; TG, Thyroglobulin; TPO, Thyroid peroxidase; TSHR, Thyroid stimulating hormone receptor].

The activity of the thyroid gland is basically controlled by the secretion of the thyroid stimulating hormone (TSH) from the pituitary gland, which in turn is under the influence of thyrotropin releasing hormone (TRH) from the hypothalamus (Mullur, Liu, & Brent, 2014). TSH is believed to stimulate growth of the follicular epithelium cells and the synthesis of thyroid hormones. The system is subjected to negative feedback control, with increased T3 inhibiting the release of TSH and TRH. T3 and T4, secreted by the thyroid gland, play an important role in the functioning of the body and the physiological effects of thyroid hormones are listed in Table 2.1. Thyroid hormones have multiple physiological functions, which can be divided into their effects on growth, metabolism and on systems (Khatawkar & Awati, 2015a).

2.2 Thyroid Neoplasms

Thyroid nodules are commonly palpable in clinical practice. They are found in 4-7% of the population by means of palpation (Brander, Viikinkoski, Nickels, & Kivisaari, 1991; Wienke, Chong, Fielding, Zou, & Mittelstaedt, 2003; Wiest et al., 1998). However, the incidence of thyroid nodules detected by ultrasonography examination can be as high as 67%, particularly in areas where iodine is not sufficiently consumed (Ezzat, Sarti, Cain, & Braunstein, 1994; Marqusee et al., 2000; Tan & Gharib, 1997).

Cancer of the thyroid gland, on the other hand, occurs in 5-10% of palpable nodules (Mazzaferri, 1992) and the overall incidence of cancer in patients selected for fine needle aspiration and cytology is slightly high, with reported detection of 9.2-13.0% cases (Hegedus, Bonnema, & Bennedbaek, 2003; Nam-Goong et al., 2004; Papini et al., 2002). Thyroid cancer is a rare malignancy. However, it is the most common form of endocrine cancer and represents 1% of all new cancer cases. The worldwide annual incidence of thyroid cancer is estimated up to 5 per 100,000 population (Constantinides & Palazzo,

Table 2.1: Physiological effects of thyroid hormones (source from Khatawkar & Awati, 2015a)

Target tissue	Effect	Mechanism
Adipose tissue	Catabolic	Stimulate lipolysis
Bone	Developmental	Promote normal growth and skeletal development
Gut	Metabolic	Increase rate of carbohydrate absorption
Heart	Chronotropic, Inotropic	Increase number of beta-adrenergic receptors Enhance response to circulating catecholamines Increase proportion of a myosin heavy chain
Lipoprotein	Metabolic	Stimulate formation of LDL receptors
Muscle	Catabolic	Increase protein breakdown
Nervous System	Developmental	Support normal brain development
Other	Calorigenic	Stimulate oxygen consumption by metabolically active tissues (except testes, uterus, lymphnodes, spleen, anterior pituitary) Increase metabolic rate

2013). In Malaysia, the population-based incidence of thyroid cancer reported by the National Cancer Registry (NCR) in 2008 was 2.8 per 100,000 population (Lim, Rampal, & Yahaya, 2008). In Kelantan, the hospital-based incidence of thyroid cancer with chronic moderate iodine deficiency was at 3.5 per 100,000 admitted patients per year (Othman, Omar, & Naing, 2009).

2.2.1 Benign thyroid tumours

The enlargement of the thyroid gland comprises a variety of conditions that can be classified as toxic or non-toxic and diffused or nodular goitre; the latter of which can be further classified as solitary thyroid nodule or multinodular goitre (Khatawkar & Awati, 2015b). Vanderpump (2011) has reported that the prevalence of solitary nodules and multinodular goitre is 3% and 1%, respectively. Recently, single and multiple thyroid nodules are found in 5.3% of women and 0.8% of men, with an increased frequency in women over 45 years of age (Medeiros-Neto, 2016). The epidemiology of goitre includes iodine deficiency, iodine excess, goitrogenic drugs and foods, as well as heavy smoking (Constantinides & Palazzo, 2013, Khatawkar & Awati, 2015b).

Thyroid nodules generally do not reflect a single disease but are clinical manifestations of a wide spectrum of thyroid diseases, ranging from hyperplastic lesions and adenomas (or carcinomas), depending on their microscopic and macroscopic histological features (Welker, 2003). They are most commonly detected in the form of benign hyperplastic lesions, which are asymptomatic (Bomeli, LeBeau, & Ferris, 2010). Nodular hyperplastic lesions that are characteristically present in benign thyroid goitre (BTG)¹ are caused by follicular cell hyperplasia at one site (termed solitary thyroid nodule) or at multiple areas

¹ The abnormal enlargement of the thyroid gland which are usually benign.

(termed multinodular goitre) within the thyroid gland (Studer & Derwahl, 1995), with the latter being more common. In Malaysia, the hospital-based incidence of nodular hyperplasia was 9.9 per 100,000 admitted patients per year (Othman et al., 2009). In some cases, hyperplastic nodules can nurture neoplastic event in the absence of external stimuli (Wang et al., 2013).

A thyroid adenoma is a benign tumour of the thyroid gland and arise from follicular cells. Follicular adenomas are further classified according to their cellular architecture and relative amounts of cellularity, which includes colloid (macrofollicular), fetal (microfollicular), Hurthle (oxyphil), and embryonal (atypical) cell types (Neki & Kazal, 2006; Zeiger & Dackiw, 2005). A follicular adenoma is a common benign neoplasm of the thyroid gland and frequently present as a single nodule.

2.2.2 Malignant thyroid tumours

Malignant thyroid tumours are classified as carcinomas based on their macroscopic and microscopic histological makeup. These abnormal growth of tissues originated from either the follicular epithelium or parafollicular cells. Thyroid cancer commonly arise from the follicular cells or thyrocytes. Clinically, thyroid cancer is normally classified into well differentiated and undifferentiated forms. While the well differentiated thyroid cancer encompass papillary and follicular carcinomas, the undifferentiated cancer comprise anaplastic carcinoma (Nguyen et al., 2015). Well differentiated thyroid cancer is generally associated with a good prognosis, with an incidence of 1 to 10 cases/100,000 people per year (Maia & Zantut-Wittmann, 2012). The calcitonin-producing parafollicular C cells of the thyroid gland gives rise to medullary thyroid carcinoma. Among all cancers of the thyroid, papillary thyroid cancer (PTC) is the most prevalent form of thyroid malignancy.

2.3 Papillary Thyroid Cancer

PTC constitutes approximately 80% of all thyroid cancer cases (Zhu et al., 2009). It is also the most prevalent thyroid cancer subtype in countries having iodine-sufficient or iodine-excess diets (Al-Salamah, Khalid, & Bismar, 2002). PTC is one of the few cancers whose incidence is on the rise (Enewold et al., 2009; Raposo et al., 2017). Possible reasons for the rising incidence of PTC remain unclear but may reflect recent improvements in the earlier detection of the cancer (Davies & Welch, 2006; Verkooijen et al., 2003).

2.3.1 Aetiology of PTC

PTC can happen at any age and has rarely been diagnosed as a congenital tumour. The incidence of PTC increases with age, and women are more frequently affected than men, in ratios of 2:1 to 4:1 (LiVolsi, 2011). Diagnosis of PTC are usually made in the third to fifth decades of the patients' life, with the mean age at 40 years.

The aetiology of PTC has evoked much interest. The only noticeably or well-established environmental factor related to the progression of PTC is a previous history of radiation exposure (Constantinides & Palazzo, 2013; Landa & Robledo, 2011). The explosion episode at the nuclear power plant in Chernobyl in April 1986 and the dropping of the atomic bomb incident in Japan in 1945 at the end of World War II have confirmed the carcinogenic effect of radiation. Others suggested risk factors include pre-existing benign thyroid disease (Smith et al., 2013) or a family history of PTC (Xu, Li, Wei, El-Naggar, & Sturgis, 2012).

2.3.2 Diagnosis of PTC

Physical examination is rarely beneficial in discriminating benign and malignant nodules, unless there is evidence of enlarged regional lymph nodes or invasion of other structures in the neck, which suggests malignancy (Mackenzie & Mortimer, 2004). The thyroid function tests, which comprise evaluation of serum TSH, free T4, and free T3, are generally not valuable in the assessment of thyroid nodules because most patients are euthyroid (Neki & Kazal, 2006).

Fine needle aspiration and cytology (FNAC) is the investigation of choice as it becomes the pivotal element in the diagnostic techniques (Maia & Zantut-Wittmann, 2012). During this procedure, the thyroid cells are classified by their cytological appearance into benign, suspicious (or indeterminate) and malignant (Constantinides & Palazzo, 2013). Aspiration smear from PTC may reveal papillary structure, but preoperative diagnosis is mainly based on the recognition of typical nuclear characteristics, such as 'Orphan Annie' nuclei intranuclear pseudoinclusions (due to cytoplasmic invaginations) and nuclear grooves (folds in the nuclear membrane) (LiVolsi, 2011; Rubin & Farber, 1994). The presence of psammoma bodies (calcium salt deposits) in a cervical lymph node forms a further evidence of PTC (Hunt & Barnes, 2003). The accuracy rate of preoperative diagnosis with FNAC is about 90% when correlated with the postoperative diagnosis of surgical specimen (Neki & Kazal, 2006).

In order to improve the diagnostic yield of FNAC, ultrasonography is usually carried out. Ultrasonography is extremely valuable in selecting appropriate nodules to aspirate within a multinodular thyroid or to select a site within a nodule (Papini et al., 2002). It can detect presence of nodules that are too small to be palpated, multiple nodules and central or lateral neck lymphadenopathy. Ultrasonography also provides precise dimensions of nodule for patient's monitoring (Bomeli et al., 2010). Ultrasound features,

such as hypoechoic appearance, microcalcifications, irregular borders, and increased vascularity, are increasingly used to help distinguish malignancy in PTC patients with benign goitre (Kim et al., 2008; Lin, 2010). Distant metastasis occurs less frequently with PTC than with other forms of thyroid malignancy (Zeiger & Dackiw, 2005). When present, the lungs and bones are most frequently involved.

2.3.3 Prognosis and treatment of PTC

Poor prognostic factors in PTC include large tumour size, older age at diagnosis, male gender and extrathyroidal growth (LiVolsi, 2011). An aggressive approach in the management and treatment of the disease may render nearly 90% of the patients cancer-free (Mazzaferri & Massoll, 2002). PTC is generally considered to be of low risk for recurrent thyroid cancer (Garas et al., 2013), with 99% survival at 20 years after surgery (Kakudo et al., 2004; Shaha et al., 1997).

Surgery is usually the first-line therapy for PTC. The extent of surgery is dependent on the size of the primary tumour and presence or absence of lymph node metastasis (Constantinides & Palazzo, 2013). In cases of malignancy with a diameter of more than 1 cm, total thyroidectomy is usually performed (Mackenzie & Mortimer, 2004). Oral administered radioiodine is usually recommended subsequent to surgery in all high-risk patients as this may destroy cancer cells in the neck. A retrospective study done by Mazzaferri (1999) showed lower recurrence rates and improved survival when the remaining thyroid tissue is ablated with radioiodine therapy.

2.3.4 Genetic alterations in PTC

Substantial molecular genetic alteration studies performed in the last two decades have given better insights in the understanding of the progression of PTC. PTC is often characterised by *RET/PTC* chromosomal rearrangements or point mutation of the *RAS* or *BRAF* proto-oncogenes, all of which are able to trigger the activation of mitogen-activated protein kinase (MAPK) cascade (Nikiforova et al., 2003; Xing, 2013). Mutations of the *BRAF*, *RAS*, or *RET* genes are found in nearly 70% of PTC cases (Nikiforova & Nikiforov, 2008). Genetic events subsequent to the mutations may further lead to other variants of PTC, i.e., classical, tall cell and follicular as well as clinico- and histopathologic features (Adeniran et al., 2006) (Table 2.2).

2.3.4.1 *BRAF* oncogene and PTC

BRAF is a member of the RAF family (A, B, and C) of serine-threonine kinases. Their activation is prompted by RAS binding and protein recruitment to the cell membrane (Nikiforov & Nikiforova, 2011). These kinases are intracellular effectors of the MAPK signalling cascade which relay the signals downstream that ultimately regulate the expression of several genes responsible for cell proliferation, differentiation, and apoptosis (Grogan, Mitmaker, & Clark, 2010).

In thyroid cancer, *BRAF* can be activated by point mutations, chromosomal rearrangement or small in-frame deletions or insertions (Nikiforov & Nikiforova, 2011). Most *BRAF* mutations are affected by a single point mutation that involves a thymine to adenine substitution at nucleotide position 1799, which results in an amino acid substitution of valine by glutamic acid at codon 600 (p.Val600Glu). The *BRAF*^{V600E} mutation in PTC has been previously described with a variable frequency ranging from 29 to 83% of cases (Xing, 2005) but has low prevalence in follicular thyroid cancer (1.4%)

(Kebebew et al., 2007). The only other *BRAF* mutation reported in thyroid tumours is the K601E mutation found in benign thyroid adenomas and the follicular variant of PTC (Soares et al., 2003; Trovisco et al., 2004).

Numerous studies have revealed that the *BRAF*^{V600E} mutation is the main genetic event in PTC, and is related with poor prognosis (Xing et al., 2005). High kinase activity of this mutant may drive genetic instability in PTC, facilitating secondary genetic alteration of members of the PI3K-AKT pathway and mediate its progression to a more aggressive cancer (Riesco-Eizaguirre & Santisteban, 2007). Vast scientific reports (Chakraborty et al., 2012; Elisei et al., 2008; Kebebew et al., 2007; Lupi et al., 2007; Yang et al., 2015), including a few meta-analyses (Lee, Lee, & Kim, 2007; Li, Lee, Schneider, & Zeiger, 2012), have acknowledged the association of this mutation with several high risk clinicopathological features, including lymph node metastases, extrathyroidal invasion, recurrence rate and advanced clinical stage. Of interest, PTC bearing *BRAF*^{V600E} mutation has been associated with the decreased expression of genes involved in thyroid hormone biosynthesis, including *NIS*, consequent treatment failure and decreased ability of tumours to trap radioiodine (Xing, 2007).

2.3.4.2 *RET/PTC* chromosomal rearrangements

The *RET/PTC* chromosomal rearrangement was first reported by Fusco et al in 1987. The proto-oncogene encodes the RET receptor, a plasma membrane bound tyrosine-kinase for ligands of the glial-derived neurotrophic factor family (Treanor, Goodman, de Sauvage, & Stone, 1996), which is expressed in the neuroendocrine and neural cells (Grogan et al., 2010). The RET protein is expressed in thyroid parafollicular or c-cells, whilst, its expression in the thyroid follicular cells remains disputable.

Table 2.2: Characteristic features of PTC with specific genetic alterations
(source from Adeniran et al., 2006)

	<i>BRAF</i>	<i>RET/PTC</i>	<i>RAS</i>
Age	Older	Younger	Average
Histopathologic variant	Classical variant Tall cell variant	Classical variant	Follicular variant
Nuclear features	Pronounced	Pronounced	Less pronounced
Psammoma bodies	Common	Very common	Rare
Extrathyroidal extension	Very common	Rare	Rare
Lymph node metastasis	Common	Very common	Rare
Tumour stage at presentation	More advance	Early	Intermediate

RET/PTC-related carcinogenesis occurs by chromosomal rearrangements, which happens when the C-terminal kinase domain of RET is linked to the promoter and N-terminal domains of unrelated gene (Fagin & Mitsiades, 2008). The rearrangement has placed *RET* under the transcriptional control of its fusion partner gene promoters (Cassol & Asa, 2011), which allows the aberrant expression of chimeric protein of the receptor in epithelial follicular thyroid cells (Nikiforov, 2002). The fusion leaves the tyrosine kinases domain of the RET receptor intact, and enables the RET/PTC chimeric oncoprotein to bind SHC protein adapter which leads to stimulation of the RAS-RAF-MAPK signalling cascade (Knauf, Kuroda, Basu, & Fagin, 2003). As a result of the rearrangement, the MAPK pathway turns out to be unrestrained and chronic (Grogan et al., 2010). It has been suggested that the rearrangement also deletes the signal sequence, the intracellular juxta membrane domains of the receptor and the extracellular ligand-binding domain, preventing it from interacting with its negative regulators, as well as re-locating the RET/PTC protein to the cytosolic compartment (Cassol & Asa, 2011).

At least 11 forms of *RET/PTC* have been described so far, and these vary according to the different fusion of genetic partners (Bongarzone et al., 1993; Ciampi & Nikiforov, 2007; Nakata et al., 1999; Nikiforov, 2002, 2008; Pierotti et al., 1993; Saenko et al., 2003; Tallini, Asa, & Fuller, 2001). Indeed, these mutations are almost exclusively found in PTC (Grogan et al., 2010). The *RET/PTC1* and *RET/PTC3* rearrangements are the most common *RET* fusion (Grogan et al., 2010; Kitamura et al., 1999), accounting together for more than 90% of all the rearrangements (Greco, Miranda, Borrello, & Pierotti, 2014). Both *RET/PTC1* and *RET/PTC3* oncogenes are created by a paracentric, intrachromosomal inversion of chromosome 10q, in which *RET* is fused to the activating genes, *CCDC6* (also known as *H4*) and *NCOA4* (also known as *ELE1* or *RFG*), respectively (Cassol & Asa, 2011). Ten separate genes located on different chromosomes (intrachromosomal rearrangements) are known to arrange with the *RET* gene, with less

frequent *RET/PTC* being produced by interchromosomal rearrangements (Greco et al., 2014).

RET/PTC rearrangements are particularly common in paediatric PTC cases and those involving radiation exposure, both from nuclear accidents, such as Chernobyl and from exposure to external beam radiation therapy (Grogan et al., 2010; Nikiforov, Rowland, Bove, Monforte-Munoz, & Fagin, 1997). In post-Chernobyl paediatric tumours *RET/PTC1* was found to be associated with classical variant of PTC, whilst, *RET/PTC3* present more commonly in solid-variant (Nikiforov et al., 1997). Indeed, medical importance of *RET/PTC* rearrangements have also been documented at a high frequency in papillary microcarcinomas, suggesting that they are an early event in carcinogenesis of PTC (Viglietto et al., 1995). In addition, introduction of *RET/PTC1* into transgenic mice has also been shown to cause a PTC-liked morphological changes (Jhiang et al., 1996).

2.3.4.3 RAS oncogenes and PTC

RAS is a small GTPase that is upstream of BRAF. Isoforms of RAS mutant play a distinct role in activating the PI3K-AKT and MAPK pathways. The KRAS is a preferential activator of the MAP kinase pathway, whereas NRAS mutant is a preferential activator of the PI3K-AKT pathway in human cancer (Haigis et al., 2008). Genetic alteration of *RAS* and *BRAF* genes are mutually exclusive in differentiated PTC, suggesting that, like *BRAF* mutation, *RAS* mutant is also capable of cause PTC independently through the MAPK signalling pathway (Brehar, Brehar, Bulgar, & Dumitrache, 2013). The active RAS proteins cause constitutive activation of downstream effector pathways that ultimately resulted in aberrant cell proliferation and differentiation.

RAS mutations were first documented in thyroid carcinomas in 1988 (Lemoine et al., 1988). Three members of the *RAS* gene family (H, N, and K) have been shown to be mutated in thyroid cancer and generally, up to 30% of human tumours are presented with *RAS* mutations (Grogan et al., 2010). The most common *RAS* mutations are found in the *NRAS* gene, followed by *HRAS*, and least frequently, *KRAS*. *RAS* mutations are found in a wide variety of thyroid tumours including follicular adenomas, follicular carcinomas, poorly differentiated carcinomas, undifferentiated carcinomas as well as papillary carcinomas. They are more frequently related to follicular tumours than PTC (Cassol & Asa, 2011). Point mutations in the *RAS* genes typically occur in codons 12, 13, and 61. The most frequent mutations lie in codon 61 of *NRAS* and to a lesser extent in *HRAS* (Fagin & Mitsiades, 2008). *RAS* mutations have been described to alter GTP-binding affinity or intrinsic GTPase activity (Cassol & Asa, 2011).

2.3.5 Biomarkers for PTC

Biomarkers, also known as biological or molecular markers, are important parameters as they provide information about the physiological changes during development and progression of diseases (Miles, Matharoo-Ball, Li, Ahmad, & Rees, 2006). In cancer, Malati (2007) has characterised useful biomarkers as those (1) that are highly specific and sensitive, (2) that have high positive and negative predictive values that are 100% accurate in distinguishing between healthy individuals and tumour patients, (4) that are capable to discriminate between neoplastic and non-neoplastic diseases, (5) that are able to predict early recurrence and have prognostic value, (6) that are clinically sensitive, with levels preceding the neoplastic process, (7) that are either specific to one type of cancer or able to universally detect all types of cancers, and last but certainly not least, (8) that are easily assayable. Recent advances in genomics and proteomics hold great potential

in biomarker discovery in thyroid cancer. In PTC, biomarkers are not only required for its early detection, but also for detecting its recurrence and persistence, and for predicting the efficiency of surgical removal of thyroid tissues, radioiodine ablation, and chemotherapy (Srinivas, Kramer, & Srivastava, 2001).

2.3.5.1 Genome-based biomarkers

Many different gene expression profiling technologies are currently in use including SAGE, oligonucleotide arrays and cDNA microarrays (Griffith, Melck, Jones, & Wiseman, 2006; Grogan et al., 2010). These technologies allow the simultaneous comparison on the expression of thousands of genes related to various diseases (Grogan et al., 2010). Changes in the patterns of gene expression in thyroid cancer are associated with the different mutations that contribute to thyroid cell carcinogenesis (Rusinek, Szpak-Ulczoł, & Jarzab, 2011). It later provides a better insight on the molecular consequences during development and progression of thyroid cancer (Griffith et al., 2006; Mazzanti et al., 2004).

Significant differences in gene expression between PTC and normal/benign thyroid tissues can be used as signature biomarkers of the cancer (Fujarewicz et al., 2007; Griffith et al., 2006; Jarzab et al., 2005). The first gene expression study in PTC has identified a gene signature that consisted of more than 220 differentially expressed genes that can discriminate the cancer from normal tissues (Huang et al., 2001). In addition, a DNA microarray analysis of PTC has also identified genetic signatures that specifically correlate mutations in *BRAF*, *RAS*, and *RET/PTC* (Giordano et al., 2005). Other genetic signatures of PTC previously identified include *FNI*, *KRT19*, *LGALS3*, *MET*, and *SERPINA1*, as well as under-expression of thyroid function-related proteins, *TPO* and *DIO1*, and the fatty acid metabolism related protein, *CRABP1* (Table 2.3).

2.3.5.2 Proteome-based biomarkers

Various proteomic techniques have been increasingly applied in the search for new diagnostic and prognostic markers in cancers (Lu et al., 2007; Steinert et al., 2002). The commonly used laboratory proteomics techniques applied in the study of PTC include two-dimensional electrophoresis (2-DE) and mass spectrometry (Table 2.3). The techniques are usually used in combination with more conventional procedures, including northern and western blotting. For a more quantitative determination of protein amounts, enzyme-linked immunosorbent assay (ELISA) is a method of choice. These techniques have been performed to identify aberrantly expressed proteins between normal and diseased conditions and between different diseased states.

By using gel based-approaches, Srisomsap et al. (2002) have demonstrated increased tissue expression of ATP5H and PHB in a group of patients with PTC, whilst Brown et al. (2006) noted differentially expressed S100A6, PRDX2, and HSP70. Fan et al. (2009) explored the serum protein profiles of patients with PTC using surface-enhanced laser desorption/ionization time-of-flight mass spectrometry (SELDI-TOF-MS) and confirmed valuable biomarkers for thyroid diagnosis. Recently, state-of-the-art proteomic techniques such as sequential window acquisition of all theoretical spectra mass spectrometry (SWATH-MS) and isobaric tag for relative and absolute quantitation (iTRAQ) have also been used to identify proteins of altered abundance in tissues of patients with PTC which can be used to discriminate the cancer from controls and follicular thyroid cancer (Martínez-Aguilar et al., 2016).

Table 2.3: Gene expression profile in patients with PTC

First Author	Sample analysed	Differentially expressed genes
Huang et al. (2001)	8 PTCs and matched normal	<p>↑ <i>CITED1, CHI3L1, SCEL, MET, LGALS3, KRT19, CST6, DUSP6, TSSC3, TIMP1, SERPINA1, PROS1, SFPTB</i></p> <p>↓ <i>MT1G, DIO1, DIO2, TPO, BCL2; DUSP1, FOSB, CRABP1</i></p>
Wasenius et al. (2003)	18 PTCs and 3 normal	<p>↑ <i>MET, MMP 11, PLAB, FN1, HIF1, HLA-DBP1, AHR, TIMP1,</i></p> <p>↓ <i>GADD153, PKD1, CYR61, HBA1, DLG3</i></p>
Hawthorn et al. (2004)	8 PTCs, 6 HNs, and matched normal	<p>↑ <i>TIMP1, GPR51, LGALS3, SERPINA1, TSSC3, IGFBP5</i></p> <p>↓ <i>TFF3, CRABP1, FCGBP, TPO, ID1, RB1</i></p>
Finley et al. (2004)	14 PTCs and 21 benign lesions	<p>↑ <i>TACSTD2, AHR, MKP2, FN1, KRT19, HGFR, LGALS3, Cathepsin C, SERPINA1, SYND4, EPS8, NRP2, ALDH4</i></p>
Yano et al. (2004)	7 PTCs and matched normal	<p>↑ <i>CCND1, FGF, VEGFB, BMP5, FGFR2, IGF1, CDH1</i></p> <p>↓ <i>TPO, NIS, TSHR</i></p>
Zhao et al. (2006)	16 PTCs, 13 FTCs, and 17 normal	<p>↑ <i>GPC1, TMSB4X, Cathepsin H, SERPINA1, CNN3, MET, LGALS3, HLA-B,</i></p> <p>↓ <i>PAX8, TG</i></p>
Fujarewicz et al. (2007)	57 PTCs, 61 benign lesions, and 62 normal	<p>↑ <i>MET, FN1, ADORA1, HMGA2, DTX4, TACSTD2, AHR, RXRG, SDC4, KRT19, ICAM1,</i></p> <p>↓ <i>DIO1, BCL2, TPO, MT1G, EMID1, CDH16, ITPR1, HGD, CA4, ID3</i></p>

Table 2.3, continued

First Author	Sample analysed	Differentially expressed genes
Murphy, Chen, and Clark (2008)	9 PTCs and 11 normal	↑ <i>CDH3, SYTL5, LRP4, CHI3L1, SCEL, NMU, SOX4, BAX, RUNX1, LGALS3, KRT19, PLAB</i>
Kim et al. (2010)	35 PTCs and matched normal	↑ <i>SLC34A2, TM7SF4, COMP, KLK7, KCNJ2, SERPINA1</i> ↓ <i>FOXA2, SLC4A4, LYVE-1, OTOS, TFCP2L1</i>
Vierlinger et al. (2011)	PTCs and nodular goitre	↑ <i>SERPINA1, KRT19, CITED1, CDH3, DPP4, TIMP1, PROS1, LAMB3</i> ↓ <i>TFF3</i>
Chung, Kim, and Kim (2012)	19 PTCs and 7 normal	↑ <i>CDH3, NGEF, PROS1, MET, CTXN1, SDC4, HPN, NRCAM, PSD3, GALE, SCEL</i> ↓ <i>LIFR, MAFB, BMP2, ANKRD37</i>

Modified from Cassol & Asa (2011)

2.3.5.3 MicroRNA biomarkers

MicroRNAs (miRNAs) belong to a class of noncoding small RNAs that are approximately 22 nucleotides in length. They have a key role in post-transcriptional gene regulation that mediates the translation and degradation of mRNA (Bartels & Tsongalis, 2009). There are two main ways in which miRNAs can contribute to cancer development (Suresh, Sethi, Ali, Giorgadze, & Sarkar, 2015). The first way is the downregulation of miRNAs which could lead to the increase expression of oncogenes. Alternatively, miRNAs upregulation could result in the silencing of tumour suppressor genes. Concentrations of different miRNAs have been linked with the metastatic and invasive potential of specific malignancies (de la Chapelle & Jazdzewski, 2011).

Several studies have confirmed that miR-146b, miR-221 and miR-222 were consistently found to be overexpressed in PTC compared to those expressed in normal thyroid tissues (He et al., 2005; Lee, Gundara, Glover, Serpell, & Sidhu, 2014; Pallante et al., 2006; Suresh, Sethi, Ali, Giorgadze, & Sarkar, 2015; Tetzlaff et al., 2007; Visone et al., 2007). These miRNAs were apparently associated with extrathyroidal extension, recurrence, lymph node or distant metastasis and *BRAF*^{V600E} mutation (Lee et al., 2014). Other commonly reported over-expressed miRNAs include miR-181b and miR-155.

2.4 Malignancy among Nodular Goitre

There has been disagreement in the literature about the possibility of thyroid cancer in patients with multiple thyroid nodules as well as those with toxic nodular goitres and Graves' disease. Early studies has suggested that patients with multiple thyroid nodules carry a lower risk of thyroid cancer than patients with only a single thyroid nodule (Barroeta et al., 2006). However, this view is no longer tenable and numerous studies

Table 2.4: Potential biomarkers for PTC from various sample using proteomic techniques

Researchers	Sample of origin	Comparison	Potential Biomarker	Regulation	Technique
Srisomsap et al. (2002)	Tissue	PTC, FTC, benign, and normal tissues	CTSB, ATP5H, and PHB	Increased	2-DE
Brown et al. (2006)	Tissue	PTC and normal tissues	S100A6, PRDX, and HSP70	Increased	2-D DIGE, MALDI-TOF MS, and IHC
Torres-Cabala et al. (2006)	Tissue and FNAC	PTC and benign tissues	LGALS1 and LGALS3	Increased	2-DE, LC-MS, and IHC
Wang et al. (2006)	Serum	PTC and healthy control	Serum expression patterns allowing discrimination between: 1) PTC vs. healthy; 2) PTC vs. benign nodes; 3) different stages of PTC; 4) different pathological types of thyroid cancer	-	SELDI-TOF MS
Laura Giusti et al. (2008)	FNAC	PTC and benign tissues	TTR, A1AT, GAPDH, LDH-B, APOA1, ANXA1, cofilin-1, and PRDX1	Increased	2-DE, MALDI-TOF MS, and Western blotting

Table 2.4, continued

Researchers	Sample of origin	Comparison	Potential Biomarker	Regulation	Technique
Moretz et al. (2008)	Serum	PTC, benign, and healthy controls	Serum expression pattern allowing discrimination between PTC vs. benign nodules	-	SELDI-TOF-MS
Fan et al. (2009)	Serum	PTC and healthy controls	APOC1 and APOC3	Decreased	SELDI-TOF-MS and ProteinChip immunoassays
Jung et al. (2010)	Tissue	PTC and normal tissues	ANXA3	Decreased	2-DE, MALDI-TOF-MS, Western blotting, Northern blotting and IHC
Sofiadis et al. (2010)	Tissue	PTC, FTC, and normal tissues	S100A6	Increased	SELDI-TOF-MS, Western blotting, and IHC
Ban et al. (2012)	Tissue	PTC and normal tissues	NPNT and MLEC	Increased	LC-MS/MS, semiquantitative RT-PCR, and IHC
Ciregia et al. (2013)	FNAC	PTC and benign tissues	Moesin and ANXA1	Increased	ELISA and Western blotting
Makki et al. (2013)	Serum	PTC and benign tissues	YKL40, GAL3, CK19, TIMP1, and ANG1	Increased	ELISA

Table 2.4, continued

Researchers	Sample of origin	Comparison	Potential Biomarker	Regulation	Technique
Ryu, Bang, Lee, Choi, and Jung (2013)	Tissue	PTC and adjacent normal tissues	Phosphatidylcholines, Sphingomyelin, and Phosphatidylinositols Lysophosphatidylcholine and Lysophosphatidylserine	Increased Decreased	MALDI-MS
Dinets et al. (2015)	Cyst fluid	PTC and benign tissues	CK19 and S100A13	Increased	LC-MS/MS, Western blotting, IHC, and ELISA
Martínez-Aguilar, Clifton-Bligh, and Molloy (2016)	Tissue	PTC, FTC, and normal tissues	ANXA1, TMSB10, GAL3, CK19, ICAM1, GALE, CRABP1, FN1, and S100A6 TPO and DEHAL1	Increased Decreased	SWATH-MS, iTRAQ-MS, and Western blotting

have reported a significant risk in the patients (McCall, Jarosz, Lawrence, & Paloyan, 1986; Miccoli et al., 2006; Pradhan, Shrestha, Shrestha, Neupane, & Bhattachan, 2011; Smith et al., 2013; Wang et al., 2013). PTC is apparently the most common variety of thyroid malignancy that was detected in patients with BTG (Gandolfi et al., 2004; Hanumanthappa et al.; Othman et al., 2009; Pelizzo, Toniato, Piotto, & Bernante, 1996; Rahman et al., 2015; Ullah et al., 2014). It is believed that the prognosis of incidental PTC is good (Wang et al., 2013). The incidence of recurrence in 317 patients who had such cases and underwent treatment was low and none of them died of cancer (Ito et al., 2007).

2.4.1 Incidence of PTC malignancy in nodular goitre

Having a background of multinodular goitre is apparently common amongst patients with thyroid cancer (Gandolfi et al., 2004; Htwe, 2012; Lin, 2010; Pang & Chen, 2007; Rahman et al., 2015). The risk of PTC in multinodular goitre is reported to vary from as low as 6% to as high as 21.2% (Bombil et al., 2014; Hanumanthappa et al.; Pang & Chen, 2007; Ullah et al., 2014). Earlier study by Alevizaki et al. (2009) has demonstrated that more than 50% of PTC were incidentally detected in elderly patients operated for pre-existing multinodular goitre. Variation in the frequencies of thyroid cancer in Graves' disease has also been observed, with 0.4% to 12.0% of the patients having PTC (Erbil et al., 2008; Gerenova, Buyschaert, De Burbure, & Daumerie, 2003; Kraimps et al., 2000). In Kelantan, a large scale study involving 1,486 patients has demonstrated that 60% of patients who were diagnosed with thyroid cancer from years 1994 to 2004 had pre-existing nodular hyperplasia (Othman et al., 2009). In addition, Ito et al. (2007) reported 317 cases of incidental PTC that were accompanied by nodular goitre (50%), hyperthyroidism (34%), adenoma (14%) and Hashimoto's disease (2%).

2.4.2 Risk predictors of PTC malignancy in nodular goitre

There is considerable variation among published risk factors for PTC malignancy in patients with benign goitre. Earlier studies comparing patients with solitary thyroid nodule with those with multiple nodular goitre showed no difference in cancer prevalence (Belfiore et al., 1992; McCall et al., 1986; Miccoli et al., 2006). However, epidemiological survey of 838 patients with multinodular goitre performed by Luo et al. (2012) showed younger age, male sex, fewer nodules, and smaller nodule size to be predictors of incidental thyroid cancer. Similar findings on higher risk of malignancy among young males with thyroid nodules has also been independently reported (Rago et al., 2010; Smith et al., 2013). On the contrary, Wang et al. (2013) reported that the female gender and multiple lesions appeared to show higher risk of malignancy, although the risk for smaller nodule size (average diameter was 4 mm) was similarly high. The data of Bombil et al. (2014) on 166 cases of PTC patients with concomitant multinodular goitre further adds to the controversy when older age (mean age was 46 years) as well as the female gender were associated with higher risk for malignancy.

CHAPTER 3: MATERIALS AND METHODS

3.1 Materials

All materials used in the course of this project and their respective manufacturers are as listed.

3.1.1 Chemicals

i. *AppliChem, Darmstadt, Germany*

Triton X-100

ii. *GE Healthcare Life Sciences, Uppsala, Sweden*

Acrylamide (MW: 71.08 g/mol)

Amberlite® XAD4

Bromophenol blue (MW: 669.99 g/mol)

Dithiothreitol (DTT)

Drystrip cover fluid

Glycerol 87% (MW: 92.09 g/mol)

Glycine (MW: 75.07 g/mol)

Immobiline pH gradient (IPG) strips, pH 4-7, 11 and 13 cm

IPG buffer, pH 4-7

N, N'-methylene-bis-acrylamide (MW: 154.17 g/mol)

Urea (MW: 60.06 g/mol)

iii. *J. Kollin Chemicals, UK*

Ethanol (MW: 46.07 g/mol)

- iv. *JT Baker*[®], Philadelphia, USA
Acetic acid (MW: 60.05 g/mol)
- v. *Merck, Darmstadt, Germany*
Acetonitrile (MW: 41.05 g/mol)
Ammonium bicarbonate (MW: 79.06 g/mol)
Ethidium bromide
Formic acid 98-100%
Glacial acetic acid 100%
Glycine
Iodoacetamide (MW: 185.00 g/mol)
Isopropanol (MW: 60.10 g/mol)
Silver nitrate (MW: 169.88 g/mol)
Sodium acetate trihydrate (MW: 36.08 g/mol)
Sodium bicarbonate (MW: 84.01 g/mol)
Sodium carbonate (MW: 58.44 g/mol)
- vi. *MP Biomedicals, Ohio, USA*
DNase, RNase-free water
- vii. *Promega, Madison, USA*
Trypsin Gold, MS grade
- viii. *Sigma-Aldrich Chemical Company, St. Louis, USA*
Agarose
EDTA-disodium salt dehydrate (MW: 372.24 g/mol)

Formaldehyde 37%

Glutaraldehyde

N, N, N', N'-Tetramethyl-ethylenediamine (MW: 116.21 g/mol)

Orange G

Sodium acetate (MW: 82.03 g/mol)

Sodium thiosulfate (MW: 158.11 g/mol)

Thiourea (MW: 76.12 g/mol)

Trizma[®] base (MW: 121.14 g/mol)

UltraPure[™] Phenol-Chloroform-Isoamyl Alcohol

ix. *Thermo Fisher Scientific, Rockford, USA*

3-[(3-Cholamidopropyl) dimethylammonio]-1-propanesulfonate hydrate

(CHAPS) (MW: 614.88 g/mol)

Potassium ferricyanide (MW: 329.26 g/mol)

Sodium dodecyl sulphate (SDS) (MW: 288.38 g/mol)

2-mercaptoethanol 99% (MW: 78.13 g/mol)

x. *Vivantis, California, USA*

Agarose, Molecular grade

3.1.2 Commercial kits and assays

i. *Abcam[®], Cambridge, UK*

Human alpha-1 antitrypsin ELISA kit

Human alpha 2-HS glycoprotein ELISA kit

ii. *Applied Biosystems, California, USA*

High Capacity RNA-to-cDNA kit
2X Fast SYBR[®] Green Master Mix

iii. *Bioassay Technology Laboratory, Shanghai, China*

ELISA kit for HSP70 (E3015Hu)

iv. *Bioline, Taunton, USA*

MyTaq Red Mix kit

v. *Covaris, Massachusetts, USA*

NGS kit

vi. *Qiagen, Hilden, Germany*

Allprep[®] DNA/RNA/Protein Mini kit

Allprotect[®] Tissue Reagent

RNase-Free DNase set

MinElute[®] Gel Extraction kit

QIAquick[®] PCR purification kit

vi. *Thermo Fisher Scientific, Rockford, USA*

Pierce BCA protein assay kit

WesternDot[™] 625 Western blot kit

3.1.3 Serological reagents

i. *Abcam[®], Cambridge, UK*

Rabbit monoclonal EP2147Y primary antibody

Rabbit polyclonal beta-actin antibody

3.1.4 DNA ladder

- i. *Fermentas Life Sciences, Massachusetts, USA*

Gene Ruler™ DNA Ladder Mix

3.1.5 Primers

- i. *AITbiotech, Pandan Crescent, Singapore*

Forward and reverse oligonucleotides for *BRAF*, *KRT10*, *LGALS3*, *NIS*, *PAX8*, *PIK3CA*, *RET*, *SLC26A4*, *TG*, *TPO*, *TRH*, *TSHR*, *TBP*, and *TSHR* genes

University of Malaysia

3.2 Methods

3.2.1 Subjects of study

A cohort of 34 unrelated patients who attended Surgery Clinic at the University of Malaya Medical Centre (UMMC), Kuala Lumpur and underwent either partial or total thyroidectomy were recruited for this study. Informed written consent was obtained from patients with papillary thyroid cancer (PTC) without any history of benign thyroid goitre (BTG) (n = 8) termed PTCa, PTC patients with a background of BTG (n = 6) termed PTCb, and those with BTG (n = 20), prior to collection of samples. Thyroid tissues were classified according to conventional histopathological criteria, as defined by World Health Organisation (WHO). The study was conducted according to the declaration of Helsinki and approval was granted by the Medical Ethics Committee of UMMC (Ref. Numb.925.8; Appendix A).

3.2.2 Medical history of patients

Table 3.1 demonstrates a profile summary of the 34 patients involved in the present study. Among these patients, nine (PCPs 3, 5, 7, 8, and 9, and BGPs 4, 8, 20, and 23) were selected for whole-exome sequencing (WES) and mutational analyses. In the second part of the present study, the thyroid tissues of one of the patients (i.e., PCP9) who had concurrent PTC (left lobe) and benign thyroid cyst² (right lobe) was subjected to proteomics as well as Ingenuity Pathway Analysis (IPA). In the final part of the study, the tissues and serum samples of all 34 patients were analysed using 2-dimensional gel electrophoresis (2-DE) and mass spectrometry.

² A noncancerous sac-like structure typically filled with liquid, semisolid, or gaseous material.

Table 3.1: Demographic and clinical profiles of subjects

Patient	Gender	Race	Age (years)	TSH ^a (mU/L)	fT4 ^b (pmol/L)	Thyroid gland status	Others
A) Patients without a background of benign thyroid goitre (PTCa)							
PCP1	Male	Indian	38	1.42	14.4	Euthyroid	Unifocal
PCP2	Female	Indian	76	1.47	13.7	Euthyroid	Unifocal
PCP3	Male	Malay	49	1.35	16.7	Euthyroid	Multifocal
PCP4	Male	Malay	60	4.63	16.7	Euthyroid	Unifocal
PCP5	Female	Malay	26	2.20	19.2	Euthyroid	Unifocal
PCP6	Female	Malay	50	0.41	17.9	Subclinical hypothyroid	Unifocal
PCP7	Female	Malay	22	2.04	14.8	Euthyroid	Unifocal
PCP11	Female	Malay	48	1.46	15.5	Euthyroid	Unifocal
B) Patients with a background of benign thyroid goitre (PTCb)							
PCP8	Male	Malay	51	1.98	17.4	Euthyroid	Unifocal
PCP9	Female	Malay	53	2.65	14.9	Euthyroid	Unifocal

Table 3.1, continued

Patient	Gender	Race	Age (years)	TSH^a (mU/L)	ft4^b (pmol/L)	Thyroid gland status	Others
PCP10	Male	Malay	35	1.10	17.9	Euthyroid	Unifocal
PCP13	Female	Indian	41	0.02	12.8	Subclinical hyperthyroid	Unifocal
PCP15	Female	Malay	36	2.50	14.5	Euthyroid	Unifocal
PCP16	Female	Malay	23	3.7	17.3	Euthyroid	Unifocal
C) Benign thyroid goitre (BTG)							
BGP1	Female	Chinese	72	1.12	16.5	Euthyroid	Multinodular
BGP2	Female	Indian	41	0.76	14.1	Euthyroid	Multinodular
BGP4	Female	Malay	42	0.59	18.2	Euthyroid	Multinodular
BGP5	Female	Chinese	66	0.12	14.3	Subclinical hyperthyroid	Multinodular
BGP6	Female	Malay	53	2.51	14.1	Euthyroid	Multinodular
BGP8	Female	Malay	60	1.15	18.5	Euthyroid	Multinodular
BGP9	Female	Indian	47	0.01	17.0	Euthyroid	Multinodular

Table 3.1, continued

Patient	Gender	Race	Age (years)	TSH^a (mU/L)	ft4^b (pmol/L)	Thyroid gland status	Others
BGP10	Female	Indian	40	1.74	13.6	Euthyroid	Multinodular
BGP11	Male	Chinese	47	0.85	18.4	Euthyroid	Multinodular
BGP12	Male	Chinese	50	<0.01	13.8	Subclinical hyperthyroid	Multinodular
BGP13	Female	Indian	36	5.2	13.5	Euthyroid	Multinodular
BGP14	Female	Indian	58	0.52	18.0	Subclinical hyperthyroid	Multinodular
BGP15	Female	Chinese	61	0.17	18.3	Subclinical hyperthyroid	Multinodular
BGP17	Female	Chinese	42	1.87	15.1	Euthyroid	Multinodular
BGP20	Female	Malay	68	0.44	17.1	Euthyroid	Multinodular
BGP21	Female	Malay	56	1.41	19.0	Euthyroid	Multinodular
BGP22	Female	Chinese	68	1.03	14.8	Euthyroid	Multinodular
BGP23	Male	Malay	63	0.37	16.0	Subclinical hyperthyroid	Multinodular
BGP24	Female	Indian	64	0.22	19.5	Euthyroid	Multinodular

Table 3.1, continued

Patient	Gender	Race	Age (years)	TSH^a (mU/L)	fT4^b (pmol/L)	Thyroid gland status	Others
BGP34	Male	Indian	51	1.01	17.1	Euthyroid	Multinodular

a) Serum TSH values of 0.55-4.78 mU/L is considered normal.

b) Serum fT4 values of 11.5-22.7 pmol/L is considered normal.

3.2.3 Sample preparation

3.2.3.1 Human tissue samples

Tissue specimens were collected from surgically removed thyroid lobes of patients who had been subjected to either partial or total thyroidectomy. Immediately after excision, samples were immersed in Allprotect[®] tissue reagent (Qiagen, Hilden, Germany) for a day at 4°C and subsequently stored at -80°C until they were tested and analysed.

3.2.3.2 Human serum samples

Six ml of pre-operative blood samples were obtained from peripheral venous puncture and collected into plain tubes without any anticoagulant. Within an hour of collection, the blood samples were immediately centrifuged at 3,000 x g for 15 minutes at 4°C. The sera in the upper layer were stored in aliquots at -80°C for future analysis.

3.2.4 Genomics analysis

3.2.4.1 Tissue lysate preparation

Frozen thyroid tissues at approximately 30 mg of weight were excised with a clean, sterile sharp scalpel. The samples were homogenised using TissueRuptor (Qiagen, Hilden, Germany) in 600 µl of RLT buffer (also known as guanidine-thiocyanate (GITC)-containing buffer) in the presence of β-mercaptoethanol.

3.2.4.2 Isolation of DNA

Homogenised tissue lysate was pipetted into a microcentrifuge tube and mixed with 800 µl of phenol-chloroform-isoamyl alcohol (25:24:1, v/v) solution. The mixture was briefly mixed by inversion until an emulsion was formed. The tube was spun for 15 minutes at 4°C at a speed of 13,000 x g. The aqueous upper phase was carefully transferred into another microcentrifuge tube. Eight hundred µl of 100% (v/v) ethanol was then added into the tube in the presence of 3 M sodium acetate (pH 5.2). The sample was spun for 15 minutes at 4°C at 13,000 x g. Supernatant was carefully discarded and the pellet was washed with 400 µl of 70% (v/v) ethanol. The tube was then centrifuged at 13,000 x g at 4°C for 15 minutes. The nucleic acid pellet was air-dried to evaporate any residual ethanol and finally reconstituted in 30 µl RNase-free water.

Total genomic DNA was further purified using the AllPrep® DNA/RNA/Protein Mini Kit (Qiagen, Hilden, Germany) according to the manufacturer's instruction with some modifications. Briefly, 500 µl of RLT buffer was added into the nucleic acid mixtures. The samples were loaded into DNA spin columns and centrifuged at 17,000 x g for 20 seconds. The DNA spin columns were then transferred into new 2 ml collection tubes. Flow-through fractions were later used for total cellular RNA (tcRNA) purification. DNA spin columns were washed with 500 µl of AW 1 buffer and followed by 500 µl of AW 2 buffer. Two hundred µl of EB buffer was then added into each column and incubated for 2 minutes at 27°C. Finally, the tubes were spun for 1 minute at 17,000 x g and DNA was collected in new microcentrifuge tubes.

3.2.4.3 Total cellular RNA (tcRNA) extraction

tcRNA was extracted using the AllPrep® DNA/RNA/Protein mini kit (Qiagen, Hilden, Germany) according to the manufacturer's instructions. Briefly, 430 µl of absolute

ethanol was added into the flow-through fraction (previously described in Section 3.2.4.2) and, subsequently transferred into an RNeasy spin column. The mixture was centrifuged at 17,000 x g for 15 seconds. The flow-through was later used for protein purification. Three hundred fifty μ l of RW 1 was then used to wash the spin column membrane. Eighty μ l of DNase I was directly added and the RNeasy spin column was incubated for 15 minutes. The column was subsequently washed with 350 μ l of RW 1 buffer and followed by 500 μ l of RPE buffer. The ready-to-use tcRNA was eluted in 30 μ l RNase free water and finally collected in a microcentrifuge tube. The eluted tcRNA was stored at -80°C for further analysis.

3.2.4.4 Determination of yield and quality of genomic DNA and tcRNA

The yield and quality of the extracted genomic DNA and tcRNA were determined using a GeneQuantpro spectrophotometer (Amersham Pharmacia Biotech, Uppsala, Sweden). Concentration was automatically calculated by the RNA/DNA calculator from the absorbance readings by assuming that 40 $\mu\text{g/ml}$ of RNA or 50 $\mu\text{g/ml}$ of DNA gave an absorbance reading of 1.0 ($A_{260} \times 40$ or $50 \mu\text{g/ml} \times \text{dilution factor}$). The quality of genomic DNA and tcRNA was estimated by measuring the A_{260}/A_{280} and A_{230}/A_{260} ratios of absorbance, respectively. Genomic DNA and tcRNA with values between 1.8 and 2.1 are considered to be of good quality.

3.2.4.5 Whole-exome sequencing

Whole-exome sequencing (WES) was performed at BGI Biotechnology Company, Beijing, China for five patients with PTC (PCP3, PCP5, PCP7, PCP8, and PCP9) and four patients with BTG (BGP4, BGP8, BGP20, and BGP23).

Six ng genomic DNA was randomly fragmented using NGS kit (Covaris, Massachusetts, USA) to produce library fragments within the range of 150-200 bps. The resulting DNA fragments were then ligated with adapters at both ends. The adapter-ligated templates were purified using the Agencourt AMPure SPRI beads and fragments with insert size of about 200 bps were excised. Extracted adapter-ligated templates were then amplified by ligation-mediated polymerase chain reaction (LM-PCR), purified and hybridised to the SureSelect Biotinylated RNA Library (BAITS) for enrichment. Hybridised fragments were bound to the streptavidin coated magnetic beads whereas non-hybridised fragments were washed away with wash buffer after 24 hours. The enrichment magnitude of captured LM-PCR products were then measured using the Agilent 2100 Bioanalyzer. Illumina Hiseq2000 platform was used for high-throughput sequencing. The raw images were then processed using Illumina base calling Software 1.7.0 to generate sequencing data of 100 pair-end reads stored in a FASTQ file, a text-based format for storing nucleotide sequence and its corresponding quality scores.

The sequencing raw data were filtered using FASQC to remove the adapter reads, low quality reads which have too many Ns and reads with unknown bases of more than 10%. The filtered clean reads were then aligned against human reference genome sequence (human genome build37 (hg19) which is available at <http://hgdownload.cse.ucsc.edu/goldenPath/hg19/bigZips/> using Burrows-Wheeler Aligner (BWA). Aligned data were generated in Sequence Alignment/Map (SAM) format and subsequently compressed to a binary format (BAM) in order to facilitate variant calling via SOAPsnp and SAMtools (<http://soap.genomics.org.cn/SOAPsv.html>) for single nucleotide variations (SNVs) and small insertions and deletions (InDels), respectively.

The certainty of each base call is recorded as a ‘Phred’ quality score, which measures the probability that a base is incorrect. The quality score of a given base, Q, is defined by the equation: $Q = -10 \log_{10} E$ where ‘E’ is the estimated probability of the wrong base call. Thus, a higher quality score indicates a smaller probability of error. A Q20 value, for example, corresponds to a 1 in 100 error probability and a Q30 value to a 1 in 1000 error rate (Table 3.2).

Table 3.2: Phred quality scores

Quality Score	Probability of Incorrect Base Call	Inferred Base Call Accuracy
10 (Q10)	1 in 10	90.0%
20 (Q20)	1 in 100	99.0%
30 (Q30)	1 in 1000	99.9%

3.2.4.6 Thyroid neoplasm-related genes screening

The variants identified were further filtered to include 36 genes which had been previously reported in four public databases, namely the NCBI dbSNP132 (http://www.ncbi.nlm.nih.gov/projects/SNP/snp_summary.cgi?build_id=132), ExAC browser (<http://exac.broadinstitute.org>), SNPedia (<http://www.snpedia.com/index.php/SNPedia>), and Ensembl (<http://www.ensembl.org/info/genome/variation/index.html>). The 36 genes are listed in Table 3.3.

Table 3.3: List of genes associated with thyroid diseases

Gene Annotation	Gene Name
<i>ADCY10</i>	Adenylate cyclase 10
<i>BGLAP</i>	Bone gamma-carboxyglutamic acid-containing protein
<i>BRAF</i>	V-raf murine sarcoma viral oncogene homolog b
<i>CALCA</i>	Calcitonin-related polypeptide alpha
<i>CCDC6</i>	Coiled-coil domain containing 6
<i>CDKN1A</i>	Cyclin-dependent kinase inhibitor 1A
<i>CTNNB1</i>	Beta-catenin
<i>EGF</i>	Epidermal growth factor
<i>GNAS</i>	Guanine nucleotide-binding protein
<i>HRAS</i>	Harvey rat sarcoma viral oncogene homolog
<i>KISS1R</i>	KISS1 receptor
<i>KRAS</i>	Kirsten rat sarcoma viral oncogene homolog
<i>KRT10</i>	Keratin 10
<i>KRT19</i>	Keratin 19
<i>LGALS3</i>	Lectin, galactoside-binding, soluble, 3
<i>LGALS3BP</i>	Lectin, galactoside-binding, soluble, 3 binding protein
<i>MEN1</i>	Multiple endocrine neoplasia type 1
<i>NKX2-1</i>	NK2 homeobox 1
<i>NRAS</i>	Neuroblastoma RAS viral (v-ras) oncogene homolog
<i>PAX8</i>	Paired box 8
<i>PIK3CA</i>	Phosphatidylinositol-4,5-biphosphate 3-kinase, catalytic subunit alpha
<i>PPARG</i>	Peroxisome proliferator-activated receptor gamma
<i>PTEN</i>	Phosphatase and tensin homolog
<i>PTH</i>	Parathyroid hormone

Table 3.3, continued

Gene Annotation	Gene Name
<i>RASSF1</i>	Ras association domain-containing protein
<i>RASSF1A</i>	Ras association domain family member 1
<i>RET</i>	Ret proto-oncogene
<i>SERPINA7</i>	Serpin peptidase inhibitor 7
<i>SLC5A5</i>	Sodium-iodide symporter
<i>SLC26A4</i>	Pendrin
<i>TG</i>	Thyroglobulin
<i>TIMP3</i>	Metallopeptidase inhibitor 3
<i>TPO</i>	Thyroid peroxidase
<i>TP53</i>	Tumour protein 53
<i>TRH</i>	Thyrotropin releasing hormone
<i>TSHR</i>	Thyroid stimulating hormone receptor

3.2.4.7 Characterisation of nucleotide alterations in thyroid neoplasm-related genes

WES analysis of the extracted DNA from the neoplastic tissues of patients with BTG and those with PTC has generated a list of novel as well as reported mutations in 36 thyroid neoplasm-related genes. Novel mutations were assessed for their effects on the encoded protein function. The mutations were analysed *in silico* for putative functional effects using the following software: Sorting Intolerant From Tolerant (SIFT) (http://sift.jcvi.org/www/SIFT_enst_submit.html), Polymorphism Phenotyping v2 (Polyphen-2) (<http://genetics.bwh.harvard.edu/pph2/>), and Mutationtaster, (<http://www.mutationtaster.org/>). The SIFT (Ng & Henikoff, 2001), PolyPhen-2 (Adzhubei et al., 2010) and Mutationtaster (Schwarz, Rödelberger, Schuelke, & Seelow, 2010) are web-based algorithms that predict how amino acid substitutions will affect protein function. Amino acid substitution results are reported as “tolerated” or as “intolerance” for SIFT while results are given as “benign”, “possibly damaging”, “probably damaging” or “unknown” for PolyPhen-2. The MutationTaster score predicts the disease potential of an alteration with score nearer to 1 has higher probability of pathogenicity.

In addition, variants that were consistently identified in PTC and/or BTG were investigated for allele frequencies and genotype distributions for all two populations. The allelic and genotypic frequencies were expressed as percentages of total alleles and genotypes. The genotypes frequencies were tested whether it corresponds with Hardy-Weinberg equilibrium (HWE) using Genepop software version 4.2 (<http://kimura.univ-montp2.fr/~rousset/Genepop.htm>) for prediction of PTC or BTG.

3.2.4.8 mRNA transcript analysis

Novel mutations identified in this study were subsequently tested using PCR direct sequencing.

(a) *Primer design*

Primer pairs of 20 bps in length for *BRAF*, *LGALS3*, *PAX8*, *PIK3CA*, *RET*, *SLC26A4*, *TG*, *TPO*, *TRH*, and *TSHR* genes (Table 3.4) were individually designed using Primer3Plus (<http://biotools.umassemed.edu/cgi-bin/primer3plus/primer3plus.cgi>) software. The sensitivity and specificity of the primer pairs were then further validated using NCBI primer blast (<http://www.ncbi.nlm.nih.gov/tools/primer-blast/>). All the primers were synthesized by AITBiotech (Singapore).

(b) *Reverse transcription of tcRNA to cDNA*

tcRNA isolated from thyroid tissues was reverse-transcribed to complementary DNA (cDNA) using the High Capacity RNA-to-cDNA Kit (Applied Biosystems, California, USA) according to the manufacturer's protocol. One μg of tcRNA was reverse-transcribed in 20 μl reaction mixture containing 20 x RT enzyme and 2 x RT buffer in a pre-heated PCR thermal cycler (Biometra, Germany). The reaction mixture was incubated at 37°C for 1 hour, followed by 95°C for 5 minutes, and finally held at 4°C until they were analysed on gel electrophoresis. cDNA samples prepared from thyroid tissue of mutation-free individuals were used as controls in the analysis.

Table 3.4: Nucleotide sequence of PCR primers for mRNA transcript analysis

Gene name	Exon	PCR primer sequence	Expected product size (bp)	Annealing temperature (°C)
<i>BRAF</i>	11 12	Forward 5' GACGGGACTCGAGTGATGAT 3' Reverse 5' CTGCTGAGGTGTAGGTGCTG 3'	155	55
	17 18	Forward 5' TTTTATGGTGGGACGAGGA 3' Reverse 5' GGACAGGAAACGCACCATA 3'	300	55
<i>LGALS3</i>	2 4	Forward 5' GAGCGGAAAATGGCAGAC 3' Reverse 5' CTGTTTGCATTGGGCTTCAC 3'	440	53
<i>PAX8</i>	7 9	Forward 5' GACTCACAGAGCAGCAGCAG 3' 5' ATGGGGAAAGGCATTGAAG 3'	411	55
<i>PIK3CA</i>	10 11	Forward 5' GAGACAATGAATTAAGGGAAAATGA 3' Reverse 5' AACAGACAGAAGCAATTTGGGTA 3'	161	50
<i>RET</i>	16 17	Forward 5' TGGCAATTGAATCCCTTTTT 3' Reverse 5' CAGTTGTCTGGCCTCTCCAT 3'	175	55
<i>SLC26A4</i>	18 19	Forward 5' TCCAAAGAATTGATGTGAATGTG 3' Reverse 5' TGGAACCTTGACCCTCTTGA 3'	177	53
<i>TG</i>	18 19	Forward 5' AGACCATCCAGACCCAAGG 3' Reverse 5' GATGTCCTCAAGCCGTGATT 3'	263	50

Table 3.4, continued

Gene name	Exon	PCR primer sequence	Expected product size (bp)	Annealing temperature (°C)
<i>TG</i>	21 23	Forward 5' CCATTTCTGCTGGAGCTTTC 3' Reverse 5' CATCACGGGGA ACTCAGAAT 3'	308	50
	33 34	Forward 5' TGCACTGGCTTTGGATTTCT 3' Reverse 5' CATCCGAAGGGATAGGTGTG 3'	170	50
<i>TPO</i>	8 9	Forward 5' TCCACCGTGTATGGCAGCTC 3' Reverse 5' CCTTCATAGGGACCCACGTA 3'	437	53
	13 15	Forward 5' AGGAAGGATGGGATTTCCAG 3' Reverse 5' GAGGTGAGACCTGCCAAGC 3'	250	53
<i>TRH</i>	2 3	Forward 5' CTCTGGCTTTGACCCTGAAC 3' Reverse 5' TGGGTTACATCGACTGACCA 3'	367	53
<i>TSHR</i>	9 10	Forward 5' CACGGGCTGACCTTTCTTAC 3' Reverse 5' GGTCTACAGAGGCGATGAGG 3'	606	53

(c) *Agarose gel electrophoresis of the PCR products and gel visualisation*

A 2% agarose was prepared in 1 x TAE Buffer (40 mM Tris, 20 mM acetic acid and 1 mM EDTA) in the presence of 0.2 µg/ml ethidium bromide. The cooled mixture was carefully poured and allowed to solidify in a minicell casting tray with a pre-inserted comb and rubber casting dams. The gel (on its bed) was placed into the electrophoresis chamber with the wells at the negative pole. The chamber was filled with 300 ml of 1 x TAE buffer and 5 µl of each samples was loaded swiftly into the designated wells using a micropipette. A standard DNA ladder marker (Fermentas Life Sciences, Massachusetts, USA) was loaded into one of the wells. Electrophoresis was then performed at 80-110 V for 50 minutes. The electric current flow was switched off when the blue dye front reached about 2-3 cm from the end of the gel. The band was visualised using a gel documentation system version 2000 (Bio-Rad Laboratories, Hercules, USA).

(d) *Purification of PCR products from PCR mixtures*

PCR products were purified using QIAquick[®] PCR Purification Kit (Qiagen, Hilden, Germany) following the manufacturer's instruction. Five volumes of PBI buffer was added to 1 volume of the PCR products and mixed by pipetting. The mixture was then transferred into a QIAquick spin column placed in a 2 ml collection tube. The column was centrifuged for 1 minute at 17,000 x g in a conventional table-top microcentrifuge. The flow-through was discarded and the column was placed back into the same collection tube. Washing was carried out by adding 750 µl of PE buffer into the column followed by centrifugation for 1 minute at 17,000 x g. The flow-through was discarded and the column was then placed into a new 1.5 ml microcentrifuge tube. The column was then incubated with 30 µl of EB buffer (10 mM Tris-Cl, pH 8.5) at room temperature for

another 1 minute followed by 1 minute of centrifugation at 17,000 x g. The purified PCR product was then stored at -20°C for further analysis.

(e) *Purification of PCR products from agarose gel*

Purification of PCR products from agarose gel was performed using MinElute® Gel Extraction Kit (Qiagen, Hilden, Germany) according to the manufacturer's protocol. The DNA fragment from the agarose gel was excised with a clean, sharp scalpel. Excess agarose was removed to minimise the size of the gel. The gel slice was then weighed in a 1.5 ml clean microcentrifuge tube. Three volumes of QG buffer were added to 1 volume of gel as recommended in the protocol. The mixture was then incubated for 10 minutes at 50°C until the gel slice was completely dissolved. The tube was vortexed for every 2-3 minutes during incubation to accelerate gel liquefying. One part of isopropanol was then added to the sample mixture.

A spin column was placed in a provided 2 ml collection tube and the sample was applied to the column. The column was centrifuged for 1 minute at 17,000 x g. The flow-through was discarded and the column was placed back in the same collection tube. To wash, 750 µl of PE buffer was added to the column, incubated at room temperature for 1 minute, followed by centrifugation for another 1 minute. The flow-through was discarded and the column was spun for an additional 1 minute at 17,000 x g to remove residual ethanol from the PE buffer. The column was then placed into a clean 1.5 ml microcentrifuge tube. Ten µl of EB buffer was dispensed directly onto the centre of the membrane of the column and incubated for 1 minute at 24°C. The column was finally spun at 17,000 x g for another 1 minute. The PCR products were kept at -20°C until further analysis.

(f) *Sanger sequencing and analysis*

Purified PCR products were sent for direct DNA sequencing at AITBiotech (Singapore). The PCR products were sequenced using the same primers used in the PCR amplification. The volume and concentration of a PCR product required for each sequence were 10 µl and 10 µM, respectively. The sequence obtained was compared to the published sequence available at NCBI gene bank database (<https://blast.ncbi.nlm.nih.gov/Blast.cgi>).

3.2.4.9 Expression analysis of *BRAF*, *NIS*, *TG*, *TPO*, and *TSHR* genes

Expression of *BRAF*, *NIS*, *TG*, *TPO*, and *TSHR* were compared between the two tissues using qRT-PCR. One µg of tcRNA extracted from the benign cyst or PTC tissue was converted to cDNA using High Capacity RNA-to-cDNA kit (Applied Biosystems, California, USA). Quantitative PCR was carried out using the StepOne Real-Time PCR System (Applied Biosystems, USA) with 40 amplification cycles. Melting curve analyses were performed for all primers to ensure single amplification product. The list of primers is shown in Table 3.5. Each reaction consisted 10 ng of cDNA, 0.2 mM forward and reverse primers, 2X Fast SYBR[®] Green Master Mix (Applied Biosystems, USA) in a final volume of 20 µl. All qRT-PCR experiments were performed in triplicates. Gene expression was normalised against a housekeeping *Tata-box binding protein (TBP)* gene. The experiment was repeated by comparing both the tissues with another 3 control (mutation-free) thyroid tissues.

Table 3.5: Sequences of the primers used for quantitative real-time PCR analysis

Genes	Exon	Primer Sequence	Fragment size (bp)	Annealing temperature (°C)
<i>TBP</i>	4 5	Forward 5' CACGAACCACGGCACTGATT 3' Reverse 5' TTTTCTTGCTGCCAGTCTGGAC 3'	89	59
<i>BRAF</i>	15 15	Forward 5' GAGTGGGTCCCATCAGTTTG 3' Reverse 5' CTGGTCCCTGTTGTTGATGTT 3'	181	59
<i>TG</i>	31/32 34/35	Forward 5' CCGGAAGAAAGTTATACTGGAAG 3' Reverse 5' TTTGAGCAATGGGCTTCTG 3'	356	59
<i>TSHR</i>	4/5 7/8	Forward 5' CCTCCTAAAGTTCCTTGGCATT 3' Reverse 5' AGGTAAACAGCATCCAGCTTTG 3'	243	59
<i>NIS</i>	1/2 3/4	Forward 5' CACCAGCACCTACGAGTACC 3' Reverse 5' CCCGGTCACTTGGTTCAG 3'	143	59
<i>TPO</i>	4 5	Forward 5' TCCAAACTTCCTGAGCCAA 3' Reverse 5' CTCCTGTGATGGGCCTGTAT 3'	241	59

3.2.5 Proteomic analysis

3.2.5.1 Extraction of protein from human tissue and serum samples

Tissue protein was extracted using the AllPrep[®] DNA/RNA/Protein Mini Kit (Qiagen, Hilden, Germany) according to the manufacturer's instruction with slight modification. Six hundred μ l of APP buffer was added to the flow through from the previous described step (Section 3.2.4.3). The mixture was then mixed vigorously and incubated at room temperature for 10 minutes to precipitate protein. The supernatant was carefully decanted after centrifugation at full speed for 10 minutes. Later, 500 μ l of 70% ethanol was added to the protein pellet and spun for another 1 minute. The supernatant layer was removed using a pipet after centrifugation at full speed for 1 minute. The protein pellet was left to dry for 10 minutes at room temperature.

The protein concentration was then determined using Pierce BCA protein assay kit according to manufacturer's instruction. The absorbance readings of bovine serum albumin standard and tissue samples were measured at 570 nm using Microplate Reader Model 680 (Bio-Rad Laboratories, Hercules, USA). Serum protein samples were directly utilised from the previous described step (Section 3.2.3.2).

3.2.5.2 2-DE

2-Dimensional electrophoresis (2-DE) involves isoelectric focusing (IEF) of proteins in their native state according to pI and subsequently, by second-dimensional electrophoresis via polyacrylamide gel electrophoresis in the presence of sodium dodecyl sulphate (SDS-PAGE), which separates the proteins according to their molecular weights.

(a) ***Rehydration of IPG gel strips***

The protein pellet from thyroid tissue was dissolved in 200 μ l of thiourea rehydration solution (7 M urea, 2 M thiourea, 2% w/v CHAPS, 0.4% v/v pH 4-7 IPG buffer). One hundred ng of dissolved tissue protein was topped up to 200 μ l with sample buffer (7 M urea, 2 M thiourea, 4% w/v CHAPS, 4% v/v pH 4-7 IPG buffer, 40 mM DTT, Orange G) and left at room temperature for 30 minutes. In case of serum samples, 7 μ l was mixed with 21 μ l sample buffer (9 M urea, 60 mM DTT, 2% (v/v) IPG buffer, 0.5% (v/v) Triton X-100) and incubated at room temperature for 30 minutes. The sample mixture was then made up to 200 μ l by addition of 172 μ l rehydration buffer (8 M urea, 0.5% (v/v) IPG buffer, 0.5% (v/v) Triton X-100) and left for another 30 minutes at room temperature.

Sample mixtures were loaded into the slots of the reswelling tray. Thirteen and 11 cm IPG drystrips pH 4-7 (GE Healthcare Life Sciences, Uppsala, Sweden) were carefully lowered with the gel sides down onto the tissue and serum mixtures, respectively. Drystrip cover fluid was pipetted over the IPG drystrips until they were fully covered to minimize evaporation and urea crystallisation. The mixtures were passively rehydrated and kept in a sealed environment for more than 12 hours at room temperature to ensure complete rehydration and sample uptake.

(b) ***First dimension separation of proteins***

The rehydrated IPG strips were placed on the drystrip ceramic tray and DTT moistened electrode strips were placed across the cathodic and anodic ends of the aligned strips. The electrodes were then positioned on the electrode strips. The IPG strips were ensured to be fully immersed with dry cover fluid. IEF of tissue and serum proteins was performed at 18°C using the following program: 1) 500 V, 1 hour, step and hold; 2) 1000 V, 1 hour, gradient; 3) 8000 V, 2.5 hours, gradient and 4) 8000 V, ~2.5 hours, step and hold. The

focused strips were either used immediately for second dimension separation or kept in -80°C in screw-cap tubes for further use.

(c) *Second dimension separation of proteins*

IPG strips were equilibrated for 15 minutes in SDS equilibration buffer (1.5 M Tris-HCl pH 8.8, 6 M urea, 29.3% glycerol, 2% SDS) contained 1% (w/v) DDT for reduction, followed by an alkylation in equilibration buffer containing 2.5% (w/v) iodoacetamide for another 15 minutes. The second dimension separation was subsequently carried out at 18°C on 8-13% SDS gel slab for tissue and serum samples using a Hoefer SE Ruby (GE, Uppsala, Sweden), with the IPG strips sealed on the top of the gels with 0.5% (w/v) agarose in SDS-electrophoresis buffer (25 mM Tris base, 198 mM glycine, 0.1% w/v SDS). The electrophoresis was completed following an optimised protocol (Phase 1: 50 V, 40 mA, 25 W for 40 minutes; Phase 2: 600 V, 40 mA, 25 W for ~2.5 hours) using the SE 600 Ruby Electrophoresis System and Power Supply-EPS601 (GE Healthcare Life Sciences, Uppsala, Sweden).

3.2.5.3 Silver staining of 2-DE gels

After electrophoresis, gels were stained according to the method described by Heukeshoven and Dernick (1988). The gel slab was immersed in fixing solution (40% (v/v) ethanol, 10% acetic acid) for at least 30 minutes. The gel was then incubated in sensitising solution (30% (v/v) ethanol, 0.5 M sodium acetate, 8 mM sodium thio-sulphate, 0.13% (v/v) glutaraldehyde) for a minimum period of 30 minutes. This was followed by three times washing for 15 minutes with double distilled water. The process was continued with staining using 5.9 mM silver nitrite in the presence of 0.02% (v/v)

formaldehyde, which required 20 minutes of incubation. The gel slab was subsequently washed for another 2 minutes and incubated with developing solution (0.24 M sodium carbonate, 0.2% (v/v) formaldehyde). The protein spots were allowed to fully develop. The gel was then soaked in stopping solution containing 40 mM EDTA disodium dihydrate followed by washing with double distilled water to prevent further colour development. The procedure was performed on a shaker as all steps in the staining technique required gentle shaking at 60 rpm.

3.2.5.4 Analysis of 2-DE gels

2-DE silver stained gels were digitised on ImageScanner (GE HealthCare, Uppsala, Sweden) which were then analysed using the ImageMaster 2D Platinum V 7.0 software (GE HealthCare, Uppsala, Sweden). Protein abundance was analysed in terms of percentage of volume contribution, which is the volume of a protein spot expressed as a percentage of the total spot volume of all detected proteins. Protein spots showing at least a 1.5-fold difference in average expression level were considered statistically significant ($p \leq 0.01$) and excised for identification by mass spectrometry.

3.2.5.5 In-gel tryptic digestion

Differentially expressed protein spots were manually excised from 2-DE gels. In-gel digestion with trypsin was performed as described by Seriramalu et al. (2010). The plugs were de-stained twice for 15 minutes with 15 mM potassium ferricyanide in 50 mM sodium thiosulfate with regular shaking at room temperature or until gel plugs became clear. Subsequently, the gel plugs were reduced in 10 mM DTT for 30 minutes at 60°C followed by alkylation with 55 mM iodoacetamide for another 20 minutes in the dark at

room temperature. They were then washed thrice with 50% acetonitrile in 100 mM ammonium bicarbonate for 20 minutes with shaking, followed by 100% acetonitrile for 15 minutes and dried using a SpeedVac at low speed. The plugs were digested overnight in 6 ng/μl trypsin in 50 mM ammonium bicarbonate at 37°C. Extraction of the peptides from the gel plugs was carried out sequentially using 50% and 100% acetonitrile followed by lyophilisation in a vacuum centrifuge until completely dry. Dried peptides were then kept in -20°C or reconstituted with 10 μl of 0.1% formic acid prior to purification using the Zip Tip C18 micropipette tips (Millipore, Billerica, MA, USA).

3.2.5.6 Q-TOF LC/MS

Digested samples were first reconstituted in 5 μl of the initial LC mobile phase (0.1% formic acid) before being injected into the Nano-flow LC 1260 series (Agilent, California, USA) directly connected to Accurate-Mass Q-TOF 6550 with a nano electrospray ionisation source. Digested peptides were enriched using an enrichment column and then separated on an HPLC Chip-Protein column (C18 reverse phase, 300 Å, 43 mm, Agilent, Santa Clara, CA, USA) with a 3-50% linear gradient of solvent B (90% acetonitrile and 0.1% formic acid) for 30 minutes with a flow rate of 0.3 μl/minute. Mass Hunter Qual acquisition software (Agilent, California, USA) was used to acquire the mass spectra (8 masses per second from 115 to 3000 m/z) followed by collision-induced dissociation of the four most intensive ions. MS/MS data were acquired in the range of 50-3000 m/z.

3.2.5.7 Database search

Spectrum Mill software (Agilent, California, USA) was set to search MS/MS acquired data against the Swiss-Prot Homo sapiens database. Mass-tolerance of precursor and

product ions was set to ± 20 and ± 50 ppm, respectively, while carbamidomethylation was specified as a fixed modification and oxidised methionine as a variable modification. A protein was considered identified according to the following selection parameters: 1) Protein score specified to be more than 20; 2) peptide mass error less than 5 ppm; 3) forward-reverse score more than two; 4) peptide score more than six and 5) Scored Peak Intensity (%SPI) more than 60 percent.

3.2.5.8 Functional analysis using Ingenuity Pathway Analysis software

Differently expressed proteins of the benign and malignant thyroid tissues from a single individual were subjected to functional analysis using IPA software (Ingenuity® Systems, <https://www.analysis.ingenuity.com>). The proteins were analysed algorithmically to generate a set of interactive networks, taking into consideration of canonical pathways, relevant biological interactions as well as cellular and disease processes based on information stored in the Ingenuity Knowledge Base. A Right-tailed Fischer's exact test was used to calculate a p value, indicating the likelihood of focused genes to belong to a network versus those obtained by chance. The IPA system computes a z-score to infer the activation status of predicted transcriptional regulators. A score ≥ 2.0 indicates significantly "activation" whereas ≤ -2.0 indicates significantly inhibition.

3.2.5.9 Western blot

Western blot was carried out to detect presence of STAT3 phosphorylated protein (pY-STAT3) in the tissue specimens. Approximately 20 μg protein sample of benign cyst and PTC tissues were separated by electrophoresis in a 12% SDS polyacrylamide gel. The separated proteins were later transferred onto a polyvinylidene difluoride membrane.

Western blot analysis was performed using rabbit monoclonal EP2147Y primary antibody (Abcam[®], Cambridge, UK) and WesternDot[™] 625 Western blot kit (Thermo Fisher Scientific, Rockford, USA) to detect presence of pY-STAT3 protein in the tissue specimens. The expression of pY-STAT3 in benign and malignant tissues was quantitated by densitometry scanning using Image-J software (<http://rsbweb.nih.gov/ij/>) and normalised to the expression of beta actin (Abcam[®], Cambridge, UK) (Shimko et al., 2014). The ratio of STAT3 variants in the benign cyst was also compared to that of the PTC.

3.2.5.10 Enzyme-linked immunosorbent assay

Serum specimens were analysed by enzyme-linked immunosorbent assay (ELISA) according to the manufacturers' instructions. ELISA was performed using anti-human alpha-1 antitrypsin (A1AT), alpha 2-HS glycoprotein (AHSG), heat shock 70 kDa protein 1A (HSP70) as primary antibodies. Cut-off parameters for tissue and serum proteins selected for ELISA in both groups of PTCa and PTCb patients were: (1) fold change (f.c.) > 2.0 and (2) $p < 0.01$. ELISA kit for HSP70 (E3015Hu) was obtained from the Bioassay Technology Laboratory, Shanghai, China. Kits for estimation of A1AT (ab108798) and AHSG (ab108855) were purchased from Abcam[®], Cambridge, UK. All readings were made on an ELISA Plate Reader (Bio-Rad, Hercules, USA). All samples, standards and blanks were analysed in duplicate.

3.2.5.11 Statistical analysis

Hardy-Weinberg (HW) exact test was used to test the genetic equilibrium of the SNVs using Genepop (version 4.2) population genetics software package. Fisher's exact

test was performed using The Statistical Package for Social Sciences (SPSS) version 24.0 (IBM, New York, NY, USA) to examine differences in genotype and allele distribution for each variant between cases.

One-way ANOVA with Tukey's post-test was performed using GraphPad Prism version 5.00 for Windows (GraphPad Software, San Diego, California, USA). The ANOVA test was used to compare mean percentages of volume contribution of the protein spots as well as protein concentrations between groups of subjects. All values are expressed as mean \pm standard error of the mean (SEM). A p value of less than 0.05 was considered significant, unless otherwise stated.

University of Malaya

CHAPTER 4: RESULTS

4.1 Genomic Studies

Nucleotide variants detected in index patients diagnosed with papillary thyroid cancer (PTC) (PCP3, PCP5, PCP7, PCP8, and PCP9) and benign thyroid goitre (BTG) (BGP4, BGP8, BGP20, and BGP23) are presented in Table 4.1. PCP5 exhibited the highest number of novel variants with 4,757 whilst the number of missense, synonymous, insertion, and deletion variants were 9,125, 10,450, 263, and 284, respectively. A total of 3,247 novel, 8,770 missense, 10,298 synonymous, 245 insertion, and 258 deletion variants were detected in PCP3. The number of variants in PCP7 was filtered to 4,512 novel, 9,019 missense, 10,617 synonymous, 267 insertion, and 275 deletion variants. As shown in the Table, 4,432 novel, 9,060 missense, 10,459 synonymous, 245 insertion, and 265 deletion variants were detected in PCP8. PCP9 has 3,908 novel, 8,975 missense, 10,430 synonymous, 277 insertion, and 271 deletion variants.

Among the patients with benign thyroid goitre, BGP20 exhibited the highest number of missense, synonymous, insertion, and deletion variants with 4,584, 9,018, 10,601, 243, and 287, respectively. A total of 8,887 missense, 10,376 for synonymous, 235 insertion, and 260 deletion variants were recorded in BGP4 of which 3,984 were novel. The number of variants in BGP8 was filtered to 3,532 novel, 8,760 missense, 10,321 synonymous, 243 insertion, and 242 deletion. Finally, 3,709 novel, 8,857 missense, 10,545 synonymous, 232 insertion, and 251 deletion variants were successfully identified in BGP23.

Table 4.1: Type of nucleotide variants identified in the index patients

Patient	Number of variant(s)				
	Novel	Missense	Synonymous	Insertion	Deletion
PCP3	3,247	8,770	10,298	245	258
PCP5	4,757	9,125	10,450	263	284
PCP7	4,512	9,019	10,617	267	275
PCP8	4,432	9,060	10,459	245	265
PCP9	3,908	8,975	10,430	277	271
BGP4	3,984	8,887	10,376	235	260
BGP8	4,584	9,018	10,601	243	287
BGP20	3,532	8,760	10,321	231	242
BGP23	3,709	8,857	10,545	232	251

4.1.1 Further analyses of the nucleotide variants in thyroid neoplasm-related genes in patients with PTC and BTG

Single nucleotide variants (SNVs) were detected in 34 out of the 36 thyroid neoplasm-related genes in patients with PTC (Figure 4.1A) and BTG (Figure 4.1B). SNVs were not detected in the *BGLAP* and *RASSF1A* genes in all of the patients. Thirteen novel SNVs in the *BRAF*, *LGALS3*, *PAX8*, *RET*, *TG*, *TPO*, and *TRH* genes were detected in patients with PTC. In the case of patients with BTG, a total of 12 novel SNVs in *BRAF*, *KRT10*, *PIK3CA*, *RASSF1*, *RET*, *SLC26A4*, *TG*, *TPO*, and *TSHR* genes were detected.

Figure 4.2 shows novel and previously reported InDel variants detected in patients with PTC (A) and BTG (B). InDel variants in the *BRAF*, *CCDC6*, *EGF*, *GNAS*, *HRAS*, *KRT19*, *LGALS3*, *PIK3CA*, *PTEN*, *RET*, *SLC26A4*, *TG*, *TP53*, and *TSHR* genes were identified in both group of patients. InDels in the *TPO* gene were detected only in the PTC patients. A novel frame shift deletion is exclusively identified in the *LGALS3* gene at position chr14:55604711, in a patient with PTC.

A summary of the number and the unique patterns of SNVs and InDels in the 34 out of the 36 thyroid neoplasm-related genes in patients with PTC and BTG are summarised in Figure 4.3. Three hundred and forty of previously described SNVs and InDels were successfully detected in 34 out of the 36 thyroid neoplasm-related genes in patients with PTC and BTG (Figure 4.3A). *TG* gene exhibited the highest number of SNVs followed by *ADCY10*. The least number of SNVs were detected in the *NRAS* and *TIMP3*. In contrast, *PIK3CA* gene carries the highest number of InDels, whilst *BRAF*, *EGF*, *GNAS*, *HRAS*, *SLC26A4*, *TP53*, and *TPO* exhibited the least number of InDel variant. Figure 4.3B shows patterns of previously documented and novel SNVs and InDels in the 34 out of the 36 candidate genes screened. Patients with PTC and BTG carried both types of

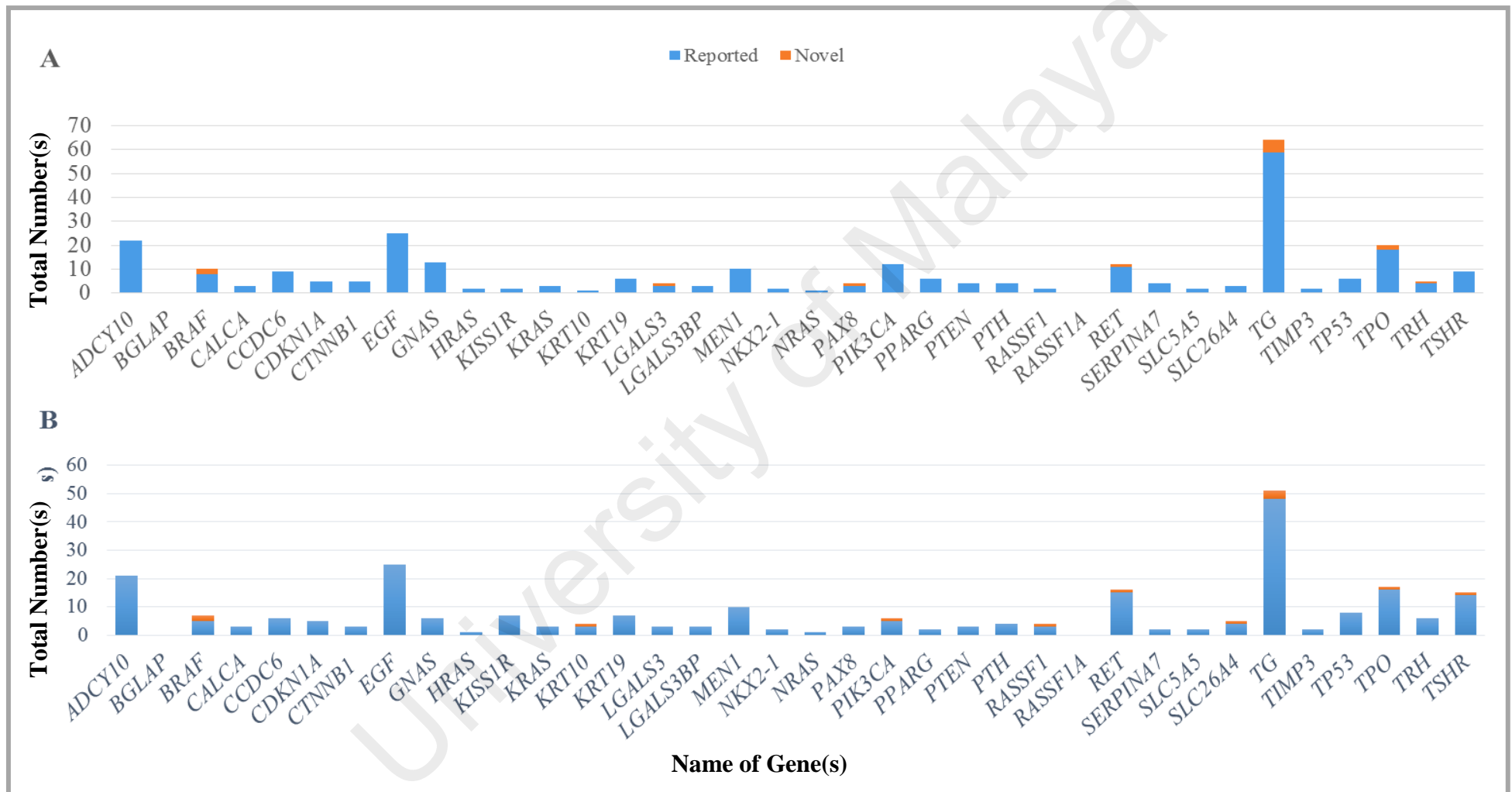


Figure 4.1: Single nucleotide variants (SNVs) detected in 34 out of 36 thyroid neoplasm-related genes in patients with A) PTC and B) BTG

[Abbreviation: *ADCY10*, Adenylate cyclase 10; *BGLAP*, Bone gamma-carboxyglutamic acid-containing protein; *BRAF*, V-raf murine sarcoma viral oncogene homolog b; *CALCA*, Calcitonin-related polypeptide alpha; *CCDC6*, Coiled-coil domain containing 6; *CDKN1A*, Cyclin-dependent kinase inhibitor 1A; *CTNNB1*, beta-Catenin; *EGF*, Epidermal growth factor; *GNAS*, Guanine nucleotide-binding protein; *HRAS*, Harvey rat sarcoma viral oncogene homolog; *KISS1R*, KISS1 receptor; *KRAS*, Kirsten rat sarcoma viral oncogene homolog; *KRT10*, Keratin 10; *KRT19*, Keratin 19; *LGALS3*, Lectin, galactoside-binding, soluble, 3 ; *LGALS3BP*, Lectin, galactoside-binding, soluble, 3 binding protein; *MEN1*, Multiple Endocrine Neoplasia Type 1; *NKX2-1*, NK2 homeobox 1; *NRAS*, Neuroblastoma RAS viral (v-ras) oncogene homolog; *PAX8*, Paired box 8; *PIK3CA*, Phosphatidylinositol-4,5-bisphosphate 3-kinase, catalytic subunit alpha; *PPARG*, Peroxisome proliferator-activated receptor gamma; *PTEN*, Phosphatase and tensin homolog; *PTH*, Parathyroid hormone; *RASSF1*, Ras association domain-containing protein; *RASSF1A*, Ras association domain family member 1; *RET*, Ret proto-oncogene; *SERPINA7*, Serpin peptidase inhibitor; *SLC5A5*, Solute carrier family 5 member 5 (Sodium Iodide Symporter); *SLC26A4*, Pendrin; *TG*, Thyroglobulin; *TIMP3*, TIMP Metallopeptidase inhibitor 3; *TP53*, Tumour protein 53; *TPO*, Thyroid peroxidase; *TRH*, Thyrotropin releasing hormone; *TSHR*, Thyroid stimulating hormone receptor]. Novel and previously reported SNVs are presented in orange and blue, respectively

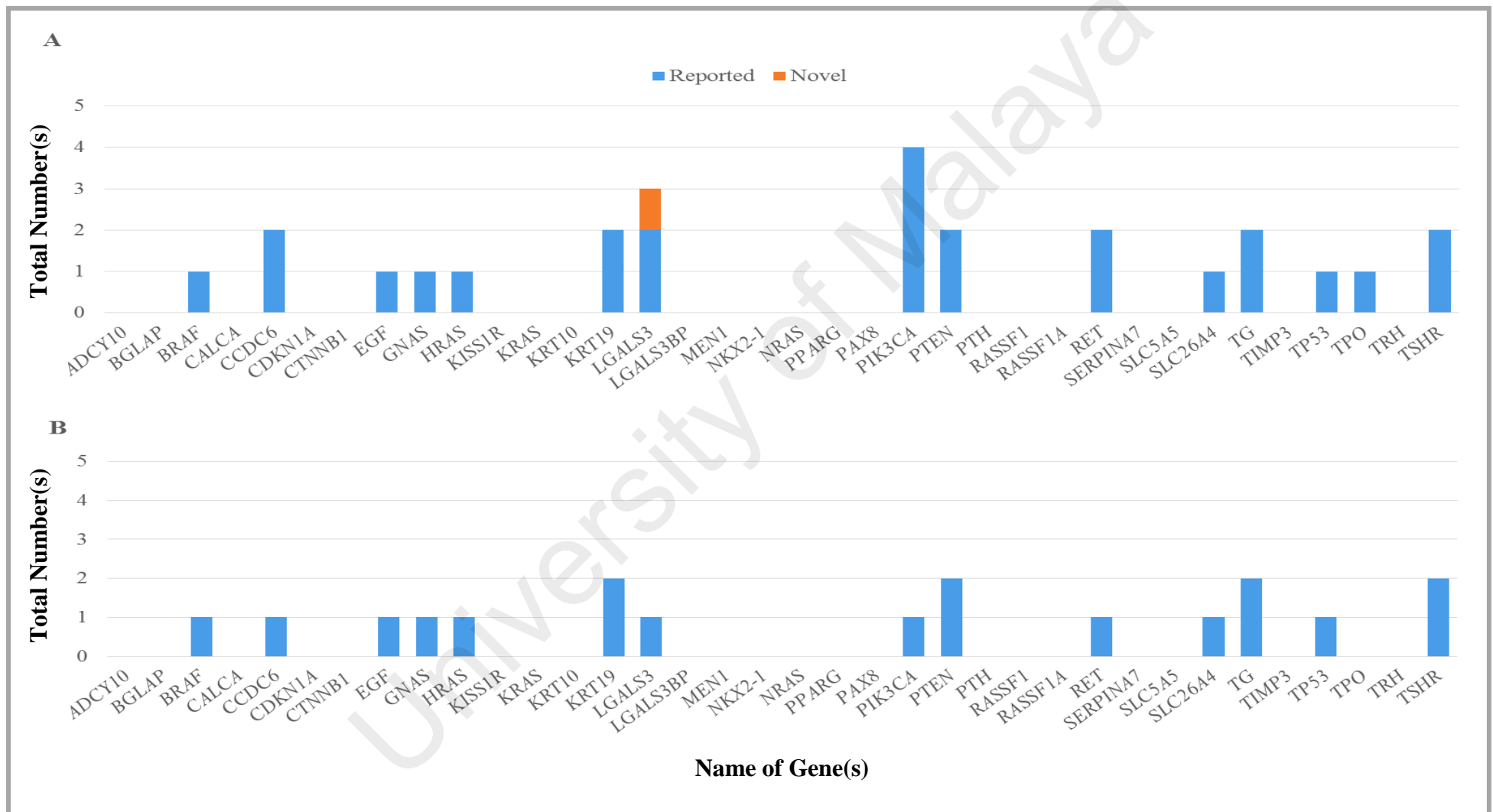


Figure 4.2: Number of insertion deletion (InDel) variants against 36 thyroid neoplasm-related genes in patients with A) PTC and B) BTG

[Abbreviation: *ADCY10*, Adenylate cyclase 10; *BGLAP*, Bone gamma-carboxyglutamic acid-containing protein; *BRAF*, V-raf murine sarcoma viral oncogene homolog b; *CALCA*, Calcitonin-related polypeptide alpha; *CCDC6*, Coiled-coil domain containing 6; *CDKN1A*, Cyclin-dependent kinase inhibitor 1A; *CTNNB1*, beta-Catenin; *EGF*, Epidermal growth factor; *GNAS*, Guanine nucleotide-binding protein; *HRAS*, Harvey rat sarcoma viral oncogene homolog; *KISS1R*, KISS1 receptor; *KRAS*, Kirsten rat sarcoma viral oncogene homolog; *KRT10*, Keratin 10; *KRT19*, Keratin 19; *LGALS3*, Lectin, galactoside-binding, soluble, 3; *LGALS3BP*, Lectin, galactoside-binding, soluble, 3 binding protein; *MEN1*, Multiple Endocrine Neoplasia Type 1; *NKX2-1*, NK2 homeobox 1; *NRAS*, Neuroblastoma RAS viral (v-ras) oncogene homolog; *PAX8*, Paired box 8; *PIK3CA*, Phosphatidylinositol-4,5-bisphosphate 3-kinase, catalytic subunit alpha; *PPARG*, Peroxisome proliferator-activated receptor gamma; *PTEN*, Phosphatase and tensin homolog; *PTH*, Parathyroid hormone; *RASSF1*, Ras association domain-containing protein; *RASSF1A*, Ras association domain family member 1; *RET*, Ret proto-oncogene; *SERPINA7*, Serpin peptidase inhibitor; *SLC5A5*, Solute carrier family 5 member 5 (Sodium Iodide Symporter); *SLC26A4*, Pendrin; *TG*, Thyroglobulin; *TIMP3*, TIMP Metallopeptidase inhibitor 3; *TP53*, Tumour protein 53; *TPO*, Thyroid peroxidase; *TRH*, Thyrotropin releasing hormone; *TSHR*, Thyroid stimulating hormone receptor]. Novel and previously reported InDel variants are presented in orange and blue, respectively.

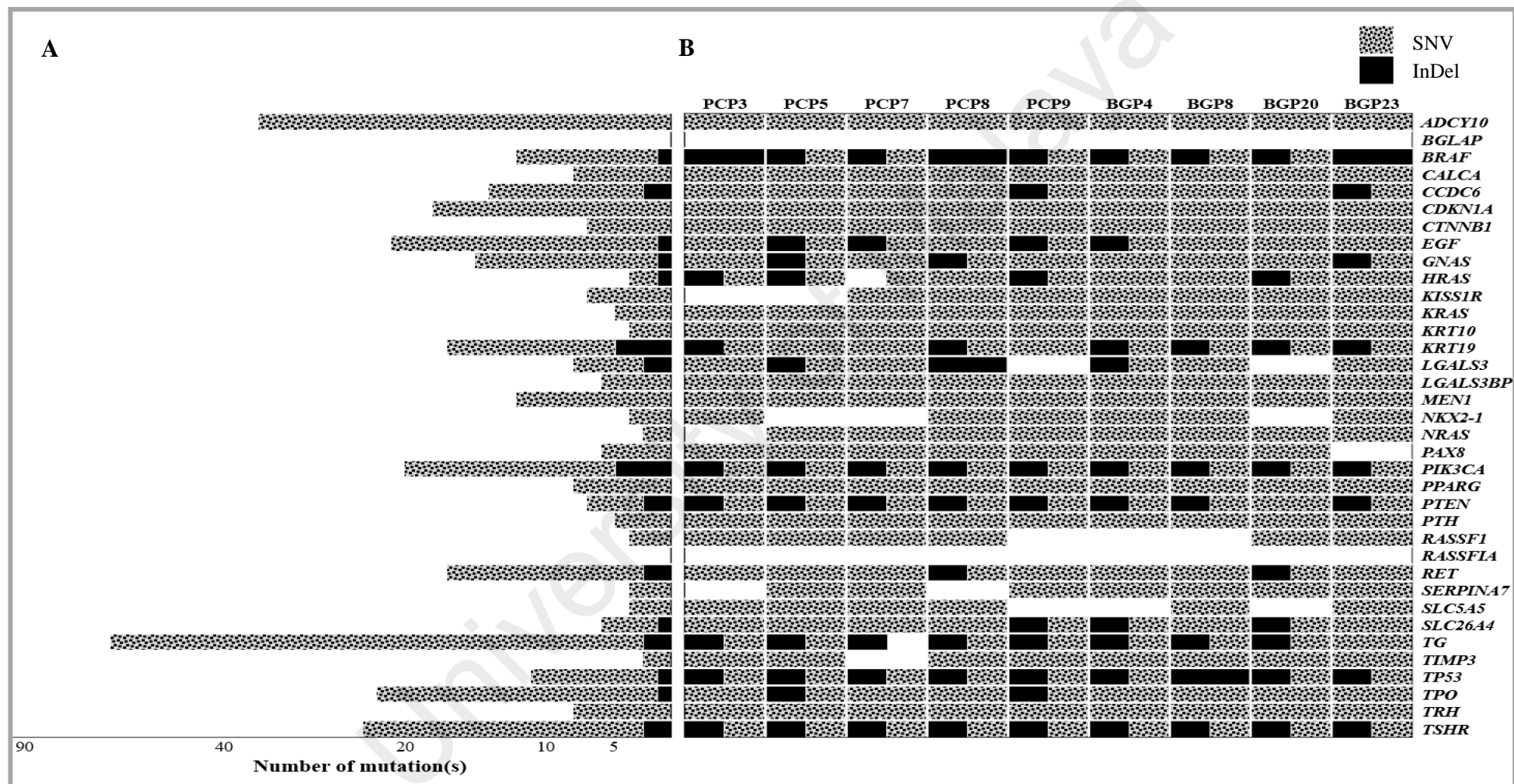


Figure 4.3: A summary of A) the number of SNVs and InDels in the 34 out of 36 thyroid neoplasm-related genes and B) patterns of SNVs and InDels in patients with PTC and BTG

[Abbreviation: *ADCY10*, Adenylate cyclase 10; *BGLAP*, Bone gamma-carboxyglutamic acid-containing protein; *BRAF*, V-raf murine sarcoma viral oncogene homolog b; *CALCA*, Calcitonin-related polypeptide alpha; *CCDC6*, Coiled-coil domain containing 6; *CDKN1A*, Cyclin-dependent kinase inhibitor 1A; *CTNNB1*, beta-Catenin; *EGF*, Epidermal growth factor; *GNAS*, Guanine nucleotide-binding protein; *HRAS*, Harvey rat sarcoma viral oncogene homolog; *KISS1R*, KISS1 receptor; *KRAS*, Kirsten rat sarcoma viral oncogene homolog; *KRT10*, Keratin 10; *KRT19*, Keratin 19; *LGALS3*, Lectin, galactoside-binding, soluble, 3; *LGALS3BP*, Lectin, galactoside-binding, soluble, 3 binding protein; *MEN1*, Multiple Endocrine Neoplasia Type 1; *NKX2-1*, NK2 homeobox 1; *NRAS*, Neuroblastoma RAS viral (v-ras) oncogene homolog; *PAX8*, Paired box 8; *PIK3CA*, Phosphatidylinositol-4,5-bisphosphate 3-kinase, catalytic subunit alpha; *PPARG*, Peroxisome proliferator-activated receptor gamma; *PTEN*, Phosphatase and tensin homolog; *PTH*, Parathyroid hormone; *RASSF1*, Ras association domain-containing protein; *RASSF1A*, Ras association domain family member 1; *RET*, Ret proto-oncogene; *SERPINA7*, Serpin peptidase inhibitor; *SLC5A5*, Solute carrier family 5 member 5 (sodium iodide symporter); *SLC26A4*, Pendrin; *TG*, Thyroglobulin; *TIMP3*, TIMP Metallopeptidase inhibitor 3; *TP53*, Tumour protein 53; *TPO*, Thyroid peroxidase; *TRH*, Thyrotropin releasing hormone; *TSHR*, Thyroid stimulating hormone receptor]. SNV and InDel are presented in black and patterned grey, respectively.

variation, SNV and InDel, in *PIK3CA* and *TSHR* genes. Alterations in *ADCY10*, *CALCA*, *CDKN1A*, *CTNNB1*, *KISSR1*, *KRAS*, *KRT10*, *KRT19*, *LGALS3BP*, *MEN1*, *NKX2-1*, *NRAS*, *PAX8*, *PTH*, *RASSF1*, *SERPINA7*, *SLC5A5*, *TIMP3*, and *TRH* genes were detected as SNV in all of the patients with PTC and BTG. Figure 4.3B also shows that all patients with PTC and BTG had InDel variations in the *BRAF*, *PIK3CA*, *TP53*, and *TSR* genes and SNVs in *ADCY10*, *CALCA*, *CCDC6*, *CDKN1A*, *CTNNB1*, *EGF*, *GNAS*, *KRAS*, *KRT10*, *KRT19*, *LGALS3BP*, *MEN1*, *PIK3CA*, *PPARG*, *PTEN*, *PTH*, *RET*, *SLC26A4*, *TG*, *TPO*, *TRH*, and *TSHR*.

In the present study, novel variants detected in 12 out of the 36 genes (*BRAF*, *KRT10*, *LGALS3*, *PAX8*, *PIK3CA*, *RASSF1*, *RET*, *SLC26A4*, *TG*, *TPO*, *TRH*, and *TSHR*) in patients with PTC and BTG were further analysed (Figure 4.4). As shown in the Figure 4.4A, novel SNVs and InDels in the *BRAF*, *RET*, *TG*, *TPO*, and *TSHR* genes are located in both the exonic and intronic regions. However, SNVs of *PAX8* and *SLC26A4* were only detected in the intronic region. *PIK3CA* gene exhibited the most number of InDel variants, whilst *TG* showed the highest number of SNVs. The highest number of novel nucleotide transition were recorded in the *BRAF* gene. BGP4 has the highest number of novel SNVs present in *BRAF*, *KRT10*, *RASSF1*, *RET*, and *TG* genes (Figure 4.4B). Interestingly, a novel InDel variant was exclusively detected in the *LGALS3* of PCP5.

Among the previously described SNVs, 24 variants in 5 thyroid neoplasm-related genes, *RET*, *TG*, *TPO*, *TRH*, and *TSHR*, were consistently detected in patients with PTC and/or BTG (Figure 4.5). Fourteen out of the 24 of the variants were shared by both group of patients. Four of them are located in the exonic regions; two non-synonymous variants in the *TG* gene namely c.3082A>G (p.Met1028Val) and c.2200T>G (p.Ser734Ala); and another two in the *TSHR* gene namely the c.742C>A (p.Arg248Ser)

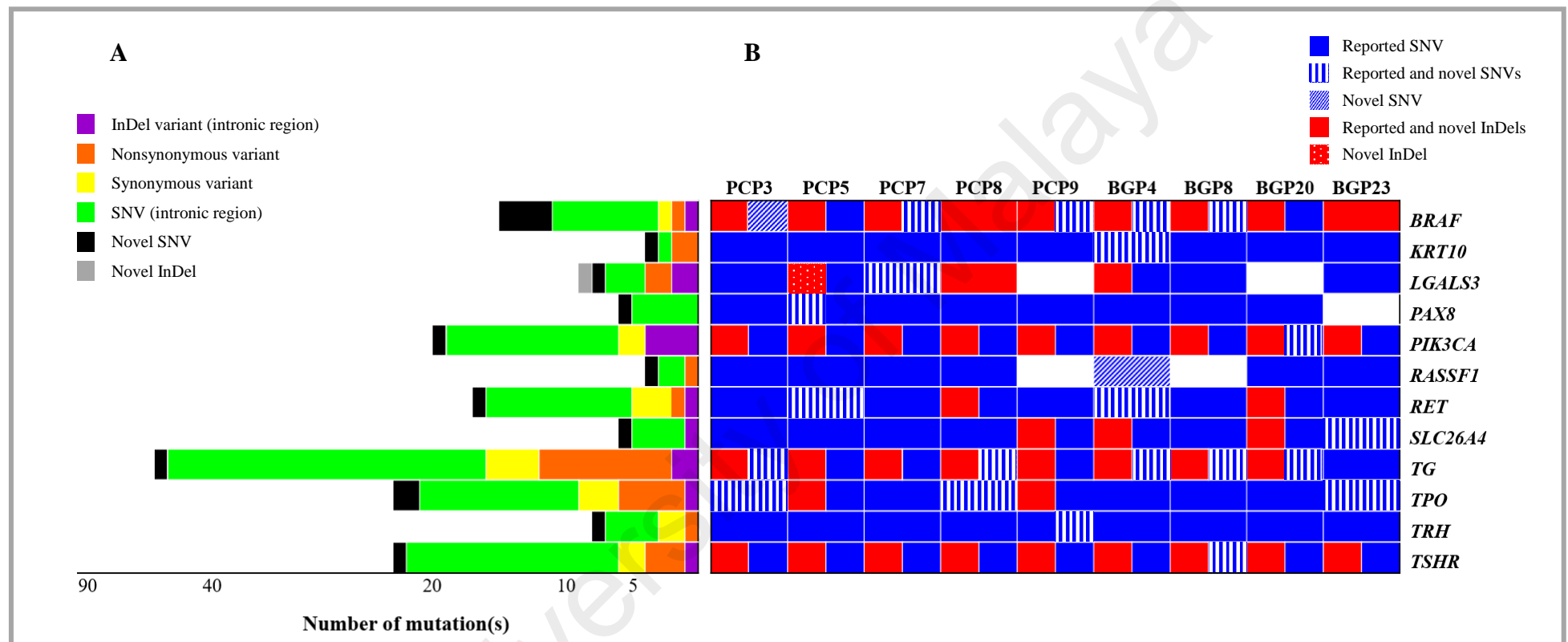


Figure 4.4: A summary of A) number of nucleotide alterations in the 12 thyroid neoplasm-related genes and B) distinct profiles of nucleotide alterations in patients with PTC and BTG

[Abbreviation: *BRAF*, V-raf murine sarcoma viral oncogene homolog b; *KRT10*, Keratin 10; *LGALS3*, Lectin, galactoside-binding, soluble, 3; *PAX8*, Paired box 8; *PIK3CA*, Phosphatidylinositol-4, 5-biphosphate 3-kinase, catalytic subunit alpha; *RASSF1*, Ras association domain-containing protein 1; *RET*, ret proto-oncogene; *SLC26A4*, Pendrin; *TG*, Thyroglobulin; *TPO*, Thyroid peroxidase; *TRH*, Thyrotropin releasing hormone; *TSHR*, Thyroid stimulating hormone receptor].

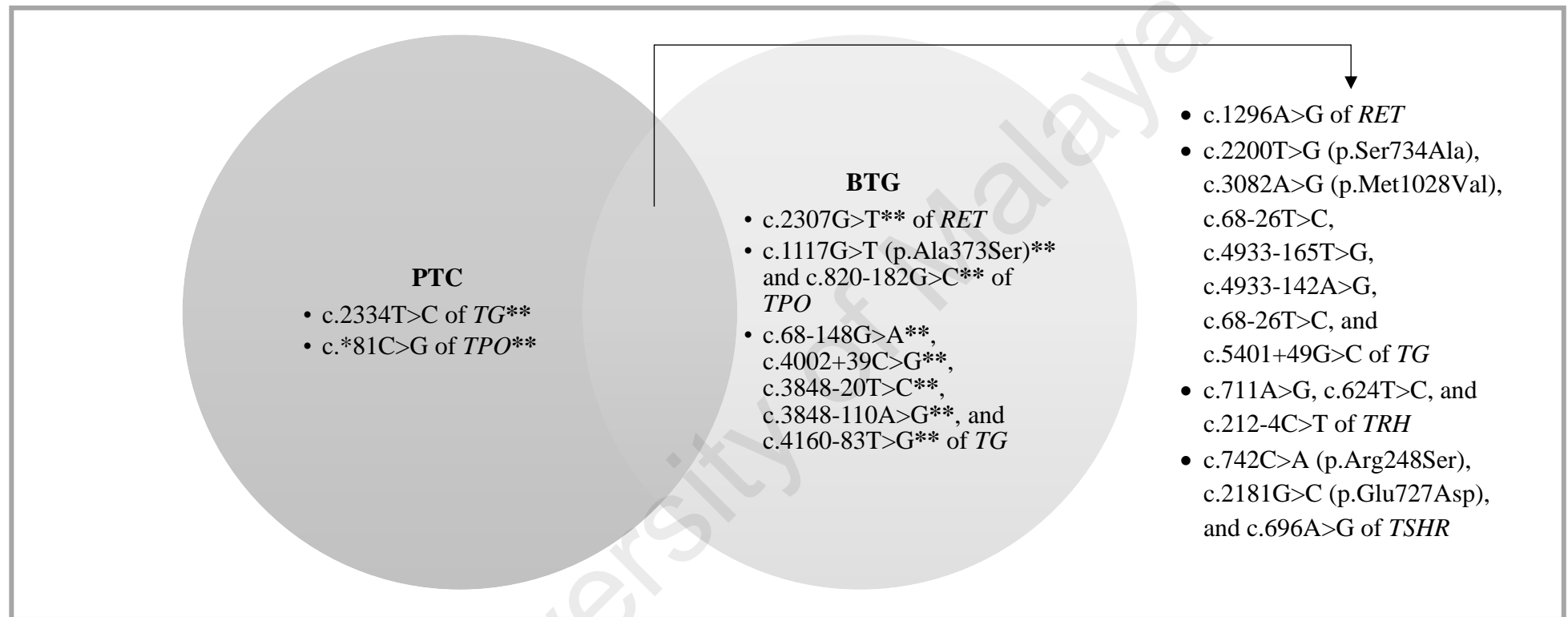


Figure 4.5: A Venn diagram to illustrate nucleotide variants that were detected in patients with PTC and BTG

Single asterisk (*) refers to a stop codon and double asterisk (**) denotes variants that were consistently identified in the respective group but not in the other group. [Abbreviation: *RET*, ret proto-oncogene; *TG*, Thyroglobulin; *TPO*, Thyroid peroxidase; *TRH*, Thyrotropin releasing hormone; *TSHR*, Thyroid stimulating hormone receptor].

and c.2181G>C (p.Glu727Asp).

In addition, synonymous variants c.711A>G and c.624T>C of *TRH*, c.1296A>G of *RET*, and c.696A>G were also present in the *TSHR* gene in both group of patients. The six intronic mutations were c.212-4C>T in the *TRH* and c.68-26T>C, c.4933-165T>G, c.4933-142A>G, c.68-26T>C, c.5401+49G>C in the *TG* genes. Variants consistently found in patients with BTG were c.820-182G>C of *TPO* as well as c.68-148G>A, c.4002+39C>G, c.3848-20T>C, c.3848-110A>G and c.4160-83T>G of mutation of *TG*, whilst the c.2334T>C of *TG* and c.*81C>G of *TPO* were detected in the malignant tissues.

Details of the reported variants found in the patients with PTC and BTG are presented in Appendices E-W.

4.1.2 Genetic susceptibility of *RET*, *TG*, *TPO* and *TSHR* genes polymorphisms on PTC and BTG

A total of five patients with PTC as well as four patients with BTG were included in the association study. Of the 24 SNVs from *RET*, *TG*, *TPO*, *TRH*, and *TSHR* genes, the genotypic frequency of only fourteen SNVs [c.2307G>T of *RET*, c.2200T>G (p.Ser734Ala), c.3082A>G (p.Met1028Val), c.68-148G>A, c.2334T>C, c.4002+39C>G, c.3848-20T>C, c.3848-110A>G, c.5401+49G>C, c.4933-165T>G, and c.4160-83T>G of *TG*, c.*81C>G of *TPO* as well as c.696A>G and c.742C>A (p.Arg248Ser) of *TSHR* genes] were consistent with the HWE in both the PTC and BTG patient subgroups. The distributions of genotypic and allelic frequencies of 14 SNVs from *RET*, *TG*, *TPO*, and *TSHR* genes in patients with PTC and BTG are tabulated in Table 4.2.

Table 4.2: Frequencies of selected SNVs genotypes and alleles in patients with PTC and BTG

Gene	SNV	Number of patients (%)		p value	Total haplotypes (%)		p value		
		PTC (n = 5)	BTG (n = 4)		PTC (n = 5)	BTG (n = 4)			
<i>RET</i>	c.2307G>T	Genotype			Allele				
		T T	0 (0%)	0 (0%)	0.17	T	8 (80%)	4 (50%)	0.32
		T G	2 (40%)	4 (100%)		G	2 (20%)	4 (50%)	
		G G	3 (60%)	0 (0%)					
	H-W, p = 1.00	H-W, p = 0.31							
<i>TG</i>	c.2200T>G (p.Ser734Ala)	Genotype			Allele				
		T T	3 (60%)	2 (50%)		T	6 (60%)	6 (75%)	0.64
		T G	0 (0%)	2 (50%)		G	4 (40%)	2 (25%)	
		G G	2 (40%)	0 (0%)	0.37				
	H-W, p = 0.05	H-W, p = 1.00							
<i>TG</i>	c.3082A>G (p.Met1028Val)	Genotype			Allele				
		A A	2 (40%)	2 (50%)	0.13	A	4 (40%)	6 (75%)	0.19
		A G	0 (0%)	2 (50%)		G	6 (60%)	2 (25%)	
		G G	3 (60%)	0 (0%)					
	H-W, p = 0.05	H-W, p = 1.00							
<i>TG</i>	c.68-148G>A	Genotype			Allele				
		G G	1 (20%)	0 (0%)	0.99	G	5 (50%)	4 (50%)	1.00
		G A	3 (60%)	4 (100%)		A	5 (50%)	4 (50%)	

Table 4.2, continued

Gene	SNV	Number of patients (%)		p value	Total haplotypes (%)		p value
		PTC (n = 5)	BTG (n = 4)		PTC (n = 5)	BTG (n = 4)	
<i>TG</i>	A A	1 (20%) H-W, p = 1.00	0 (0%) H-W, p = 0.34				
<i>TG</i>	c.2334T>C	Genotype T T T C C C H-W, p = 1.00	Genotype 2 (40%) 2 (50%) 2 (50%) 0 (0%) H-W, p = 1.00	p value 0.99	Allele T C	Total haplotypes (%) 7 (70%) 3 (30%) 6 (75%) 2 (25%)	p value 1.00
<i>TG</i>	c.4002+39C>G	Genotype G G G C C C H-W, p = 0.33	Genotype 3 (60%) 1 (20%) 1 (20%) 0 (0%) 3 (75%) 1 (25%) H-W, p = 1.00	p value 0.19	Allele G C	Total haplotypes (%) 7 (70%) 3 (30%) 3 (37.5%) 5 (62.5%)	p value 0.34
<i>TG</i>	c.3848-20T>C	Genotype C C C T T T H-W, p = 0.33	Genotype 3 (60%) 1 (20%) 1 (20%) 0 (0%) 3 (75%) 1 (25%) H-W, p = 1.00	p value 0.19	Allele C T	Total haplotypes (%) 7 (70%) 3 (30%) 3 (37.5%) 5 (62.5%)	p value 0.34
<i>TG</i>	c.3848-110A>G	Genotype G G G A	Genotype 3 (60%) 1 (20%) 0 (0%) 3 (75%)	p value 0.19	Allele G A	Total haplotypes (%) 7 (70%) 3 (30%) 3 (37.5%) 5 (62.5%)	p value 0.34

Table 4.2, continued

Gene	SNV	Number of patients (%)		p value	Total haplotypes (%)		p value
		PTC (n = 5)	BTG (n = 4)		PTC (n = 5)	BTG (n = 4)	
<i>TG</i>	A A	1 (20%) H-W, p = 0.33	1 (25%) H-W, p = 1.00				
<i>TG</i>	c.5401+49G>C	Genotype G G G C C C H-W, p = 1.00	Genotype 1 (25%) 3 (75%) 0 (0%) H-W, p = 1.00	0.52	Allele G C	8 (80%) 2 (20%) 5 (62.5%) 3 (37.5%)	0.61
<i>TG</i>	c.4933-165T>G	Genotype G G G T T T H-W, p = 1.00	Genotype 1 (25%) 2 (50%) 1 (25%) H-W, p = 1.00	0.71	Allele G T	8 (80%) 2 (20%) 4 (50%) 4 (50%)	0.32
<i>TG</i>	c.4160-83T>G	Genotype G G G T T T H-W, p = 1.00	Genotype 0 (0%) 3 (75%) 1 (25%) H-W, p = 0.14	0.19	Allele G T	7 (70%) 3 (30%) 3 (37.5%) 5 (62.5%)	0.34
<i>TPO</i>	c.*81C>G	Genotype G G G C	Genotype 0 (0%) 4 (100%)	1.00	Allele G C	4 (40%) 6 (60%) 4 (50%) 4 (50%)	1.00

Table 4.2, continued

Gene	SNV	Number of patients (%)		p value	Total haplotypes (%)		p value		
		PTC (n = 5)	BTG (n = 4)		PTC (n = 5)	BTG (n = 4)			
<i>TPO</i>		C C	1 (20%) H-W, p = 0.11	0 (0%) H-W, p = 1.00					
<i>TSHR</i>	c.696A>G	Genotype							
		G G	0 (0%)	0 (0%)	0.17	G	2 (20%)	4 (50%)	0.32
		G A	2 (40%)	4 (100%)		A	8 (80%)	4 (50%)	
		A A	3 (60%)	0 (0%)					
			H-W, p = 0.05	H-W, p = 1.00					
<i>TSHR</i>	c.742C>A (p.Arg248Ser)	Genotype							
		A A	0 (0%)	0 (0%)	1.00	A	5 (50%)	4 (50%)	1.00
		A C	5 (100%)	4 (100%)		C	5 (50%)	4 (50%)	
		C C	0 (0%)	0 (0%)					
			H-W, p = 1.00	H-W, p = 1.00					

Using the Fisher's exact test analysis, it was found that there was no significant association between *RET*, *TG*, *TPO*, and *TSHR* genotype and susceptibility to PTC and BTG (p value = 0.13 to 1.00). With respect to the alleles, the statistical test also resulted in no significant association between polymorphisms at the *RET*, *TG*, *TPO*, and *TSHR* loci and both thyroid neoplasm subgroups, PTC and BTG (p value = 0.13 to 1.00).

4.1.3 Characterisation of novel variants in the individual index patients

Table 4.3 shows novel nucleotide variants detected in the individual index patients. PCP3 is a heterozygote for four novel mutations; chr7:140477939C>G, which is located in intron 11 of the *BRAF* gene, chr8:133984762G>T and chr8:133984834C>T in intron 33 of the *TG* gene, and a non-synonymous c.1082G>T mutation in exon 8 of the *TPO* gene. The c.1082G>T mutation is expected to convert an arginine (R) to leucine (L) at amino acid 361 (p.Arg361Leu).

PCP5 carries a novel heterozygous c.19-50_53CTGdel mutation in intron 1 of the *LGALS3* gene. Deletion of the 3 nucleotides are expected to lead to a frame shift deletion in the *LGALS3* gene. Apart from the c.19-50_53CTGdel mutation, PCP5 is also a heterozygote for a novel c.894G>A mutation in exon 8 of the *PAX8* gene and chr10:43617643 G>A mutation in intron 16 of the *RET* gene.

In the case of PCP7, a novel chr7:140434597G>A in intron 17 of the *BRAF* gene was detected in the patient. It was revealed that PCP7 was a heterozygote for the mutation. A non-synonymous, heterozygous c.158C>A mutation was also detected in exon 3 of the *LGALS3* gene. The mutation is expected to change an alanine (A) to aspartic acid (D) at amino acid 53 (p.Ala53Asp).

Table 4.3: Summary of detected nucleotide variants of the candidate genes in patients with PTC and BTG

Patient	Gene	Location	Base Change	Variant Type	Variant Annotation
PCP3	<i>BRAF</i>	chr7:140477939 intron 11	C>G	SNV	n.a.
	<i>TG</i>	chr8:133984762 intron 33	G>T	SNV	n.a.
		chr8:133984834 intron 33	C>T	SNV	n.a.
	<i>TPO</i>	chr2:1481120 exon 8	G>T	non-synonymous	c.1082G>T p.Arg361Leu
PCP5	<i>LGALS3</i>	chr14:55604711 intron 1	CTG/-	frame shift deletion	c.19-50_53CTGdel
	<i>PAX8</i>	chr2:113994182 exon 8	C>T	synonymous	c.894G>A p.Val298Val
	<i>RET</i>	chr10:43617643 intron 16	G>A	SNV	n.a.
PCP7	<i>BRAF</i>	chr7:140434597 intron 17	G>A	SNV	n.a.
	<i>LGALS3</i>	chr14:55604902 exon 3	C>A	non-synonymous	c.158C>A p.Ala53Asp
PCP8	<i>TG</i>	chr8:133935658 exon 22	A>G	non-synonymous	c.4604A>G p.Asp1535Gly
		chr8:133920671 intron 18	A>T	SNV	n.a.
	<i>TPO</i>	chr2:1500368 exon 13	C>T	synonymous	c.1698C>T p.Asp566Asp
PCP9	<i>BRAF</i>	chr7:140434597 intron 17	G>A	SNV	n.a.

Table 4.3, continued

Patient	Gene	Location	Base Change	Variant Type	Variant Annotation
PCP9	<i>TRH</i>	chr3:129695683 exon 3	G>A	non-synonymous	c.353G>A p.Arg118Gln
BGP4	<i>BRAF</i>	chr7:140449357 intron 15	G>A	SNV	n.a.
	<i>KRT10</i>	chr17:389747824 intron 7	T>C	SNV	n.a.
	<i>RASSF1</i>	chr3:50375431 exon 2	A>C	non-synonymous	c.262A>C p.Thr88Pro
	<i>RET</i>	chr10:4359585 intron 1	G>T	SNV	n.a.
	<i>TG</i>	chr8:133981747 exon 32	T>C	non-synonymous	c.5908T>C p.Phe1970Leu
		chr8:133920671 intron 18	A>T	SNV	n.a.
BGP8	<i>BRAF</i>	chr7:140434586 intron 17	G>A	SNV	n.a.
	<i>TG</i>	chr8:133920671 intron 18	A>T	SNV	n.a.
		chr8:133935725 exon 22	G>A	synonymous	c.4671G>A p.Glu1557Glu
	<i>TSHR</i>	chr14:81609812 exon 10	C>T	synonymous	c.1410C>T p.Ile470Ile
BGP20	<i>PIK3CA</i>	chr3:178936810 intron 10	T>C	SNV	n.a.
	<i>TG</i>	chr8:133920671 intron 18	A>T	SNV	n.a.

Table 4.3, continued

Patient	Gene	Location	Base Change	Variant Type	Variant Annotation
BGP23	<i>SLC26A4</i>	chr7:107344934 intron 18	C>T	SNV	n.a.
	<i>TPO</i>	chr2:1481120 exon 8	G>T	non-synonymous	c.1082G>T p.Arg361Leu

As shown in the Table 4.3, PCP8 carries a heterozygous c.4604A>G mutation in exon 22 of the *TG*. The nucleotide transition was predicted to change an aspartic acid (D) to glycine (G) at codon 1535 (p.Asp1535Gly). The other novel mutations, c.1698C>T and chr8:133920671A>T were detected in exon 13 of the *TPO* and intron 18 of the *TG* gene, respectively.

In the case of PCP9, a heterozygous novel mutation in intron 17 of the *BRAF* gene (chr7:140434597G>A) and a nucleotide transition of G to A at cDNA position 353 (c.353G>A) of the *TRH* gene were detected. The c.353G>A mutation is predicted to change in amino acid at codon 118 from an arginine (R) to glutamine (Q) (p.Arg118Gln).

Using similar strategy, potential disease-causing variants in patients with BTG were filtered out from publically available databases. The novel variants that remained after filtering are detailed in Table 4.3. BGP4 was presented with nucleotide transition of T to C at cDNA position 5908 (c.5908T>C) in exon 32 of the *TG* gene. The non-synonymous mutation is predicted to change phenylalanine (F) to leucine (L) at amino acid 1970 (p.Phe1970Leu). Another novel non-synonymous, c.262A>C, was detected in the *RASSF1* of BGP4. The nucleotide change was predicted to cause an amino acid substitution of threonine (T) to proline (L) at amino acid 88 (p.Thr88Pro). The other four novel intronic mutations occurred in intron 15 of *BRAF* (chr7:140449357G>A), intron 7 of *KRT10* (chr17:389747824T>C), intron 1 of *RET* (chr10:4359585G>T), and intron 18 of *TG* (chr8:133920671A>T). WES has revealed that the patient was heterozygotes for all of the mutations.

As shown in the Table, BGP8 is a heterozygote for four novel mutations namely the chr7:140434586G>A in intron 17 of the *BRAF*, chr8:133920671A>T in intron 18 of the *TG*, a c.4671G>A in exon 22 of the *TG* and c.1410C>T in exon 10 of the *TSHR* genes.

For BGP20, a novel heterozygous chr3:178936810T>C which is located in intron 10 of *PIK3CA* gene was detected along with another novel mutation, chr8:133920671C>T in intron 18 of the *TG* gene.

One of the novel mutations, chr7:107344934C>T, which is located in intron of the *SLC26A4* gene, was detected in BGP23. Analysis of the benign tissue of BGP23 also revealed the presence of c.1082G>T change in the *TPO* gene which appeared to change an arginine (R) to leucine (L) at amino acid 361 (p.Arg361Leu). He was shown to carry the mutations in heterozygous form.

4.1.3.1 *In silico* analysis of the novel non-synonymous variants in the *LGALS3*, *RASSF1*, *TG*, *TPO*, and *TRH* genes

The c.158C>A variant in the *LGALS3* gene in PCP7 is predicted to change an alanine (A) to aspartic acid (D) at amino acid 53 (p.Ala53Asp). *In silico* evaluation using SIFT, PolyPhen2, and MutationTaster algorithms suggested that the substitution of Ala-53 to Asp-53 is “benign or tolerated” to the *LGALS3* protein activity. The complete analyses results are shown in Figures 4.6.

The c.262A>C variant in the *RASSF1* gene in BGP4 is expected to replace Thr with Pro at amino acid 88 (p.Thr88Pro). *In silico* analyses predicted that the variant is possibly damaging. The complete analyses results are shown in Figure 4.7.

The c.5908T>C mutation detected in the benign tissue of BGP4 suggested that the substitution of Phe-1970 to Leu-170 is probably damaging to the *TG* protein activity. The algorithm analyses using SIFT, PolyPhen2, and MutationTaster are summarised in Figure 4.8.

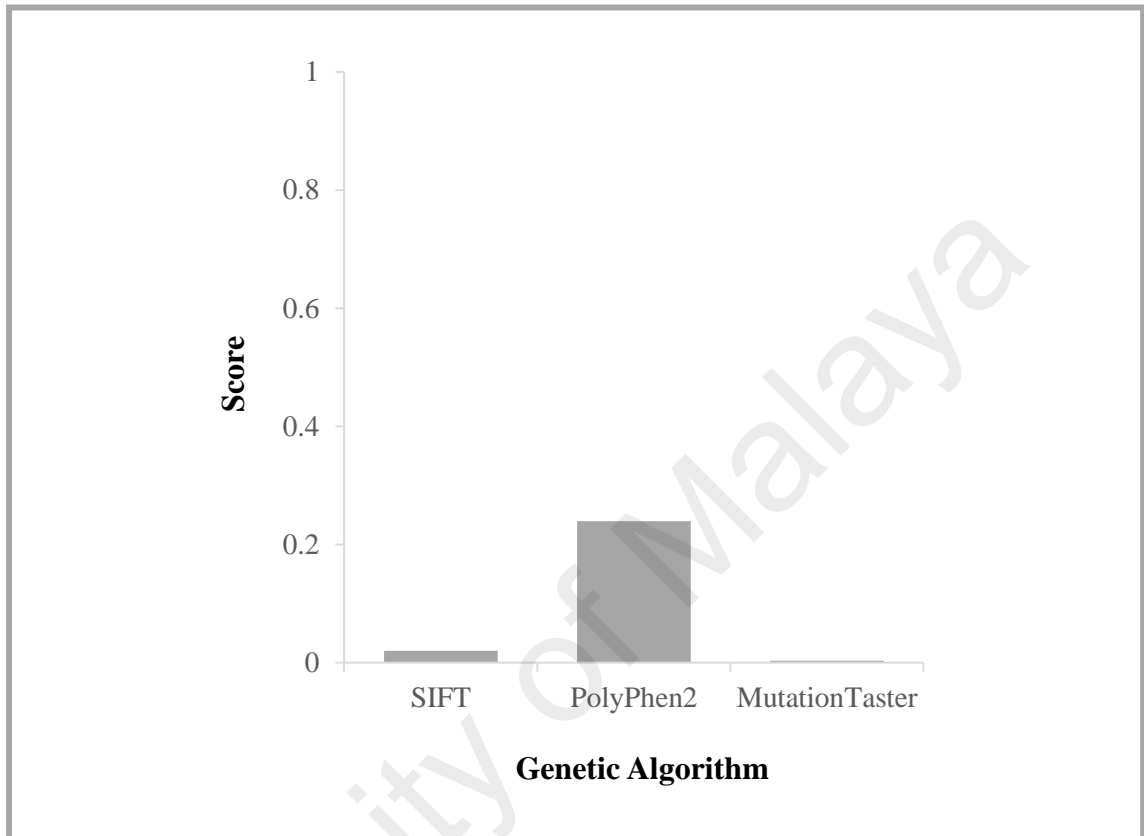


Figure 4.6: Genetic algorithm analysis of a novel variant c.158C>A (p.Ala53Asp) of *LGALS3* gene in a patient with PTC (PCP7)

The Sorting Intolerant From Tolerant (SIFT) score represents the probability that an amino acid substitution is damaging with value below or equal to 0.05 indicates that the mutation is “damaging”. A mutation is predicted to be “tolerated” if the score is more than 0.05. The Polymorphism Phenotyping v2 (PolyPhen2) score represents the probability that a substitution is damaging with value nearer 1 are more confidently predicted to be deleterious. A mutation is predicted to be probably damaging if the score is more than 0.85, possibly damaging if the score is in between 0.85 to 0.15, benign if the score is less than 0.15. The MutationTaster score predicts the disease potential of an alteration with score nearer to 1 has higher probability of pathogenicity.

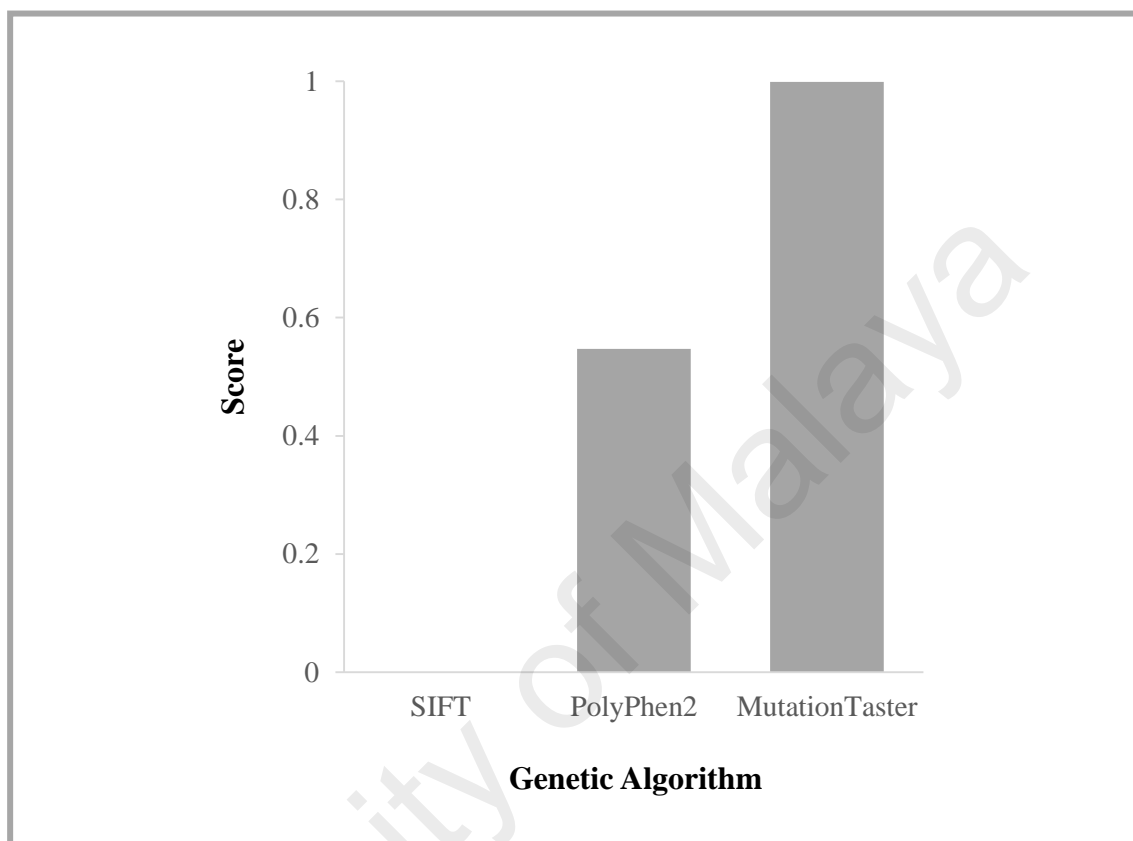


Figure 4.7: Genetic algorithm analysis of a novel variant c.262A>C (p.Thr88Pro) of *RASSF1* gene in a patient with BTG (BGP4)

The Sorting Intolerant From Tolerant (SIFT) score represents the probability that an amino acid substitution is damaging with value below or equal to 0.05 indicates that the mutation is “damaging”. A mutation is predicted to be “tolerated” if the score is more than 0.05. The Polymorphism Phenotyping v2 (PolyPhen2) score represents the probability that a substitution is damaging with value nearer 1 are more confidently predicted to be deleterious. A mutation is predicted to be probably damaging if the score is more than 0.85, possibly damaging if the score is in between 0.85 to 0.15, benign if the score is less than 0.15. The MutationTaster score predicts the disease potential of an alteration with score nearer to 1 has higher probability of pathogenicity.

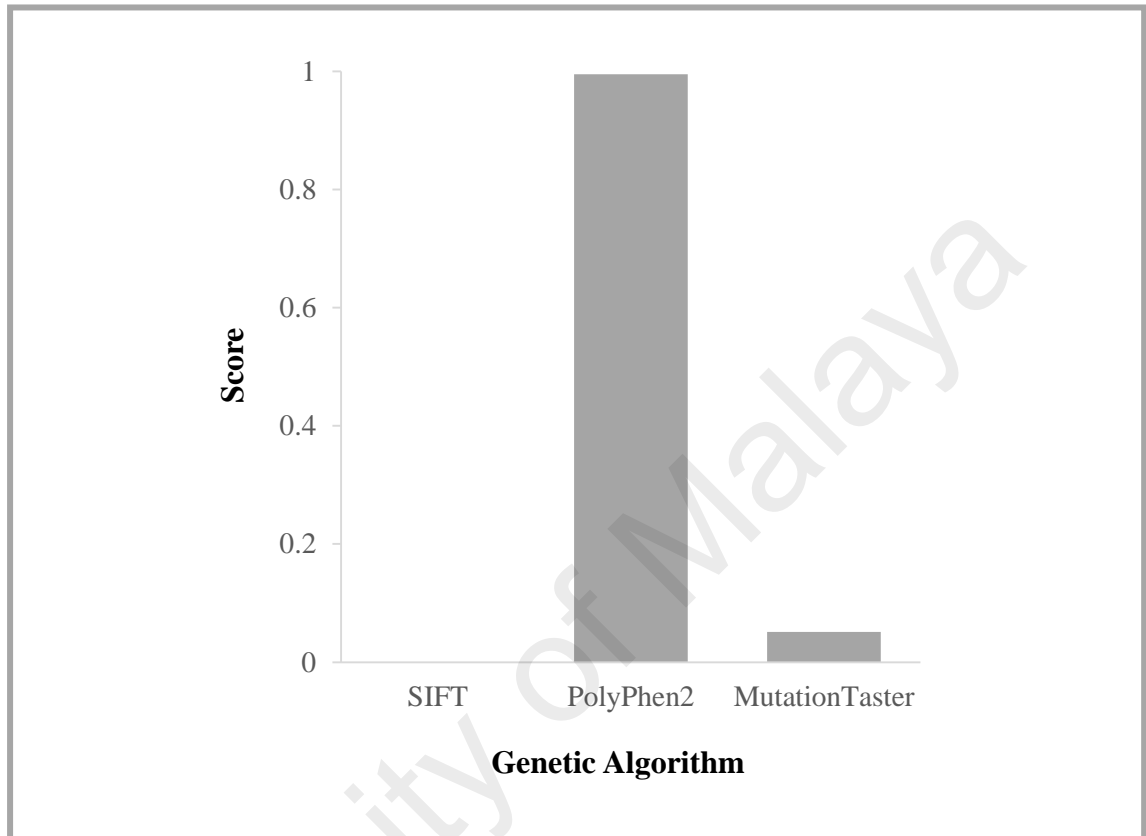


Figure 4.8: Genetic algorithm analysis of a novel variant c.5908T>C (p.Phe1970Leu) of *TG* gene in a patient with BTG (BGP4)

The Sorting Intolerant From Tolerant (SIFT) score represents the probability that an amino acid substitution is damaging with value below or equal to 0.05 indicates that the mutation is “damaging”. A mutation is predicted to be “tolerated” if the score is more than 0.05. The Polymorphism Phenotyping v2 (PolyPhen2) score represents the probability that a substitution is damaging with value nearer 1 are more confidently predicted to be deleterious. A mutation is predicted to be probably damaging if the score is more than 0.85, possibly damaging if the score is in between 0.85 to 0.15, benign if the score is less than 0.15. The MutationTaster score predicts the disease potential of an alteration with score nearer to 1 has higher probability of pathogenicity.

PCP8 was presented with c.4604A>G mutation in the *TG* gene. The effect of the substitution of Asp-1535 by glycine on *TG* activity was predicted to be damaging to the *TG* protein activity. The complete analyses results are shown in Figure 4.9.

PCP3 and BGP23 were presented with nucleotide transition of G to T at cDNA position 1082 (c.1082G>T) of the *TPO* gene. The algorithms predicted that substitutions of Arg-361 by a leucine (L) on protein activity is possibly damaging (Figure 4.10).

The c.353G>A mutation of *TRH* was predicted to change arginine (R) to glutamine (Q) at amino acid 118 (p.Arg118Gln). The effect of the substitution of Arg-118 by a glutamine on protein activity is probably damaging to the *TRH* protein activity. The algorithm analyses are summarised in Figure 4.11.

4.1.3.2 The effect of the novel mutations in the *BRAF*, *LGALS3*, *PAX8*, *PIK3CA*, *RET*, *SLC26A4*, *TG*, *TPO*, and *TSHR* genes on intronic splicing

Table 4.4 shows DNA sequencing results on the effect of novel exonic and intronic alterations namely chr7:140477939C>G and chr7:140434597G>A of *BRAF*, c.158C>A (p.Ala53Asp) of *LGALS3*, c.894G>A of *PAX8*, chr3:178936810T>C of *PIK3CA*, chr10:43617643G>A of *RET*, chr7:107344934C>T of *SLC26A4*, c.4604A>G (p.Asp1535Gly), c.4671G>A, chr8:133920671A>T, chr8:133984762G>T, and chr8:133984834C>T of *TG*, c.1082G>T (p.Arg361Leu), c.1698C>T of *TPO*, and c.1410C>T of *TSHR* on intronic splicing. Normal exon-exon junctions associated with the respective mutations were detected except for the c.19-50_53CTGdel of the *LGALS3* gene.

The novel mutation, c.19-50_53CTGdel, which is located in intron 3 of the *LGALS3* gene, was only detected in PCP5 (Figure 4.12A). Two amplicons of 412 bps

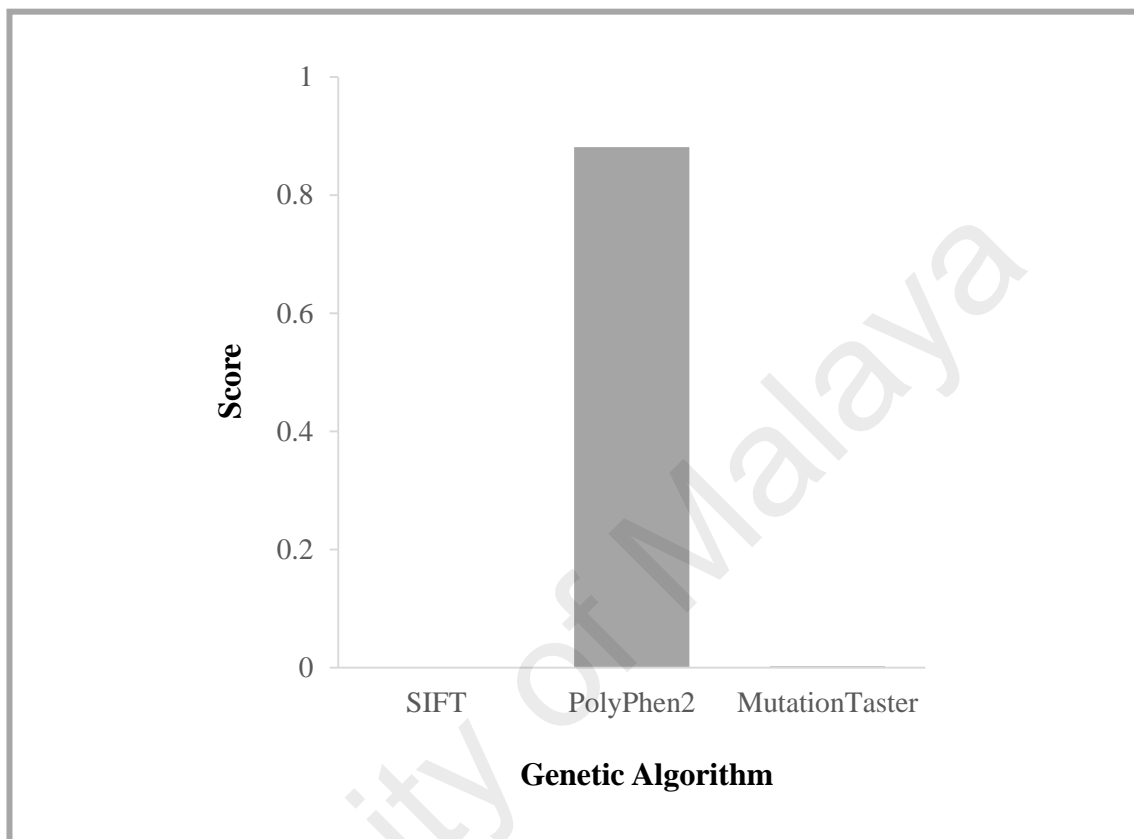


Figure 4.9: Genetic algorithm analysis of a novel variant c.4604A>G (p.Asp1535Gly) of *TG* gene in a patient with PTC (PCP8)

The Sorting Intolerant From Tolerant (SIFT) score represents the probability that an amino acid substitution is damaging with value below or equal to 0.05 indicates that the mutation is “damaging”. A mutation is predicted to be “tolerated” if the score is more than 0.05. The Polymorphism Phenotyping v2 (PolyPhen2) score represents the probability that a substitution is damaging with value nearer 1 are more confidently predicted to be deleterious. A mutation is predicted to be probably damaging if the score is more than 0.85, possibly damaging if the score is in between 0.85 to 0.15, benign if the score is less than 0.15. The MutationTaster score predicts the disease potential of an alteration with score nearer to 1 has higher probability of pathogenicity.

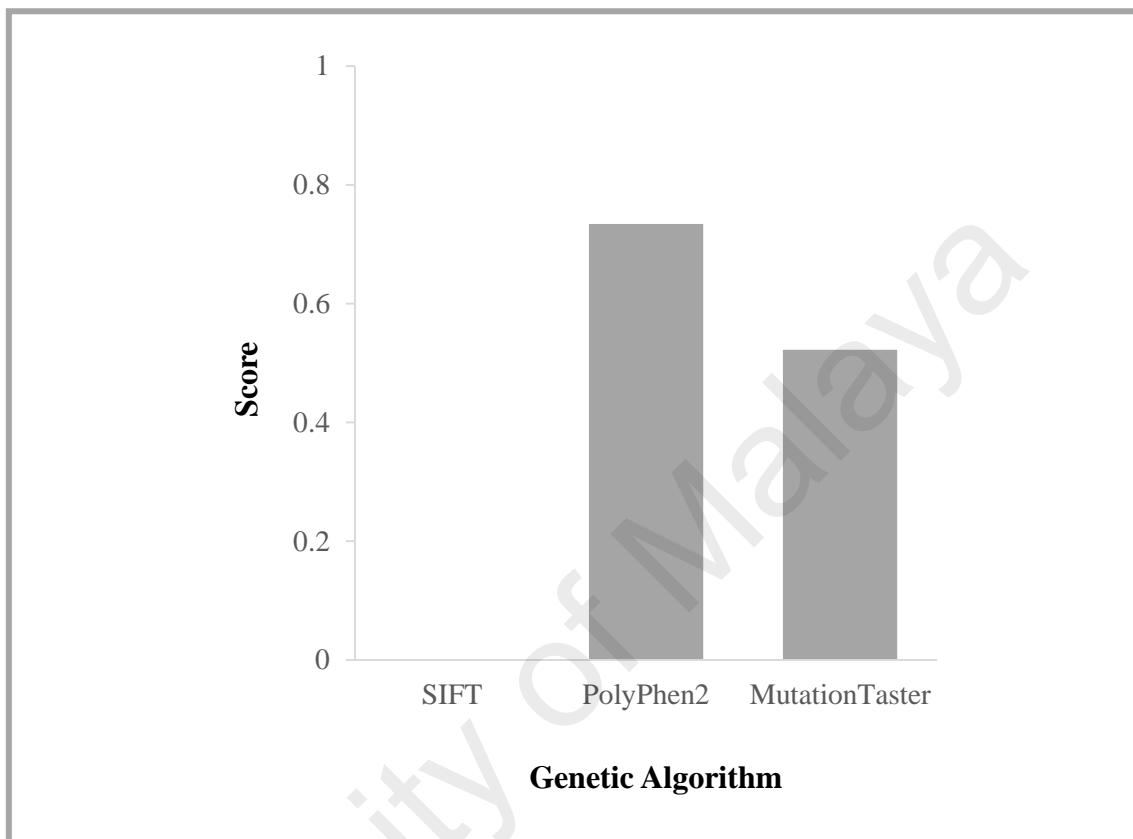


Figure 4.10: Genetic algorithm analysis of a novel variant c.1082G>T (p.Arg361Leu) of *TPO* gene in patients with PTC (PCP3) and those with BTG (BGP23)

The Sorting Intolerant From Tolerant (SIFT) score represents the probability that an amino acid substitution is damaging with value below or equal to 0.05 indicates that the mutation is “damaging”. A mutation is predicted to be “tolerated” if the score is more than 0.05. The Polymorphism Phenotyping v2 (PolyPhen2) score represents the probability that a substitution is damaging with value nearer 1 are more confidently predicted to be deleterious. A mutation is predicted to be probably damaging if the score is more than 0.85, possibly damaging if the score is in between 0.85 to 0.15, benign if the score is less than 0.15. The MutationTaster score predicts the disease potential of an alteration with score nearer to 1 has higher probability of pathogenicity.

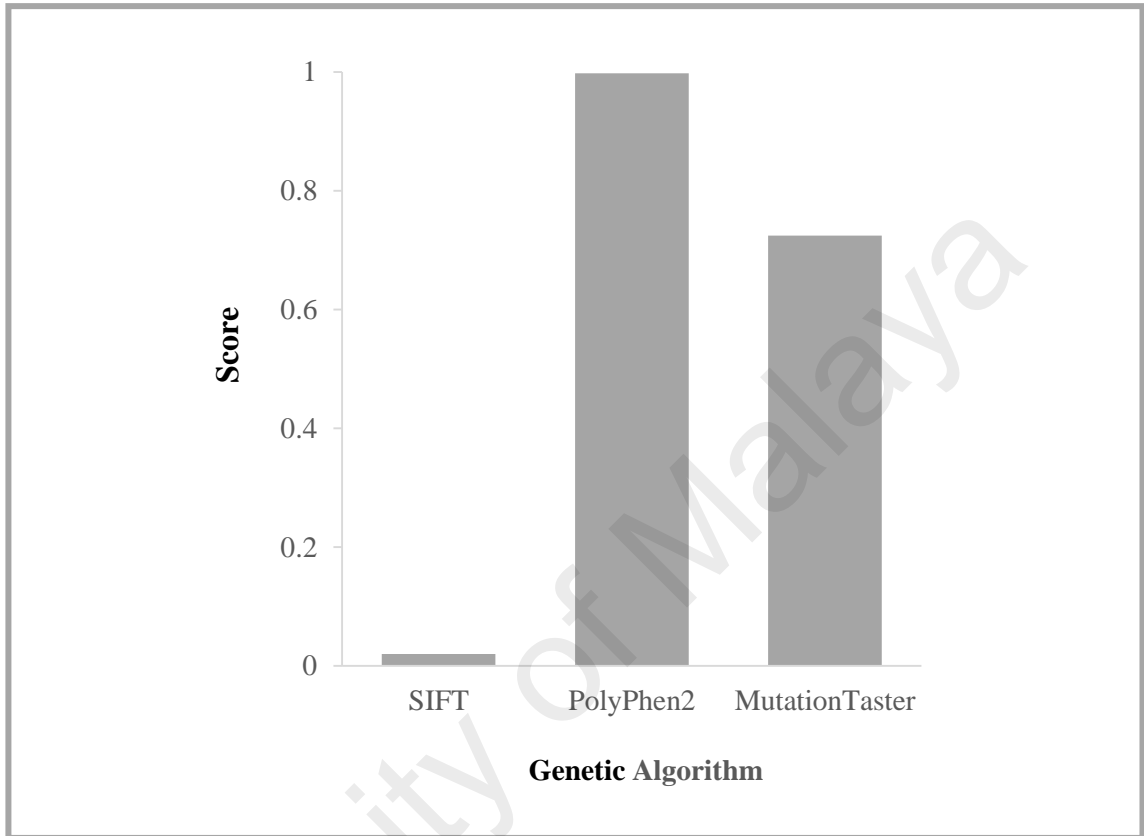


Figure 4.11: Algorithm analysis of a novel variant c.353G>A (p.Arg118Gln) of *TRH* gene in a patient with PTC (PCP9)

The Sorting Intolerant From Tolerant (SIFT) score represents the probability that an amino acid substitution is damaging with value below or equal to 0.05 indicates that the mutation is “damaging”. A mutation is predicted to be “tolerated” if the score is more than 0.05. The Polymorphism Phenotyping v2 (PolyPhen2) score represents the probability that a substitution is damaging with value nearer 1 are more confidently predicted to be deleterious. A mutation is predicted to be probably damaging if the score is more than 0.85, possibly damaging if the score is in between 0.85 to 0.15, benign if the score is less than 0.15. The MutationTaster score predicts the disease potential of an alteration with score nearer to 1 has higher probability of pathogenicity.

Table 4.4: The effect of the novel mutations in the *BRAF*, *LGALS3*, *PAX8*, *PIK3CA*, *RET*, *SLC26A4*, *TG*, *TPO*, and *TSHR* genes on intronic splicing

Gene	Patient	Variant location	Variant Annotation	Electropherogram	Exon-exon boundary	Forward (F) / Reverse (R) sequencing
<i>BRAF</i>	PCP3	chr7:140477939	C>G	<p>G G C A T G G T G A T G Exon 11 Exon 12</p>	11/12	F
<i>BRAF</i>	PCP7	chr7:140434597	G>A	<p>C C C C A A A T T C T C Exon 17 Exon 18</p>	17/18	F
<i>LGALS3</i>	PCP7	chr14:55604902	c.158C>A p.Ala53Asp	<p>C C A C C C A T T G T G Exon 3 Exon 4</p>	3/4	F
<i>PAX8</i>	PCP5	chr2:113994182	c.894G>A p.Val298Val	<p>G A G C A G G G C C T C Exon 7 Exon 8</p>	7/8	F

Table 4.4, continued

Gene	Patient	Variant location	Variant Annotation	Electropherogram	Exon-exon boundary	Forward (F) / Reverse (R) sequencing
<i>PIK3CA</i>	BGP20	chr3:178936810	T>C	<p>60 G T C A C A G A C A C T 70 Exon 10 Exon 11</p>	10/11	F
<i>RET</i>	PCP5	chr10:43617643	G>A	<p>30 A G T A T G T A T G G T Exon 16 Exon 17</p>	16/17	F
<i>SLC26A4</i>	BGP23	chr7:107344934	C>T	<p>10 T T C A G T A T T A T G Exon 18 Exon 19</p>	18/19	F
<i>TG</i>	PCP8, BGP8, and 20	chr8:133920671	A>T	<p>100 G A T C C A G G T G A A 110 Exon 18 Exon 19</p>	18/19	F

Table 4.4, continued

Gene	Patient	Variant location	Variant Annotation	Electropherogram	Exon-exon boundary	Forward (F) / Reverse (R) sequencing
<i>TG</i>	PCP8	chr8:133935658	c.4604A>G p.Asp1535Gly	<p>170 G T T T G A T G A T 180 G C Exon 22 Exon 23</p>	22/23	F
<i>TG</i>	BGP8	chr8:133935725	c.4671G>A p.Glu1557Glu	<p>G T T T G A 170 T G A T G C Exon 22 Exon 23</p>	22/23	F
<i>TG</i>	PCP3	chr8:133984762 chr8:133984834	G>T C>T	<p>T C A G G A 10 G T A G A G Exon 33 Exon 34</p>	33/34	F
<i>TPO</i>	BGP23	chr2:1481120	c.1082G>T p.Arg361Leu	<p>C A C C A G 320 A T C A T C Exon 8 Exon 9</p>	8/9	F

Table 4.4, continued

Gene	Patient	Variant location	Variant Annotation	Electropherogram	Exon-exon boundary	Forward (F) / Reverse (R) sequencing
<i>TPO</i>	PCP8	chr2:1500368	c.1698C>T p.Asp566Asp		13/14	F
<i>TSHR</i>	BGP8	chr14:81609812	c.1410C>T p.Ile470Ile		9/10	F

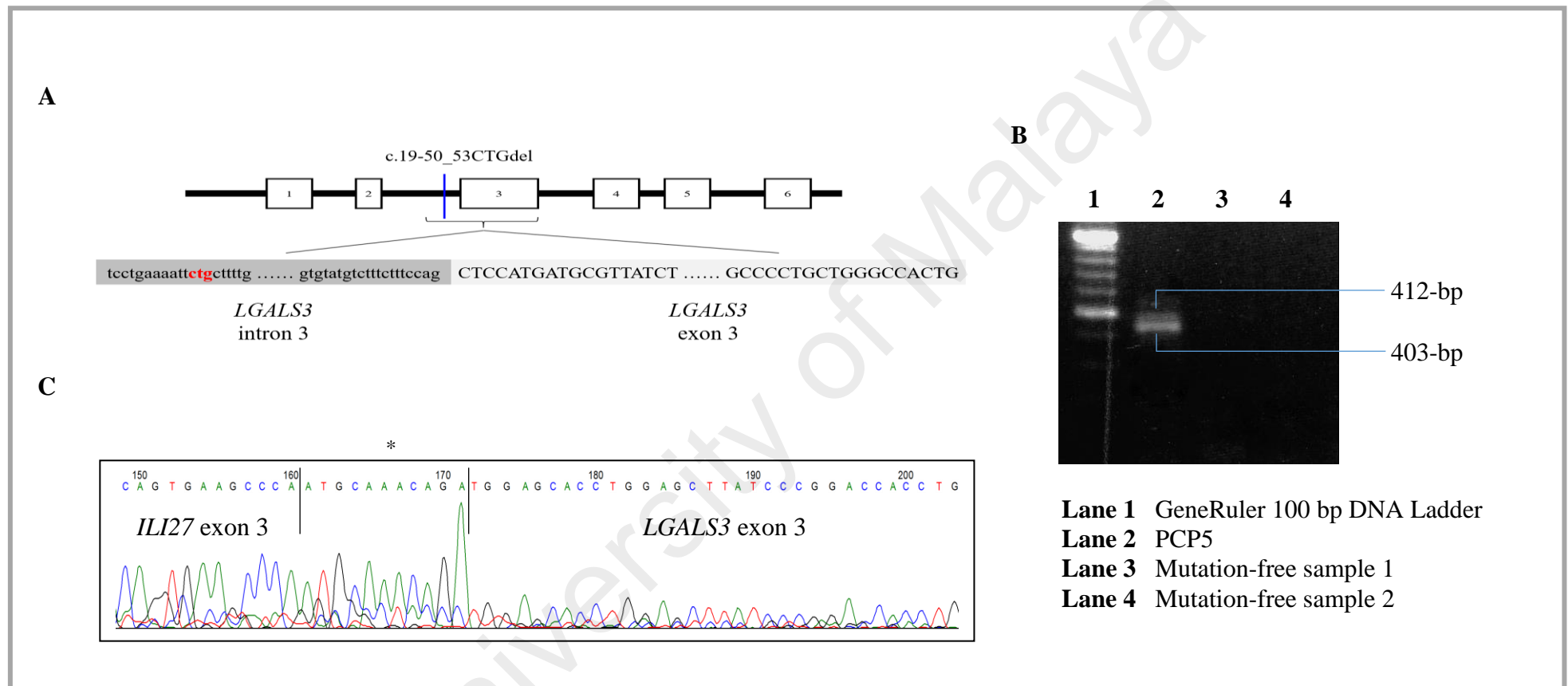


Figure 4.12: Transcript analysis of the *LGALS3* gene in a patient with PTC, PCP5, with a novel c.19-50_53CTGdel

A) A schematic diagram to illustrate the location of the c.19-50_53CTGdel mutation in intron 3, B) An agarose gel electrophoresis of PCR products, and C) A chromatography profile of cDNA showing exon-exon junction between *LGALS3* and *ILI27* genes. Single asterisk (*) denotes an unknown origin based on the public database.

and 403 bps were detected (Figure 4.12B). Sequence analysis of the cDNA revealed that the higher molecular weight band contained an additional sequence preceding the third exon of the *LGALS3* gene (Figure 4.12C). The additional sequence of 144-bps (ATCTGGAGAGTCCAGTTGCTCCCAGTGACTGCGGAATATCCACAAAGCTGCCGAAGCAACTCCGCCCCCATTGGCAATGGCCGCCGCGGACATCATCTTGGCTGCTATGGAGGACGAGGCGATTCCCGCCACAGTGAAGCCCA) originated from chr14:94582157 in exon 3 until chr14:94582799 in exon 4 of interferon, alpha-inducible protein 27 (*IFI27*) gene. Furthermore, the insertion was derived from the sequence corresponding to the minus strain of *IFI27*. An insertion of 11-bps (ATGCAAACAGA) between the fusion cDNA did not originate from the known reference sequences.

Transcription analysis of chr7:140449357G>A of *BRAF*, chr17:389747824T>C of *KRT10*, chr3:50375431A>C of *RASSF1*, chr10:4359585G>T of *RET*, chr8:133981747T>C and chr8:133920671A>T of *TG* mutations detected in the benign tissue of BGP4 could not be further validated due to low concentration of RNA.

4.1.4 Further evaluation on a novel c.353G>A (p.Arg118Gln) mutation in PCP9

The concurrent presence of a benign thyroid cyst and PTC in PCP9 provided an avenue to study the molecular differences between the two tissue areas. When DNA extracted from the benign thyroid cyst and PTC lesions of the patient were subjected to direct DNA sequencing, novel c.353G>A mutation in the *TRH* gene was detected only in the benign cyst (Figure 4.13). qRT-PCR analyses of selective genes, *BRAF*, *NIS*, *TG*, *TPO*, and *TSHR*, in the benign cyst, PTC lesion and three control tissues revealed that *NIS* transcript was not detected in both the benign and PTC tissues. Whilst *TG* was also not expressed in the PTC tissue, enhanced expression of *TG* relative to the controls was detected in the

benign cyst. The expression of *BRAF* and *TSHR* genes was relatively higher in the benign tissue compared to that of PTC. When compared with the three *BRAF* mutation-free control tissues, the benign cyst showed high expression of all the selected genes except *TPO*. However, only the expression of the *BRAF* gene in the PTC tissue was higher than that of the three control tissues (Figure 4.14).

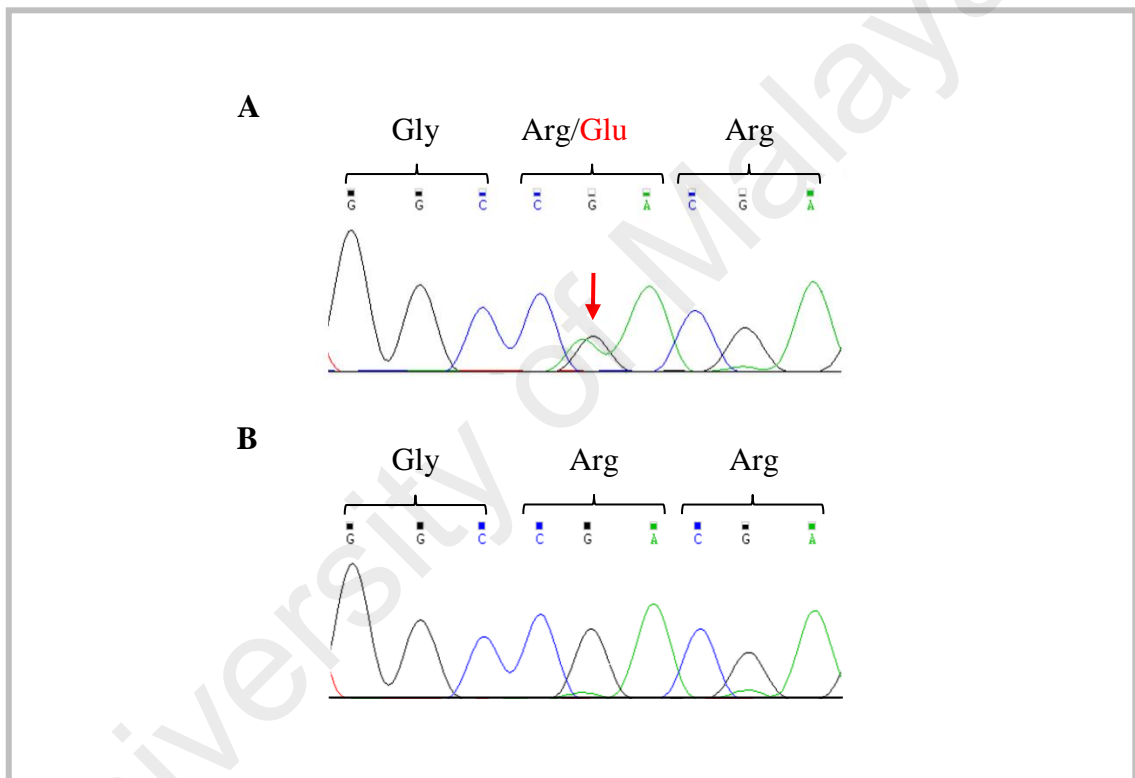


Figure 4.13: DNA sequencing electropherograms showing the A) c.353G>A (p.Arg118Gln) mutation in exon 3 of the *TRH* gene and B) wild type allele

The location of the nucleotide transition is indicated by red arrow.

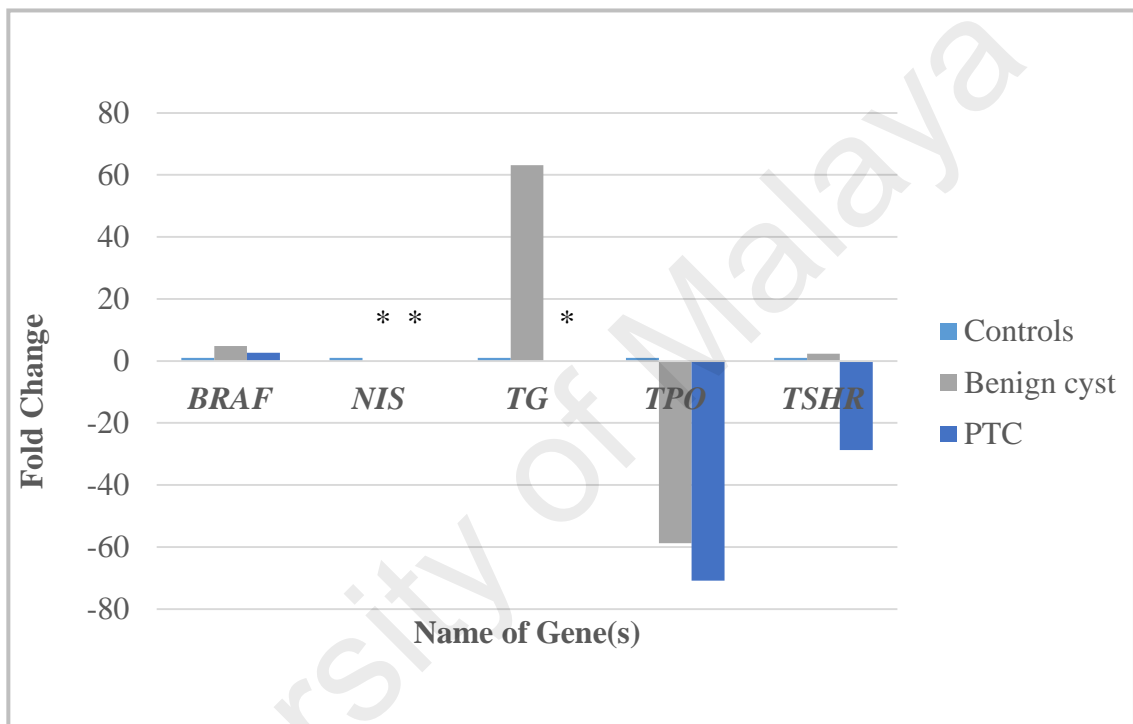


Figure 4.14: Real time PCR analysis

Comparison of the *BRAF*, *NIS*, *TG*, *TPO*, and *TSHR* gene expression level between benign cyst and lesion areas of thyroid tissue of PCP9. Single asterisk (*) denotes for undetected expression.

4.2 Proteomic Studies

Genomic alterations are believed to have an influence in the expression patterns of proteins that are related to the development and progression of PTC. In the initial part of the present study, WES analysis of extracted DNA from the malignant tissue of a patient with PTC revealed mutations of c.1799T>A (p.Val600Glu) and c.353G>A (p.Arg118Gln) in the *BRAF* and the *TRH* genes, respectively. When the benign cyst of the same patient was subjected to direct PCR screening for both the mutations, only the c.353G>A mutation of the *TRH* gene was detected. Furthermore, both the benign and malignant tissues also showed decrease or loss of expression of multiple iodide metabolism genes with elevated *BRAF* expression. Following up on these leads, two proteomics investigations were performed in the present study.

In the first proteomics study, the role of the altered expression of proteins in the benign cyst and PTC tissue of the same patient on the underlying mechanisms that led to the malignant transformation was initially evaluated using two-dimensional electrophoresis (2-DE). This was then followed by further data mining of proteins of altered abundances using Ingenuity Pathway Analysis (IPA). For confirmation of presence or absence of proteins in normal and lesion areas of the thyroid tissue, the extracted protein samples were also analysed by sodium dodecyl sulphate-polyacrylamide gel electrophoresis (SDS-PAGE) and Western blotting. The ultimate outcome of this integrated analysis may reflect the actual molecular events that underlie the pathophysiology of PTC.

In the second proteomics study, thyroid tissues and serum samples of patients with PTC but without a history of BTG (termed PTCa; n = 8), PTC patients with a background of BTG (termed PTCb; n = 6), and patients with BTG (n = 20), were analysed using similar gel-based proteomic analysis. Differences in the profiles of protein abundances

in PTCa and PTCb, relative to BTG, would form a preliminary reflection that the two thyroid cancers are etiologically and mechanistically different.

4.2.1 Protein profiles of concurrent benign thyroid cyst and malignant tissues of a patient with PTC

Considerable cases of PTC have been detected to arise from benign form goitres such as follicular adenoma, colloid nodules, benign cysts or nodular thyroiditis (Gandolfi et al., 2004, Hegedus et al., 2003, Sachmechi et al., 2000). A study carried out in Hospital Universiti Sains Malaysia (HUSM) from years 1994 to 2004 has also shown that 60% of thyroid cancer that were detected occurred with a background of prolonged goitre (Othman et al., 2009). In view of the increased risk of the Malaysian goitrous patients developing into thyroid cancer, a case of concurrent benign thyroid cyst and PTC was examined using gel-based proteomics with the aim of elucidating the molecular mechanisms underlying tumourigenesis of a long-standing thyroid nodule. A more detailed medical description of the patient is described in Section 3.2.2.

4.2.1.1 2-DE tissue profiles

Figure 4.35 shows representative protein profiles of the benign thyroid cyst and PTC tissues when analysed by 2-DE. Each tissue was analysed in triplicate to ensure reproducibility. Image analysis of silver stained gels showed an average of 670 and 668 spots from the benign cyst and PTC tissues, respectively. Only spots that appeared in all gel images from each tissue were compared and subjected to statistical analysis ($p < 0.01$). Quantitative analysis of the 2-DE gels revealed 27 proteins spots with more than 1.5 fold changes between the two tissues. Twenty-three of the spots, which comprised

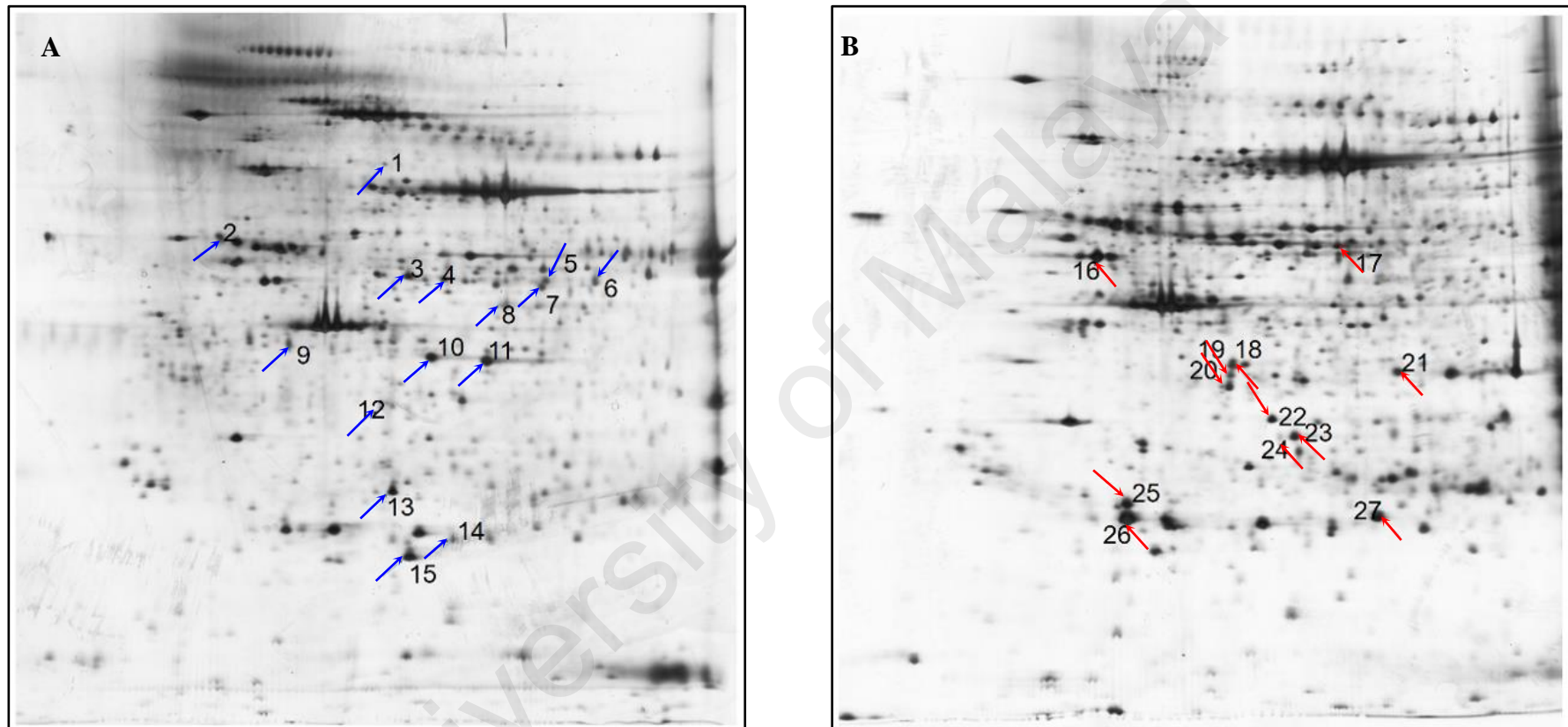


Figure 4.15: Representative 2-DE maps of benign thyroid cyst and PTC tissue

Figure demonstrates 2-DE maps of (A) benign thyroid cyst and (B) PTC tissue from the same patient. The proteins were separated on a pH 4-7 nonlinear IPG strip, followed by a 8-15% SDS-polyacrylamide gel. The gel was silver-stained and spots of altered abundance (indicated by arrows) were analysed by Q-TOF LC/MS. The acidic sides of the 2-DE gels are to the left and relative molecular mass declines from the top for all panels.

21 proteins, were subsequently identified by tandem mass spectrometry (MS/MS) and database query (Table 4.5).

4.2.1.2 Pathway interactions and biological process analysis

Analysis of the 21 proteins using IPA identified two associated “cancer, endocrine system disorders, organismal injury and abnormalities” (Figure 4.16, panel A) and “amino acid metabolism, small molecule biochemistry, nucleic acid metabolism” networks (Figure 4.16, panel B), with scores of 44 and 10, respectively. A score of 2 or higher indicates at least a 99% confidence of not being generated by random chance and higher scores indicate a greater confidence. Cancer related signalling pathways such as p38/ERK 1/2 MAPK, PKC(s), and Akt/NF- κ B pathways were shown in the “cancer, endocrine system disorders, organismal injury, and abnormalities” network.

Canonical pathway analysis ranked the “acute phase response signalling” at the top with the highest significance ($p < 6.85 \times 10^{-07}$) and indicated that this pathway was “activated” (z-score: 2) in the benign tissue. Other pathways, namely “coagulation system”, “extrinsic prothrombin activation pathway”, “intrinsic prothrombin activation pathway” and “G-protein signalling mediated by Tubby protein”, were particularly relevant to the data set but the activity patterns of these pathways were not available.

The five top-most predicted activated upstream regulators by z-score for the data set (using benign tissue as reference) were fenofibrate, PPARA, HRAS, D-glucose, and nitrofurantoin. However, none of these regulators was significantly “activated” (z-score ≥ 2.0) in the PTC tissue. In contrast, the five most predicted inhibited upstream regulators were PD98059, STAT3, L-triiodothyronine, MYC, and TP53. IL6 was ranked behind TP53 with a score of -1.341. Amongst these regulators, only PD98059 was significantly

Table 4.5: List of proteins with differential abundance identified by Q-TOF LC/MS

Spot No.	Anova Value	Fold Ratio	Tissue Proteins	SWISS PROT Acc. No.	Theoretical Mass (kDa)	MS/MS Search Score	Coverage (%) (Number of Peptide)
1	<0.001	6.51	Acylamino-acid-releasing enzyme (APEH)	P13798	82.19	40.83	4 (3)
2	<0.001	2.33	Alpha-1-antitrypsin (SERPINA1)	P01009	46906.80	125.07	28.7 (9)
3	<0.001	2.82	Fibrinogen gamma chain (FGG)	P02679	52.14	179.45	26.9 (11)
4	0.005	7.60	Fibrinogen gamma chain (FGG)	P02679	52.14	57.96	7.9 (4)
7	<0.001	13.57	4-trimethylaminobutyraldehyde dehydrogenase (ALDH9A1)	P49189	54.71	65.03	9.7 (5)
8	0.003	1.68	26S protease regulatory subunit 7 (PSMC2)	P35998	49.03	102.00	17.3 (7)
9	0.006	6.59	Haptoglobin (HP)	P00738	45.89	104.06	15.5 (6)
10	<0.001	10.49	Fibrinogen beta chain (FGB)	P02675	56611.80	275.42	40.9 (17)
11	<0.001	14.48	Fibrinogen beta chain (FGB)	P02675	56611.80	160.33	27.4 (11)
12	0.001	2.50	Guanine nucleotide-binding protein G(I)/G(S)/G(T) subunit beta-2 (GNB2)	P62879	38072.10	127.22	25.2 (8)
13	0.003	7.02	Prohibitin (PHB)	P35232	29.86	106.16	26.4 (7)

Table 4.5, continued

Spot No.	Anova Value	Fold Ratio	Tissue Proteins	SWISS PROT Acc. No.	Theoretical Mass (kDa)	MS/MS Search Score	Coverage (%) (Number of Peptide)
14	0.009	3.90	Thioredoxin-dependent peroxide reductase, mitochondrial (PRDX3)	P30048	28034.50	45.89	15.6 (4)
15	0.002	5.85	Peroxisredoxin-2 (PRDX2)	P32119	22062.70	126.14	36.8 (8)
16	0.009	-2.31	ATP synthase subunit beta, mitochondrial (ATP5B)	P06576	56558.90	311.99	40.2 (17)
17	0.003	-2.02	Selenium-binding protein 1 (SELENBP1)	Q13228	52960.50	150.42	25.4 (10)
18	0.002	-5.07	Actin, cytoplasmic 2 (ACTG1)	P63261	42134.40	57.41	9.8 (4)
20	<0.01	-2.84	Guanine nucleotide-binding protein G(I)/G(S)/G(T) subunit beta-1 (GNB1)	P62873	38175.10	98.75	22.3 (6)
21	0.003	-12.11	Annexin A1 (ANXA1)	P04083	38941.80	21.86	4.9 (2)
22	0.002	2.32	Annexin A3 (ANXA3)	P12429	36545.80	206.29	23.2 (13)
23	0.001	3.90	3-hydroxyisobutyrate dehydrogenase, mitochondrial (HIBADH)	P31937	35727.70	58.97	17.2 (4)

Table 4.5, continued

Spot No.	Anova Value	Fold Ratio	Tissue Proteins	SWISS PROT Acc. No.	Theoretical Mass (kDa)	MS/MS Search Score	Coverage (%) (Number of Peptide)
24	0.005	1.90	F-actin-capping protein subunit beta (CAPZB)	P47756	31635.20	67.03	16.2 (4)
25	0.007	-9.80	Cathepsin B (CTSB)	P07858	38790.80	67.75	14.7 (4)
26	0.007	-2.70	Apolipoprotein A-I (APOA1)	P02647	38790.80	117.35	28.8 (7)

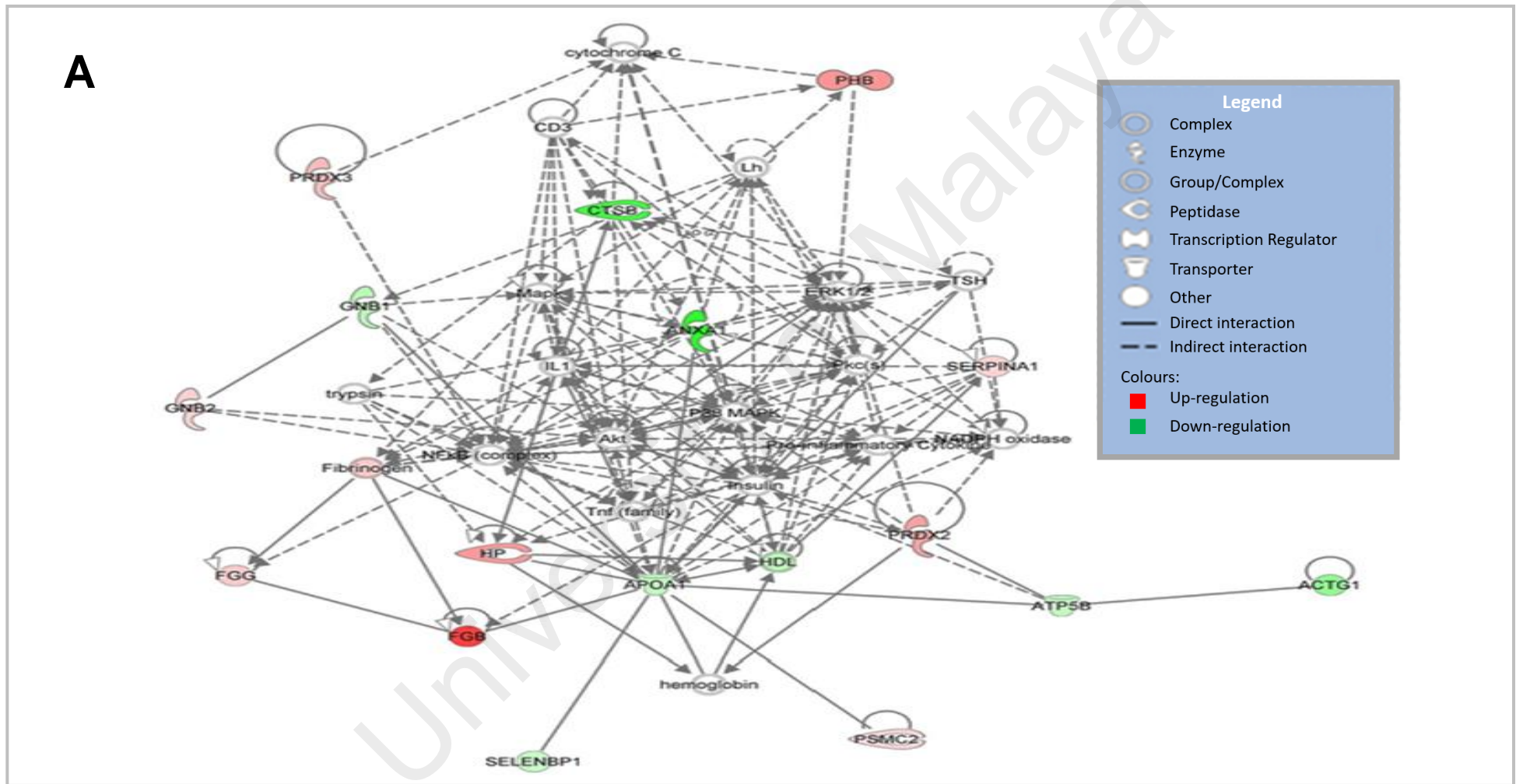


Figure 4.16: IPA graphical representation of the molecular relationships in A) “cancer, endocrine system disorders, organismal injury, and abnormalities” network and B) “amino acid metabolism, small molecule biochemistry, nuclei acid metabolism” network in benign cyst vs PTC tissues

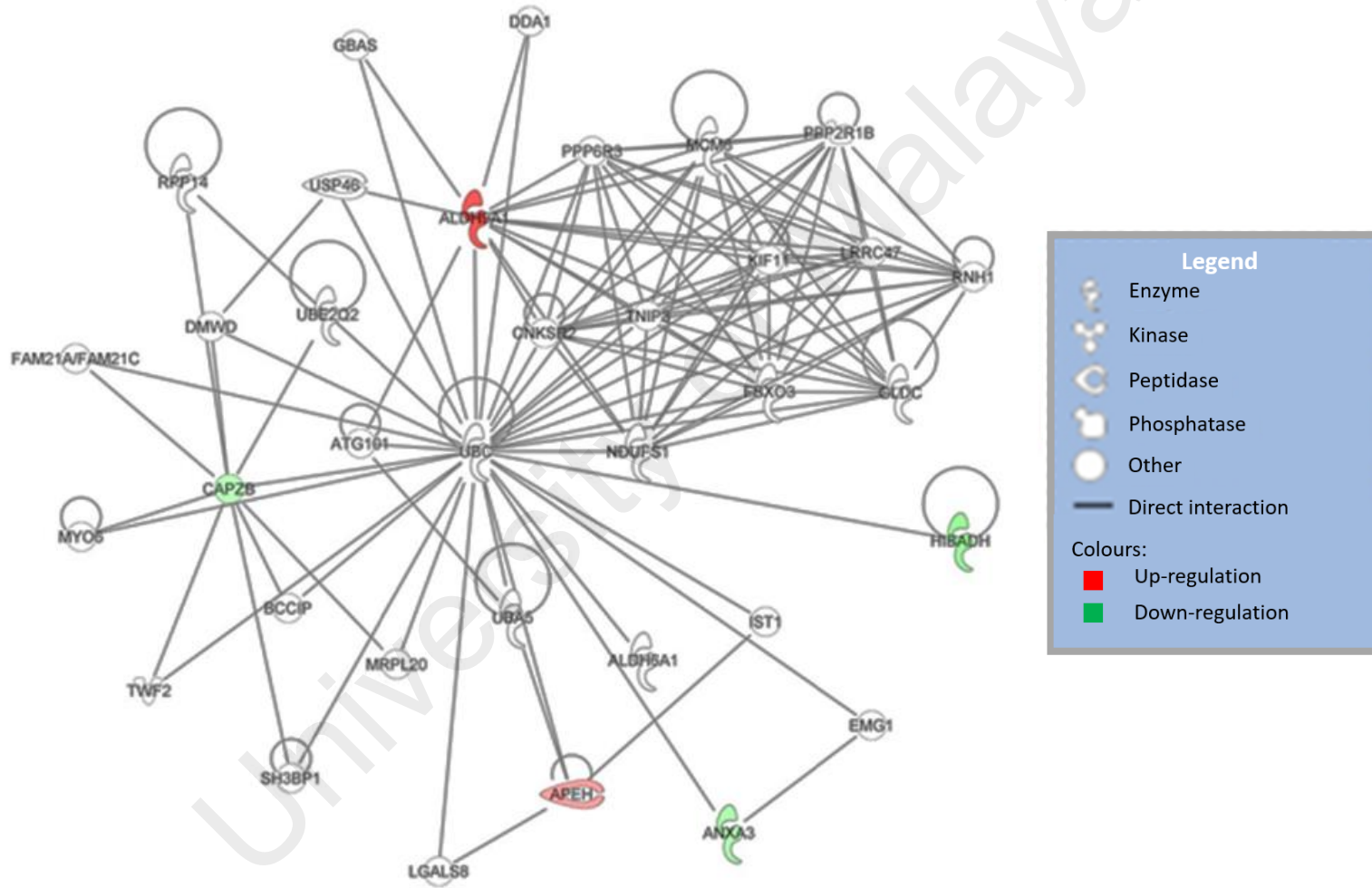
B

Figure 4.16, continued

Each network is displayed graphically as nodes (genes) and edges (the biological relationships between the nodes). Nodes in red indicate up-regulated genes while those in green represent down-regulated genes. Nodes without colours indicate unaltered expression. Various shapes of the nodes represent the functional class of the proteins. The different arrow shapes represent different types of interactions. Edges are displayed with various labels that describe the nature of the relationship between the nodes. [Abbreviation: ACTG1, Actin Gamma 1; ALDH5A1, Aldehyde Dehydrogenase 5 Family Member A1; ALDHA1, Aldehyde Dehydrogenase Isoform 1A1; ANXA1, Annexin A1; ANXA3, Annexin A3; APEH, Acylaminoacyl-Peptide Hydrolase; APOA4, Apolipoprotein A4; ATG101, Autophagy-Related Protein 101; ATP5B, Mitochondrial Membrane ATP Synthase; BCCIP, BRCA2 And CDKN1A Interacting Protein; CAPZB, F-actin-capping protein subunit beta; CD3, Cluster Of Differentiation E; CNKSR2, Connector Enhancer Of Kinase Suppressor Of Ras 2; CTSB, Cathepsin B; DDA1, DET1 And DDB1 Associated 1; DMWD, Dystrophia Myotonica WD Repeat-Containing Protein; EMG1, Ribosomal RNA Small Subunit Methyltransferase NEP1; ERK1/2, Extracellular Signal-Regulated Kinase 1 and 2; FAM21A/FAM21C, Family With Sequence Similarity 21, Member A/C; FGB, Fibrinogen Beta Chain; FGG, Fibrinogen Gamma Chain; GBAS, Glioblastoma Amplified Sequence; GLDC, Glycine Decarboxylase; GNB1, G Protein Subunit Beta 1; GNB2, G Protein Subunit Beta 2; HDL, High Density Lipoprotein; HIBADH, 3-Hydroxyisobutyrate Dehydrogenase; HP, Haptoglobin; IL1, Interleukin-1; IST1, Increased Sodium Tolerance 1 Homolog; KIF11, Kinesin Family Member 11; LGALS8, Lectin, Galactoside Binding Soluble 8; Lh, Luteinising Hormone; LRRC47, Leucine Rich Repeat Containing 47; Map, Mitogen-Activated Protein; MCM3, Minichromosome Maintenance Complex Component 3; MRPL20, Mitochondrial Ribosomal Protein L20; MYO5A, Myosin VA; NDUFS1, NADH Ubiquinone Oxidoreductase Core Subunit S1; NFKB, Nuclear Factor Kappa B; P38 MAPK, P38 Mitogen-Activated Protein Kinase 14; PHB, Prohibitin; PKC(s), Protein Kinase C; PPP2R1B, Protein Phosphatase 2 Regulatory Subunit A, Beta; PPP6R3, Protein Phosphatase 6 Regulatory Subunit 3; PRDX2, Peroxiredoxin 2; PRDX3, Peroxiredoxin 3; PSMC2, Proteasome 26S Subunit, Atpase 2; RNH1, Ribonuclease/Angiogenin Inhibitor 1; RPP14, Ribonuclease P/MRP Subunit P14; SELENBP1, Selenium Binding Protein 1; SERPINA1, Serpin peptidase inhibitor 1; SH3BP1, SH3 Domain Binding Protein 1; Tnf, Tumour Necrosis Factor; TNIP2, TNFAIP3 Interacting Protein 2; TSH, Thyroid Stimulating Hormone; TWF2, Twinfilin Actin Binding Protein 2; UBA5, Ubiquitin Like Modifier Activating Enzyme 5; UBC, Ubiquitin C; UBE2Q2, Ubiquitin Conjugating Enzyme E2 Q2; USP46, Ubiquitin Specific Peptidase 46].

“inhibited” in the PTC tissue with a score of less than -2. However, STAT3 was shown to be significantly activated (z-score ≥ 2.0) when cancer tissue was used as a reference gel in the comparison (Table 4.6).

For the diseases and functions analyses, benign cold thyroid nodule was the most relevant disease based on the data set with a p value of less than 5.28×10^{-07} . “Metabolism of carbohydrate”, “synthesis of lipid”, and “metabolism of protein” were likely to be activated in the PTC tissue. However, “necrosis of epithelial tissue”, “apoptosis”, “cell death”, and “necrosis” were likely to be inhibited in the benign tissue whilst “proliferation of cell” was likely to be activated (Table 4.7).

In addition, seven molecules namely, ANXA1, APOA1, HP, PHB, PRDX2, PRDX3, and SERPINA1, are apparently related to “free radical scavenging” including two potent scavengers of H_2O_2 namely PRDX2 and PRDX3, which are also an indication of oxidative stress (Table 4.8).

4.2.1.3 Quantitative western blot analysis of STAT3 phosphorylation

Western blot analysis of pY-STAT3 showed presence of two distinct 75 (predicted molecular weight: 88 kDa) and 28 kDa bands and one faint 67 kDa band in the benign cyst, whilst only the 75 and 67 kDa bands were detected in the PTC tissue. A distinct 42 kDa band which corresponds to beta-actin was observed in both tissues (Figure 4.17, panel A). Densitometric evaluation of the blots using Image-J algorithm showed similar total expression of pY-STAT3 in both the benign and PTC tissues. However, the 28 kDa pY-STAT3 fragment, which was termed STAT3 ϵ in the present study, was only expressed in the benign tissue. In contrast, the levels of the 75 and 67 kDa pY-STAT3 proteins found in the PTC tissue appeared 3- and 5-folds higher respectively, compared

Table 4.6: Upstream regulators predicted to be regulated in different tissues using IPA software

Upstream regulators	Gene symbol	Molecular type	Activation z-score ^a		Molecules
			PTC vs Benign	Benign vs PTC	
Interleukin 6	IL6	cytokine	-1.34	1.35	ANXA1, APOA1, FGB, FGG, HP, PHB, SERPINA1
V-myc avian myelocytomatosis viral oncogene homolog	MYC	transcription regulator	-1.73	1.73	CAPZB, CTSB, PHB, PRDX2, PRDX3, SERPINA1
Signal transducer and activator of transcription 3	STAT3	transcription regulator	-2.00	2.21	CTSB, FGB, FGG, HP, PHB, SERPINA1
L-triiodothyronine	T3	chemical-endogenous mammalian	-1.73	1.73	APOA1, HP, PRDX2, PRDX3
Tumour protein 53	TP53	transcription regulator	-1.50	1.50	ALDH9A1, ANXA1, ANXA3, APOA1, CTSB, PRDX2, PRDX3
PD98059	-	chemical-kinase inhibitor	-2.21	2.21	ANXA1, APOA1, CTSB, SELENBP1, SERPINA1
Fenofibrate	-	chemical drug	1.96	-1.96	APOA1, FGB, FGG, HP

Table 4.6, continued

Upstream regulators	Gene symbol	Molecular type	Activation z-score ^a		Molecules
			PTC vs Benign	Benign vs PTC	
Peroxisome proliferator-activated receptor alpha	PPARA	ligand-dependant nuclear receptor	1.29	-1.29	ALDH9A1, APOA1, ATP5B, FGB, FGG, SELENBP1
Harvey rat sarcoma viral oncogene homolog	HRAS	enzyme	1.00	-1.00	ANXA1, CTSB, HP, PHB
D-glucose	-	chemical drug	1.00	-1.00	ACTG1, ANXA3, ATP5B, CTSB
Nitrofurantoin	-	chemical-endogenous mammalian	0.82	-0.82	ACTG1, CTSB, FGB, PRDX2, SELENBP1, SERPINA1

^a Activation z-score of more than 2 is considered activated while less than -2 is considered inhibited. This score was generated by the IPA software.

Table 4.7: Prediction of disease or function annotation in different tissues using IPA software

Disease or function annotation	Activation z-score ^a		Molecules
	PTC vs Benign	Benign vs PTC	
Cell death and survival			
Apoptosis	1.65	-1.65	ANXA1, APOA1, CTSB, GNB2, PHB, PRDX2, PRDX3, SELENBP1, SERPINA1
Cell death	1.93	-1.93	ANXA1, APOA1, BRAF, CNB2, CTSB, PHB, PRDX2, PRDX3, SELENBP1, SERPINA1
Necrosis	1.30	-1.30	ANXA1, APOA1, CTSB, GNB2, PHB, PRDX2, PRDX3, SERPINA1
Necrosis of epithelial tissue	1.97	-1.97	CTSB, PRDX2, PRDX3, SERPINA1
Cellular growth and proliferation			
Proliferation of cell	-1.94	1.94	ACTG1, ANXA1, APOA1, ATP5B, BRAF, CTSB, GNB1, PHB, PRDX2, PRDX3, PSMC2, SELENBP1, SERPINA1, TG, TPO, TSHR
Cancer, organismal injury and abnormalities			
Growth of tumour	-1.49	1.49	ANXA1, APOA1, BRAF, CTSB, PHB, TG
Carbohydrate metabolism			
Metabolism of carbohydrate	1.98	-1.98	APOA1, CTSB, GNB1, PRDX2
Lipid metabolism and small molecule			
Synthesis of lipid	1.67	-1.67	ANXA1, APOA1, PHB, PRDX2, SERPINA1
Protein synthesis			
Metabolism of protein	1.10	-1.10	ANXA1, APEH, APOA1, CTSB, PSMC2, SERPINA1

^a Activation z-score of more than 2 is considered activated while less than -2 is considered inhibited. This score was generated by the IPA software.

Table 4.8: Involvement of the seven identified proteins in the free radical scavenging activity

Function Annotations	<i>p</i> value	Molecules
Metabolism of reactive oxygen species	2.12E ⁻⁰⁶	ANXA1, APOA1, HP, PHB, PRDX2*, PRDX3*, SERPINA1
Synthesis of reactive oxygen species	2.49E ⁻⁰⁵	ANXA1, APOA1, HP, PHB, PRDX2*, SERPINA1
Reduction of hydrogen peroxide	4.55E ⁻⁰⁵	PRDX2*, PRDX3*
Reduction of monohydroperoxylinoleic acid	3.10E ⁻⁰³	PRDX2*
Metabolite removal of superoxide	3.10E ⁻⁰²	PRDX2*

* An indication of oxidative stress level

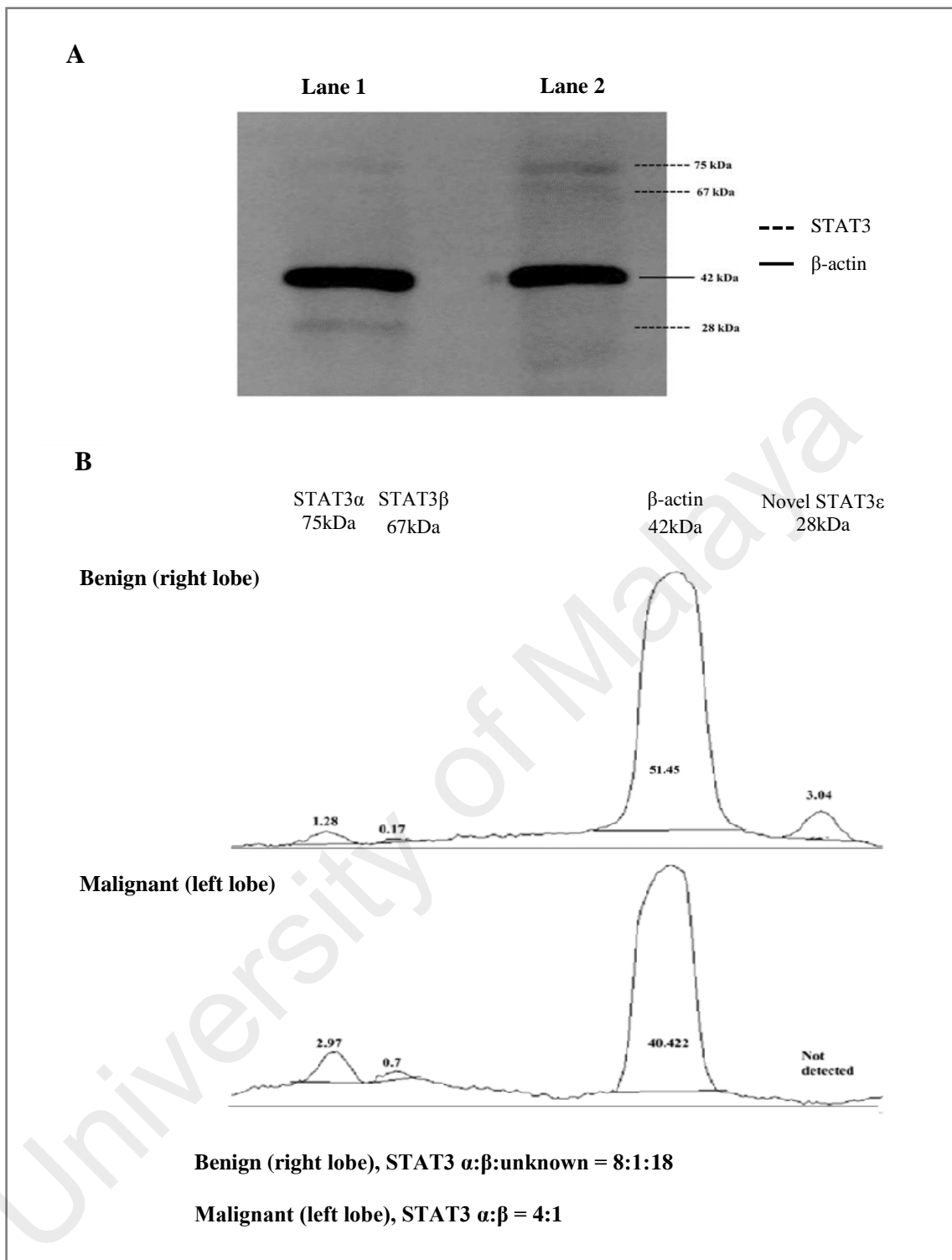


Figure 4.17: Western blot and Image-J densitometric analyses

Thyroid tissue protein samples were first tested with anti-pYSTAT3 antibody followed by anti- β actin antibody (loading control). Equal amount of microsomal protein (20 μ g) for each sample (100ng for the positive control) was used. A) Representative western blot gel picture: Lane 1: benign cyst protein sample; Lane 2: PTC protein sample and B) Image-J densitometric quantification of pY-STAT3 isoforms and β -actin in the benign cyst and PTC sample.

to the benign tissue. The three 75, 67, and 28 kDa variants of pY-STAT3 were expressed in ratio of 8:1:18 in the benign tissue, while the ratio of the 75 to 67 kDa pY-STAT3 variants was 4:1 in the malignant tissue (Figure 4.17, panel B).

4.2.2 Proteomic analyses of patients with BTG, PTCa, and PTCb

PTC is mainly diagnosed using fine-needle aspiration biopsy. This most common form of well-differentiated thyroid cancer occurs with or without a background of BTG. In the present study, a gel-based proteomics analysis was performed to analyse the expression of proteins in tissue and serum samples of PTC patients with (PTCb; n = 6) and without a history of BTG (PTCa; n = 8) relative to patients with BTG (n = 20). This was followed by confirmation of the levels of proteins which showed significant altered abundances of more than two-fold difference ($p < 0.01$) in the tissue and serum samples of the same subjects using ELISA.

4.2.2.1 2-DE tissue profiles

Separation of thyroid tissue samples from BTG (n = 20), PTCa (n = 8), and PTCb (n = 6) patients involved in the present study by 2-DE generated similar profiles. An average of 758 protein spots was matched when the 2-DE profiles of the patients were analysed using ImageMaster™ 2D Platinum software. Panels A, B, and C of Figure 4.18 demonstrate representative 2-DE gel images of patients with BTG, PTCa, and PTCb, respectively. Six protein spots, with altered abundance by more than 1.5 fold, were detected when 2-DE gels of PTCa and PTCb were compared with those of BTG. Analysis by Q-TOF LC/MS and database query identified the proteins as alpha-1 antitrypsin (A1AT; three different protein species), heat shock 70 kDa protein (HSP70), protein

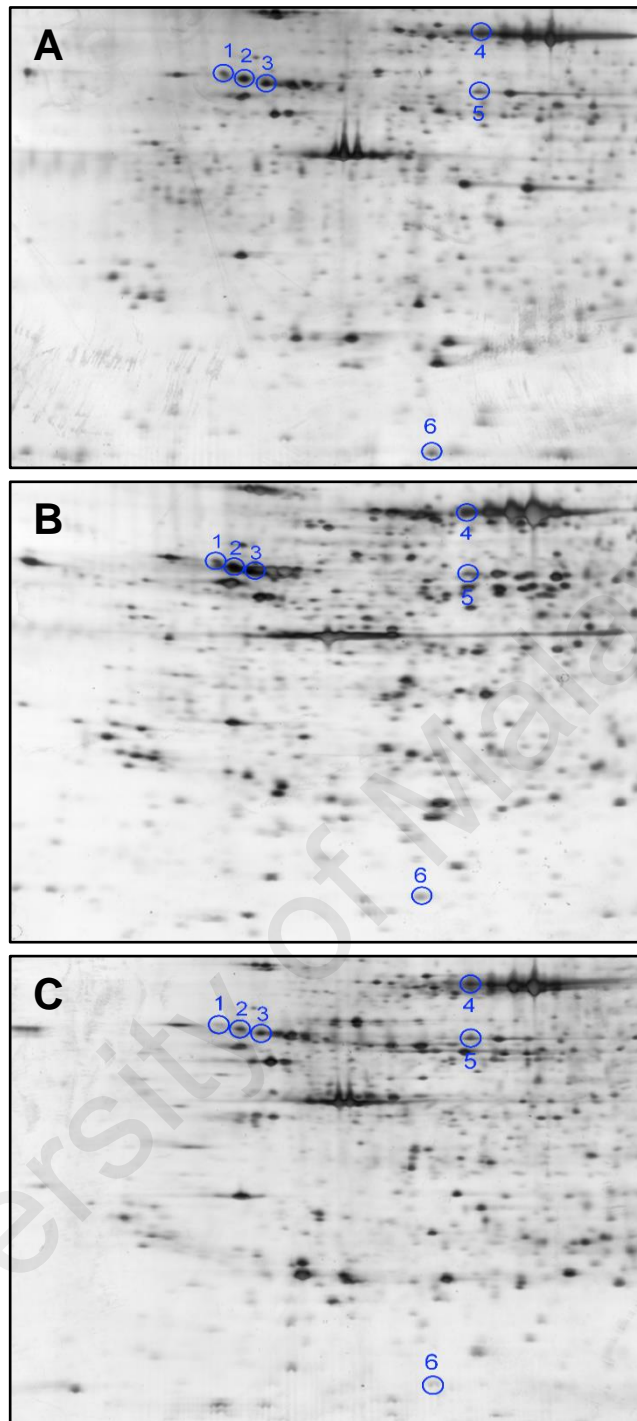


Figure 4.18: Representative 2-DE tissue protein profiles of BTG, PTCa, and PTCb patients

Tissue samples of (A) BTG (n = 20), (B) PTCa (n = 8), and (C) PTCb (n = 6) patients were subjected to 2-DE and silver staining. Spots circled in blue are those that showed significant differential abundance in PTCa and/or PTCb patients, relative to patients with BTG. For all panels, the acidic sides of the gels are to the left and relative molecular mass declines from the top.

disulfide isomerase (PDI), and ubiquitin-conjugating enzyme E2 N (UBE2N) (Table 4.9).

Figure 4.19 demonstrates the relative abundance of proteins that were significantly different ($p \leq 0.01$) in the thyroid tissues of patients with PTCa ($n = 8$) and PTCb ($n = 6$) compared to those with BTG ($n = 20$). Two protein spots of altered abundance, including higher levels of A1ATb ($p = 0.01$; f.c. = +1.5) and HSP70 ($p = 0.003$; f.c. = +2.3) were identified in the PTCa patients compared to those with BTG (panels A and B respectively). In the case of PTCb patients, the expression of A1ATb ($p = 0.002$; f.c. = -2.8), A1ATc ($p = 0.003$; f.c. = -2.4), A1ATd ($p = 0.008$; f.c. = -2.3), PDI ($p = 0.009$; f.c. = -2.0), and UBE2N ($p = 0.003$; f.c. = -2.1) was significantly lower than those of the BTG patients (panels C, D, E, F, and G, respectively).

4.2.2.2 2-DE serum profiles

Substantially less spots were resolved when serum samples of the same patients were analysed by 2-DE. The representative 2-DE serum protein profiles of patients with BTG (Panel A), PTCa (Panel B), and PTCb (Panel C) are shown in Figure 4.20. An average of 377 spots was matched when a total of 34 2-DE gels (BTG; $n = 20$; PTCa; $n = 8$; PTCb; $n = 6$) were analysed using ImageMaster™ 2D Platinum software. Among these, five demonstrated statistically significant variation ($p \leq 0.01$), with more than 1.5-fold difference of abundance.

Table 4.9: Identification of spots from 2-DE tissue proteins profiles using Q-TOF LC/MS

Spot No.	Tissue Proteins	SWISS PROT Acc. No.	Theoretical Mass (Da)	MS/MS Search Score	Coverage (%) (Number of Peptide)
1	Alpha-1 antitrypsin b (A1ATb)	P01009	46906.8	125.1	28.7 (9)
2	Alpha-1 antitrypsin c (A1ATc)	P01009	46906.8	127.3	19.8 (9)
3	Alpha-1 antitrypsin d (A1ATd)	P01009	46906.8	139.8	17.9 (9)
4	Heat shock 70 kDa protein (HSP70)	P08107	70336.2	90.8	10.2 (5)
5	Protein disulfide isomerase (PDI)	P30101	57180.7	259.9	33.8 (17)
6	Ubiquitin-conjugating enzyme E2 N (UBE2N)	P61088	17194.6	44.9	19.0 (3)

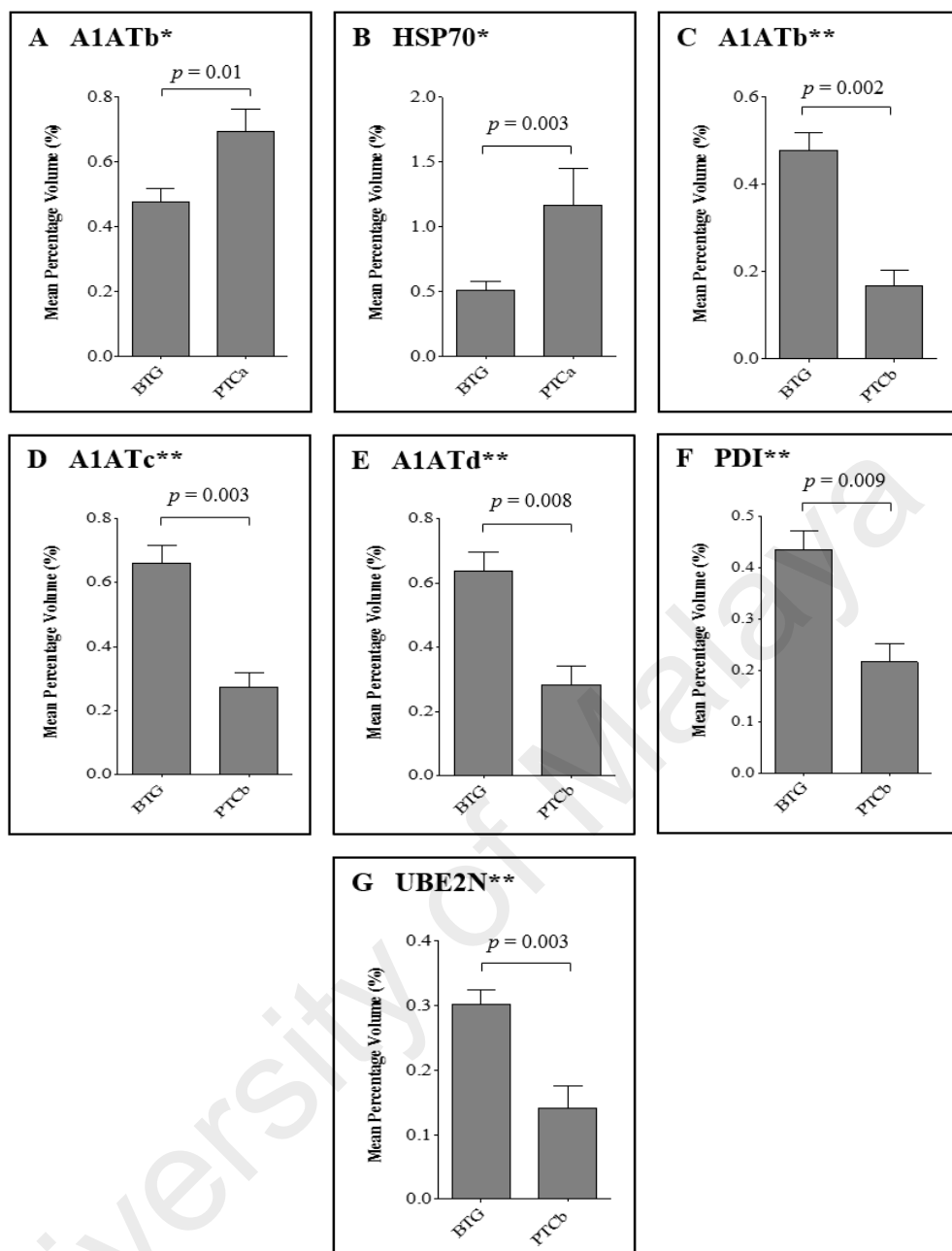


Figure 4.19: Percentage volume contribution of 2-DE tissue proteins that were differentially expressed in patients with BTG, PTCa, and PTCb

Percentage of volume contribution (%vol) of tissue protein spots was analysed using ImageMaster™ 2D Platinum software, version 7.0. Standard errors of the mean (SEM) were from biological replicates. Single asterisk (*) denotes differentially expressed proteins in PTCa patients (n = 8) compared to those with BTG (n = 20) and double asterisks (**) refer to proteins that were differentially expressed in PTCb (n = 6) compared to BTG (n = 20) patients.

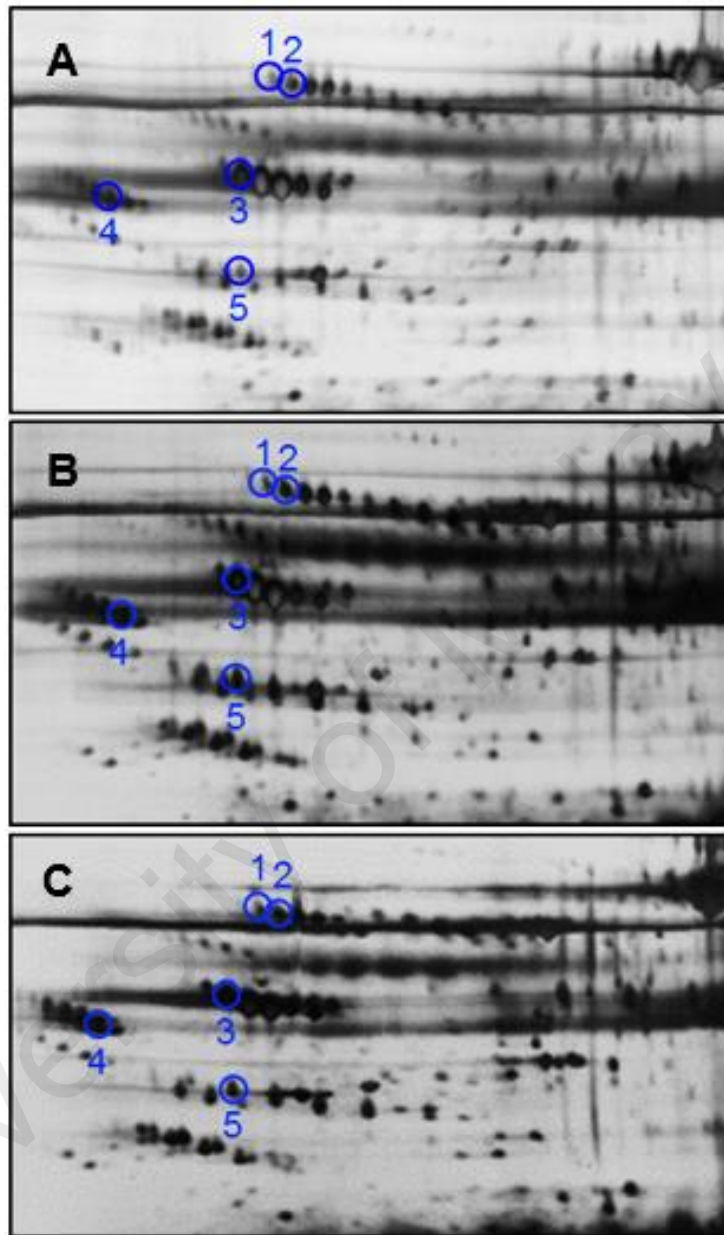


Figure 4.20: 2-DE analyses of serum proteins derived from BTG, PTCa, and PTCb patients

Serum samples of (A) BTG (n = 20), (B) PTCa (n = 8), and (C) PTCb (n = 6) patients were subjected to 2-DE and silver staining. Circles in blue refer to spots that showed differential abundance in PTCa and/or PTCb patients compared to those with BTG. The acidic sides of the 2-DE gels are to the left and relative molecular mass declines from the top for all panels.

Five spots of significant altered abundance were detected in the 2-DE profiles of PTCa or PTCb patients compared to those of patients with BTG. When the five protein spots of altered abundance were subjected to Q-TOF LC/MS analysis and database query, three were identified as A1AT, AHSG, and apolipoprotein A-IV (APOA4), whilst the other two spots were those of alpha 1-beta glycoprotein (A1B) (Table 4.10). Both protein species of A1B (A1Ba, $p = 0.008$; f.c. = +1.62, A1Bb, $p = 0.003$; f.c. = +1.82) and A1ATa ($p = 7.3E-04$; f.c. = +2.29) were apparently overexpressed in patients with PTCa compared to those with BTG (Figure 4.21, panels A, B and C) whilst patients with PTCb demonstrated higher expression of AHSG ($p = 0.006$; f.c. = +2.11) and APOA4 ($p = 0.009$; f.c. = +1.77) (Figure 4.21, panels D and E).

4.2.2.3 Analysis of tissue and serum proteins expression by ELISA

For confirmation of the detected proteins of altered abundances which showed more than two-fold difference ($p < 0.01$) in patients with PTCa and PTCb relative to BTG patients, ELISA was performed on the tissue and serum proteins (Figure 4.22). Our results indicate that the expression of tissue A1AT was significantly higher for PTCa but not significantly different for PTCb (panel A). In case of HSP70, ELISA was not able to detect significant differences of the tissue protein in both groups of patients with PTCa and PTCb compared to those with BTG (panel B). A1AT was also found to be significantly enhanced in the sera of patients with PTCa compared to those with BTG while its levels in PTCb patients appeared lower than those with BTG (panel C). Serum AHSG was enhanced in both PTCa and PTCb patients although significant difference was only detected in patients with PTCb (panel D).

Table 4.10: List of serum proteins with differential abundance identified by Q-TOF LC/MS

Spot No.	Serum Proteins	SWISS PROT Acc. No.	Theoretical Mass (Da)	MS/MS Search Score	Coverage (%) (Number of Peptide)
1	Alpha 1-beta glycoprotein a (A1Ba)	P04217	54823.0	140.7	24.4 (8)
2	Alpha 1-beta glycoprotein b (A1Bb)	P04217	54823.0	49.7	6.8 (3)
3	Alpha-1 antitrypsin a (A1ATa)	P01009	46906.8	308.5	45.2 (21)
4	Alpha-2-HS glycoprotein (AHSG)	P02765	40122.7	100.2	21.5 (6)
5	Apolipoprotein A-IV (APOA4)	P06727	45371.0	61.4	10.1 (4)

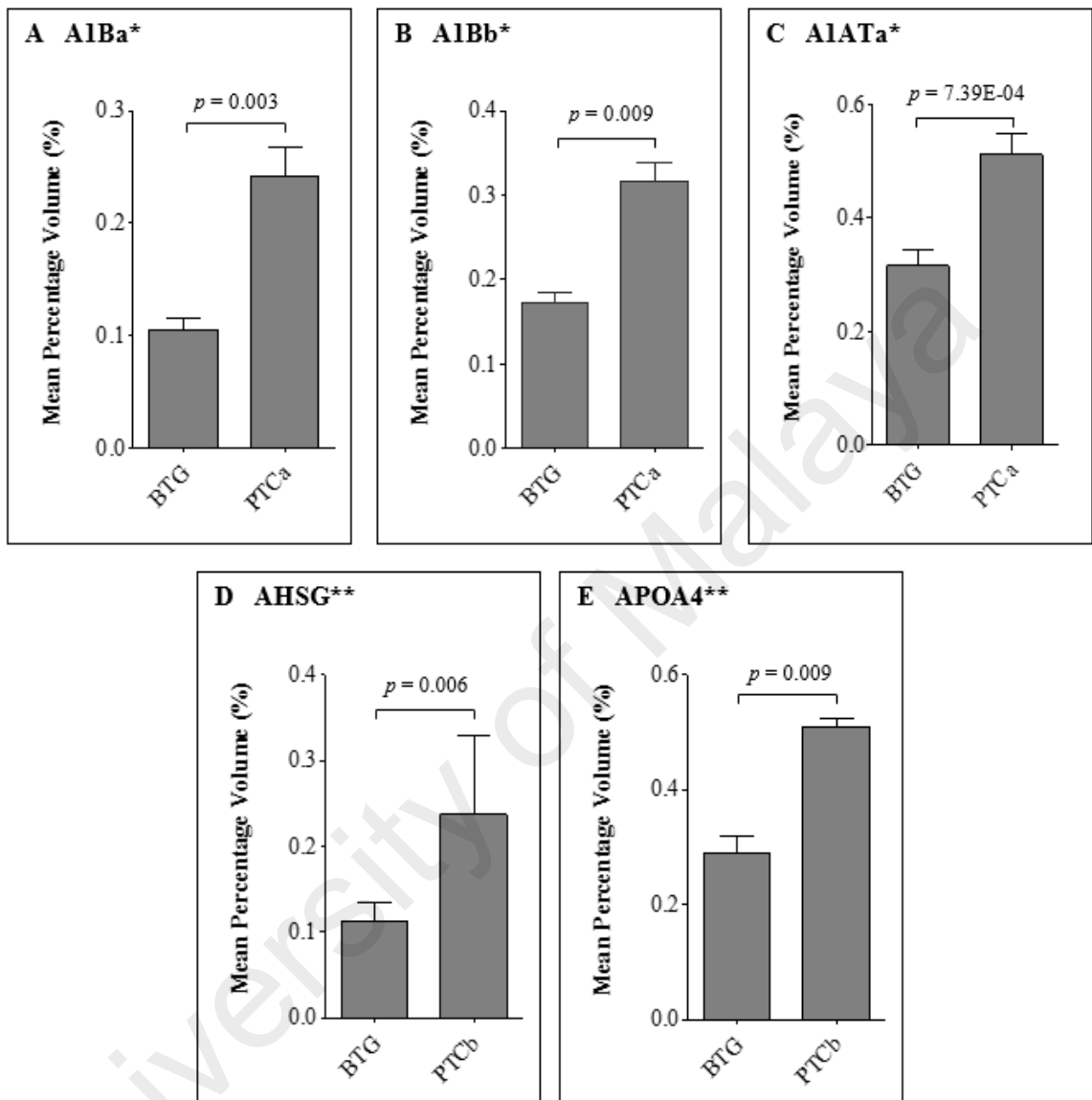


Figure 4.21: Average percentage of volumes that were differentially expressed between BTG, PTCa, and PTCb patients

Percentage of volume contribution (%vol) of serum protein spots was analysed using ImageMaster™ 2D Platinum software, version 7.0. Standard errors of the mean (SEM) were from biological replicates. Single asterisk (*) denotes differentially expressed proteins in PTCa patients (n = 8) compared to those with BTG (n = 20) and double asterisks (**) refer to proteins that were differentially expressed in PTCb (n = 6) compared to BTG (n = 20) patients.

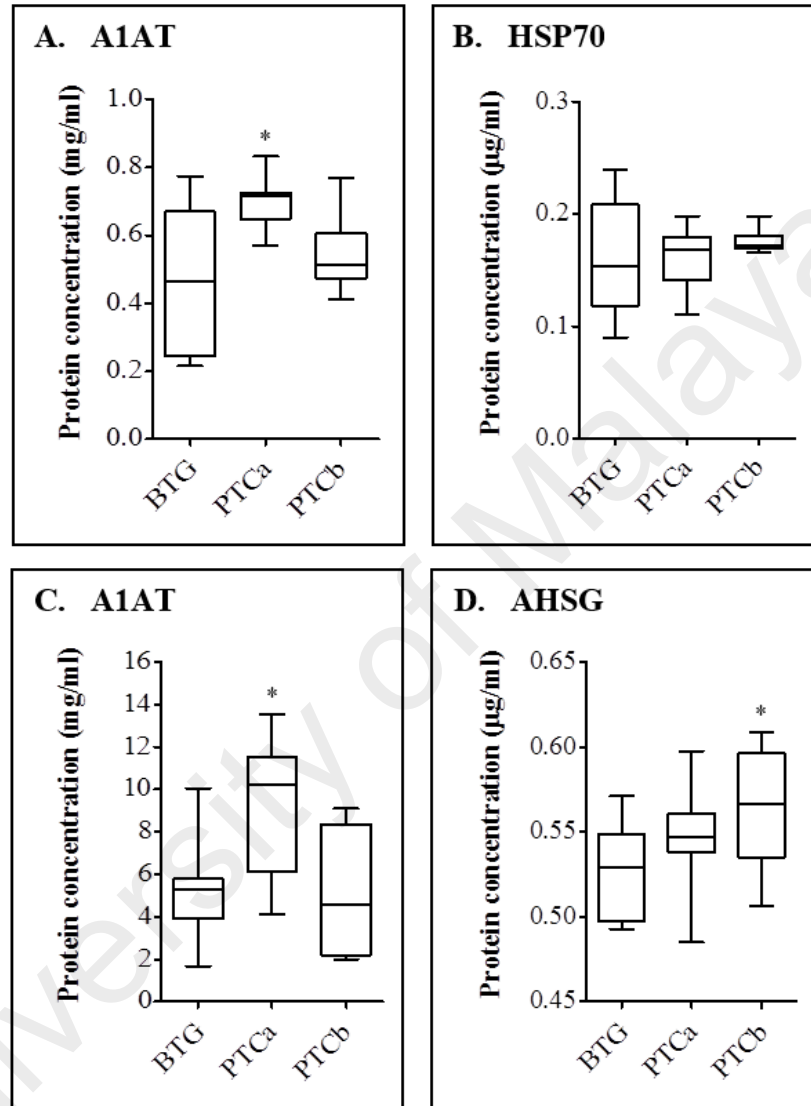


Figure 4.22: ELISA analyses of tissue (panels A and B) and serum (panels C and D) proteins in BTG, PTCa, and PTCb patients

ELISA was performed using antihuman A1AT, HSP70, and AHSG as primary antibodies. Single (*) asterisk denotes a p value of < 0.05 when PTCa ($n = 8$) and PTCb ($n = 6$) were compared to BTG ($n = 20$). Assay was performed in duplicate and data are presented as mean \pm standard error of the mean (SEM) from biological replicates.

CHAPTER 5: DISCUSSION

Cancers may develop as a result of many factors. Modifications in the genome and in gene expression patterns that are vital for cellular regulatory processes such as DNA duplication, differentiation, growth, and apoptosis could be the contributing factors. Although the exact cause of thyroid cancer in most patients is still uncertain, current emerging evidence shows that genetic mutations play an important role in the development and progression of papillary thyroid cancer (PTC) (Xing, 2013). PTC showed concordant alteration of many genes including the *BRAF*, *MET*, *PAX8*, *RET*, and *TRK* (Segev, Umbricht, & Zeiger, 2003). In addition, benign thyroid goitre (BTG) have also recently been thought as a condition with a risk associated malignancy (Palo & Mishra, 2017).

There is a wide range of studies that are now applying genomic technology to improve understanding of genetic pathology of diseases (Lowe & Reddy, 2015). The latest genomic technology such as next generation sequencing (NGS) offers a different scale of nucleotide sequencing from transcriptome, exome and up to the whole genome. Sequencing of whole exome regions has the potential to reveal predisposing variants in common diseases and cancers as well as causes of large number of rare, mostly monogenic, genetic disorders (Rabbani, Tekin, & Mahdieh, 2014). This approach has been shown to be able to aid/ help in the identification of molecular diagnosis in nearly 30% of clinically unclear cases.

In the present study, genetic alterations that could be associated to thyroid tumour were screened in patients with PTC and BTG using whole-exome sequencing (WES). The study focused mainly on thyroid neoplasm-related genes. WES analysis successfully identified 340 variants in 34 out of the 36 thyroid neoplasm-related genes screened. This included earlier reported pathogenic mutations, such as the c.1799T>A (Jo et al., 2006;

Nucera, Goldfarb, Hodin, & Parangi, 2009; Zhang et al., 2016) and c.861-170A>T in the *BRAF* (Yang, Huang, & Jing, 2016), c.191C>A and c.292A>C in the *LGALS3* (de Mendonça Belmont, da Silva, de Melo Vilar, Bezerra, & da Silva Araujo, 2016) and the c.215C>G in the *TP53* (Shi et al., 2012; Vymetalkova et al., 2015) genes.

The significance of *BRAF* mutations in the pathogenesis of PTC was first reported in 2003 (Soares et al., 2003; Xu, Quiros, Gattuso, Ain, & Prinz, 2003). Whilst some study showed that the mutations were restricted to PTC and have not been found in other types of well-differentiated thyroid follicular neoplasm (Cohen et al., 2003; Kimura et al., 2003; Trovisco et al., 2004; Xu et al., 2003), others demonstrated that *BRAF* mutations also occur in poorly differentiated and anaplastic cancers (Nikiforova et al., 2003; Xing, 2005). In the present study, two previously reported mutations in the *BRAF* gene, c.1799T>A (Val600Glu) and c.861-170A>T, were exclusively detected in malignant thyroid lesions of PTC patients, PCP9 and PCP5, respectively. The c.1799T>A (p.Val600Glu) mutation is a non-synonymous variant of the *BRAF* gene that is predicted to be functionally deleterious (Estep, Palmer, McCormick, & Rauen, 2007). *BRAF*^{V600E} was initially discovered in PTC in 2003 (Nikiforova et al., 2003; Soares et al., 2003; Xu et al., 2003). The *BRAF*^{V600E} is commonly found in patients with PTC with varying prevalence of 29% to 83% (Elisei et al., 2008; Trovisco et al., 2004; Xing, 2005; Xu et al., 2003). In this study, a lower frequency of the mutation (20%) was detected in the PTC patients supporting the findings by (Namba et al., 2003). The *BRAF*^{V600E} is also associated with more aggressive variants of PTC, presented with 77%, 60%, and 12% in tall cell PTCs, conventional PTCs and follicular variant PTCs, respectively (Xing, 2005). The mutation has been identified in ovarian and colorectal cancers as well as melanoma (Qu et al., 2013; Singer et al., 2003; Yuen et al., 2002).

BRAF is a serine threonine kinase that activate mitogen-activated protein kinase (MEK), which in turn activates mitogen-activated protein kinase (MAPK) and other downstream targets of MAPK signalling pathway (Li et al., 2012). The $BRAF^{V600E}$ mutation strongly increases BRAF kinase activity resulted in excessive activation of MAPK signalling pathway (Cantwell-Dorris, O'Leary, & Sheils, 2011). Ultimately, the activation leads to uncontrolled proliferation of thyroid cancer cells (Puxeddu, Durante, Avenia, Filetti, & Russo, 2008; Sumimoto, Imabayashi, Iwata, & Kawakami, 2006; Xing, 2007). The $BRAF^{V600E}$ is believed to be involved in the early stages of tumour development of PTC by inducing tumour initiation, increasing growth and promoting survival of the cancerous cells (Knauf & Fagin, 2009; Tang & Lee, 2010). It has been shown that $BRAF^{V600E}$ promotes the invasion of tumour cells in a rat thyroid cell line model (Mesa et al., 2006). An *in vivo* study conducted by Knauf et al. (2005) showed that transgenic mice develop PTC after injection of the $BRAF^{V600E}$ protein into the thyroid gland.

In addition, the presence of $BRAF^{V600E}$ mutation correlates with poor prognostic features (such as extrathyroidal extension, lymph node metastasis or advanced tumour stage) in PTC patients (Huang et al., 2014; Li et al., 2012). The association of $BRAF^{V600E}$ mutation with clinical manifestations of PTC is controversial (Tang & Lee, 2010). While some studies have shown that $BRAF^{V600E}$ is associated with an advanced stage of the disease at diagnosis (Kebebew et al., 2007; Namba et al., 2003; Nikiforova & Nikiforov, 2008), but this correlation has not been confirmed by other groups (Fugazzola et al., 2006; Kim et al., 2012; Xu et al., 2003).

The c.861-170A>T mutation of the *BRAF* which was detected in PCP5 was described as a potential susceptible locus for PTC in Chinese population (Jiang et al., 2016). Inconsistent result was reported by Yang et al. (2016) where the c.861-170A>T mutation

was involved in the progression of PTC rather than as a risk factor. An earlier study by Qiang Zhang et al. (2013) found that those carrying the variant are more likely to suffer from PTC at an earlier age (< 45 years), as also observed in the present study, but appeared to be less susceptible to develop lymph node metastases.

Apart from the *BRAF* gene, mutations in the *TP53* gene were also detected in this study. A non-synonymous c.215C>G nucleotide transition that was predicted to change of arginine to proline at codon 72 in exon 4 (p.Arg72 Pro) was detected in two patients with BTG (BGP4 and BGP23) and five patients with PTC (PCP3, PCP5, PCP7, PCP8, and PCP9). *TP53* gene encodes a tumour suppressor, p53. p53 is one of the most vital tumour suppressors in human cells to maintain genomic stability and regulating cell growth as well as apoptosis (Levine, 1997; Meek, 2004; Vogelstein, Lane, & Levine, 2000). Kinetically, p53 containing Arg-72 seems to induce apoptosis much faster and protecting cells from carcinogenesis compared to the mutated p53 with Pro-72 (Bergamaschi et al., 2006; Dumont, Leu, Della Pietra, George, & Murphy, 2003; Muller, Vousden, & Norman, 2011).

Meta-analysis carried out by Wang et al. (2014) suggested that the c.215C>G (p.Arg72Pro) mutation of *TP53* was associated with a risk of developing thyroid cancer. Furthermore, several reports have also described the association between the *TP53* Arg72Pro polymorphism and PTC risk in different populations (Boltze et al., 2002; Chen et al., 2015; Granja et al., 2004; Rogounovitch et al., 2006; Wu, Guo, & Guo, 2014). Previously reported cases showed many human tumours such as osteosarcoma, bladder, oesophageal, gastric, and ovarian cancers, carries the c.215C>G (p.Arg72Pro) mutation in the *TP53* gene (Bellini, Cadamuro, Succi, Proença, & Silva, 2012; Lin et al., 2013; Ru et al., 2015; Schildkraut et al., 2009). The co-segregating c.782+92T>G and c.782+72C>T polymorphisms in intron 7 of the *TP53* gene were found to be in positive

association with many types of malignancies such as stomach and colon cancer (Palacio-Rúa, Isaza-Jiménez, Ahumada-Rodríguez, Ceballos-García, & Muñetón-Peña, 2014). Furthermore, an epidemiological study by Schildkraut et al. (2009) has shown an association between the c.782+92T>G variant of *TP53* gene and risk of ovarian cancer.

In the present study, WES analysis of extracted DNA from the thyroid tissues also revealed two previously reported pathogenic mutations in the *LGALS3* gene; c.191C>A and c.292A>C as well as a novel c.19-50_52CTGdel mutation. *LGALS3* encodes galectin 3 (GAL3), a beta-galactoside-binding lectin which is involved in tumour progression (Raz et al., 1991), cell differentiation (Ohannesian, Lotan, & Lotan, 1994), adhesion (Woynarowska et al., 1994) and apoptosis resistance (Akahani, Nangia-Makker, Inohara, Kim, & Raz, 1997). GAL3 is also believed to be associated with thyroid cancer (Chiu et al., 2010). GAL3 is differentially expressed in thyroid cancer compared with benign and normal thyroid specimens, suggesting that GAL3 is a good diagnostic marker for thyroid cancer (Balan, Nangia-Makker, & Raz, 2010; Karger et al., 2012; Sumana, ShaShidhar, & Shivarudrappa, 2015).

The c.191C>A mutation (p.Pro64His) was detected in BTG patients, BGP4, BGP8, and BGP 23. The functional germline mutation of *LGALS3*^{P64H} has resulted in the susceptibility of galectin-3 to cleavage by matrix metalloproteinases (MMPs), MMP-2 and MMP-9 (Cardoso & Bustos, 2016). The MMPs are believed to play a role in the initiation and development of tumour vascularisation (Bergers et al., 2000; Ribatti & Crivellato, 2012). The substitution of proline-64 by a histidine is associated with the development of breast cancer (Balan et al., 2008). According to the study, H/H allele is associated with higher breast cancer risk in both Caucasian and Asian women.

Another previously reported non-synonymous variant, c.292A>C in the *LGALS3* gene (p.Thr98Pro) was successfully identified in 5 patients (PCP 3 and 5, and BGP 4, 8, and

23). The functional implication of this change on thyroid cancer risk is still uncertain. It was reported that the polymorphism is a genetic predisposition factor for rheumatoid arthritis in Taiwan (Hu, Chang, Wu, Tsai, & Hsu, 2011).

In the present study, WES analysis detected a novel frame-shift deletion (c.19-50_52CTGdel) in the *LGALS3* gene in only one patient with PTC, PCP5. Further transcript analysis showed the presence of a chimeric RNA comprises exons from *IFI27* and *LGALS3* genes. WES data for the respective patient did not find any evidence of *IFI27-LGALS3* gene fusion or *IFI27* mutation. Both of the *LGALS3* and *IFI27* genes are located on chromosome 14 at q22.3 and q32.13, respectively. It has been demonstrated that *LGALS3* was involved in modulating inflammation and cell apoptosis (Henderson & Sethi, 2009; Li, Li, & Gao, 2014). The *IFI27* is known to influence apoptosis by sending extracellular signals to activate pro-apoptotic genes (Rosebeck & Leaman, 2008). RNA processing events of two pre-mRNAs that are transcribed from different genes lead to a fusion RNA (Akiva et al., 2006; Kannan et al., 2011; Zhou, Liao, Zheng, & Shen, 2012). Fusion RNAs may simply be RNA chimeras resulted from trans-splicing, transcription of short homologous sequence slippage, and/or read through transcription (Zhou et al., 2012). The slippage occurs at a region where the two genes are homologous in the DNA sequence, which is typically short (Peng et al., 2015). They are thus referred to as “short homologous sequence” (SHS). SHSs between two loci are essential for effective template-switching to generate the chimeric RNAs (Li, Zhao, Jiang, & Wang, 2009). The model is simpler from the natural trans-splicing as spliceosome is not involved during the generation of mature chimeric RNAs. This transcriptional slippage

is possible if both of the gene loci become simultaneously active and share one transcription factory³.

In this study, the generation of *IFI27-LGALS3* chimeric RNA, can likely be explained through the transcriptional slippage model (Figure 5.1A). The present result shows that the homology sequence 5' GTGAAGCCCAATGCAAACA 3' acts as a linker for exon 3 of the *LGALS3* gene and minus strand RNA of exon 4 of the *IFI27* gene through an SHS-dependent mechanism (Figure 5.1B). After the pre-mRNA fragment of *LGALS3* is transcribed, the SHS at its 5' end of pre-mRNA (exon 4) "misaligns" with the SHSs at another locus of *IFI27* in exon 3. A chimeric *IFI27-LGALS3* RNA is then generated once the transcription process continues on the new template. Fusion RNA conserves an open reading frame which could create various novel proteins with aberrant functions (Fang, Wei, Kang, & Landweber, 2012). Many previous results suggest that transcriptional slippage is possible to cause human disease (van den Hurk, Willems, Bloemen, & Martens, 2001). However, the significance of the *IFI27-LGALS3* chimeric RNA remains, to the best of our knowledge, unknown.

A previously reported polymorphism in adenoma and follicular thyroid cancer tumour cases (G. Wu et al., 2005), c.3075C>T of the *PIK3CA* gene, was also identified in this study in a patient with PTC (PCP5). The *PIK3CA* gene encodes the phosphatidylinositol 3'-kinase (PI3K) catalytic subunit (Karakas, Bachman, & Park, 2006). PI3K is a member of the PTEN/PI3K/AKT pathway that plays an important role in regulating cell growth and proliferation as well as in tumourigenesis and progression. Mutations in the *PIK3CA* gene have been commonly detected in follicular and anaplastic thyroid cancer but is

³ Active transcription units are clustered in the nucleus, at a number of specialised, discrete sites.

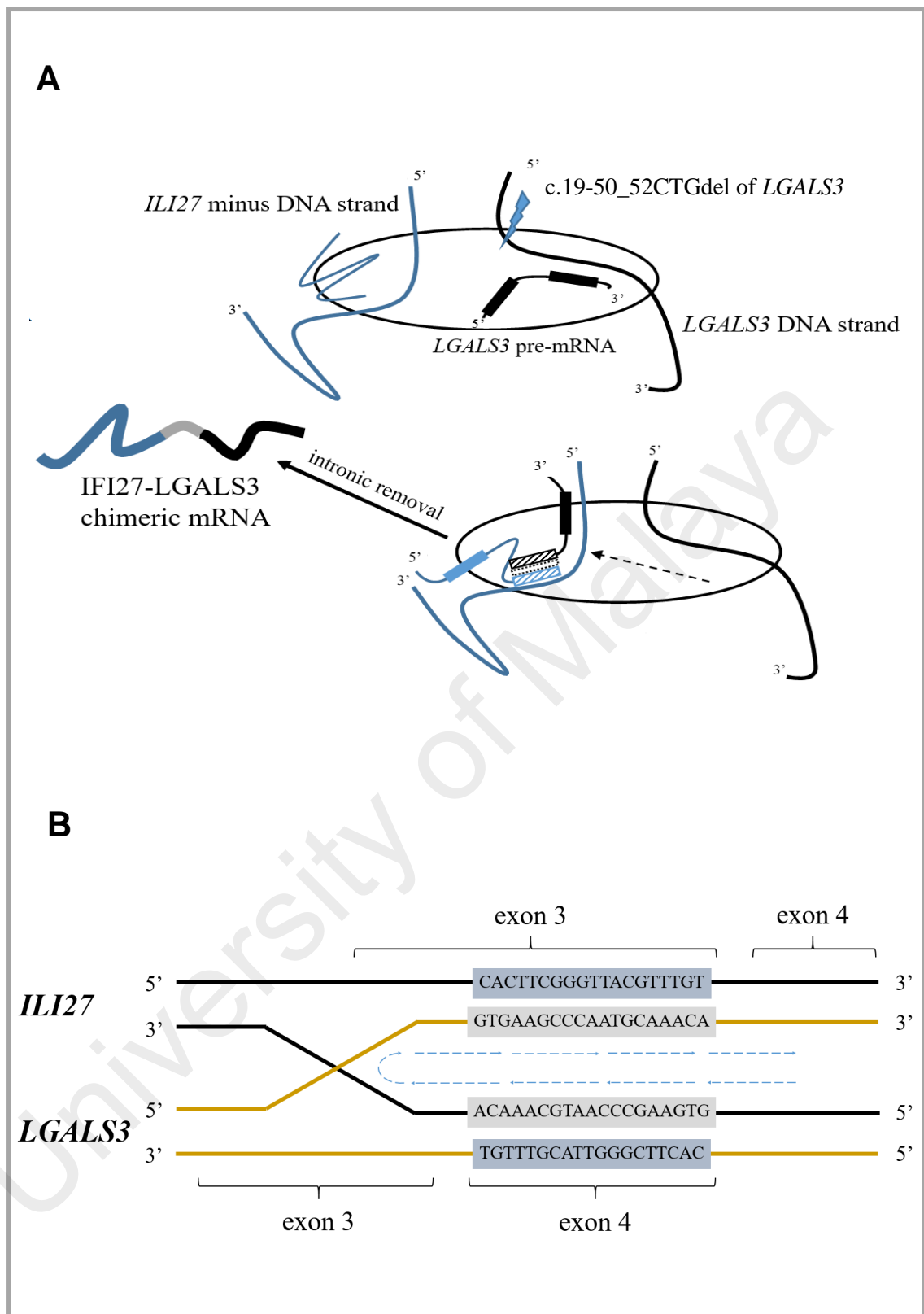


Figure 5.1: RNA processing events that generate IFI27-LGALS3 chimeric mRNA of PCP5

A) Short homologous sequences (SHSs) slippage model of the IFI27-LGALS3 chimeric mRNA and B) a transcription starts from *ILI27* gene with a SHS sequence in exon 3 pairing with a SHS sequence in exon 4 in *LGALS3* gene.

uncommon in PTC (Wang et al., 2007). At present, it is not known if the mutation is the underlying genetic cause of PTC in this patient.

As for the *RET* proto-oncogene, WES analysis successfully identified a non-synonymous variant, c.833C>A, in a patient with BTG, BGP4. The c.833C>A nucleotide transition is predicted to replace threonine by asparagine at amino acid 278 (p.Thr278Asn). The proto-oncogene encodes a transmembrane tyrosine kinase receptor that governs cell differentiation and proliferation (Elisei et al., 2014). Although the role of c.833C>A (p.Thr278Asn) is unknown, the mutation has been previously reported in carriers presented familial medullary thyroid carcinoma in a Chinese Han family (Qi et al., 2014).

It is now well recognised that polymorphisms may have a relatively strong influence on cancer predisposition (Dunning et al., 1999; Gianfagna, Feo, Van Duijn, Ricciardi, & Boccia, 2008; Y. Lu et al., 2017). Studies have revealed that the incidence and development of thyroid neoplasms is also associated with gene polymorphisms (Brand et al., 2009; Chiang et al., 2008; Gong et al., 2016; Lin et al., 2016; Wang et al., 2016). Previous studies have reported the association of *BRAF*, *KRAS*, *MET*, *TTF1*, and *TTF2* genes polymorphisms with significantly greater incidence of PTC (Gao, Chen, Niu, Lin, & Li, 2015; Jiang et al., 2016; Ning et al., 2016; Ning et al., 2015; Wang et al., 2016). In the present study, the possible association of 14 gene polymorphisms with PTC or BTG among Malaysians was investigated. The c.2200T>G (p.Ser734Ala), c.3082A>G (p.Met1028Val), c.68-148G>A, c.2334T>C, c.4002+39C>G, c.3848-20T>C, c.3848-110A>G, c.5401+49G>C, c.4933-165T>G, and c.4160-83T>G of *TG*, c.*81C>G of *TPO* as well as c.696A>G and c.742C>A (p.Arg248Ser) of *TSHR* have not been used in previous association studies except for the c.2307G>T of *RET*. It has been observed that there is no association of the polymorphisms at the *TG*, *TPO*, *TSHR* and *RET* loci with

susceptibility of the diseases. Lack of association observed in this study could be due to the small number of subjects who were involved in this study. Thus, a future study involving a larger number of patients with PTC and BTG should be carried out to ensure a conclusive finding. The effects of genetic variants within the iodine metabolism genes in relation to PTC or BTG, to the best of our knowledge, were not frequently reported in the literature. While most molecular research have considered autoimmune thyroid disease and non-medullary thyroid cancer to be associated with *TG* (Ban et al., 2012; Matakidou et al., 2004; Wang, Wang, Sun, & Qie, 2015), Akdi et al. (2011) provided the first documentation on *TG* gene as a susceptibility factor for differentiated thyroid cancer. The finding has been supported in a recent study by (Abidi, Fayaz, & Fard, 2017) which evidence a significant association of D1312G polymorphism in an Iranian population.

Previous research has shown the association of *TPO* genetic variants with significantly greater incidence of differentiated thyroid cancer (Cipollini et al., 2013), whilst, to date, there is no reported study on the association of *TSHR* with the development of PTC or BTG. Limited study of an association between polymorphism at the *RET* locus and PTC has been reported so far. A recent research has documented that G691S polymorphism of *RET* is associated with the occurrence and development of PTC in the Han population in southern China (Wang et al., 2016). Santos, Azevedo, Martins, Rodrigues, and Lemos (2014) reported that there is a significant risk between *RET* S836S polymorphism and PTC, and that the G691S/S904S polymorphisms might be related to tumour behaviour. In contrast to the present study, one study found that the L769L and G691S variants within *RET* represented the strongest association with PTC (Lesueur et al., 2002).

Human serum and tissues contain an extensive variation of different proteins and peptides. Alterations in the production of specific proteins and enzymes can arise due to different physiological states and origins of diseases (Malati, 2007). This leads to

differences in the protein composition in the tissues and serum, which can then serve as indicators for development and progression of diseases. Hence, the aberrantly expressed proteins and peptides can be utilised as valuable biomarkers, enabling diagnosis as well as prognosis of different diseased conditions.

The previous discussion of the genomic findings of the present thesis has generated a list of putative pathogenic mutations, which opens up new avenues for studies to identify their correlations with the development and progression of PTC at the protein level. Although BTG cannot be termed a premalignant disease, epidemiological and histopathological data appear to suggest that this condition has a significant potential risk for progression into malignancy (Arora, Scognamiglio, Zhu, & Fahey Iii, 2008; Htwe, 2012; Pradhan et al., 2011). In Malaysia, approximately 60% of the reported thyroid cancer cases comprise those with PTC with the concurrent presence of BTG (Othman et al., 2009). This strongly suggests that BTG, when prolonged, may develop into PTC. Currently, the molecular pathways involved in thyroid carcinogenesis are increasingly being unravelled. With the integration of genomic and proteomic investigations, a better understanding of the molecular events that underlie the development and progression of PTC may be achieved.

The concurrent manifestation of a benign thyroid cyst and PTC in a single patient provided an opportunity for a study on the differences between tissues obtained from the benign and malignant tumours of the same individual. Using current state-of-the-art OMIC technologies, the genes as well as proteins of the two tissues may be unravelled and possible transitional changes that might have occurred during malignancy may be speculated.

In this study, when the benign and malignant thyroid tissues from a single patient with concurrent benign thyroid cyst and PTC were analysed, mutation of *BRAF* (*BRAF*^{V600E})

was exclusively detected in the PTC tissue of the patient. The same tissue was also shown to exhibit loss of mRNA expression of *TG* and *NIS*, and reduced expression of *TPO*. The decreased or loss of expression of *TG*, *NIS*, and *TPO* genes, due to the continued activation of the MAPK pathway caused by the gain-of-function in *BRAF*^{V600E} mutation, has been earlier demonstrated in cases of PTC (Durante et al., 2007; Espadinha, Santos, Sobrinho, & Bugalho, 2009; Lazar et al., 1999; Riesco-Eizaguirre, Gutierrez-Martinez, Garcia-Cabezas, Nistal, & Santisteban, 2006; Romei et al., 2008). The fact that several *in vitro* and animal models studies have shown an association between *BRAF*^{V600E} oncogene activation and lower mRNA expression levels of some thyroid differentiation genes such as *TPO*, *TG*, and *NIS* further corroborates this postulation (Knauf et al., 2005; Mitsutake et al., 2006; Puxeddu et al., 2008). On the other hand, *NIS* expression was not detected in the benign tissue of the same patient in the present study, and the expression of *TG* and *BRAF* was also found to be highly active whilst *TPO* appeared to be markedly reduced.

Hydrogen peroxide (H₂O₂) is a reactive oxygen species (ROS) continuously produced during stimulation of the thyroid follicular cells, or thyrocytes, by thyroid stimulating hormone (TSH). The thyroid gland fully utilizes H₂O₂ as a substrate of thyroid peroxidase (TPO) in the iodination of thyroglobulin (TG) and biosynthesis of thyroid hormones (Corvilain, Van Sande, Laurent, & Dumont, 1991). In contrast to the decreased expression of *TPO*, further analysis showed that *TSHR*, which is regulated by *TSH*, was positively expressed in the benign tissue of the patient when compared to three *BRAF*^{V600E} mutation-free control tissues. A continuous stimulation of thyrocytes by TSH, under the situation when TPO was not active, may have created an H₂O₂-rich environment in the benign tissue and caused oxidative stress to the cells. Such a condition may have led to upregulation of TG in the thyrocytes, which was also observed in the benign cyst of the patient. The presence of TG is crucial as it is known to act as a powerful suppressor for

H₂O₂ production by regulating the expression of dual oxidases (DUOXs) (Yoshihara et al., 2012).

Excessive ROS can cause cellular injury and mediate peroxidation of lipids, oxidation of proteins, damage to nucleic acids, enzyme inhibition and apoptosis of cells (Fulda, Gorman, Hori, & Samali, 2010; Sharma, Jha, Dubey, & Pessarakli, 2012). Survival of the host depends largely on the ability of cells to handle oxidative insults, either through adaptation, resistance of stress and repair or removal of damaged molecules or cells. In the present study, a possible active network involved in the benign cyst has been elucidated by IPA analysis, based on proteins that were detected to be differentially expressed between the benign thyroid cyst and PTC tissue, with a suggestive network “acute phase response signalling”. The concurrent involvement of “coagulation system”, “intrinsic prothrombin activation pathway”, and “extrinsic prothrombin activation pathway” in the same tissue implies injury and/or inflammation, and has frequently been associated with pathogenesis of various types of cancer (Hanahan & Weinberg, 2011). Although they are known to be closely related, the exact signalling mechanism that links oxidative stress with chronic inflammation as well as cancer remains inconclusive (Reuter, Gupta, Chaturvedi, & Aggarwal, 2010). As thyroid epithelial cells are constantly exposed to ROS, thyrocytes may activate numerous enzymatic systems, such as glutathione peroxidase, catalase, superoxide dismutases, and peroxiredoxins (PRDXs) to limit cellular injuries (Gérard, Many, Daumerie, Knoop, & Colin, 2005; Kim et al., 2000; Mono et al., 1997; Mutaku, Poma, Many, Deneff, & van Den Hove, 2002). The presence of PRDX2 and PRDX3 in the benign cyst was confirmed by mass spectrometry analysis in the present study. These results, together with the earlier reported data of Kang et al. (1998) and Kim et al. (2000), provide indirect evidence that the proteins were likely to have been generated in response to the increased amounts of H₂O₂. In addition, PRDX2 and PRDX3 may have also acted as major apoptosis mediators to protect the cells against

the apoptosis-inducing effects of high levels of H₂O₂ (Kang et al., 1998). Indeed, the expression of the proteins has been closely associated with cervical cancer (Kim et al., 2009), whereas lung (Lehtonen et al., 2004) and ovarian cancers (Pylväs, Puistola, Kauppila, Soini, & Karihtala, 2010) exhibited at least one of the PRDX isoforms.

A recent study has shown that the release of PRDX2 may function as an inflammatory mediator by triggering macrophages to produce tumour necrosis factor- α (TNF- α) (Salzano et al., 2014), whilst others postulated involvement of H₂O₂ insults in the tissue which could induce the production of interleukin 6 (IL6) (Colston, Chandrasekar, & Freeman, 2002; Wu et al., 2010) as observed in the present study. In fact, *BRAF*^{V600E} mutation has been shown to induce the secretion of IL6 in mediating melanoma growth (Sumimoto et al., 2006; Whipple & Brinckerhoff, 2014). In any case, TNF α and IL6 are both major inflammatory cytokines involved in cancer-related inflammation (Kishimoto, 2005), which are under the control of transcription factors, nuclear factor- κ B (NF- κ B) and signal transducers and activators of transcription (STAT3) (Mantovani, Allavena, Sica, & Balkwill, 2008). Recently, the association of H₂O₂ with STAT3 signalling was also unveiled when Sobotta et al. (2015) demonstrated the modulation of cytokine-induced STAT3 signalling by the expression of PRDX2 which functions as a H₂O₂ signal receptor and transmitter in transcription factor redox regulation. Dangerous liaisons between STAT3 and NF- κ B are believed to be attributed to their ability to control the expression of anti-apoptotic and pro-proliferative genes in premalignant cells and their neoplastic progeny (Grivennikov & Karin, 2010). In thyroid cancer cell lines, *BRAF*^{V600E} apparently activates the NF- κ B signalling pathway leading to an acquisition of apoptotic resistance and promotion of invasion (Palona et al., 2006).

STAT3, a cytoplasmic protein, is a family member of transcription factors that transduce short-term cytoplasmic signals. The protein, which is constitutively expressed

in a wide range of tissues, is believed to play a role in the maintenance of cellular homeostasis by regulating a number of genes involved in the inflammatory response as well as apoptosis, differentiation, and stem cell maintenance (Resemann, Watson, & Lloyd-Lewis, 2014). The STAT3 transcript generates two isoforms, STAT3 α and STAT3 β , that are generated by alternative splicing of exon 23, with STAT3 β being a truncated version of STAT3 α (Zhang & Lai, 2014). The expression STAT3 β is found in various cell types but its amount is lower than that of STAT3 α (Caldenhoven et al., 1996; Schaefer, Sanders, & Nathans, 1995). Higher expression and activation of STAT3 have been detected in thyroid cancer, including lymphatic metastasis of PTC (J. Zhang et al., 2011). Consistent with this, a histological analysis revealed that STAT3 is specifically regulated in PTC but not in follicular thyroid cancer, signifying that STAT3 activation may be involved in the establishment of the papillary phenotype (Trovato et al., 2003).

The roles of STAT3 in tumourigenesis are surrounded by controversies. Whilst some studies showed that tyrosine-phosphorylated or activated STAT3 (pY-STAT3) can promote tumourigenesis (Azare et al., 2007; Diaz et al., 2006; Tye et al., 2012) and considered it as a product of an oncogene (Bromberg et al., 1999), others demonstrated that the protein inhibited growth of tumour and induced cell apoptosis (de la Iglesia et al., 2008; Lee et al., 2012). Consistent with the later notion, STAT3 deficiency appeared to facilitate tumourigenesis in a murine model of *BRAF*^{V600E}-induced PTC (Couto et al., 2012). Increased STAT3 is believed to induce the transcription of tumour suppressor insulin-like growth factor binding protein 7, which later negatively regulated aerobic glycolysis and decreasing energy metabolism in cancer cells.

More recently, a 67 kDa isoform of STAT3, the STAT3 β , has been suggested to act as a dominant negative factor to STAT3 α (75 kDa) and contributed to the opposing function of STAT3 (Zhang & Lai, 2014). Consistent with this view, a malignant tissue which

showed strong activation levels of STAT3 β has been shown to have higher rates of cell necrosis and apoptosis than that of the benign cyst (Baran-Marszak et al., 2004). STAT3 β has been previously reported in various malignancies, including prostate (Ni, Lou, Leman, & Gao, 2000), ovarian, breast (Burke et al., 2001) and lung cancers (G. Xu, Zhang, & Zhang, 2009) as well as melanoma (Niu et al., 1999). It has also been shown to halt the transcriptional activation of several STAT3 downstream targets including cyclin D1, myeloid cell leukaemia 1, and B-cell lymphoma-extra large (Bcl-XL), leading to inhibition of tumour growth and promoting apoptosis (Epling-Burnette et al., 2001; Karni, Jove, & Levitzki, 1999; Sinibaldi et al., 2000).

In the present study, however, a 28 kDa fragment of STAT3 with at least 2 fold higher levels than STAT3 α , was instead detected as the main pY-STAT3 isoform in the benign cyst. The fragment, which is termed as STAT3 ϵ in the present study, was not detected in the PTC tissue of the same patient. This, together with the western blot results which showed amounts of pY-STAT3 in both the benign cyst and PTC tissues of the patient implicate the role of STAT3 ϵ in maintaining cell survival and higher proliferation rates in the benign cyst. This hypothesis was further strengthened when IPA predicted that STAT3 and V-myc avian myelocytomatosis viral oncogene homolog (MYC), a proto-oncogene that is a downstream target for many signals such as MAPK and STAT3 pathways and known to induce cell proliferation, reduce apoptosis, and promote tumour progression (Dang, 2013), were likely to be activated in the benign cyst. MYC was estimated to have contributed to cause at least 40% of tumours (Miller, Thomas, Islam, Muench, & Sedoris, 2012). In spite that it is known to be up-regulated in PTC (Zhu, Zhao, Park, Willingham, & Cheng, 2014) as well as many other cancers (Chen, Wu, Tanaka, & Zhang, 2014), overexpression of MYC alone is inefficient at causing malignant transformation (Loosveld et al., 2014).

IPA analysis performed in the present study had also predicted that the PTC cells were likely to display inhibition of p53, which functions as a tumour suppressor by preventing cells with mutated or damaged DNA from dividing (Zilfou & Lowe, 2009). Reduced or loss of p53 function is common at a late stage of tumour development (Muller et al., 2011). However, Niu et al. (2005) and Muller et al. (2011) have successfully restored the expression of p53 by blocking STAT3 in cancer cells, demonstrating involvement of STAT3 in mediating p53 inhibition. Since both tissues in the present study had presented similar amounts of total pY-STAT3, the STAT3 ϵ that was detected in the benign cyst may have interfered with the binding of STAT3 to the p53 promoter, and hence, retained the p53 function that helped prevent/delay the malignant transformation of the cells. In addition, IPA also revealed an increase in glucose and protein metabolisms and production of lipids in the PTC cells. This is in agreement with the fact that cancer cells frequently exhibit specific alterations in their metabolic activity, termed as the Warburg effect, to support its rapid proliferation (Vander Heiden, Cantley, & Thompson, 2009). Hence, when taken together, the data of the present study, appear to suggest that prolonged H₂O₂ insults in the patient might have resulted in extreme oxidative stress that interfered with the MAPK and STAT3 pathways, which then led to *BRAF*^{V600E} mutation and consequential loss of function of p53 as well as the altered metabolisms and malignant transformation that occurred in PTC (Figure 5.2).

Patients with PTC comprise those with (termed PTCb in this thesis) and without (termed PTCa in this thesis) a history BTG. The association between patients with BTG and those with PTCb is well recognised (Hanumanthappa et al., 2012). In 2004, Gandolfi et al. reported detection of unsuspected PTC in 14% of BTG patients after postoperative histopathologic examination, and stressed that the risk of malignancy in BTG should not be undervalued. More recently, Thavarajah and Weber (2012) performed global gene expression analysis to evaluate for dissimilarities in gene expression patterns between

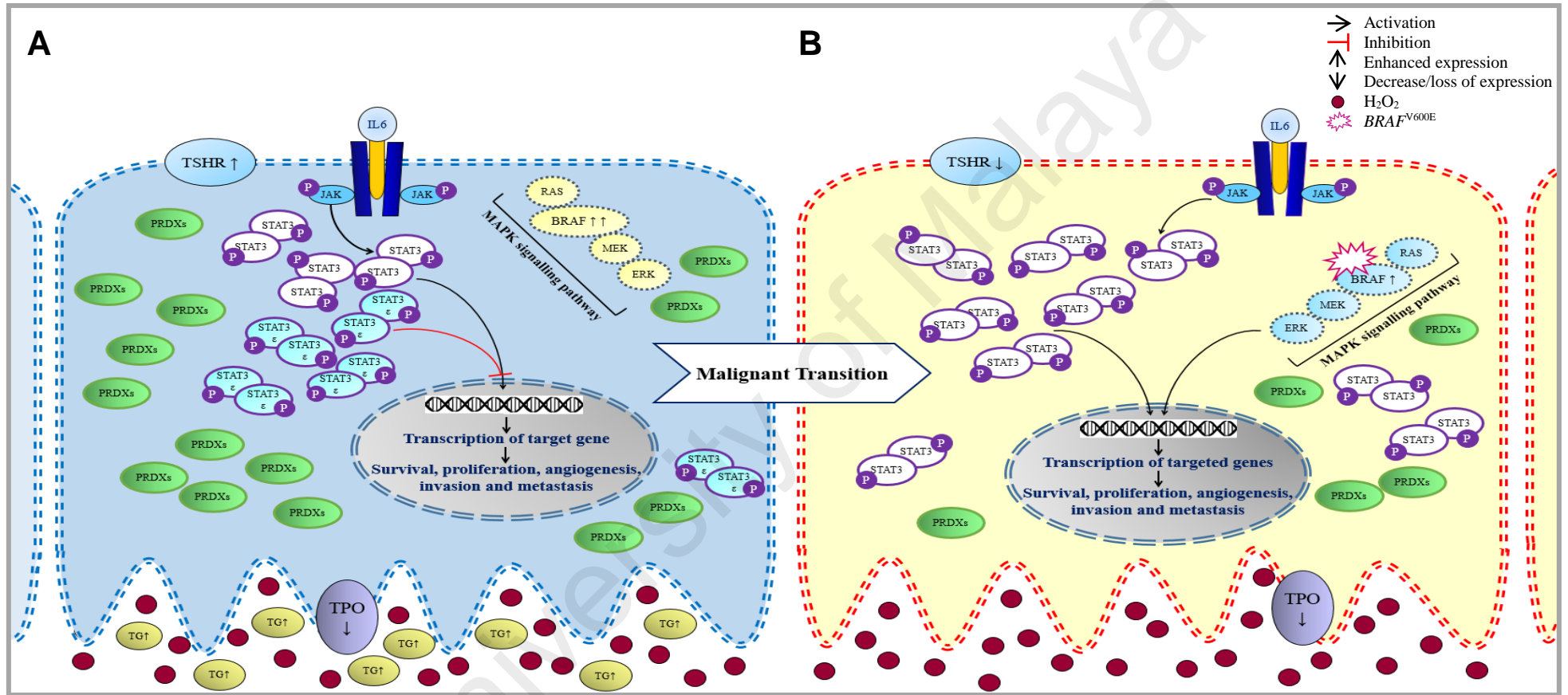


Figure 5.2: Proposed transitional changes in A) benign thyroid cyst and B) PTC tissue in a single patient, PCP9

[Abbreviation: BRAF, V-ras murine sarcoma viral oncogene homolog b; IL6, Interleukin 6; JAK, Janus kinase; MAPK, Mitogen-activated protein kinase; P, Phosphorylated; PRDXs, Peroxiredoxins; STAT3, Signal transducer and activator of transcription 3; TG, Thyroglobulin; TPO, Thyroid peroxidase; TSHR, Thyroid stimulating hormone receptor].

patients confirmed with multinodular goitre with those who had unsuspected PTC. In their report, they claimed to be able to accurately distinguish between hyperplastic nodules of the patients from those associated with PTC based on the gene expression patterns, and hypothesised factors that may influence genesis of PTC. Unlike PTCb, PTCa is a PTC that has no known association with BTG. However, to date, comparative studies of the expression of proteins in the tissue and serum samples of PTC patients with and without benign background have not been performed.

In the present study, the thyroid tissue and serum samples of patients with BTG and those with PTCa and PTCb were analysed using gel-based proteomics. This is to identify tissue and serum proteins of altered abundance in patients with PTCa and PTCb relative to those expressed in patients with BTG as the two types of PTC maybe totally unrelated, both etiologically as well as mechanistically.

In the first part of the study, image analysis of thyroid tissue samples resolved by 2-DE demonstrated enhanced expression of alpha-1 antitrypsin (A1AT) and heat shock 70 kDa (HSP70) in patients with PTCa compared to those with BTG. A1AT is an inhibitor of plasma serine proteases involved in the regulation of the activity of many serum enzymes. The protein, which shares DNA sequence homology with other members of the family of serine protease inhibitors like alpha-1 antichymotrypsin and antitrombin III, has been previously reported to be elevated in PTC compared to the benign tissues (Poblete, Nualart, del Pozo, Perez, & Figueroa, 1996). A1AT may play a role in influencing tissue repair *in vivo* by directly stimulating fibroblast proliferation and extracellular matrix production. Higher levels of A1AT within tumour tissues may lead to the desmoplastic response and often associated with disease progression (Dabbagh et al., 2001). The state of A1AT abundance within the neoplastic tissue may also signify a protective mechanism by the host tissue to the proteases produced by tumour cells. In an

experimental model *in vitro*, A1AT was found to hinder the activation of progelatinase A (MMP-2) and tumour cell invasion by inhibiting the activity of serine proteinase (Shamamian et al., 2001). Several studies have shown that A1AT blocks the activity of caspase-3, an intra-cellular cysteine protease which plays a vital role in cell apoptosis (Petrache et al., 2006; Zhang et al., 2007).

Elevated levels of HSP70 by more than two-fold difference in patients with PTC have also been previously reported by Brown et al. (2006), and this is in line with the 2-DE data of the present study. However, ELISA analysis performed in the present study was not able to validate these results. HSP70 is a member of the highly conserved heat shock proteins consisting of molecular chaperones, which is present in every membranous organelle of all cells (Sherman & Gabai, 2015). The protein has been identified as a protector against cellular stress (Wang et al., 2002) and also involved in inflammation (Vabulas et al., 2002). HSP70 is normally kept at low levels, however, it is highly elevated in breast cancer (Ciocca et al., 1993). This observation was later extended to other types of tumours including cervix (Hellman et al., 2004), colon (Hwang et al., 2003), liver (Luk et al., 2006) and prostate (Alaiya et al., 2001). Higher levels of HSP70 is likely a consequence of its critical role in cancer cell signalling and survival pathways by (a) inhibiting both p53-dependent and -independent senescence as well as the intrinsic and extrinsic apoptosis pathways and (b) stabilising lysosome function in tumour cells and allows for autophagy (Murphy, 2013).

In the case of tissue samples of patients with PTCb, image analysis of 2-DE gels demonstrated lower levels of A1AT, protein disulfide isomerase (PDI), and ubiquitin conjugating enzyme E2N (UBE2N), relative to their BTG counterparts. The lower expression of A1AT in PTCb patients appears to be in direct contrast to that detected in patients with PTCa, and hence, points to a different mechanism that may be involved in

malignant transformation of PTCb as opposed to PTCa. In the present study, the different altered expression of A1AT in the tissue samples of patients with PTCa and PTCb were also validated using ELISA. However, to date, PTCb is the only cancer whose tissue expression of A1AT is shown to be relatively lower than those in BTG tissues.

An earlier study conducted by Netea-Maier et al. (2008) by examining differences of protein abundances between follicular adenoma and follicular cancer tissues has also shown a statistically significant difference in the levels of PDI, which is one of 20 proteins belonging to a family of enzymes that mediate oxidative protein folding in the endoplasmic reticulum (Kozlov, Määttänen, Thomas, & Gehring, 2010). PDI, a member of the thioredoxin superfamily of redox proteins, is capable of protecting cancer cells from apoptosis and silencing of the PDI gene to induce substantial cytotoxicity (Lovat et al., 2008). It is also believed to regulate STAT3 signalling and proliferation, which is thought to trigger malignancy (Coe, Jung, Groenendyk, Prins, & Michalak, 2010). The respective protein has been shown to be up-regulated in the melanoma cell lines (Caputo et al., 2011) and lung adenocarcinoma (Tufo et al., 2014).

UBE2N, also known as Ubc13, is believed to control protein-protein interactions involved in DNA damage repair and protein kinase activation (Wu et al., 2009). It plays a critical role in the activation of NF- κ B (Cheng et al., 2014) and MAPKs signalling (Tseng et al., 2010; Yamamoto et al., 2006) in most immune cells. UBE2N has been previously reported to be overexpressed in patients with triple-negative breast cancer as well as in six different neuroblastoma cell lines (Cheng et al., 2014; Lino et al., 2014). The role of UBE2N in the development of neuroblastoma was explained by p53 inactivation through formation of monomeric p53 that results in its cytoplasmic translocation and subsequent loss of function (Cheng et al., 2014). This same mechanism may also occur in the development of PTCb as supported by our observation of decreased

UBE2N abundance in the PTCb tissues although further investigations are needed for absolute confirmation.

When similar gel-based experiments were performed on serum samples of the same groups of PTCa, PTCb, and BTG patients, only A1AT was consistently detected to be of altered abundance. HSP70, PDI, and UB2EN, which were earlier shown to be differently expressed in the tissue samples of patients with PTCa or PTCb, were either not detected or not significantly different when compared to patients with BTG. Among the proteins identified, A1AT demonstrated significantly higher abundance in serum samples of PTCa patients compared to those of BTG. Earlier studies have also demonstrated significantly increased levels of blood A1AT in a good number of cancers including gastrointestinal cancer (Solakidi, Dessypris, Stathopoulos, Androulakis, & Sekeris, 2004), hepatocellular carcinoma (Hong & Hong, 1991), infiltrating ductal breast carcinoma (Hamrita et al., 2009), lung cancer (Patz Jr et al., 2007) and pancreatic adenocarcinoma (Trachte et al., 2002) but the present study, performed by 2-DE as well as ELISA, is the first to report on the enhanced levels of A1AT in the serum samples of PTCa patients.

A1AT is mainly synthesised in the liver cells and known to be present in abundance in the blood. Enhanced levels of A1AT in the blood circulation of patients with cancer are believed to be due to additional production of the protease inhibitor by the tumour cells (Poblete et al., 1996). Whilst this may be true in PTCa, it is not quite the same in the case of PTCb as our earlier analysis has shown decreased levels of A1AT in the cancer tissues of the PTCb patients. Hence, in case of the latter, enhanced abundance of serum A1AT detected is more likely to be a result of excess cell death or damage as earlier suggested by Anderson and Anderson (2002). Enhanced levels of A1AT in the blood circulation of cancer patients is likely due to the non-specific acute phase reaction in response to inflammation accompanying tumour progression (Bergin, Hurley,

McElvaney, & Reeves, 2012; Jonigk et al., 2013). Hence, the enhance production of A1AT in PTCa may generally regarded as one of the defence mechanism of the body against cancer growth.

Apart from A1AT, elevated levels of alpha 1-beta glycoprotein (A1B) were further detected in the serum analyses of patients with PTCa. A member of the immunoglobulin superfamily, A1B is believed to be a secreted plasma protein (Ishioka, Takahashi, & Putnam, 1986). Although the function of A1B is unknown, overabundance of the protein in serum samples has been previously reported in patients with endometrial and cervical cancers (Abdul- Rahman, Lim, & Hashim, 2007) as well as cervical squamous cell carcinoma (Looi et al., 2009). These findings suggest that the protein may be involved in carcinogenesis.

In contrast to patients with PTCa, serum analyses of PTCb patients demonstrated relatively higher levels of alpha 2-HS glycoprotein (AHSG) and apolipoprotein A4 (APOA4) relative to those from patients with BTG. Significant higher levels of AHSG in the PTCb patients relative to those with BTG were also detected in the ELISA experiments. AHSG, which is also known as fetuin-A, is a member of the cystatin family of proteins that has been linked to a number of cellular functions such as brain development, bone remodelling, and immune functions (Arnaud & Kalabay, 2002). The binding of AHSG to annexin surface receptor of tumour cells in a Ca^{2+} -dependent fashion triggers the PI3K-AKT signalling pathway leading to tumour establishment and growth (Kundranda et al., 2005). Furthermore, the absence of ASHG has been proved to reduce the number of tumours per mouse by 30% without altering the tumour onset or conversion of benign papilloma to squamous cell carcinoma (Leite-Browning et al., 2004). Earlier studies have reported its reduced abundance in patients with acute myeloid leukaemia (Kwak et al., 2004), lung squamous cell carcinoma (Dowling et al., 2012), and germ-line

ovarian carcinoma (Chen, Lim, Peh, Abdul-Rahman, & Hashim, 2008), whilst hypopharyngeal squamous cell carcinoma (Tian et al., 2015) and pancreatic ductal adenocarcinoma (Chen et al., 2014) showed elevated levels of ASHG.

APOA4 is a plasma lipoprotein which controls multiple metabolic pathways such as lipid and glucose metabolism. The protein is primarily synthesised by the small intestine and liver, followed by secretion into the blood (Wang et al., 2015). Plasma APOA4 levels correlate with the high-density lipoproteins levels. APOA4 has anti-inflammatory and anti-oxidative properties (Khovidhunkit et al., 2004; Recalde et al., 2004). The levels of APOA4 have been similarly shown to be able to discriminate malignant from benign cases in ovarian (Timms et al., 2014) and endometrial neoplasms (Wang et al., 2011).

When taken together, the data from tissue and serum analyses of PTCa and PTCb patients relative to those with BTG generally points to differences in the two distinct cancers of the thyroid although it is currently not possible to rule out that they may also be due other reasons such as the different stages of the malignant disease. Both PTCa and PTCb distinguish themselves from BTG in different types of tissue and serum proteins of altered abundance. While lower levels of tissue A1AT, PDI, and UBE2N appeared to be associated with PTCb, higher abundances of A1AT and HSP70 seemed apparent in PTCa. In case of the serum proteins, higher abundances of A1AT and A1B were detected in PTCa, while PTCb was associated with enhanced APOA4 and AHSG. Because of their distinctive altered abundances, these proteins have strong potentials to be used as tissue or serum biomarkers for distinguishing the three different thyroid neoplasms although this requires further extensive validation in clinically representative populations.

CHAPTER 6: CONCLUSION

In the present study, tissues of patients with benign thyroid goitre (BTG) and papillary thyroid cancer (PTC) were systematically investigated for molecular alterations. In the genomics study, whole-exome sequencing (WES) performed on tissues of four with BTG and five patients with PTC detected 340 of previously described variants in 36 thyroid neoplasm-related genes. This included earlier reported pathogenic mutations, such as c.1799T>A (p.Val600Glu) and c.861-170A>T of *BRAF*, c.191C>A (p.Pro64His) and c.292A>C of *LGALS3*, as well as c.215C>G (p.Arg72Pro) of *TP53* genes. Screening of nucleotide alterations in the thyroid neoplasm-related genes showed that the *TG* gene exhibited the highest number of variations. The least number of variants was detected in *NRAS* and *TIMP3* genes. None of the variants was found in *BGLAP* and *RASSF1A* genes. The findings of this study also revealed a total of 23 novel variants in 12 candidate genes. Among these were five non-synonymous novel mutations of the *RASSF1*, *TG*, *TPO*, and *TRH* genes, which affected normal activities of their respective proteins. In addition, another novel intronic c.19-50_53CTGdel mutation of *LGALS3*, was also detected and believed to cause misalignment of the mRNA molecule with *ILI27*, creating a novel *LGALS3-IFI27* chimeric mRNA. The data generated from the present study suggests that these novel mutations may have an impact on disease-causing effects.

In the case study report, the benign and malignant tissues of a patient with concurrent benign thyroid cyst and PTC were both detected for the c.353G>A (p.Arg118Gln) mutation of the *TRH* gene, when analysed by PCR-direct sequencing and WES, respectively. However, the malignant tissue further showed presence of the c.1799T>A (p.Val600Glu) mutation in the *BRAF* gene, which was not detected in the benign cyst. Data generated from proteomics analysis of both the benign and malignant tissues further led to the speculation that the malignancy in the patient may have been due to *BRAF*^{V600E}

mutation that was initiated from prolonged H₂O₂ insults attributed to the germ line *TRH*^{R118Q} mutation.

Using 2-DE gel-based approach together with silver staining detection method, an attempt to establish 2-DE profiles of high abundance tissue and serum proteins of PTC patients without (PTCa) and with a history of BTG (PTCb) as well as those with BTG were methodically performed. The data of the present study showed that PTCa and PTCb distinguished themselves from BTG in the types of tissue and serum proteins of altered abundance. Comparative ImageMaster™ analyses had resulted in higher levels of alpha-1 antitrypsin (A1AT) and heat shock 70 kDa protein in tissue samples of patients with PTCa compared to those with BTG. For PTCb, marked aberration in the abundance of tissue proteins were observed for A1AT, protein disulfide isomerase and ubiquitin conjugating enzyme E2N. In case of the serum proteins, higher levels of A1AT and alpha 1-beta glycoprotein were associated with PTCa, while higher levels of apolipoprotein A-IV and alpha 2-HS glycoprotein (AHSG) seemed apparent in the PTCb. The different altered expression of tissue and serum A1AT as well as serum AHSG were validated by ELISA. The distinctive altered abundances of the tissue and serum proteins that were detected from the proteomics analysis, in essence, form preliminary indications that PTCa and PTCb are two distinct cancers of the thyroid that are etiologically and mechanistically different. These proteins also stand to have a potential use as tissue or serum biomarkers to discriminate the three different thyroid neoplasms although this requires further validation in clinically representative populations.

REFERENCES

- Abdul- Rahman, P. S., Lim, B. K., & Hashim, O. H. (2007). Expression of high-abundance proteins in sera of patients with endometrial and cervical cancers: analysis using 2- DE with silver staining and lectin detection methods. *Electrophoresis*, 28(12), 1989-1996.
- Abidi, M., Fayaz, S., & Fard, E. P. (2017). Association of the Asp1312Gly *thyroglobulin* gene polymorphism with susceptibility to differentiated thyroid cancer in an Iranian population. *Asian Pacific Journal of Cancer Prevention: APJCP*, 18(2), 503.
- Adeniran, A. J., Zhu, Z., Gandhi, M., Steward, D. L., Fidler, J. P., Giordano, T. J., . . . Nikiforov, Y. E. (2006). Correlation between genetic alterations and microscopic features, clinical manifestations, and prognostic characteristics of thyroid papillary carcinomas. *The American Journal of Surgical Pathology*, 30(2), 216-222.
- Adzhubei, I. A., Schmidt, S., Peshkin, L., Ramensky, V. E., Gerasimova, A., Bork, P., . . . Sunyaev, S. R. (2010). A method and server for predicting damaging missense mutations. *Nature Methods*, 7(4), 248-249.
- Akahani, S., Nangia-Makker, P., Inohara, H., Kim, H. R. C., & Raz, A. (1997). Galectin-3: a novel antiapoptotic molecule with a functional BH1 (NWGR) domain of Bcl-2 family. *Cancer Research*, 57(23), 5272-5276.
- Akdi, A., Pérez, G., Pastor, S., Castell, J., Biarnés, J., Marcos, R., & Velázquez, A. (2011). Common variants of the *thyroglobulin* gene are associated with differentiated thyroid cancer risk. *Thyroid*, 21(5), 519-525.
- Akgül, Ö., Ocak, S., Göçmen, E., Koc, M., & Tez, M. (2010). Clinical significance of cellular microfollicular lesions in goiter. *The Endocrinologist*, 20(3), 115-116.
- Akiva, P., Toporik, A., Edelheit, S., Peretz, Y., Diber, A., Shemesh, R., . . . Sorek, R. (2006). Transcription-mediated gene fusion in the human genome. *Genome Research*, 16(1), 30-36.
- Al-Salamah, S. M., Khalid, K., & Bismar, H. A. (2002). Incidence of differentiated cancer in nodular goiter. *Saudi Medical Journal*, 23(8), 947-952.
- Alaiya, A., Oppermann, M., Langridge, J., Roblick, U., Egevad, L., Brändstedt, S., . . . Jörnvall, H. (2001). Identification of proteins in human prostate tumor material by two-dimensional gel electrophoresis and mass spectrometry. *Cellular and Molecular Life Sciences*, 58(2), 307-311.
- Alevizaki, M., Papageorgiou, G., Rentziou, G., Saltiki, K., Marafelia, P., Loukari, E., . . . Dimopoulos, M. A. (2009). Increasing prevalence of papillary thyroid carcinoma in recent years in Greece: the majority are incidental. *Thyroid*, 19(7), 749-754.

- Anderson, N. L., & Anderson, N. G. (2002). The human plasma proteome history, character, and diagnostic prospects. *Molecular and Cellular Proteomics*, 1(11), 845-867.
- Arnaud, P., & Kalabay, L. (2002). Alpha2- HS glycoprotein: a protein in search of a function. *Diabetes/Metabolism Research and Reviews*, 18(4), 311-314.
- Arora, N., Scognamiglio, T., Zhu, B., & Fahey III, T. J. (2008). Do benign thyroid nodules have malignant potential? An evidence-based review. *World Journal of Surgery*, 32(7), 1237-1246.
- Azare, J., Leslie, K., Al-Ahmadie, H., Gerald, W., Weinreb, P. H., Violette, S. M., & Bromberg, J. (2007). Constitutively activated Stat3 induces tumorigenesis and enhances cell motility of prostate epithelial cells through integrin β 6. *Molecular and Cellular Biology*, 27(12), 4444-4453.
- Balan, V., Nangia-Makker, P., & Raz, A. (2010). Galectins as cancer biomarkers. *Cancers*, 2(2), 592-610.
- Balan, V., Nangia-Makker, P., Schwartz, A. G., Jung, Y. S., Tait, L., Hogan, V., . . . Wu, G. S. (2008). Racial disparity in breast cancer and functional germ line mutation in galectin-3 (rs4644): A pilot study. *Cancer Research*, 68(24), 10045-10050.
- Ban, Y., Tozaki, T., Taniyama, M., Skrabanek, L., Nakano, Y., Ban, Y., & Hirano, T. (2012). Multiple SNPs in intron 41 of *thyroglobulin* gene are associated with autoimmune thyroid disease in the Japanese population. *PLoS One*, 7(5), e37501.
- Ban, Y., Yamamoto, G., Takada, M., Hayashi, S., Ban, Y., Shimizu, K., . . . Hirano, T. (2012). Proteomic profiling of thyroid papillary carcinoma. *Journal of Thyroid Research*, 2012, 815079. doi: 10.1155/2012/815079.
- Baran-Marszak, F., Feuillard, J., Najjar, I., Le Clorennec, C., Béchet, J.-M., Dusanter-Fourt, I., . . . Fagard, R. (2004). Differential roles of STAT1 α and STAT1 β in fludarabine-induced cell cycle arrest and apoptosis in human B cells. *Blood*, 104(8), 2475-2483.
- Baris, O., Mirebeau-Prunier, D., Savagner, F., Rodien, P., Ballester, B., Loriol, B., . . . Malthiery, Y. (2005). Gene profiling reveals specific oncogenic mechanisms and signaling pathways in oncocytic and papillary thyroid carcinoma. *Oncogene*, 24(25), 4155-4161. doi: 10.1038/sj.onc.1208578.
- Barroeta, J. E., Wang, H., Shiina, N., Gupta, P. K., LiVolsi, V. A., & Baloch, Z. W. (2006). Is fine-needle aspiration (FNA) of multiple thyroid nodules justified? *Endocrine Pathology*, 17(1), 61-66.
- Bartels, C. L., & Tsongalis, G. J. (2009). MicroRNAs: novel biomarkers for human cancer. *Clinical Chemistry*, 55(4), 623-631.
- Belfiore, A., La Rosa, G. L., La Porta, G. A., Giuffrida, D., Milazzo, G., Lupo, L., . . . Vigneri, R. (1992). Cancer risk in patients with cold thyroid nodules: relevance of iodine intake, sex, age, and multinodularity. *The American Journal of Medicine*, 93(4), 363-369.

- Bellini, M. F., Cadamuro, A. C. T., Succi, M., Proença, M. A., & Silva, A. E. (2012). Alterations of the *TP53* gene in gastric and esophageal carcinogenesis. *BioMed Research International*, 2012.
- Bergamaschi, D., Samuels, Y., Sullivan, A., Zvelebil, M., Breysens, H., Bisso, A., . . . Gasco, M. (2006). iASPP preferentially binds p53 proline-rich region and modulates apoptotic function of codon 72-polymorphic p53. *Nature Genetics*, 38(10), 1133-1141.
- Bergers, G., Brekken, R., McMahon, G., Vu, T. H., Itoh, T., Tamaki, K., . . . Werb, Z. (2000). Matrix metalloproteinase-9 triggers the angiogenic switch during carcinogenesis. *Nature Cell Biology*, 2(10), 737-744.
- Bergin, D. A., Hurley, K., McElvaney, N. G., & Reeves, E. P. (2012). Alpha-1 antitrypsin: A potent anti-inflammatory and potential novel therapeutic agent. *Archivum Immunologiae et Therapiae Experimentalis*, 60(2), 81-97.
- Blankenship, D. R., Chin, E., & Terris, D. J. (2005). Contemporary management of thyroid cancer. *American Journal of Otolaryngology*, 26(4), 249-260.
- Boltze, C., Roessner, A., Landt, O., Szibor, R., Peters, B., & Schneider-Stock, R. (2002). Homozygous proline at codon 72 of p53 as a potential risk factor favoring the development of undifferentiated thyroid carcinoma. *International Journal of Oncology*, 21(5), 1151-1154.
- Bombil, I., Bentley, A., Kruger, D., & Luvhengo, T. E. (2014). Incidental cancer in multinodular goitre post thyroidectomy. *South African Journal of Surgery*, 52(1), 5-9.
- Bomeli, S. R., LeBeau, S. O., & Ferris, R. L. (2010). Evaluation of a thyroid nodule. *Otolaryngology Clinic of North America*, 43(2), 229-238, vii. doi: 10.1016/j.otc.2010.01.002.
- Bongarzone, I., Monzini, N., Borrello, M., Carcano, C., Ferraresi, G., Arighi, E., . . . Pierotti, M. (1993). Molecular characterization of a thyroid tumor-specific transforming sequence formed by the fusion of ret tyrosine kinase and the regulatory subunit RI alpha of cyclic AMP-dependent protein kinase A. *Molecular and Cellular Biology*, 13(1), 358-366.
- Brand, O. J., Barrett, J. C., Simmonds, M. J., Newby, P. R., McCabe, C. J., Bruce, C. K., . . . Hunt, P. J. (2009). Association of the *thyroid stimulating hormone receptor* gene (*TSHR*) with Graves' disease. *Human Molecular Genetics*, 18(9), 1704-1713.
- Brander, A., Viikinkoski, P., Nickels, J., & Kivisaari, L. (1991). Thyroid gland: US screening in a random adult population. *Radiology*, 181(3), 683-687. doi: 10.1148/radiology.181.3.1947082.
- Brehar, A., Brehar, F., Bulgar, A., & Dumitrache, C. (2013). Genetic and epigenetic alterations in differentiated thyroid carcinoma. *Journal of Medicine and Life*, 6(4), 403.

- Bromberg, J. F., Wrzeszczynska, M. H., Devgan, G., Zhao, Y., Pestell, R. G., Albanese, C., & Darnell, J. E. (1999). Stat3 as an oncogene. *Cell*, 98(3), 295-303.
- Brown, L. M., Helmke, S. M., Hunsucker, S. W., Netea-Maier, R. T., Chiang, S. A., Heinz, D. E., . . . Haugen, B. R. (2006). Quantitative and qualitative differences in protein expression between papillary thyroid carcinoma and normal thyroid tissue. *Molecular Carcinogenesis*, 45(8), 613-626. doi: 10.1002/mc.20193.
- Burke, W. M., Jin, X., Lin, H. J., Huang, M., Liu, R., Reynolds, R. K., & Lin, J. (2001). Inhibition of constitutively active Stat3 suppresses growth of human ovarian and breast cancer cells. *Oncogene*, 20(55), 7925-7934.
- Bursuk, E. (2012). Introduction to Thyroid: Anatomy and Functions. In L. S. Ward (Ed.), *Thyroid and parathyroid diseases-new insights into some old and some new Issues*. doi: 10.5772/37942.
- Caldenhoven, E., van Dijk, T. B., Solari, R., Armstrong, J., Raaijmakers, J. A., Lammers, J. W. J., . . . de Groot, R. P. (1996). STAT3 β , a splice variant of transcription factor STAT3, is a dominant negative regulator of transcription. *Journal of Biological Chemistry*, 271(22), 13221-13227.
- Cantwell-Dorris, E. R., O'Leary, J. J., & Sheils, O. M. (2011). BRAFV600E: Implications for carcinogenesis and molecular therapy. *Molecular Cancer Therapeutics*, 10(3), 385-394.
- Caputo, E., Maiorana, L., Vasta, V., Pezzino, F. M., Sunkara, S., Wynne, K., . . . Libra, M. (2011). Characterization of human melanoma cell lines and melanocytes by proteome analysis. *Cell Cycle*, 10(17), 2924-2936.
- Cardoso, A. C. F., Andrade, L. N. de S., & Bustos, S. O., Chammas, R. (2016). Galectin-3 determines tumor cell adaptive strategies in stressed tumor microenvironments. *Frontiers in Oncology*, 6, 127.
- Carlé, A., Krejbjerg, A., & Laurberg, P. (2014). Epidemiology of nodular goitre. Influence of iodine intake. *Best Practice and Research: Clinical Endocrinology and Metabolism*, 28(4), 465-479.
- Cassol, C. A., & Asa, S. L. (2011). Molecular pathology of thyroid cancer. *Diagnostic Histopathology*, 17(3), 124-139.
- Chakraborty, A., Narkar, A., Mukhopadhyaya, R., Kane, S., D'Cruz, A., & Rajan, M. G. (2012). BRAF V600E mutation in papillary thyroid carcinoma: Significant association with node metastases and extra thyroidal invasion. *Endocrine Pathology*, 23(2), 83-93.
- Chandramouli, K., & Qian, P. Y. (2009). Proteomics: challenges, techniques and possibilities to overcome biological sample complexity. *Human Genomics and Proteomics*, 2009. doi: 10.4061/2009/239204.
- Chen, B. J., Wu, Y. L., Tanaka, Y., & Zhang, W. (2014). Small molecules targeting c-Myc oncogene: promising anti-cancer therapeutics. *International Journal of Biological Sciences*, 10(10), 1084.

- Chen, J., Wu, W., Chen, L., Ma, X., Zhao, Y., Zhou, H., . . . Hu, L. (2014). Expression and clinical significance of AHSG and complement C3 in pancreatic ductal adenocarcinoma. *Zhonghua Yi Xue Za Zhi*, *94*(28), 2175-2179.
- Chen, R., Liu, S., Ye, H., Li, J., Du, Y., Chen, L., . . . Mao, Y. (2015). Association of *p53* rs1042522, *MDM2* rs2279744, and *p21* rs1801270 polymorphisms with retinoblastoma risk and invasion in a Chinese population. *Scientific Reports*, *5*, 13300.
- Chen, Y., Lim, B. K., Peh, S. C., Abdul-Rahman, P. S., & Hashim, O. H. (2008). Profiling of serum and tissue high abundance acute-phase proteins of patients with epithelial and germ line ovarian carcinoma. *Proteome Science*, *6*(1), 20.
- Cheng, J., Fan, Y., Xu, X., Zhang, H., Dou, J., Tang, Y., . . . Zhao, Y. (2014). A small-molecule inhibitor of UBE2N induces neuroblastoma cell death via activation of *p53* and *JNK* pathways. *Cell Death and Disease*, *5*(2), e1079.
- Chiang, F. Y., Wu, C. W., Hsiao, P. J., Kuo, W. R., Lee, K. W., Lin, J. C., . . . Juo, S. H. H. (2008). Association between polymorphisms in DNA base excision repair genes *XRCC1*, *APE1*, and *ADPRT* and differentiated thyroid carcinoma. *Clinical Cancer Research*, *14*(18), 5919-5924.
- Chiu, C. G., Strugnell, S. S., Griffith, O. L., Jones, S. J., Gown, A. M., Walker, B., . . . Wiseman, S. M. (2010). Diagnostic utility of galectin-3 in thyroid cancer. *The American Journal of Pathology*, *176*(5), 2067-2081.
- Cho, W. C. S. (2010). Omics approaches in cancer research In: W. Cho (Ed.) *An omics perspective on cancer research*. Springer, Dordrecht.
- Chow, L. S., Gharib, H., Goellner, J. R., & van Heerden, J. A. (2001). Nondiagnostic thyroid fine-needle aspiration cytology: management dilemmas. *Thyroid*, *11*(12), 1147-1151. doi: 10.1089/10507250152740993.
- Chung, K. W., Kim, S. W., & Kim, S. W. (2012). Gene expression profiling of papillary thyroid carcinomas in Korean patients by oligonucleotide microarrays. *Journal of the Korean Surgical Society*, *82*(5), 271-280. doi: 10.4174/jkss.2012.82.5.271.
- Ciampi, R., & Nikiforov, Y. E. (2007). *RET/PTC* rearrangements and *BRAF* mutations in thyroid tumorigenesis. *Endocrinology*, *148*(3), 936-941.
- Ciocca, D. R., Clark, G. M., Tandon, A. K., Fuqua, S. A., Welch, W. J., & McGuire, W. L. (1993). Heat shock protein hsp70 in patients with axillary lymph node-negative breast cancer: prognostic implications. *Journal of the National Cancer Institute*, *85*(7), 570-574.
- Cipollini, M., Pastor, S., Gemignani, F., Castell, J., Garritano, S., Bonotti, A., . . . Marcos, R. (2013). *TPO* genetic variants and risk of differentiated thyroid carcinoma in two European populations. *International Journal of Cancer*, *133*(12), 2843-2851.
- Ciregia, F., Giusti, L., Molinaro, A., Niccolai, F., Agretti, P., Rago, T., . . . Iacconi, P. (2013). Presence in the pre-surgical fine-needle aspiration of potential thyroid

biomarkers previously identified in the post-surgical one. *PLoS One*, 8(9), e72911.

- Citterio, C. E., Machiavelli, G. A., Miras, M. B., Gruñeiro-Papendieck, L., Lachlan, K., Sobrero, G., . . . Testa, G. (2013). New insights into *thyroglobulin* gene: molecular analysis of seven novel mutations associated with goiter and hypothyroidism. *Molecular and Cellular Endocrinology*, 365(2), 277-291.
- Coe, H., Jung, J., Groenendyk, J., Prins, D., & Michalak, M. (2010). ERp57 modulates STAT3 signaling from the lumen of the endoplasmic reticulum. *Journal of Biological Chemistry*, 285(9), 6725-6738.
- Cohen, Y., Xing, M., Mambo, E., Guo, Z., Wu, G., Trink, B., . . . Sidransky, D. (2003). *BRAF* mutation in papillary thyroid carcinoma. *Journal of the National Cancer Institute*, 95(8), 625-627.
- Colston, J. T., Chandrasekar, B., & Freeman, G. L. (2002). A novel peroxide-induced calcium transient regulates interleukin-6 expression in cardiac-derived fibroblasts. *Journal of Biological Chemistry*, 277(26), 23477-23483.
- Comino-Mendez, I., Gracia-Aznarez, F. J., Schiavi, F., Landa, I., Leandro-Garcia, L. J., Leton, R., . . . Cascon, A. (2011). Exome sequencing identifies *MAX* mutations as a cause of hereditary pheochromocytoma. *Nature Genetics*, 43(7), 663-667. doi: 10.1038/ng.861.
- Constantinides, V., & Palazzo, F. (2013). Goitre and thyroid cancer. *Medicine*, 41(9), 546-550.
- Corvilain, B., Van Sande, J., Laurent, E., & Dumont, J. E. (1991). The H₂O₂-generating system modulates protein iodination and the activity of the pentose phosphate pathway in dog thyroid. *Endocrinology*, 128(2), 779-785.
- Couto, J. P., Daly, L., Almeida, A., Knauf, J. A., Fagin, J. A., Sobrinho-Simões, M., . . . Lyden, D. (2012). STAT3 negatively regulates thyroid tumorigenesis. *Proceedings of the National Academy of Sciences*, 109(35), E2361-E2370.
- Dabbagh, K., Laurent, G. J., Shock, A., Leoni, P., Papakrivopoulou, J., & Chambers, R. C. (2001). Alpha-1-antitrypsin stimulates fibroblast proliferation and procollagen production and activates classical MAP kinase signalling pathways. *Journal of Cellular Physiology*, 186(1), 73-81.
- Dang, C. V. (2013). MYC, metabolism, cell growth, and tumorigenesis. *Cold Spring Harbor Perspectives in Medicine*, 3(8), a014217.
- Davies, L., & Welch, H. G. (2006). Increasing incidence of thyroid cancer in the United States, 1973-2002. *Jama*, 295(18), 2164-2167.
- de la Chapelle, A., & Jazdzewski, K. (2011). MicroRNAs in thyroid cancer. *The Journal of Clinical Endocrinology and Metabolism*, 96(11), 3326-3336.

- de la Iglesia, N., Konopka, G., Puram, S. V., Chan, J. A., Bachoo, R. M., You, M. J., . . . Bonni, A. (2008). Identification of a PTEN-regulated STAT3 brain tumor suppressor pathway. *Genes and Development*, 22(4), 449-462.
- de Mendonça Belmont, T. F., da Silva, A. S., de Melo Vilar, K., Medeiros, F.S., Vasconcelos, L. R. S., dos Anjos, A. C. M., . . . da Silva Araujo, A. (2016). Single nucleotide polymorphisms at+ 191 and+ 292 of *galectin-3* gene (*LGALS3*) related to lower GAL-3 serum levels are associated with frequent respiratory tract infection and vaso-occlusive crisis in children with sickle cell anemia. *PLoS One*, 11(9), e0162297.
- Diaz, N., Minton, S., Cox, C., Bowman, T., Gritsko, T., Garcia, R., . . . Seijo, E. (2006). Activation of stat3 in primary tumors from high-risk breast cancer patients is associated with elevated levels of activated SRC and survivin expression. *Clinical Cancer Research*, 12(1), 20-28.
- Dinets, A., Pernemalm, M., Kjellin, H., Sviatoha, V., Sofiadis, A., Juhlin, C. C., . . . Hoog, A. (2015). Differential protein expression profiles of cyst fluid from papillary thyroid carcinoma and benign thyroid lesions. *PLoS One*, 10(5), e0126472. doi: 10.1371/journal.pone.0126472.
- Dowling, P., Clarke, C., Hennessy, K., Torralbo- Lopez, B., Ballot, J., Crown, J., . . . Lynch, V. (2012). Analysis of acute- phase proteins, AHSG, C3, CLI, HP and SAA, reveals distinctive expression patterns associated with breast, colorectal and lung cancer. *International Journal of Cancer*, 131(4), 911-923.
- Dralle, H., Machens, A., Basa, J., Fatourechi, V., Franceschi, S., Hay, I. D., . . . Sherman, S. I. (2015). Follicular cell-derived thyroid cancer. *Nature Reviews Disease Primers*, 1, 15077. doi: 10.1038/nrdp.2015.77.
- Dumont, P., Leu, J.-J., Della Pietra, A. C., George, D. L., & Murphy, M. (2003). The codon 72 polymorphic variants of *p53* have markedly different apoptotic potential. *Nature Genetics*, 33(3), 357-365.
- Dunning, A. M., Healey, C. S., Pharoah, P. D., Teare, M. D., Ponder, B. A., & Easton, D. F. (1999). A systematic review of genetic polymorphisms and breast cancer risk. *Cancer Epidemiology and Prevention Biomarkers*, 8(10), 843-854.
- Durante, C., Puxeddu, E., Ferretti, E., Morisi, R., Moretti, S., Bruno, R., . . . Verrienti, A. (2007). *BRAF* mutations in papillary thyroid carcinomas inhibit genes involved in iodine metabolism. *The Journal of Clinical Endocrinology and Metabolism*, 92(7), 2840-2843.
- Eberhardt, N. L., Grebe, S. K., McIver, B., & Reddi, H. V. (2010). The role of the *PAX8/PPAR* gamma fusion oncogene in the pathogenesis of follicular thyroid cancer. *Molecular and Cell Endocrinology*, 321(1), 50-56. doi: 10.1016/j.mce.2009.10.013.
- Elisei, R., Molinaro, E., Agate, L., Bottici, V., Viola, D., Biagini, A., . . . Vivaldi, A. (2014). *RET* oncogene and thyroid carcinoma. *Journal of Genetic Syndromes and Gene Therapy*, 5(1), 1.

- Elisei, R., Ugolini, C., Viola, D., Lupi, C., Biagini, A., Giannini, R., . . . Basolo, F. (2008). *BRAFV600E* mutation and outcome of patients with papillary thyroid carcinoma: a 15-year median follow-up study. *The Journal of Clinical Endocrinology and Metabolism*, *93*(10), 3943-3949.
- Enewold, L., Zhu, K., Ron, E., Marrogi, A. J., Stojadinovic, A., Peoples, G. E., & Devesa, S. S. (2009). Rising thyroid cancer incidence in the United States by demographic and tumor characteristics, 1980-2005. *Cancer Epidemiology, Biomarkers and Prevention*, *18*(3), 784-791. doi: 10.1158/1055-9965.EPI-08-0960.
- Epling-Burnette, P., Liu, J. H., Catlett-Falcone, R., Turkson, J., Oshiro, M., Kothapalli, R., . . . Karras, J. (2001). Inhibition of STAT3 signaling leads to apoptosis of leukemic large granular lymphocytes and decreased Mcl-1 expression. *Journal of Clinical Investigation*, *107*(3), 351.
- Erbil, Y., Barbaros, U., Özbey, N., Kapran, Y., Tükenmez, M., Bozbora, A., & Özarmağan, S. (2008). Graves' disease, with and without nodules, and the risk of thyroid carcinoma. *The Journal of Laryngology and Otology*, *122*(3), 291-295.
- Espadinha, C., Santos, J. R., Sobrinho, L. G., & Bugalho, M. J. (2009). Expression of iodine metabolism genes in human thyroid tissues: evidence for age and *BRAFV600E* mutation dependency. *Clinical Endocrinology (Oxf)*, *70*(4), 629-635.
- Estep, A. L., Palmer, C., McCormick, F., & Rauen, K. A. (2007). Mutation analysis of *BRAF*, *MEK1* and *MEK2* in 15 ovarian cancer cell lines: implications for therapy. *PLoS One*, *2*(12), e1279.
- Ezzat, S., Sarti, D. A., Cain, D. R., & Braunstein, G. D. (1994). Thyroid incidentalomas. Prevalence by palpation and ultrasonography. *Archives of Internal Medicine*, *154*(16), 1838-1840.
- Fagin, J. A., & Mitsiades, N. (2008). Molecular pathology of thyroid cancer: diagnostic and clinical implications. *Best Practice and Research. Clinical endocrinology and Metabolism*, *22*(6), 955-969.
- Fan, Y., Shi, L., Liu, Q., Dong, R., Zhang, Q., Yang, S., . . . Wang, J. (2009). Discovery and identification of potential biomarkers of papillary thyroid carcinoma. *Molecular Cancer*, *8*, 79. doi: 10.1186/1476-4598-8-79.
- Fang, W., Wei, Y., Kang, Y., & Landweber, L. F. (2012). Detection of a common chimeric transcript between human chromosomes 7 and 16. *Biology Direct*, *7*(1), 49.
- Finley, D. J., Arora, N., Zhu, B., Gallagher, L., & Fahey III, T. J. (2004). Molecular profiling distinguishes papillary carcinoma from benign thyroid nodules. *The Journal of Clinical Endocrinology and Metabolism*, *89*(7), 3214-3223. doi: 10.1210/jc.2003-031811.
- Finn, S., Smyth, P., O'Regan, E., Cahill, S., Toner, M., Timon, C., . . . Sheils, O. (2007). Low-level genomic instability is a feature of papillary thyroid carcinoma: an array comparative genomic hybridization study of laser capture microdissected

papillary thyroid carcinoma tumors and clonal cell lines. *Archives of Pathology and Laboratory Medicine*, 131(1), 65-73. doi: 10.1043/1543-2165(2007)131[65:LGIIAF]2.0.CO;2.

- Fugazzola, L., Puxeddu, E., Avenia, N., Romei, C., Cirello, V., Cavaliere, A., . . . Rossi, S. (2006). Correlation between *B-RAFV600E* mutation and clinic-pathologic parameters in papillary thyroid carcinoma: data from a multicentric Italian study and review of the literature. *Endocrine-related Cancer*, 13(2), 455-464.
- Fujarewicz, K., Jarzab, M., Eszlinger, M., Krohn, K., Paschke, R., Oczko-Wojciechowska, M., . . . Swierniak, A. (2007). A multi-gene approach to differentiate papillary thyroid carcinoma from benign lesions: gene selection using support vector machines with bootstrapping. *Endocrine-related Cancer*, 14(3), 809-826.
- Fulda, S., Gorman, A. M., Hori, O., & Samali, A. (2010). Cellular stress responses: cell survival and cell death. *International Journal of Cell Biology*, 2010.
- Gandolfi, P. P., Frisina, A., Raffa, M., Renda, F., Rocchetti, O., Ruggeri, C., & Tombolini, A. (2004). The incidence of thyroid carcinoma in multinodular goiter: retrospective analysis. *Acta Biomed*, 75(2), 114-117.
- Gao, Y., Chen, F., Niu, S., Lin, S., & Li, S. (2015). Replication and meta-Analysis of common gene mutations in *TTF1* and *TTF2* with papillary thyroid cancer. *Medicine*, 94(36).
- Garas, G., Jarral, O., Tolley, N., Palazzo, F., Athanasiou, T., & Zacharakis, E. (2013). Is there survival benefit from life-long follow-up after treatment for differentiated thyroid cancer? *International Journal of Surgery*, 11(2), 116-121.
- Garcia-Rostan, G., Costa, A. M., Pereira-Castro, I., Salvatore, G., Hernandez, R., Hermsem, M. J., . . . Santoro, M. (2005). Mutation of the *PIK3CA* gene in anaplastic thyroid cancer. *Cancer Research*, 65(22), 10199-10207.
- Gérard, A. C., Many, M.-C., Daumerie, C., Knoops, B., & Colin, I. (2005). Peroxiredoxin 5 expression in the human thyroid gland. *Thyroid*, 15(3), 205-209.
- Geranova, J., Buysschaert, M., De Burbure, C., & Daumerie, C. (2003). Prevalence of thyroid cancer in Graves' disease: a retrospective study of a cohort of 103 patients treated surgically. *European Journal of Internal Medicine*, 14(5), 321-325.
- Gianfagna, F., Feo, E. D., Van Duijn, C. M., Ricciardi, G., & Boccia, S. (2008). A systematic review of meta-analyses on gene polymorphisms and gastric cancer risk. *Current Genomics*, 9(6), 361-374.
- Gilissen, C., Hoischen, A., Brunner, H. G., & Veltman, J. A. (2011). Unlocking Mendelian disease using exome sequencing. *Genome Biology*, 12(9), 228.
- Giordano, T. J., Kuick, R., Thomas, D. G., Misek, D. E., Vinco, M., Sanders, D., . . . Shedden, K. (2005). Molecular classification of papillary thyroid carcinoma: distinct *BRAF*, *RAS*, and *RET/PTC* mutation-specific gene expression profiles discovered by DNA microarray analysis. *Oncogene*, 24(44), 6646-6656.

- Giusti, L., Iaconi, P., Ciregia, F., Giannaccini, G., Donatini, G. L., Basolo, F., . . . Lucacchini, A. (2008). Fine-needle aspiration of thyroid nodules: proteomic analysis to identify cancer biomarkers. *Journal of Proteome Research*, 7(9), 4079-4088.
- Gong, J., Jiang, S., Wang, D., Dong, H., Chen, G., Fang, K., . . . Lu, F. (2016). Association of polymorphisms of rs179247 and rs12101255 in *thyroid stimulating hormone receptor* intron 1 with an increased risk of Graves' disease: a meta-analysis. *Journal of Huazhong University of Science and Technology*, 36(4), 473-479.
- Granja, F., Morari, J., Morari, E. C., Correa, L. A., Assumpção, L. g. V., & Ward, L. S. (2004). Proline homozygosity in codon 72 of *p53* is a factor of susceptibility for thyroid cancer. *Cancer Letters*, 210(2), 151-157.
- Greco, A., Miranda, C., Borrello, M. G., & Pierotti, M. A. (2014). Chapter 16 - Thyroid Cancer. In G. Dellaire, J. N. Berman & R. J. Arceci (Eds.), *Cancer genomics* (pp. 265-280). Boston: Academic Press.
- Greenbaum, D., Colangelo, C., Williams, K., & Gerstein, M. (2003). Comparing protein abundance and mRNA expression levels on a genomic scale. *Genome Biology*, 4(9), 117. doi: 10.1186/gb-2003-4-9-117.
- Griffith, O. L., Melck, A., Jones, S. J., & Wiseman, S. M. (2006). Meta-analysis and meta-review of thyroid cancer gene expression profiling studies identifies important diagnostic biomarkers. *Journal of Clinical Oncology*, 24(31), 5043-5051.
- Grivennikov, S. I., & Karin, M. (2010). Dangerous liaisons: STAT3 and NF- κ B collaboration and crosstalk in cancer. *Cytokine and Growth Factor Reviews*, 21(1), 11-19.
- Grogan, R. H., Mitmaker, E. J., & Clark, O. H. (2010). The evolution of biomarkers in thyroid cancer-from mass screening to a personalized biosignature. *Cancers*, 2(2), 885-912.
- Haigis, K. M., Kendall, K. R., Wang, Y., Cheung, A., Haigis, M. C., Glickman, J. N., . . . Shannon, K. M. (2008). Differential effects of oncogenic K-Ras and N-Ras on proliferation, differentiation and tumor progression in the colon. *Nature Genetics*, 40(5), 600-608.
- Hamrita, B., Chahed, K., Trimeche, M., Guillier, C. L., Hammann, P., Chaïeb, A., . . . Chouchane, L. (2009). Proteomics-based identification of α 1-antitrypsin and haptoglobin precursors as novel serum markers in infiltrating ductal breast carcinomas. *Clinica Chimica Acta*, 404(2), 111-118.
- Hanahan, D., & Weinberg, R. A. (2011). Hallmarks of cancer: the next generation. *Cell*, 144(5), 646-674.
- Hanumanthappa, M. B., Gopinathan, S., Suvarna, R., Guruprasad Rai D., Shetty, G., Shetty, A., . . . Shetty, N. (2012). The incidence of malignancy in multi-nodular goitre: a prospective study at a tertiary academic centre. *Journal of Clinical and Diagnostic Research*, 6(2), 267-270.

- Hawthorn, L., Stein, L., Varma, R., Wiseman, S., Loree, T., & Tan, D. (2004). TIMP1 and SERPIN-A overexpression and TFF3 and CRABP1 underexpression as biomarkers for papillary thyroid carcinoma. *Head Neck*, 26(12), 1069-1083. doi: 10.1002/hed.20099.
- He, H., Jazdzewski, K., Li, W., Liyanarachchi, S., Nagy, R., Volinia, S., . . . Suster, S. (2005). The role of microRNA genes in papillary thyroid carcinoma. *Proceedings of the National Academy of Sciences of the United States of America*, 102(52), 19075-19080.
- Hegedus, L., Bonnema, S. J., & Bennedbaek, F. N. (2003). Management of simple nodular goiter: current status and future perspectives. *Endocrine Reviews*, 24(1), 102-132. doi: 10.1210/er.2002-0016.
- Hellman, K., Alaiya, A., Schedvins, K., Steinberg, W., Hellström, A., & Auer, G. (2004). Protein expression patterns in primary carcinoma of the vagina. *British Journal of Cancer*, 91(2), 319-326.
- Henderson, N. C., & Sethi, T. (2009). The regulation of inflammation by galectin- 3. *Immunological Reviews*, 230(1), 160-171.
- Heukeshoven, J., & Dernick, R. (1988). Improved silver staining procedure for fast staining in PhastSystem Development Unit. I. Staining of sodium dodecyl sulfate gels. *Electrophoresis*, 9(1), 28-32.
- Honda, K., Ono, M., Shitashige, M., Masuda, M., Kamita, M., Miura, N., & Yamada, T. (2013). Proteomic approaches to the discovery of cancer biomarkers for early detection and personalized medicine. *Japanese Journal of Clinical Oncology*, 43(2), 103-109. doi: 10.1093/jjco/hys200.
- Hong, W. S., & Hong, S. I. (1991). Clinical usefulness of alpha-1-antitrypsin in the diagnosis of hepatocellular carcinoma. *Journal of Korean Medical Science*, 6(3), 206-213.
- Howell, G. M., Hodak, S. P., & Yip, L. (2013). RAS mutations in thyroid cancer. *Oncologist*, 18(8), 926-932. doi: 10.1634/theoncologist.2013-0072.
- Htwe, T. T. (2012). Thyroid malignancy among goitrous thyroid lesions: a review of hospital-based studies in Malaysia and Myanmar. *Singapore Medical Journal*, 53(3), 159-163.
- Hu, C.-Y., Chang, S.-K., Wu, C.-S., Tsai, W.-I., & Hsu, P.-N. (2011). Galectin-3 gene (LGALS3) + 292C allele is a genetic predisposition factor for rheumatoid arthritis in Taiwan. *Clinical Rheumatology*, 30(9), 1227.
- Huang, F., Fang, W., Ye, L., Zhang, X., Shen, L., Han, R., . . . Wang, W. (2014). BRAF mutation correlates with recurrent papillary thyroid carcinoma in Chinese patients. *Current Oncology*, 21(6), e740.
- Huang, Y., Prasad, M., Lemon, W. J., Hampel, H., Wright, F. A., Kornacker, K., . . . de la Chapelle, A. (2001). Gene expression in papillary thyroid carcinoma reveals highly consistent profiles. *Proceedings of the National Academy of Sciences of*

the United States of America, 98(26), 15044-15049. doi: 10.1073/pnas.251547398.

- Hunt, J. L., & Barnes, E. L. (2003). Non-tumor-associated psammoma bodies in the thyroid. *American Journal of Clinical Pathology*, 119(1), 90-94.
- Hwang, T. S., Han, H. S., Choi, H. K., Lee, Y. J., Kim, Y. J., Han, M. Y., & Park, Y. M. (2003). Differential, stage- dependent expression of Hsp70, Hsp110 and Bcl- 2 in colorectal cancer. *Journal of Gastroenterology and Hepatology*, 18(6), 690-700.
- Ishioka, N., Takahashi, N., & Putnam, F. W. (1986). Amino acid sequence of human plasma alpha 1B-glycoprotein: homology to the immunoglobulin supergene family. *Proceedings of the National Academy of Sciences*, 83(8), 2363-2367.
- Ito, Y., Higashiyama, T., Takamura, Y., Miya, A., Kobayashi, K., Matsuzuka, F., . . . Miyauchi, A. (2007). Prognosis of patients with benign thyroid diseases accompanied by incidental papillary carcinoma undetectable on preoperative imaging tests. *World Journal of Surgery*, 31(8), 1672.
- Jarzab, B., Wiench, M., Fujarewicz, K., Simek, K., Jarzab, M., Oczko-Wojciechowska, M., . . . Swierniak, A. (2005). Gene expression profile of papillary thyroid cancer: sources of variability and diagnostic implications. *Cancer Research*, 65(4), 1587-1597. doi: 10.1158/0008-5472.CAN-04-3078.
- Jhiang, S., Sagartz, J., Tong, Q., Parker-Thornburg, J., Capen, C., Cho, J. Y., . . . Ledent, C. (1996). Targeted expression of the *ret/PTC1* oncogene induces papillary thyroid carcinomas. *Endocrinology*, 137(1), 375-378.
- Jiang, R., Zhao, C., Xu, H., Zhao, M., Sun, X., Wang, X., & Song, W. (2016). Correlation between polymorphisms of *BRAF* gene and papillary thyroid carcinoma. *Clinical Endocrinology (Oxf)*, 84(3), 431-437.
- Jo, Y. S., Li, S., Song, J. H., Kwon, K. H., Lee, J. C., Rha, S. Y., . . . Ro, H. K. (2006). Influence of the *BRAF* V600E mutation on expression of vascular endothelial growth factor in papillary thyroid cancer. *The Journal of Clinical Endocrinology and Metabolism*, 91(9), 3667-3670.
- Jonigk, D., Al-Omari, M., Maegel, L., Müller, M., Izykowski, N., Hong, J., . . . Mahadeva, R. (2013). Anti-inflammatory and immunomodulatory properties of α 1-antitrypsin without inhibition of elastase. *Proceedings of the National Academy of Sciences*, 110(37), 15007-15012.
- Jung, E. J., Moon, H. G., Park, S. T., Cho, B. I., Lee, S. M., Jeong, C. Y., . . . Hong, S. C. (2010). Decreased annexin A3 expression correlates with tumor progression in papillary thyroid cancer. *Proteomics Clinical Applications*, 4(5), 528-537. doi: 10.1002/prca.200900063.
- Kakudo, K., Tang, W., Ito, Y., Mori, I., Nakamura, Y., & Miyauchi, A. (2004). Papillary carcinoma of the thyroid in Japan: subclassification of common type and identification of low risk group. *Journal of Clinical Pathology*, 57(10), 1041-1046. doi: 10.1136/jcp.2004.017889.

- Kang, S. W., Chae, H. Z., Seo, M. S., Kim, K., Baines, I. C., & Rhee, S. G. (1998). Mammalian peroxiredoxin isoforms can reduce hydrogen peroxide generated in response to growth factors and tumor necrosis factor- α . *Journal of Biological Chemistry*, 273(11), 6297-6302.
- Kannan, K., Wang, L., Wang, J., Ittmann, M. M., Li, W., & Yen, L. (2011). Recurrent chimeric RNAs enriched in human prostate cancer identified by deep sequencing. *Proceedings of the National Academy of Sciences*, 108(22), 9172-9177.
- Karakas, B., Bachman, K., & Park, B. (2006). Mutation of the *PIK3CA* oncogene in human cancers. *British Journal of Cancer*, 94(4), 455-459.
- Karger, S., Krause, K., Gutknecht, M., Schierle, K., Graf, D., Steinert, F., . . . Führer, D. (2012). *ADM3*, *TFF3* and *LGALS3* are discriminative molecular markers in fine-needle aspiration biopsies of benign and malignant thyroid tumours. *British Journal of Cancer*, 106(3), 562-568.
- Karni, R., Jove, R., & Levitzki, A. (1999). Inhibition of pp 60 c-Src reduces *Bcl-XL* expression and reverses the transformed phenotype of cells overexpressing EGF and HER-2 receptors. *Oncogene*, 18(33), 4654-4662.
- Kebebew, E., Weng, J., Bauer, J., Ranvier, G., Clark, O. H., Duh, Q.-Y., . . . Griffin, A. (2007). The prevalence and prognostic value of *BRAF* mutation in thyroid cancer. *Annals of Surgery*, 246(3), 466.
- Khatawkar, A., & Awati, S. M. (2015a). Thyroid gland-historical aspects, embryology, anatomy and physiology. *IAIM*, 2(9), 165-171.
- Khatawkar, A. V., & Awati, S. (2015b). Multi-nodular goiter: epidemiology, etiology, pathogenesis and pathology. *IAIM*, 2(9), 152-156.
- Khovidhunkit, W., Duchateau, P. N., Medzihradzsky, K. F., Moser, A. H., Naya-Vigne, J., Shigenaga, J. K., . . . Feingold, K. R. (2004). Apolipoproteins A-IV and AV are acute-phase proteins in mouse HDL. *Atherosclerosis*, 176(1), 37-44.
- Kim, H., Lee, T.-H., Park, E. S., Suh, J. M., Park, S. J., Chung, H. K., . . . Shong, M. (2000). Role of peroxiredoxins in regulating intracellular hydrogen peroxide and hydrogen peroxide-induced apoptosis in thyroid cells. *Journal of Biological Chemistry*, 275(24), 18266-18270.
- Kim, H. S., Kim, D. H., Kim, J. Y., Jeoung, N. H., Lee, I. K., Bong, J. G., & Jung, E. D. (2010). Microarray analysis of papillary thyroid cancers in Korean. *The Korean Journal of Internal Medicine*, 25(4), 399-407. doi: 10.3904/kjim.2010.25.4.399.
- Kim, J. Y., Lee, C. H., Kim, S. Y., Jeon, W. K., Kang, J. H., An, S. K., & Jun, W. S. (2008). Radiologic and pathologic findings of nonpalpable thyroid carcinomas detected by ultrasonography in a medical screening center. *Journal of Ultrasound in Medicine*, 27(2), 215-223.
- Kim, K., Yu, M., Han, S., Oh, I., Choi, Y. J., Kim, S., . . . Choe, W. (2009). Expression of human peroxiredoxin isoforms in response to cervical carcinogenesis. *Oncology Reports*, 21(6), 1391-1396.

- Kim, S. J., Lee, K. E., Myong, J. P., Park, J. H., Jeon, Y. K., Min, H. S., . . . Youn, Y. K. (2012). *BRAF* V600E mutation is associated with tumor aggressiveness in papillary thyroid cancer. *World Journal of Surgery*, 36(2), 310-317.
- Kimura, E. T., Nikiforova, M. N., Zhu, Z., Knauf, J. A., Nikiforov, Y. E., & Fagin, J. A. (2003). High prevalence of *BRAF* mutations in thyroid cancer. *Cancer Research*, 63(7), 1454-1457.
- Kishimoto, T. (2005). Interleukin-6: from basic science to medicine-40 years in immunology. *Annual Review of Immunology*, 23, 1-21.
- Kitamura, Y., Minobe, K., Nakata, T., Shimizu, K., Tanaka, S., Fujimori, M., . . . Emi, M. (1999). *Ret/PTC3* is the most frequent form of gene rearrangement in papillary thyroid carcinomas in Japan. *Journal of Human Genetics*, 44(2), 96-102.
- Knauf, J. A., & Fagin, J. A. (2009). Role of MAPK pathway oncoproteins in thyroid cancer pathogenesis and as drug targets. *Current Opinion in Cell Biology*, 21(2), 296-303.
- Knauf, J. A., Kuroda, H., Basu, S., & Fagin, J. A. (2003). *RET/PTC*-induced dedifferentiation of thyroid cells is mediated through Y1062 signaling through SHC-RAS-MAP kinase. *Oncogene*, 22(28), 4406-4412.
- Knauf, J. A., Ma, X., Smith, E. P., Zhang, L., Mitsutake, N., Liao, X.-H., . . . Fagin, J. A. (2005). Targeted expression of *BRAF*V600E in thyroid cells of transgenic mice results in papillary thyroid cancers that undergo dedifferentiation. *Cancer Research*, 65(10), 4238-4245.
- Koussounadis, A., Langdon, S. P., Um, I. H., Harrison, D. J., & Smith, V. A. (2015). Relationship between differentially expressed mRNA and mRNA-protein correlations in a xenograft model system. *Scientific Reports*, 5, 10775. doi: 10.1038/srep10775.
- Kozlov, G., Määttänen, P., Thomas, D. Y., & Gehring, K. (2010). A structural overview of the PDI family of proteins. *The FEBS journal*, 277(19), 3924-3936.
- Kraimps, J., Bouin- Pineau, M., Mathonnet, M., De Calan, L., Ronceray, J., Visset, J., . . . Barbier, J. (2000). Multicentre study of thyroid nodules in patients with Graves' disease. *British Journal of Surgery*, 87(8), 1111-1113.
- Krause, K., Jessnitzer, B., & Fuhrer, D. (2009). Proteomics in thyroid tumor research. *The Journal of Clinical Endocrinology and Metabolism*, 94(8), 2717-2724. doi: 10.1210/jc.2009-0308.
- Kundranda, M. N., Henderson, M., Carter, K. J., Gorden, L., Binhazim, A., Ray, S., . . . Jahnen-Dechent, W. (2005). The serum glycoprotein fetuin-A promotes Lewis lung carcinoma tumorigenesis via adhesive-dependent and adhesive-independent mechanisms. *Cancer Research*, 65(2), 499-506.
- Kwak, J. Y., Ma, T. Z., Yoo, M. J., Choi, B. H., Kim, H. G., Kim, S. R., . . . Kwak, Y. G. (2004). The comparative analysis of serum proteomes for the discovery of

- biomarkers for acute myeloid leukemia. *Experimental Hematology*, 32(9), 836-842.
- Landa, I., & Robledo, M. (2011). Association studies in thyroid cancer susceptibility: are we on the right track? *Journal of Molecular Endocrinology*, 47(1), R43-58.
- Lazar, V., Bidart, J.-M., Caillou, B., Mahé, C., Lacroix, L., Filetti, S., & Schlumberger, M. (1999). Expression of the *Na⁺/I⁻ symporter* gene in human thyroid tumors: a comparison study with other thyroid-specific genes. *The Journal of Clinical Endocrinology and Metabolism*, 84(9), 3228-3234.
- Lee, J., Kim, J. C., Lee, S.-E., Quinley, C., Kim, H., Herdman, S., . . . Raz, E. (2012). Signal transducer and activator of transcription 3 (STAT3) protein suppresses adenoma-to-carcinoma transition in *Apcmin/+* mice via regulation of Snail-1 (SNAI) protein stability. *Journal of Biological Chemistry*, 287(22), 18182-18189.
- Lee, J. C., Gundara, J. S., Glover, A., Serpell, J., & Sidhu, S. B. (2014). MicroRNA expression profiles in the management of papillary thyroid cancer. *Oncologist*, 19(11), 1141-1147.
- Lee, J. H., Lee, E. S., & Kim, Y. S. (2007). Clinicopathologic significance of *BRAF* V600E mutation in papillary carcinomas of the thyroid. *Cancer*, 110(1), 38-46.
- Lehtonen, S. T., Svensk, A. M., Soini, Y., Pääkkö, P., Hirvikoski, P., Kang, S. W., . . . Kinnula, V. L. (2004). Peroxiredoxins, a novel protein family in lung cancer. *International Journal of Cancer*, 111(4), 514-521.
- Leite-Browning, M. L., McCawley, L. J., Jahnen-Dechent, W., King, L. E., Matrisian, L. M., & Ochieng, J. (2004). Alpha 2-HS glycoprotein (fetuin-A) modulates murine skin tumorigenesis. *International Journal of Oncology*, 25(2), 319-324.
- Lemoine, N. R., Mayall, E. S., Wyllie, F. S., Farr, C. J., Hughes, D., Padua, R. A., . . . Wynford-Thomas, D. (1988). Activated ras oncogenes in human thyroid cancers. *Cancer Research*, 48(16), 4459-4463.
- Lennon, N. J., Adalsteinsson, V. A., & Gabriel, S. B. (2016). Technological considerations for genome-guided diagnosis and management of cancer. *Genome Medicine*, 8(1), 112.
- Lesueur, F., Corbex, M., McKay, J., Lima, J., Soares, P., Griseri, P., . . . Papotti, M. (2002). Specific haplotypes of the *RET* proto-oncogene are over-represented in patients with sporadic papillary thyroid carcinoma. *Journal of Medical Genetics*, 39(4), 260-265.
- Levine, A. J. (1997). p53, the cellular gatekeeper for growth and division. *Cell*, 88(3), 323-331.
- Li, C., Lee, K. C., Schneider, E. B., & Zeiger, M. A. (2012). *BRAF* V600E mutation and its association with clinicopathological features of papillary thyroid cancer: a meta-analysis. *The Journal of Clinical Endocrinology and Metabolism*, 97(12), 4559-4570.

- Li, L.-c., Li, J., & Gao, J. (2014). Functions of galectin-3 and its role in fibrotic diseases. *Journal of Pharmacology and Experimental Therapeutics*, *351*(2), 336-343.
- Li, X., Zhao, L., Jiang, H., & Wang, W. (2009). Short homologous sequences are strongly associated with the generation of chimeric RNAs in eukaryotes. *Journal of Molecular Evolution*, *68*(1), 56-65.
- Lim G. C. C., Rampal, S., & Halimah, Y. (Eds). (2008). *Cancer incidence inpeninsular Malaysia, 2003-2005: The third report of the National Cancer Registry, Malaysia*. National Cancer Registry. Kuala Lumpur.
- Lin, H. Y., Yang, M. C., Huang, C. H., Wu, W. J., Yu, T. J., & Lung, F. W. (2013). Polymorphisms of *TP53* are markers of bladder cancer vulnerability and prognosis. In *Urologic oncology: seminars and original investigations* (Vol. 31, No. 7, pp. 1231-1241). Elsevier.
- Lin, J. D. (2010). Thyroid cancer in thyroid nodules diagnosed using ultrasonography and fine needle aspiration cytology. *Journal of Medical Ultrasound*, *18*(3), 91-104.
- Lin, J. D., Yang, S. F., Wang, Y. H., Fang, W. F., Lin, Y. C., Lin, Y. F., . . . Cheng, C.-W. (2016). Analysis of associations of human *BAFF* gene polymorphisms with autoimmune thyroid diseases. *PLoS One*, *11*(5), e0154436.
- Lino, M. A. M., Palacios-Rodríguez, Y., Rodríguez-Cuevas, S., Bautista-Piña, V., Marchat, L. A., Ruíz-García, E., . . . Díaz-Chávez, J. (2014). Comparative proteomic profiling of triple-negative breast cancer reveals that up-regulation of RhoGDI-2 is associated to the inhibition of caspase 3 and caspase 9. *Journal of Proteomics*, *111*, 198-211.
- LiVolsi, V. A. (2011). Papillary thyroid carcinoma: an update. *Modern Pathology*, *24 Suppl 2*, S1-9. doi: 10.1038/modpathol.2010.129.
- Looi, M. L., Karsani, S. A., Rahman, M. A., Dali, A. Z. H. M., Ali, S. A. M., Ngah, W. Z. W., & Yusof, Y. A. M. (2009). Plasma proteome analysis of cervical intraepithelial neoplasia and cervical squamous cell carcinoma. *Journal of Biosciences*, *34*(6), 917-925.
- Loosveld, M., Bonnet, M., Gon, S., Montpellier, B., Quilichini, B., Navarro, J. M., . . . Morgado, E. (2014). MYC fails to efficiently shape malignant transformation in T- cell acute lymphoblastic leukemia. *Genes, Chromosomes and Cancer*, *53*(1), 52-66.
- Lovat, P. E., Corazzari, M., Armstrong, J. L., Martin, S., Pagliarini, V., Hill, D., . . . Redfern, C. P. (2008). Increasing melanoma cell death using inhibitors of protein disulfide isomerases to abrogate survival responses to endoplasmic reticulum stress. *Cancer Research*, *68*(13), 5363-5369.
- Lowe, W. L., & Reddy, T. E. (2015). Genomic approaches for understanding the genetics of complex disease. *Genome Research*, *25*(10), 1432-1441.

- Lu, M., Faull, K. F., Whitelegge, J. P., He, J., Shen, D., Saxton, R. E., & Chang, H. R. (2007). Proteomics and mass spectrometry for cancer biomarker discovery. *Biomarker Insights*, 2, 347.
- Lu, Y., Zhu, X., Zhang, C., Jiang, K., Huang, C., & Qin, X. (2017). Role of *CYP2E1* polymorphisms in breast cancer: a systematic review and meta-analysis. *Cancer Cell International*, 17(1), 11.
- Luk, J. M., Lam, C. T., Siu, A. F., Lam, B. Y., Ng, I. O., Hu, M. Y., . . . Fan, S. T. (2006). Proteomic profiling of hepatocellular carcinoma in Chinese cohort reveals heat-shock proteins (Hsp27, Hsp70, GRP78) up-regulation and their associated prognostic values. *Proteomics*, 6(3), 1049-1057.
- Luo, J., McManus, C., Chen, H., & Sippel, R. S. (2012). Are there predictors of malignancy in patients with multinodular goiter? *Journal of Surgical Research*, 174(2), 207-210.
- Lupi, C., Giannini, R., Ugolini, C., Proietti, A., Berti, P., Minuto, M., . . . Miccoli, P. (2007). Association of *BRAF* V600E mutation with poor clinicopathological outcomes in 500 consecutive cases of papillary thyroid carcinoma. *The Journal of Clinical Endocrinology and Metabolism*, 92(11), 4085-4090.
- Mackenzie, E. J., & Mortimer, R. H. (2004). 6: Thyroid nodules and thyroid cancer. *The Medical Journal of Australia*, 180(5), 242-247.
- Maia, F. F., & Zantut-Wittmann, D. E. (2012). Thyroid nodule management: clinical, ultrasound and cytopathological parameters for predicting malignancy. *Clinics*, 67(8), 945-954.
- Makki, F. M., Taylor, S. M., Shahnavaaz, A., Leslie, A., Gallant, J., Douglas, S., . . . Hart, R. D. (2013). Serum biomarkers of papillary thyroid cancer. *Journal of Otolaryngology Head and Neck Surgery*, 42, 16. doi: 10.1186/1916-0216-42-16.
- Malati, T. (2007). Tumour markers: an overview. *Indian Journal of Clinical Biochemistry*, 22(2), 17-31.
- Mantovani, A., Allavena, P., Sica, A., & Balkwill, F. (2008). Cancer-related inflammation. *Nature*, 454(7203), 436-444.
- Marqusee, E., Benson, C. B., Frates, M. C., Doubilet, P. M., Larsen, P. R., Cibas, E. S., & Mandel, S. J. (2000). Usefulness of ultrasonography in the management of nodular thyroid disease. *Annals of Internal Medicine*, 133(9), 696-700.
- Martínez-Aguilar, J., Clifton-Bligh, R., & Molloy, M. P. (2016). Proteomics of thyroid tumours provides new insights into their molecular composition and changes associated with malignancy. *Scientific Reports*, 6, 23660.
- Matakidou, A., Hamel, N., Popat, S., Henderson, K., Kantemiroff, T., Harmer, C., . . . Foulkes, W. D. (2004). Risk of non-medullary thyroid cancer influenced by polymorphic variation in the *thyroglobulin* gene. *Carcinogenesis*, 25(3), 369-373.

- Mazzaferrri, E., & Massoll, N. (2002). Management of papillary and follicular (differentiated) thyroid cancer: new paradigms using recombinant human thyrotropin. *Endocrine-related Cancer*, 9(4), 227-247.
- Mazzaferrri, E. L. (1992). Thyroid cancer in thyroid nodules: finding a needle in the haystack. *The American Journal of Medicine*, 93(4), 359-362.
- Mazzaferrri, E. L. (1999). An overview of the management of papillary and follicular thyroid carcinoma. *Thyroid*, 9(5), 421-427.
- Mazzanti, C., Zeiger, M. A., Costourous, N., Umbricht, C., Westra, W. H., Smith, D., . . . Libutti, S. K. (2004). Using gene expression profiling to differentiate benign versus malignant thyroid tumors. *Cancer Research*, 64(8), 2898-2903.
- McCall, A., Jarosz, H., Lawrence, A., & Paloyan, E. (1986). The incidence of thyroid carcinoma in solitary cold nodules and in multinodular goiters. *Surgery*, 100(6), 1128-1132.
- Medeiros-Neto, G. (2000). Multinodular goiter. In L. J. De Groot, G. Chrousos, K. Dungan, K. R. Feingold, A. Grossman, J. M. Hershman, . . . A. Vinik (Eds.), *Endotext [Internet]*. South Dartmouth, Massachusetts: MDText.com, Inc.
- Meek, D. W. (2004). The p53 response to DNA damage. *DNA Repair*, 3(8), 1049-1056.
- Mesa, C., Mirza, M., Mitsutake, N., Sartor, M., Medvedovic, M., Tomlinson, C., . . . Fagin, J. A. (2006). Conditional activation of *RET/PTC3* and *BRAFV600E* in thyroid cells is associated with gene expression profiles that predict a preferential role of BRAF in extracellular matrix remodeling. *Cancer Research*, 66(13), 6521-6529.
- Miccoli, P., Minuto, M. N., Galleri, D., D'Agostino, J., Basolo, F., Antonangeli, L., . . . Berti, P. (2006). Incidental thyroid carcinoma in a large series of consecutive patients operated on for benign thyroid disease. *ANZ Journal of Surgery*, 76(3), 123-126.
- Miles, A. K., Matharoo-Ball, B., Li, G., Ahmad, M., & Rees, R. C. (2006). The identification of human tumour antigens: current status and future developments. *Cancer Immunology, Immunotherapy*, 55(8), 996-1003.
- Miller, D. M., Thomas, S. D., Islam, A., Muench, D., & Sedoris, K. (2012). c-Myc and cancer metabolism. *Clinical Cancer Research*, 18(20); 5546-5553.
- Mitsutake, N., Miyagishi, M., Mitsutake, S., Akeno, N., Mesa, C., Knauf, J. A., . . . Fagin, J. A. (2006). BRAF mediates RET/PTC-induced mitogen-activated protein kinase activation in thyroid cells: functional support for requirement of the RET/PTC-RAS-BRAF pathway in papillary thyroid carcinogenesis. *Endocrinology*, 147(2), 1014-1019.
- Mono, T., Shinohara, R., Iwase, K., Kotake, M., Hamada, M., Uchimura, K., . . . Ishizuki, Y. (1997). Changes in free radical scavengers and lipid peroxide in thyroid glands of various thyroid disorders. *Hormone and Metabolic Research*, 29(07), 351-354.

- Moore, K. L., & Persaud, T. V. N. (2003). *The developing human: clinically oriented embryology*. Philadelphia, Pa: Saunders.
- Mordente, A., Meucci, E., Martorana, G. E., & Silvestrini, A. (2015). Cancer biomarkers discovery and validation: state of the art, problems and future perspectives. *Advances in Experimental Medicine and Biology*, 867, 9-26. doi: 10.1007/978-94-017-7215-0_2.
- Moretz, W. H., 3rd, Gourin, C. G., Terris, D. J., Xia, Z. S., Liu, Z., Weinberger, P. M., . . . Adam, B. L. (2008). Detection of papillary thyroid carcinoma with serum protein profile analysis. *Archives of Otolaryngology Head and Neck Surgery*, 134(2), 198-202. doi: 10.1001/archoto.2007.34.
- Muller, P. A., Vousden, K. H., & Norman, J. C. (2011). p53 and its mutants in tumor cell migration and invasion. *The Journal of Cell Biology*, 192(2), 209-218.
- Mullur, R., Liu, Y.-Y., & Brent, G. A. (2014). Thyroid hormone regulation of metabolism. *Physiological Reviews*, 94(2), 355-382.
- Murphy, K. M., Chen, F., & Clark, D. P. (2008). Identification of immunohistochemical biomarkers for papillary thyroid carcinoma using gene expression profiling. *Human Pathology*, 39(3), 420-426. doi: 10.1016/j.humpath.2007.07.015.
- Murphy, M. E. (2013). The HSP70 family and cancer. *Carcinogenesis*, 34(6), 1181-1188.
- Mutaku, J., Poma, J., Many, M., Deneff, J., & van Den Hove, M. (2002). Cell necrosis and apoptosis are differentially regulated during goitre development and iodine-induced involution. *Journal of Endocrinology*, 172(2), 375-386.
- Nagy, R., & Ringel, M. D. (2015). Genetic predisposition for nonmedullary thyroid cancer. *Hormones and Cancer*, 6(1), 13-20. doi: 10.1007/s12672-014-0205-y.
- Nakata, T., Kitamura, Y., Shimizu, K., Tanaka, S., Fujimori, M., Yokoyama, S., . . . Emi, M. (1999). Fusion of a novel gene, *ELKS*, to *RET* due to translocation t(10;12)(q11;p13) in a papillary thyroid carcinoma. *Genes, Chromosomes and Cancer*, 25(2), 97-103.
- Nam-Goong, I. S., Kim, H. Y., Gong, G., Lee, H. K., Hong, S. J., Kim, W. B., & Shong, Y. K. (2004). Ultrasonography-guided fine-needle aspiration of thyroid incidentaloma: correlation with pathological findings. *Clinical Endocrinology (Oxf)*, 60(1), 21-28.
- Namba, H., Nakashima, M., Hayashi, T., Hayashida, N., Maeda, S., Rogounovitch, T. I., . . . Yamashita, S. (2003). Clinical implication of hot spot *BRAF* mutation, V599E, in papillary thyroid cancers. *The Journal of Clinical Endocrinology and Metabolism*, 88(9), 4393-4397.
- Neki, N., & Kazal, H. (2006). Solitary thyroid nodule-an insight. *Journal, Indian Academy of Clinical Medicine*, 7(4), 328-323.
- Netea-Maier, R. T., Hunsucker, S. W., Hoevenaars, B. M., Helmke, S. M., Slootweg, P. J., Hermus, A. R., . . . Duncan, M. W. (2008). Discovery and validation of protein

- abundance differences between follicular thyroid neoplasms. *Cancer Research*, 68(5), 1572-1580.
- Ng, P. C., & Henikoff, S. (2001). Predicting deleterious amino acid substitutions. *Genome Research*, 11(5), 863-874.
- Nguyen, Q. T., Lee, E. J., Huang, M. G., Park, Y. I., Khullar, A., & Plodkowski, R. A. (2015). Diagnosis and treatment of patients with thyroid cancer. *American Health and Drug Benefits*, 8(1), 30.
- Ni, Z., Lou, W., Leman, E. S., & Gao, A. C. (2000). Inhibition of constitutively activated Stat3 signaling pathway suppresses growth of prostate cancer cells. *Cancer Research*, 60(5), 1225-1228.
- Nikiforov, Y. E. (2002). *RET/PTC* rearrangement in thyroid tumors. *Endocrine Pathology*, 13(1), 3.
- Nikiforov, Y. E. (2008). Thyroid carcinoma: molecular pathways and therapeutic targets. *Modern Pathology*, 21, S37-S43.
- Nikiforov, Y. E., & Nikiforova, M. N. (2011). Molecular genetics and diagnosis of thyroid cancer. *Nature Reviews Endocrinology*, 7(10), 569-580.
- Nikiforov, Y. E., Rowland, J. M., Bove, K. E., Monforte-Munoz, H., & Fagin, J. A. (1997). Distinct pattern of *ret* oncogene rearrangements in morphological variants of radiation-induced and sporadic thyroid papillary carcinomas in children. *Cancer Research*, 57(9), 1690-1694.
- Nikiforova, M. N., Kimura, E. T., Gandhi, M., Biddinger, P. W., Knauf, J. A., Basolo, F., . . . Fusco, A. (2003). *BRAF* mutations in thyroid tumors are restricted to papillary carcinomas and anaplastic or poorly differentiated carcinomas arising from papillary carcinomas. *The Journal of Clinical Endocrinology and Metabolism*, 88(11), 5399-5404.
- Nikiforova, M. N., & Nikiforov, Y. E. (2008). Molecular genetics of thyroid cancer: implications for diagnosis, treatment and prognosis. *Expert Review of Molecular Diagnostics*, 8(1), 83-95.
- Ning, L., Rao, W., Yu, Y., Liu, X., Pan, Y., Ma, Y., . . . Yu, Q. (2016). Association between the *KRAS* Gene Polymorphisms and Papillary Thyroid Carcinoma in a Chinese Han Population. *Journal of Cancer*, 7(15), 2420.
- Ning, L., Yu, Y., Liu, X., Ai, L., Zhang, X., Rao, W., . . . Yu, Q. (2015). Association analysis of *MET* gene polymorphism with papillary thyroid carcinoma in a Chinese population. *International Journal of Endocrinology*, 2015.
- Niu, G., Heller, R., Catlett-Falcone, R., Coppola, D., Jaroszeski, M., Dalton, W., . . . Yu, H. (1999). Gene therapy with dominant-negative Stat3 suppresses growth of the murine melanoma B16 tumor *in vivo*. *Cancer Research*, 59(20), 5059-5063.

- Niu, G., Wright, K. L., Ma, Y., Wright, G. M., Huang, M., Irby, R., . . . Pardoll, D. (2005). Role of Stat3 in regulating p53 expression and function. *Molecular and Cellular Biology*, 25(17), 7432-7440.
- Nucera, C., Goldfarb, M., Hodin, R., & Parangi, S. (2009). Role of B-Raf V600E in differentiated thyroid cancer and preclinical validation of compounds against B-Raf V600E. *Biochimica et Biophysica Acta-Reviews on Cancer*, 1795(2), 152-161.
- Ohannesian, D. W., Lotan, D., & Lotan, R. (1994). Concomitant increases in galectin-1 and its glycoconjugate ligands (carcinoembryonic antigen, lamp-1, and lamp-2) in cultured human colon carcinoma cells by sodium butyrate. *Cancer Research*, 54(22), 5992-6000.
- Othman, N. H., Omar, E., & Naing, N. N. (2009). Spectrum of thyroid lesions in hospital Universiti Sains Malaysia over 11 years and a review of thyroid cancers in Malaysia. *Asian Pacific Journal of Cancer Prevention*, 10(1), 87-90.
- Palacio-Rúa, K., Isaza-Jiménez, L., Ahumada-Rodríguez, E., Ceballos-García, H., & Muñetón-Peña, C. (2014). Genetic analysis in *APC*, *KRAS*, and *TP53* in patients with stomach and colon cancer. *Revista de Gastroenterología de México (English Edition)*, 79(2), 79-89.
- Pallante, P., Visone, R., Ferracin, M., Ferraro, A., Berlingieri, M., Troncione, G., . . . Negrini, M. (2006). MicroRNA deregulation in human thyroid papillary carcinomas. *Endocrine-related Cancer*, 13(2), 497-508.
- Palo, S., & Mishra, D. (2017). Prevalence of malignancy in multinodular goiter and solitary thyroid nodule: a histopathological audit. *International Journal of Research in Medical Sciences*, 4(6), 2319-2323.
- Palona, I., Namba, H., Mitsutake, N., Starenki, D., Podtcheko, A., Sedliarou, I., . . . Umezawa, K. (2006). *BRAF*V600E promotes invasiveness of thyroid cancer cells through nuclear factor κ B activation. *Endocrinology*, 147(12), 5699-5707.
- Pang, H. N., & Chen, C. M. (2007). Incidence of cancer in nodular goitres. *Annals of the Academy of Medicine Singapore*, 36(4), 241-243.
- Pang, W. W., Abdul-Rahman, P. S., Izlina Wan-Ibrahim, W., & Haji Hashim, O. (2010). Can the acute-phase reactant proteins be used as cancer biomarkers? *International Journal of Biological Markers*, 25(1), 1.
- Papini, E., Guglielmi, R., Bianchini, A., Crescenzi, A., Taccogna, S., Nardi, F., . . . Pacella, C. M. (2002). Risk of malignancy in nonpalpable thyroid nodules: predictive value of ultrasound and color-Doppler features. *The Journal of Clinical Endocrinology and Metabolism*, 87(5), 1941-1946.
- Park, S. M., & Chatterjee, V. K. (2005). Genetics of congenital hypothyroidism. *Journal of Medical Genetics*, 42(5), 379-389. doi: 10.1136/jmg.2004.024158.
- Parsa, N. (2012). Environmental factors inducing human cancers. *Iranian Journal of Public Health*, 41(11), 1-9.

- Patz Jr, E. F., Campa, M. J., Gottlin, E. B., Kusmartseva, I., Guan, X. R., & Herndon, J. E. (2007). Panel of serum biomarkers for the diagnosis of lung cancer. *Journal of Clinical Oncology*, 25(35), 5578-5583.
- Pelizzo, M., Toniato, A., Piotto, A., & Bernante, P. (1996). Cancer in multinodular goiter. *Annali Italiani di Chirurgia*, 67(3), 351-356.
- Peng, Z., Yuan, C., Zellmer, L., Liu, S., Xu, N., & Liao, D. J. (2015). Hypothesis: artifacts, including spurious chimeric RNAs with a short homologous sequence, caused by consecutive reverse transcriptions and endogenous random primers. *Journal of Cancer*, 6(6), 555.
- Petrache, I., Fijalkowska, I., Medler, T. R., Skirball, J., Cruz, P., Zhen, L., . . . Tuder, R. M. (2006). α -1 Antitrypsin inhibits caspase-3 activity, preventing lung endothelial cell apoptosis. *The American Journal of Pathology*, 169(4), 1155-1166.
- Pierotti, M., Arighi, E., Bongarzone, I., Borrello, M., Butti, G., Greco, A., . . . Sozzi, G. (1993). *RET/ptc* and *TRK* oncogenes in papillary thyroid carcinoma. In *Tyrosine Phosphorylation/Dephosphorylation and Downstream Signalling* (pp. 87-98). Springer, Berlin, Heidelberg.
- Poblete, M. T., Nualart, F., del Pozo, M., Perez, J. A., & Figueroa, C. D. (1996). Alpha1-antitrypsin expression in human thyroid papillary carcinoma. *The American Journal of Surgical Pathology*, 20(8), 956-963.
- Pradhan, G., Shrestha, R., Shrestha, S., Neupane, J., & Bhattachan, C. (2011). The incidence of thyroid carcinoma in multinodular goiter: prospective study. *Nepal Medical College Journal*, 13(3), 169-171.
- Puxeddu, E., Durante, C., Avenia, N., Filetti, S., & Russo, D. (2008). Clinical implications of *BRAF* mutation in thyroid carcinoma. *Trends in Endocrinology and Metabolism*, 19(4), 138-145.
- Pylväs, M., Puistola, U., Kauppila, S., Soini, Y., & Karihtala, P. (2010). Oxidative stress-induced antioxidant enzyme expression is an early phenomenon in ovarian carcinogenesis. *European Journal of Cancer*, 46(9), 1661-1667.
- Qi, X. P., Zhang, R. X., Cao, J. L., Chen, Z. G., Jin, H. Y., & Yang, R. R. (2014). The rare intracellular *RET* mutation p. S891A in a Chinese Han family with familial medullary thyroid carcinoma. *Journal of Biosciences*, 39(3), 505.
- Qu, K., Pan, Q., Zhang, X., Rodriguez, L., Zhang, K., Li, H., . . . Cheng, S.-M. (2013). Detection of *BRAF* V600 mutations in metastatic melanoma: comparison of the Cobas 4800 and Sanger sequencing assays. *The Journal of Molecular Diagnostics*, 15(6), 790-795.
- Rabbani, B., Tekin, M., & Mahdieh, N. (2014). The promise of whole-exome sequencing in medical genetics. *Journal of Human Genetics*, 59(1), 5-15.
- Rago, T., Fiore, E., Scutari, M., Santini, F., Di Coscio, G., Romani, R., . . . Miccoli, P. (2010). Male sex, single nodularity, and young age are associated with the risk of finding a papillary thyroid cancer on fine-needle aspiration cytology in a large

- series of patients with nodular thyroid disease. *European Journal of Endocrinology*, 162(4), 763-770.
- Rahman, M. M., Ali, M. I., Karim, M. A., Arafat, M. S., Hanif, M., & Tarafder, K. H. (2015). Frequency of malignancy in multinodular goitre. *Bangladesh Journal of Otorhinolaryngology*, 20(2), 75-79.
- Raposo, L., Morais, S., Oliveira, M. J., Marques, A. P., Jose Bento, M., & Lunet, N. (2017). Trends in thyroid cancer incidence and mortality in Portugal. *European Journal of Cancer Prevention*, 26(2), 135-143. doi: 10.1097/CEJ.0000000000000229.
- Raz, A., Carmi, P., Raz, T., Hogan, V., Mohamed, A., & Wolman, S. R. (1991). Molecular cloning and chromosomal mapping of a human galactoside-binding protein. *Cancer Research*, 51(8), 2173-2178.
- Recalde, D., Ostos, M. A., Badell, E., Garcia-Otin, A.-L., Pidoux, J., Castro, G., . . . Scott-Algara, D. (2004). Human apolipoprotein A-IV reduces secretion of proinflammatory cytokines and atherosclerotic effects of a chronic infection mimicked by lipopolysaccharide. *Arteriosclerosis, Thrombosis, and Vascular Biology*, 24(4), 756-761.
- Resemann, H. K., Watson, C. J., & Lloyd-Lewis, B. (2014). The Stat3 paradox: a killer and an oncogene. *Molecular and Cellular Endocrinology*, 382(1), 603-611.
- Reuter, S., Gupta, S. C., Chaturvedi, M. M., & Aggarwal, B. B. (2010). Oxidative stress, inflammation, and cancer: how are they linked? *Free Radical Biology and Medicine*, 49(11), 1603-1616.
- Ribatti, D., & Crivellato, E. (2012). Mast cells, angiogenesis, and tumour growth. *Biochimica et Biophysica Acta-Molecular Basis of Disease*, 1822(1), 2-8.
- Riesco-Eizaguirre, G., Gutierrez-Martinez, P., Garcia-Cabezas, M., Nistal, M., & Santisteban, P. (2006). The oncogene *BRAFV600E* is associated with a high risk of recurrence and less differentiated papillary thyroid carcinoma due to the impairment of Na⁺/I⁻ targeting to the membrane. *Endocrine-related Cancer*, 13(1), 257-269.
- Riesco-Eizaguirre, G., & Santisteban, P. (2007). New insights in thyroid follicular cell biology and its impact in thyroid cancer therapy. *Endocrine-related Cancer*, 14(4), 957-977.
- Ris-Stalpers, C., & Bikker, H. (2010). Genetics and phenomics of hypothyroidism and goiter due to *TPO* mutations. *Molecular and Cellular Endocrinology*, 322(1-2), 38-43. doi: 10.1016/j.mce.2010.02.008.
- Rogounovitch, T. I., Saenko, V. A., Ashizawa, K., Sedliarou, I. A., Namba, H., Abrosimov, A. Y., . . . Petoukhova, N. S. (2006). *TP53* codon 72 polymorphism in radiation-associated human papillary thyroid cancer. *Oncology Reports*, 15(4), 949-956.

- Romei, C., Ciampi, R., Faviana, P., Agate, L., Molinaro, E., Bottici, V., . . . Pinchera, A. (2008). *BRAFV600E* mutation, but not *RET/PTC* rearrangements, is correlated with a lower expression of both thyroperoxidase and sodium iodide symporter genes in papillary thyroid cancer. *Endocrine-related Cancer*, *15*(2), 511-520.
- Rosebeck, S., & Leaman, D. W. (2008). Mitochondrial localization and pro-apoptotic effects of the interferon-inducible protein ISG12a. *Apoptosis*, *13*(4), 562-572.
- Ru, J. Y., Cong, Y., Kang, W. B., Yu, L., Guo, T., & Zhao, J. N. (2015). Polymorphisms in *TP53* are associated with risk and survival of osteosarcoma in a Chinese population. *International Journal of Clinical and Experimental Pathology*, *8*(3), 3198.
- Rubin, E., & Farber, J. L. (1994). *Pathology*. Philadelphia: J.B. Lippincott Company.
- Rusinek, D., Szpak-Ulczo, S., & Jarzab, B. (2011). Gene expression profile of human thyroid cancer in relation to its mutational status. *Journal of Molecular Endocrinology*, *47*(3), R91-R103.
- Ryu, J., Bang, G., Lee, J., Choi, S., & Jung, Y. (2013). Lipid MALDI MS profiling accurately distinguishes papillary thyroid carcinoma from normal tissue. *Journal of Proteomics and Bioinformatics*, *6*, 065-071. doi: 10.4172/jpb.1000263.
- Sachmechi, I., Miller, E., Varatharajah, R. C., A. , Carroll, Z., Kissin, E., & Rosner, F. (2000). Thyroid carcinoma in single cold nodules and in cold nodules of multinodular goiters. *Endocrine Practice*, *6*(1), 5-7.
- Saenko, V., Rogounovitch, T., Shimizu-Yoshida, Y., Abrosimov, A., Lushnikov, E., Roumiantsev, P., . . . Ohtsuru, A. (2003). Novel tumorigenic rearrangement, $\Delta rfp/ret$, in a papillary thyroid carcinoma from externally irradiated patient. *Mutation Research/Fundamental and Molecular Mechanisms of Mutagenesis*, *527*(1), 81-90.
- Sallam, R. M. (2015). Proteomics in cancer biomarkers discovery: challenges and applications. *Disease Markers*, *2015*, 1-12. doi: 10.1155/2015/321370a.
- Salzano, S., Checconi, P., Hanschmann, E.-M., Lillig, C. H., Bowler, L. D., Chan, P., . . . Sacre, S. (2014). Linkage of inflammation and oxidative stress via release of glutathionylated peroxiredoxin-2, which acts as a danger signal. *Proceedings of the National Academy of Sciences*, *111*(33), 12157-12162.
- Santos, M., Azevedo, T., Martins, T., Rodrigues, F. J., & Lemos, M. C. (2014). Association of *RET* genetic polymorphisms and haplotypes with papillary thyroid carcinoma in the Portuguese population: a case-control study. *PLoS One*, *9*(10), e109822.
- Schaefer, T. S., Sanders, L. K., & Nathans, D. (1995). Cooperative transcriptional activity of Jun and Stat3 beta, a short form of Stat3. *Proceedings of the National Academy of Sciences*, *92*(20), 9097-9101.
- Schildkraut, J. M., Goode, E. L., Clyde, M. A., Iversen, E. S., Moorman, P. G., Berchuck, A., . . . Peplonska, B. (2009). Single nucleotide polymorphisms in the *TP53* region

- and susceptibility to invasive epithelial ovarian cancer. *Cancer Research*, 69(6), 2349-2357.
- Schwarz, J. M., Rödelsperger, C., Schuelke, M., & Seelow, D. (2010). MutationTaster evaluates disease-causing potential of sequence alterations. *Nature Methods*, 7(8), 575-576.
- Seeböck, R., Haybaeck, J., & Tsybrovskyy, O. (2017). Molecular Aspects of Thyroid Carcinogenesis. In *Mechanisms of Molecular Carcinogenesis-Volume 1* (pp. 175-184). Cham: Springer International Publishing.
- Segev, D. L., Umbricht, C., & Zeiger, M. A. (2003). Molecular pathogenesis of thyroid cancer. *Surgical Oncology*, 12(2), 69-90.
- Seriramalu, R., Pang, W. W., Jayapalan, J. J., Mohamed, E., Abdul- Rahman, P. S., Bustam, A. Z., . . . Hashim, O. H. (2010). Application of champedak mannose-binding lectin in the glycoproteomic profiling of serum samples unmasks reduced expression of alpha- 2 macroglobulin and complement factor B in patients with nasopharyngeal carcinoma. *Electrophoresis*, 31(14), 2388-2395.
- Shaha, A. R., Shah, J. P., & Loree, T. R. (1997). Low-risk differentiated thyroid cancer: the need for selective treatment. *Annals of Surgical Oncology*, 4(4), 328-333.
- Shamamian, P., Schwartz, J. D., Pocock, B. J., Monea, S., Whiting, D., Marcus, S. G., & Mignatti, P. (2001). Activation of progelatinase A (MMP- 2) by neutrophil elastase, cathepsin G, and proteinase- 3: a role for inflammatory cells in tumor invasion and angiogenesis. *Journal of Cellular Physiology*, 189(2), 197-206.
- Sharma, J., Milas, M., Weber, C. J., & Carlson, G. W. (2010). Neck. In W. C. Wood, C. A. Staley & J. E. Skandalakis (Eds.), *Anatomic basis of tumor surgery* (pp. 55-128). Berlin, Heidelberg: Springer Berlin Heidelberg.
- Sharma, P., Jha, A. B., Dubey, R. S., & Pessarakli, M. (2012). Reactive oxygen species, oxidative damage, and antioxidative defense mechanism in plants under stressful conditions. *Journal of Botany*, 2012.
- Shendure, J., & Ji, H. (2008). Next-generation DNA sequencing. *Nature Biotechnology*, 26(10), 1135-1145. doi: 10.1038/nbt1486.
- Sherman, M. Y., & Gabai, V. L. (2015). Hsp70 in cancer: back to the future. *Oncogene*, 34(32), 4153-4161.
- Shi, M., Huang, R., Pei, C., Jia, X., Jiang, C., & Ren, H. (2012). TP53 codon 72 polymorphism and glioma risk: a meta-analysis. *Oncology Letters*, 3(3), 599-606.
- Shimko, M. J., Zacccone, E. J., Thompson, J. A., Schwegler- Berry, D., Kashon, M. L., & Fedan, J. S. (2014). Nerve growth factor reduces amiloride- sensitive Na⁺ transport in human airway epithelial cells. *Physiological Reports*, 2(7), e12073.
- Singer, G., Oldt III, R., Cohen, Y., Wang, B. G., Sidransky, D., Kurman, R. J., & Shih, I.-M. (2003). Mutations in *BRAF* and *KRAS* characterize the development of low-

grade ovarian serous carcinoma. *Journal of the National Cancer Institute*, 95(6), 484-486.

Singh, V. (2014). *Textbook of anatomy head, neck, and brain* (Volume 3). Elsevier Health Sciences.

Sinibaldi, D., Wharton, W., Turkson, J., Bowman, T., Pledger, W. J., & Jove, R. (2000). Induction of p21^{WAF1/CIP1} and cyclin D1 expression by the Src oncoprotein in mouse fibroblasts: role of activated STAT3 signaling. *Oncogene*, 19(48), 5419-5427.

Smith, J. J., Chen, X., Schneider, D. F., Broome, J. T., Sippel, R. S., Chen, H., & Solórzano, C. C. (2013). Cancer after thyroidectomy: a multi-institutional experience with 1,523 patients. *Journal of the American College of Surgeons*, 216(4), 571-577.

Soares, P., Trovisco, V., Rocha, A. S., Lima, J., Castro, P., Preto, A., . . . Sobrinho-Simoes, M. (2003). *BRAF* mutations and *RET/PTC* rearrangements are alternative events in the etiopathogenesis of PTC. *Oncogene*, 22(29), 4578-4580.

Sobotta, M. C., Liou, W., Stöcker, S., Talwar, D., Oehler, M., Ruppert, T., . . . Dick, T. P. (2015). Peroxiredoxin-2 and STAT3 form a redox relay for H₂O₂ signaling. *Nature Chemical Biology*, 11(1), 64-70.

Sofiadis, A., Becker, S., Hellman, U., Hultin-Rosenberg, L., Dinets, A., Hulchiy, M., . . . Larsson, C. (2012). Proteomic profiling of follicular and papillary thyroid tumors. *European Journal of Endocrinology*, 166(4), 657-667. doi: 10.1530/EJE-11-0856.

Sofiadis, A., Dinets, A., Orre, L. M., Branca, R. M., Juhlin, C. C., Foukakis, T., . . . Lehtio, J. (2010). Proteomic study of thyroid tumors reveals frequent up-regulation of the Ca²⁺-binding protein S100A6 in papillary thyroid carcinoma. *Thyroid*, 20(10), 1067-1076. doi: 10.1089/thy.2009.0400.

Solakidi, S., Dessypris, A., Stathopoulos, G. P., Androulakis, G., & Sekeris, C. E. (2004). Tumour-associated trypsin inhibitor, carcinoembryonic antigen and acute-phase reactant proteins CRP and α 1-antitrypsin in patients with gastrointestinal malignancies. *Clinical Biochemistry*, 37(1), 56-60.

Srinivas, P. R., Kramer, B. S., & Srivastava, S. (2001). Trends in biomarker research for cancer detection. *The Lancet Oncology*, 2(11), 698-704.

Srisomsap, C., Subhasitanont, P., Otto, A., Mueller, E. C., Punyarit, P., Wittmann-Liebold, B., & Svasti, J. (2002). Detection of cathepsin B up-regulation in neoplastic thyroid tissues by proteomic analysis. *Proteomics*, 2(6), 706-712. doi: 10.1002/1615-9861(200206)2:6<706::AID-PROT706>3.0.CO;2-E.

Stathatos, N. (2016). Anatomy and physiology of the thyroid gland: clinical correlates to thyroid cancer. In *Thyroid cancer* (pp. 3-8). New York, NY: Springer.

Steinert, R., Von Hoegen, P., Fels, L., Günther, K., Lippert, H., & Reymond, M. (2002). Proteomic prediction of disease outcome in cancer: clinical framework and

current status. *American Journal of Pharmacogenomics: Genomics-related Research in Drug Development and Clinical Practice*, 3(2), 107-115.

Studer, H., & Derwahl, M. (1995). Mechanisms of nonneoplastic endocrine hyperplasia—a changing concept: a review focused on the thyroid gland. *Endocrine Reviews*, 16(4), 411-426.

Sumana, B., ShaShidhar, S., & Shivarudrappa, A. (2015). Galectin-3 immunohistochemical expression in thyroid neoplasms. *Journal of Clinical and Diagnostic Research*, 9(11), EC07.

Sumimoto, H., Imabayashi, F., Iwata, T., & Kawakami, Y. (2006). The BRAF–MAPK signaling pathway is essential for cancer-immune evasion in human melanoma cells. *Journal of Experimental Medicine*, 203(7), 1651-1656.

Suresh, R., Sethi, S., Ali, S., Giorgadze, T., & Sarkar, F. H. (2015). Differential expression of microRNAs in papillary thyroid carcinoma and their role in racial disparity. *Journal of Cancer Science and Therapy*, 7(5), 145.

Tallini, G., Asa, S. L., & Fuller, G. N. (2001). *RET* oncogene activation in papillary thyroid carcinoma. *Advances in Anatomic Pathology*, 8(6), 345-354.

Tan, G. H., & Gharib, H. (1997). Thyroid incidentalomas: management approaches to nonpalpable nodules discovered incidentally on thyroid imaging. *Annals of Internal Medicine*, 126(3), 226-231.

Tang, K.-T., & Lee, C.-H. (2010). *BRAF* mutation in papillary thyroid carcinoma: pathogenic role and clinical implications. *Journal of the Chinese Medical Association*, 73(3), 113-128.

Tetzlaff, M. T., Liu, A., Xu, X., Master, S. R., Baldwin, D. A., Tobias, J. W., . . . Baloch, Z. W. (2007). Differential expression of miRNAs in papillary thyroid carcinoma compared to multinodular goiter using formalin fixed paraffin embedded tissues. *Endocrine Pathology*, 18(3), 163-173.

Thavarajah, S., & Weber, F. (2012). Genetic background may confer susceptibility to PTC in benign multinodular thyroid disease. *Journal of Cancer Therapy*, 3(06), 997.

Tian, W.-D., Li, J.-Z., Hu, S.-W., Peng, X.-W., Li, G., Liu, X., . . . Li, X.-P. (2015). Proteomic identification of alpha-2-HS-glycoprotein as a plasma biomarker of hypopharyngeal squamous cell carcinoma. *International Journal of Clinical and Experimental Pathology*, 8(8), 9021.

Torres-Cabala, C., Bibbo, M., Panizo-Santos, A., Barazi, H., Krutzsch, H., Roberts, D. D., & Merino, M. J. (2006). Proteomic identification of new biomarkers and application in thyroid cytology. *Acta Cytol*, 50(5), 518-528.

Trachte, A. L., Suthers, S. E., Lerner, M. R., Hanas, J. S., Jupe, E. R., Sienko, A. E., . . . Postier, R. G. (2002). Increased expression of alpha-1-antitrypsin, glutathione S-transferase π and vascular endothelial growth factor in human pancreatic adenocarcinoma. *The American Journal of Surgery*, 184(6), 642-647.

- Treanor, J. J., Goodman, L., de Sauvage, F., & Stone, D. M. (1996). Characterization of a multicomponent receptor for GDNF. *Nature*, 382(6586), 80.
- Trovato, M., Grosso, M., Vitarelli, E., Ruggeri, R., Alesci, S., Trimarchi, F., . . . Benvenaga, S. (2003). Distinctive expression of STAT3 in papillary thyroid carcinomas and a subset of follicular adenomas. *Histology and Histopathology*, 18(2), 393-400.
- Trovisco, V., Vieira de Castro, I., Soares, P., Máximo, V., Silva, P., Magalhaes, J., . . . Sobrinho-Simões, M. (2004). *BRAF* mutations are associated with some histological types of papillary thyroid carcinoma. *The Journal of Pathology*, 202(2), 247-251.
- Tseng, P.-H., Matsuzawa, A., Zhang, W., Mino, T., Vignali, D. A., & Karin, M. (2010). Different modes of ubiquitination of the adaptor TRAF3 selectively activate the expression of type I interferons and proinflammatory cytokines. *Nature Immunology*, 11(1), 70-75.
- Tufo, G., Jones, A., Wang, Z., Hamelin, J., Tajeddine, N., Esposti, D., . . . Migdal, C. (2014). The protein disulfide isomerases PDIA4 and PDIA6 mediate resistance to cisplatin-induced cell death in lung adenocarcinoma. *Cell Death and Differentiation*, 21(5), 685-695.
- Tye, H., Kennedy, C. L., Najdovska, M., McLeod, L., McCormack, W., Hughes, N., . . . Ishikawa, T. O. (2012). STAT3-driven upregulation of TLR2 promotes gastric tumorigenesis independent of tumor inflammation. *Cancer Cell*, 22(4), 466-478.
- Ullah, I., Hafeez, M., Ahmad, N., Muahammad, G., & Gandapur, S. (2014). Incidence of thyroid malignancy in multinodular goiter. *Cell*, 92, 333-9115307.
- Vabulas, R. M., Ahmad-Nejad, P., Ghose, S., Kirschning, C. J., Issels, R. D., & Wagner, H. (2002). HSP70 as endogenous stimulus of the Toll/interleukin-1 receptor signal pathway. *Journal of Biological Chemistry*, 277(17), 15107-15112.
- van den Hurk, W. H., Willems, H. J., Bloemen, M., & Martens, G. J. (2001). Novel frameshift mutations near short simple repeats. *Journal of Biological Chemistry*, 276(15), 11496-11498.
- Vander Heiden, M. G., Cantley, L. C., & Thompson, C. B. (2009). Understanding the Warburg effect: the metabolic requirements of cell proliferation. *Science*, 324(5930), 1029-1033.
- Vanderpump, M. P. (2011). The epidemiology of thyroid disease. *British Medical Bulletin*, 99, 39-51. doi: 10.1093/bmb/ldr030.
- Varambally, S., Yu, J., Laxman, B., Rhodes, D. R., Mehra, R., Tomlins, S. A., . . . Chinnaiyan, A. M. (2005). Integrative genomic and proteomic analysis of prostate cancer reveals signatures of metastatic progression. *Cancer Cell*, 8(5), 393-406. doi: 10.1016/j.ccr.2005.10.001.
- Verkooijen, H. M., Fioretta, G., Pache, J. C., Franceschi, S., Raymond, L., Schubert, H., & Bouchardy, C. (2003). Diagnostic changes as a reason for the increase in

papillary thyroid cancer incidence in Geneva, Switzerland. *Cancer Causes and Control*, 14(1), 13-17.

- Vierlinger, K., Mansfeld, M. H., Koperek, O., Nohammer, C., Kaserer, K., & Leisch, F. (2011). Identification of SERPINA1 as single marker for papillary thyroid carcinoma through microarray meta analysis and quantification of its discriminatory power in independent validation. *BMC Medical Genomics*, 4, 30. doi: 10.1186/1755-8794-4-30.
- Viglietto, G., Chiappetta, G., Martinez-Tello, F. J., Fukunaga, F. H., Tallini, G., Rigopoulou, D., . . . Fusco, A. (1995). *RET/PTC* oncogene activation is an early event in thyroid carcinogenesis. *Oncogene*, 11(6), 1207-1210.
- Visone, R., Russo, L., Pallante, P., De Martino, I., Ferraro, A., Leone, V., . . . Croce, C. M. (2007). MicroRNAs (miR)-221 and miR-222, both overexpressed in human thyroid papillary carcinomas, regulate p27Kip1 protein levels and cell cycle. *Endocrine-related Cancer*, 14(3), 791-798.
- Vogelstein, B., Lane, D., & Levine, A. J. (2000). Surfing the p53 network. *Nature*, 408(6810), 307-310.
- Vucic, E. A., Thu, K. L., Robison, K., Rybaczyk, L. A., Chari, R., Alvarez, C. E., & Lam, W. L. (2012). Translating cancer 'omics' to improved outcomes. *Genome Research*, 22(2), 188-195. doi: 10.1101/gr.124354.111.
- Vymetalkova, V., Soucek, P., Kunicka, T., Jiraskova, K., Brynychova, V., Pardini, B., . . . Kozevnikovova, R. (2015). Genotype and haplotype analyses of *TP53* gene in breast cancer patients: association with risk and clinical outcomes. *PLoS One*, 10(7), e0134463.
- Wang, D. G., Chen, J. Y., Zhang, H. Y., Zhang, F. F., Yang, L. J., & Mu, Y. H. (2016). The correlation analysis of *RET* gene polymorphism with papillary thyroid carcinoma. *International Journal of Clinical and Experimental Pathology*, 9(10), 10707-10713.
- Wang, F., Kohan, A. B., Lo, C. M., Liu, M., Howles, P., & Tso, P. (2015). Apolipoprotein A-IV: a protein intimately involved in metabolism. *Journal of Lipid Research*, 56(8), 1403-1418.
- Wang, F., Wang, P., Wang, B., Fu, Z. J., Yuan, Y., Yan, S. L., . . . Wang, Y. G. (2014). Association between *TP53* Arg72Pro polymorphism and thyroid carcinoma risk. *Tumor Biology*, 35(3), 2723-2728. doi: 10.1007/s13277-013-1359-x.
- Wang, F., Yan, D., Ji, X., Han, J., Chen, M., Qiao, H., & Zhang, S. (2016). rs965513 polymorphism as a common risk marker is associated with papillary thyroid cancer. *Oncotarget*, 7(27), 41336.
- Wang, J. X., Yu, J. k., Wang, L., Liu, Q. L., Zhang, J., & Zheng, S. (2006). Application of serum protein fingerprint in diagnosis of papillary thyroid carcinoma. *Proteomics*, 6(19), 5344-5349.

- Wang, K., Kan, J., Yuen, S. T., Shi, S. T., Chu, K. M., Law, S., . . . Leung, S. Y. (2011). Exome sequencing identifies frequent mutation of *ARID1A* in molecular subtypes of gastric cancer. *Nature Genetics*, *43*(12), 1219-1223. doi: 10.1038/ng.982.
- Wang, L. Q., Wang, T. Y., Sun, Q. L., & Qie, Y. Q. (2015). Correlation between thyroglobulin gene polymorphisms and autoimmune thyroid disease. *Molecular Medicine Reports*, *12*(3), 4469-4475.
- Wang, S. F., Zhao, W. H., Wang, W. B., Teng, X. D., Teng, L. S., & Ma, Z. M. (2013). Clinical features and prognosis of patients with benign thyroid disease accompanied by an incidental papillary carcinoma. *Asian Pacific Journal of Cancer Prevention*, *14*(2), 707-711.
- Wang, Y. S., Cao, R., Jin, H., Huang, Y. P., Zhang, X. Y., Cong, Q., . . . Xu, C. J. (2011). Altered protein expression in serum from endometrial hyperplasia and carcinoma patients. *Journal of Hematology and oncology*, *4*(1), 15.
- Wang, Y., Hou, P., Yu, H., Wang, W., Ji, M., Zhao, S., . . . Shi, B. (2007). High prevalence and mutual exclusivity of genetic alterations in the phosphatidylinositol-3-kinase/akt pathway in thyroid tumors. *The Journal of Clinical Endocrinology and Metabolism*, *92*(6), 2387-2390.
- Ward, L. S., Morari, E. C., Leite, J. L., Bufalo, N. E., Guilhen, A. C., Araujo, P. P., . . . Matos, P. S. (2007). Identifying a risk profile for thyroid cancer. *Arquivos Brasileiros de Endocrinologia e Metabologia*, *51*(5), 713-722.
- Wasenius, V. M., Hemmer, S., Kettunen, E., Knuutila, S., Franssila, K., & Joensuu, H. (2003). *Hepatocyte growth factor receptor, matrix metalloproteinase-11, tissue inhibitor of metalloproteinase-1, and fibronectin* are up-regulated in papillary thyroid carcinoma: a cDNA and tissue microarray study. *Clinical Cancer Research*, *9*(1), 68-75.
- Whipple, C., & Brinckerhoff, C. (2014). *BRAFV600E* melanoma cells secrete factors that activate stromal fibroblasts and enhance tumourigenicity. *British Journal of Cancer*, *111*(8), 1625-1633.
- Wienke, J. R., Chong, W. K., Fielding, J. R., Zou, K. H., & Mittelstaedt, C. A. (2003). Sonographic features of benign thyroid nodules: interobserver reliability and overlap with malignancy. *Journal of Ultrasound in Medicine*, *22*(10), 1027-1031.
- Wiest, P. W., Hartshorne, M. F., Inskip, P. D., Crooks, L. A., Vela, B. S., Telepak, R. J., . . . Tekkel, M. (1998). Thyroid palpation versus high-resolution thyroid ultrasonography in the detection of nodules. *Journal of Ultrasound in Medicine*, *17*(8), 487-496.
- Wojnarowska, B., Skrincosky, D. M., Haag, A., Sharma, M., Matta, K., & Bernacki, R. J. (1994). Inhibition of lectin-mediated ovarian tumor cell adhesion by sugar analogs. *Journal of Biological Chemistry*, *269*(36), 22797-22803.
- Wu, B., Guo, D., & Guo, Y. (2014). Association between *p53* Arg72Pro polymorphism and thyroid cancer risk: a meta-analysis. *Tumor biology*, *35*(1), 561.

- Wu, G., Mambo, E., Guo, Z., Hu, S., Huang, X., Gollin, S. M., . . . Xing, M. (2005). Uncommon mutation, but common amplifications, of the *PIK3CA* gene in thyroid tumors. *The Journal of Clinical Endocrinology and Metabolism*, *90*(8), 4688-4693.
- Wu, W. C., Hu, D. N., Gao, H. X., Chen, M., Wang, D., Rosen, R., & McCormick, S. A. (2010). Subtoxic levels hydrogen peroxide-induced production of interleukin-6 by retinal pigment epithelial cells. *Molecular Vision*, *16*, 1864.
- Wulfkuhle, J. D., Paweletz, C. P., Steeg, P. S., Petricoin, E. F., 3rd, & Liotta, L. (2003). Proteomic approaches to the diagnosis, treatment, and monitoring of cancer. *Advances in Experimental Medicine and Biology*, *532*, 59-68.
- Xing, M. (2005). *BRAF* mutation in thyroid cancer. *Endocrine-related Cancer*, *12*(2), 245-262.
- Xing, M. (2007). *BRAF* mutation in papillary thyroid cancer: pathogenic role, molecular bases, and clinical implications. *Endocrine Reviews*, *28*(7), 742-762.
- Xing, M. (2013). Molecular pathogenesis and mechanisms of thyroid cancer. *Nature Reviews Cancer*, *13*(3), 184-199.
- Xing, M., Westra, W. H., Tufano, R. P., Cohen, Y., Rosenbaum, E., Rhoden, K. J., . . . Tallini, G. (2005). *BRAF* mutation predicts a poorer clinical prognosis for papillary thyroid cancer. *The Journal of Clinical Endocrinology and Metabolism*, *90*(12), 6373-6379.
- Xu, L., Li, G., Wei, Q., El- Naggari, A. K., & Sturgis, E. M. (2012). Family history of cancer and risk of sporadic differentiated thyroid carcinoma. *Cancer*, *118*(5), 1228-1235.
- Xu, G., Zhang, C., & Zhang, J. (2009). Dominant negative STAT3 suppresses the growth and invasion capability of human lung cancer cells. *Molecular Medicine Reports*, *2*(5), 819-824.
- Xu, X., Quiros, R. M., Gattuso, P., Ain, K. B., & Prinz, R. A. (2003). High prevalence of *BRAF* gene mutation in papillary thyroid carcinomas and thyroid tumor cell lines. *Cancer Research*, *63*(15), 4561-4567.
- Yamamoto, M., Okamoto, T., Takeda, K., Sato, S., Sanjo, H., Uematsu, S., . . . Ishii, K. J. (2006). Key function for the Ubc13 E2 ubiquitin-conjugating enzyme in immune receptor signaling. *Nature Immunology*, *7*(9), 962-970.
- Yang, L. B., Sun, L. Y., Jiang, Y., Tang, Y., Li, Z. H., Zhang, H. Y., . . . Ye, F. (2015). The clinicopathological features of *BRAF* mutated papillary thyroid cancers in Chinese patients. *International Journal of Endocrinology*, *2015*.
- Yang, Z., Huang, J. X., & Jing, W. N. (2016). Role of single nucleotide polymorphisms of *KRAS* and *BRAF* genes in susceptibility for papillary thyroid carcinoma and patients' prognosis. *International Journal of Clinical and Experimental Pathology*, *9*(3), 3859-3864.

- Yano, Y., Uematsu, N., Yashiro, T., Hara, H., Ueno, E., Miwa, M., . . . Uchida, K. (2004). Gene expression profiling identifies platelet-derived growth factor as a diagnostic molecular marker for papillary thyroid carcinoma. *Clinical Cancer Research*, 10(6), 2035-2043.
- Yoshihara, A., Hara, T., Kawashima, A., Akama, T., Tanigawa, K., Wu, H., . . . Ishii, N. (2012). Regulation of dual oxidase expression and H₂O₂ production by thyroglobulin. *Thyroid*, 22(10), 1054-1062.
- Yuen, S. T., Davies, H., Chan, T. L., Ho, J. W., Bignell, G. R., Cox, C., . . . Chan, A. S. (2002). Similarity of the phenotypic patterns associated with *BRAF* and *KRAS* mutations in colorectal neoplasia. *Cancer Research*, 62(22), 6451-6455.
- Zeiger, M. A., & Dackiw, A. P. (2005). Follicular thyroid lesions, elements that affect both diagnosis and prognosis. *Journal of Surgical Oncology*, 89(3), 108-113.
- Zhang, B., Lu, Y., Campbell-Thompson, M., Spencer, T., Wasserfall, C., Atkinson, M., & Song, S. (2007). α 1-Antitrypsin protects β -cells from apoptosis. *Diabetes*, 56(5), 1316-1323.
- Zhang, H. F., & Lai, R. (2014). STAT3 in cancer-friend or foe? *Cancers*, 6(3), 1408-1440.
- Zhang, J., Gill, A., Atmore, B., Johns, A., Delbridge, L., Lai, R., & McMullen, T. (2011). Upregulation of the signal transducers and activators of transcription 3 (STAT3) pathway in lymphatic metastases of papillary thyroid cancer. *International Journal of Clinical and Experimental Pathology*, 4(4), 356.
- Zhang, Q., Liu, S. Z., Guan, Y. X., Chen, Q. J., & Zhu, Q. Y. (2016). Meta-analyses of association between *BRAF*V600E mutation and clinicopathological features of papillary thyroid carcinoma. *Cellular Physiology and Biochemistry*, 38(2), 763-776.
- Zhang, Q., Song, F., Zheng, H., Zhu, X., Song, F., Yao, X., . . . Chen, K. (2013). Association between single-nucleotide polymorphisms of *BRAF* and papillary thyroid carcinoma in a Chinese population. *Thyroid*, 23(1), 38-44.
- Zhao, J., Leonard, C., Brunner, E., Gemenjager, E., Heitz, P. U., & Odermatt, B. (2006). Molecular characterization of well-differentiated human thyroid carcinomas by cDNA arrays. *International Journal of Oncology*, 29(5), 1041-1051.
- Zhou, J., Liao, J., Zheng, X., & Shen, H. (2012). Chimeric RNAs as potential biomarkers for tumor diagnosis. *BMB Reports*, 45(3), 133-140.
- Zhu, C., Zheng, T., Kilfoy, B. A., Han, X., Ma, S., Ba, Y., . . . Zhang, Y. (2009). A birth cohort analysis of the incidence of papillary thyroid cancer in the United States, 1973-2004. *Thyroid*, 19(10), 1061-1066. doi: 10.1089/thy.2008.0342.
- Zhu, X., Zhao, L., Park, J. W., Willingham, M. C., & Cheng, S. Y. (2014). Synergistic signaling of *KRAS* and thyroid hormone receptor β mutants promotes undifferentiated thyroid cancer through *MYC* up-regulation. *Neoplasia*, 16(9), 757-769.

Zilfou, J. T., & Lowe, S. W. (2009). Tumor suppressive functions of p53. *Cold Spring Harbor Perspectives in Biology*, 1(5), a001883.

University of Malaya

LIST OF PUBLICATIONS

List of ISI-publications

- 1) **Mardiaty Iryani Abdullah**, Ching Chin Lee, Sarni Mat Junit, Khoon Leong Ng and Onn Haji Hashim. Tissue and serum samples of patients with papillary thyroid cancer with and without benign background demonstrate different altered expression of proteins. PeerJ 2016; 4:e2450, doi: 10.7717/peerj.2450.
- 2) Ching Chin Lee, **Mardiaty Iryani Abdullah**, Sarni Mat Junit, Khoon Leong Ng, Sing Ying Wong, Nur Siti Fatimah Ramli and Onn Haji Hashim. Malignant transformation of benign thyroid nodule is caused by prolonged H₂O₂ insult that interfered with the STAT3 pathway? Int J Clin Exp Med 2016; 9(9): 18601-18617.
- 3) **Mardiaty Iryani Abdullah**, Nur Siti Fatimah Ramli, Khoon Leong Ng, Onn Haji Hashim and Sarni Mat Junit. Discovery of genetic alterations in patients with benign thyroid goitre and papillary thyroid cancer by whole-exome sequencing. (Manuscript in preparation).
- 4) **Mardiaty Iryani Abdullah**, Khoon Leong Ng, Sarni Mat Junit and Onn Haji Hashim. Papillary thyroid cancer: An updated review. (Manuscript in preparation)